AD_____

AWARD NUMBER: W81XWH-05-2-0034

TITLE: Topical Application of Liposomal Antioxidants for Protection Against CEES Induced Skin Damage

PRINCIPAL INVESTIGATOR: William L. Stone, Ph.D.
Victor Paromov, Ph.D.
Hongsong Yang, M.D.

CONTRACTING ORGANIZATION: East Tennessee State University
Johnson City, Tennessee 37614

REPORT DATE: June 2008

TYPE OF REPORT: Final

PREPARED FOR: U.S. Army Medical Research and Materiel Command
Fort Detrick, Maryland 21702-5012

REPORT DOCUMENTATION PAGE

Form Approved
OMB No. 0704-0188

1. REPORT DATE	2. REPORT TYPE	3. DATES COVERED
01-06-2008	Final	1 Jul 2005 – 30 May 2008

4. TITLE AND SUBTITLE

Topical Application of Liposomal Antioxidants for Protection Against CEES Induced Skin Damage

5a. CONTRACT NUMBER

5b. GRANT NUMBER
W81XWH-05-2-0034

5c. PROGRAM ELEMENT NUMBER

6. AUTHOR(S)
William L. Stone, Ph.D.; Victor Paromov, Ph.D.
Hongsong Yang, M.D.

E-Mail: stone@etsu.edu

5d. PROJECT NUMBER

5e. TASK NUMBER

5f. WORK UNIT NUMBER

7. PERFORMING ORGANIZATION NAME(S) AND ADDRESS(ES)

East Tennessee State University
Johnson City, Tennessee 37614

8. PERFORMING ORGANIZATION REPORT NUMBER

9. SPONSORING / MONITORING AGENCY NAME(S) AND ADDRESS(ES)
U.S. Army Medical Research and Materiel Command
Fort Detrick, Maryland 21702-5012

10. SPONSOR/MONITOR'S ACRONYM(S)

11. SPONSOR/MONITOR'S REPORT NUMBER(S)

12. DISTRIBUTION / AVAILABILITY STATEMENT
Approved for Public Release; Distribution Unlimited

13. SUPPLEMENTARY NOTES

14. ABSTRACT
This study was successful in developing an effective prophylactic therapy against skin damage caused by an analog of mustard gas, 2-chloroethylethyl sulfide (CEES) using in vitro model systems. The therapy is based on the topical application of antioxidant liposomes. Both EpiDerm cultured human skin tissues as well as cultured keratinocytes were used as the in vitro model systems. Our results show that CEES pathophysiology involves oxidative stress and liposomes containing both water- and lipid-soluble antioxidants are, therefore, likely to be effective therapeutic agents for protecting US military and civilians from a chemical warfare agent such as mustard gas (HD). In summary, we have determined the therapeutic efficacy as well as the chemical and physical stability of various antioxidant liposome formulations for future testing in animal models.

15. SUBJECT TERMS
skin, CEES, toxicity, liposomes, antioxidants, vitamin E, protection, keratinocytes

16. SECURITY CLASSIFICATION OF:			17. LIMITATION OF ABSTRACT	18. NUMBER OF PAGES	19a. NAME OF RESPONSIBLE PERSON
a. REPORT	b. ABSTRACT	c. THIS PAGE			USAMRMC
U	U	U	UU	137	19b. TELEPHONE NUMBER *(include area code)*

TABLE OF CONTENTS:

ABBREVIATIONS:

ALA, α-Lipoic acid
AT, α-tocopherol
CEES, half mustard or 2-chloroethyl-ethyl sulfide
CAM, calcein AM
Car-DCFH DA, carboxy-dichloroflurescin diaceatate
DEVD-AFC, peptido (DEVD)-7-Amino-4-trifluoromethylcoumarin
DMSO, dimethyl sulfoxide, a solvent
GSH, reduced glutathione and an antioxidant
GT, γ-tocopherol
HD, sulfur mustard or bis-2-(chloroethyl) sulfide
IL-1β, interleukin-1 beta
LPS, lipopolysaccaride
MNNG, N-methyl-N'-nitro-N-nitrosoguanidine
MTT, 3-(4, 5-dimethylthiazolyl-2)-2,5-diphenyltetrazolium bromide
NAC, N-acetyl-L-cysteine
NFκB, nuclear factor kappa-B
PI, propidium iodide
PMA, phorbol myristate acetate
ROS, reactive oxygen species
TBHP, tert-butyl hydroperoxide
TNF-α, tumor necrosis factor-alpha

INTRODUCTION:

Sulfur Mustard (HD): The sulfur mustard (bis-2-(chloroethyl) sulfide) could effectively be used to produce casualties in the battlefield and to force opposing troops to wear full protective equipment thereby slowing down the tempo of military operations. It could also be used with devastating results against civilian targets, and such use of HD by S. Hussein's military forces in Iraq has been well documented. The extensive and slow healing skin lesions following exposure to HD would also place a heavy burden on the medical services of military and public health organizations.

Effects of HD on human skin: A characteristic of sulfur mustard exposure is the occurrence of a symptom free period of some hours post exposure. The duration of this period and the severity of the subsequent lesions are dependent upon the mode of exposure, the environmental temperature and individual to individual variations. In the first hour after exposure to mustard gas vapor or liquid there are usually no signs or symptoms but nausea, vomiting and eye smarting have been occasionally reported. Post-exposure (up to 24 hours) skin inflammation ensues followed by lesion formation and blistering.

Treatment of HD: There is no antidote or effective treatment for mustard gas toxicity either for skin or lung exposure.

Mechanism of CEES/HD-induced skin damage: Oxidative stress is an important mechanism for HD induced skin injury. HD and its analog 2-chloroethylethyl sulfide (CEES) induce alkylation of DNA and rapid oxidation of intracellular proteins and lipids. CEES and HD are known also to react with the major intracellular antioxidant GSH; depleting it with a subsequent loss of protection against reactive oxygen species (ROS) and an activation of inflammatory responses.

Considerable evidence suggests that HD toxicity is associated with an increased generation of damaging free radical production and promote apoptosis. As detailed below, we have found that oxidative stress and pro-inflammatory cytokines play a key role in the toxicity of CEES. The PI's laboratory is part of a DOD funded group termed the "Advanced Medical Countermeasure Consortium". This group is systematically evaluating the overall hypothesis that oxidative stress, pro-inflammatory agents, and apoptotic cell signaling are the key factors in the toxicity of mustard gas. In recent years, there has been an enormous expansion of findings on the molecular mechanism of inflammatory responses and its relationship to oxidative stress [1-4].

We are currently taking advantage of this rich wealth of background information to help define the molecular links between inflammatory agents, oxidative stress and mustard gas toxicity. We have found that macrophages exposed to CEES have a decreased level of intracellular GSH, which is even further diminished in the presence of LPS [5]. Pretreatment of the macrophages with N-acetyl cysteine (NAC) protects against the loss of intracellular GSH. NAC serves to promote the synthesis of GSH and this is the likely

mechanism for the protective effect of NAC against CEES/HD toxicity as reported by the PI's laboratory and other researchers.

The HD-induced depletion of GSH together with protein and lipid oxidation has far reaching consequences that have not been previously appreciated. HD-induced pathophysiology may occur in large part due to a disruption of redox homeostasis. Redox homeostasis is dependent upon the balance between oxidants and antioxidants. Redox sensitive gene expression is determined by the cellular redox status. Signal transduction events induced by endogenous stimuli alter the redox state of the cell. GSH depletion influences a variety of cellular signaling process, such as activation and phosphorylation of stress kinases (JNK, p38, PI-3K) via sensitive cysteine-rich domains; activation of sphingomyelinase ceramide pathway, and activation of AP-1 and NFkB, with subsequent gene transcription [6, 7]. GSH levels are inversely related to the activity of NFkB [9]. NFkB regulates many genes involved in inflammation such as: inducible nitric oxide sythase (iNOS), proinflammatory cytokines, Il-1, TNF-alpha, interleukin 6 (IL-6), chemokine, IL-8, E-selectin, vascular cell adhesion molecule 1 (ICAM-1), and granulocyte-macrophage colony stimulating factor (GM-CSF) [6, 8].

Arroyo *et al.* [9] found a dose dependent increase in TNF- alpha, IL-6, IL1 beta in SM treated human keratinocyte cells. Signal transduction has also been demonstrated for CEES, wherein TNF-alpha, sphingomyelinase levels, caspase 3, 8, and 9 were all elevated [10]. Stone *et al.* [5] have found that inflammatory cytokines exacerbate the toxicity of CEES. In proliferating cells GSH levels are rapidly depleted by TNF-alpha. It is postulated that oxidative stress induced by CEES is further amplified by the loss of GSH and inflammatory cytokine production, thus exacerbating CEES-induced pathophysiology.

Rationale for the use of Liposomal Antioxidants: One way of reversing or preventing the ROS-induced cellular injury to skin is via topical application of antioxidants. Vitamin E (tocopherols and tocotrienols), GSH, N-acetylcysteine (NAC), α-Lipoic acid (ALA), ethyl pyruvate are very effective antioxidants. Their antioxidative potential and importance in skin pathophysiology had been tested previously in a large number of investigations [2, 11-14]. However, the delivery of antioxidants to skin remains problematic in some cases as intact skin allows the passage of small lipophilic substances but, in most cases, efficiently retards the diffusion of water-soluble molecules.

Liposomes are phospholipid vesicles composed of lipid bilayers enclosing an aqueous compartment. Hydrophilic molecules can be encapsulated in the aqueous spaces and lipophilic molecules can be incorporated into the lipid bilayers. Liposomes are unique in their ability to simultaneously deliver both water-soluble (in their aqueous inner space) and lipid-soluble antioxidants (in the phospholipid bilayer) to cells and tissues. They represent an ideal drug delivery system that enhances penetration of the active ingredient into the skin, localizes the drug at the site of action, and reduces percutaneous absorption.

The term "antioxidant liposome" is relatively new and refers to liposomes containing lipid soluble chemical antioxidants, water-soluble chemical antioxidants, enzymatic

antioxidants, or combinations of these various antioxidants. Stone et al. [15] have reviewed the use of antioxidant liposomes in the general area of free radical biology and medicine as well as the relevant application of this technology to weapons of mass destruction. Antioxidant liposomes hold great promise for the treatment of many diseases and conditions in which oxidative stress plays a prominent role. Several studies have clearly indicated that the liposomal antioxidant formulations compared to that of the free non-encapsulated antioxidants exert a far superior protective effect against oxidative stress-induced tissue injuries.

Military Significance: The overall objective of this study was to develop an effective prophylactic therapy against CEES-induced skin damage (analogous to HD effect) based on the topical application of antioxidant liposomes. Our preliminary data suggested that antioxidant liposomes are very effective in preventing CEES toxicity to stimulated macrophages. This study examined the effectiveness of various liposome formulations in ameliorating the CEES-induced skin injury in a human skin model (EpiDerm).

We have found liposomal preparations that would be useful in treating both lung and skin injuries in the battlefield thus preserving combat effectiveness. Furthermore, the timely administration of this treatment regimen will also avert the devastating results of CEES/HD against civilians that might be exposed during a terrorist attack. In this investigation, we also addressed practical issues with regards to large scale preparation, storage and pharmacological stability.

BODY

We originally proposed using EpiDerm cultured human skin tissues as a working model to study CEES cytotoxicity and the potential protective effects of antioxidant liposomes. However, EpiDerm tissues are very expensive and, in order to optimally utilize our resources, we utilized cultured normal human epidermal keratinocytes (NHEK) purchased from Cambrex in our first series of experiments. In addition, we used cultured 1106 KERTr human keratinocytes (ATCC) and immortalized human keratinocytes HaCaT purchased from Cell-Lines-Service (Germany), which are easy to culture and allow unlimited number of passages, whereas NHEK spontaneously transform after a few passages (a major and costly limitation). These issues were discussed and recommended by USAMRICD scientist Dr. R. Ray who specializes in studies of HD toxicity mechanisms. We studied the protective effect of antioxidant liposomes in cultured human keratinocytes, optimized antioxidant liposome formulations, and then performed the final experiments with the human EpiDerm tissues. In this report, we will detail the results of each specific task (hyperlinked below). In addition, our final series of experiments with the Epiderm Model are detailed separately.

Task 1: We characterized the toxicity of CEES to keratinocytes or the EpiDerm model as a function of CEES dose and exposure time. We determined: (1) how apoptosis contributes to CEES induced toxicity by measuring both capase-3; (2) if immuno-stimulators (LPS, PMA) and pro-inflammatory cytokines (TNF-α, IL-1β) increase CEES toxicity to human keratinocytes/EpiDerm tissues. It is postulated that apoptosis is the major cell death mechanism at low doses of CEES or HD whereas necrosis is the dominant mechanism at higher concentrations of CEES or HD and long-time exposures. We further anticipated that immuno-stimulators such as pro-inflammatory cytokines, LPS and PMA would enhance CEES toxicity to human keratinocytes.

Task 2:. We determined the influence of CEES on various oxidative stress parameters using cultured human keratinocytes and later, the EpiDerm model.

Task 3: We examined the pharmacokinetics of antioxidant liposomes following their topical application to the human keratinocytes or EpiDerm tissues.

Task 4: Cultured human keratinocytes and EpiDerm system were utilized to determine the most protective antioxidant liposome formulations.

Task 5: We explored the possibility of manufacturing antioxidant liposomes in large scale industrial quantities and attempted to optimize the antioxidant liposome formulations in order to enhance their long-term physical, chemical and therapeutic stability.

Results

Task 5- Characterization of Antioxidant Liposomes

As mentioned in the Introduction, liposomes are unique in their ability to effectively deliver both water- and lipid-soluble antioxidants to skin cells. As liposomes are artificially made vehicles, the question of their long-term stability especially under non-optimal conditions (high temperature, dry air) is of high importance. Therefore, we addressed the question of the liposome stability at the beginning of our studies.

Relevant to **Task 5**, we obtained the instrumentation required to prepare antioxidant liposomes in large quantities and characterize their particle size distribution. In order to manufacture large unilamellar antioxidant liposomes in quantities up to 10-20 L per day, we have optimized a micro-fluidizing technique. Using the M-110L Laboratory Microfluidizer® Processo,r we can produce liposomes at a rate of 270 ml/min at 18,000 PSI. This device was chosen since this technique can be scaled-up to industrial levels without changing liposomes properties/characteristics, which is important for future FDA considerations.

The PI and Dr. Hongsong Yang were trained by the Field Representative of Microfluidics Company on the use of M-110L Laboratory Microfluidizer® Processor and the Model 380 Nicomp particle size analyzer.

A long range consideration in the formulation of antioxidant liposomes is the very high cost of highly purified phosphatidyl choline typically used to make antioxidant liposomes. Purified phosphatidyl choline (i.e., dipalmitoyl phosphatidyl choline), although useful for *in vitro* testing would be too expensive for a commercial product useful to the DOD. The PI, therefore, initiated conversations with the American Lecithin Co. (www.americanlecithin.com) which has extensive experience and expertise in the use of soybean phosphatidyl choline to make liposomes. We have tested PL 85 G phosphatidyl choline, phospholipon 90G and phospholipon 90H (fully hydrogenated) in our preparations of antioxidant liposomes. These products possess high quality at low cost and relevant FDA files are on record. Liposomes prepared from phospholipon 90H and 90G showed the highest uniformity and stability and, therefore, were used in our studies focused on protecting human keratinocytes from a mustard gas analog toxicity.

In our previous results, we found that alpha-tocopherol containing liposomes were effective in protecting macrophages from CEES induced cytotoxicity. α-Tocopherol is the primary form of vitamin E found in plasma and is the primary lipid soluble antioxidant in blood. We have found, however, that γ-tocopherol is taken up by cells in culture to higher extent then α-tocopherol [16]. In the experiments preformed here, we tested liposomes made with either α-tocopherol or γ-tocopherol or mixtures of both. γ-Tocopherol is also very expensive and a commercial antioxidant-liposome formulation based on this vitamin

E isoform would be prohibitively expensive. The PI has, therefore, also made contact with commercial suppliers of mixed tocopherols with high a content of γ-tocopherol. The DSM Nutritional Products (www.dsm.com) supplied us with 100 g quantities of mixed tocopherols (with a very high content of γ-tocopherol) for testing in the antioxidant liposomes.

The liposomes have been characterized by measuring: 1) particle size distribution using a dynamic light scattering Model 380 Nicomp particle analyzer; (2) liposome antioxidant (e.g., vitamin E) content composition and stability; and (3) potential liposome cytotoxicity in human skin cells using the MTT assay (**see Task 1**). In addition, liposomes containing encapsulated water-soluble antioxidants, such as GSH and NAC, were tested on their chemical stability (GSH oxidation) and physical stability (GSH leakiness).

Table 1 shows the typical chemical compositions of our antioxidant liposome formulation along with their average size distribution. The following large unilamellar liposomal (LUV) formulations were made: (1) "Blank liposomes" ; (2) "G-liposomes" [G-L] containing 75 mM GSH); (3) "T-liposomes" [T-L] with 6.67% mol./mol. α-tocopherol ; (4) "2x-T-liposomes" [2xT-L] with 13.33% mol./mol. α-tocopherol); (5) "G/T-liposomes" [GT-L] with a lipid composition the same as for "T-liposomes", containing 75 mM GSH; (6) "NAC-liposomes" containing 75 mM NAC); (7) "NAC/T-liposomes" [NT-L] with the same lipid composition "T-liposomes" and containing 75 mM NAC);. Aliquots of these liposomes were: (1) stored at room temperature; (2) refrigerator at 4°C; (3) stored with or without EDTA or urate as chelating agents.

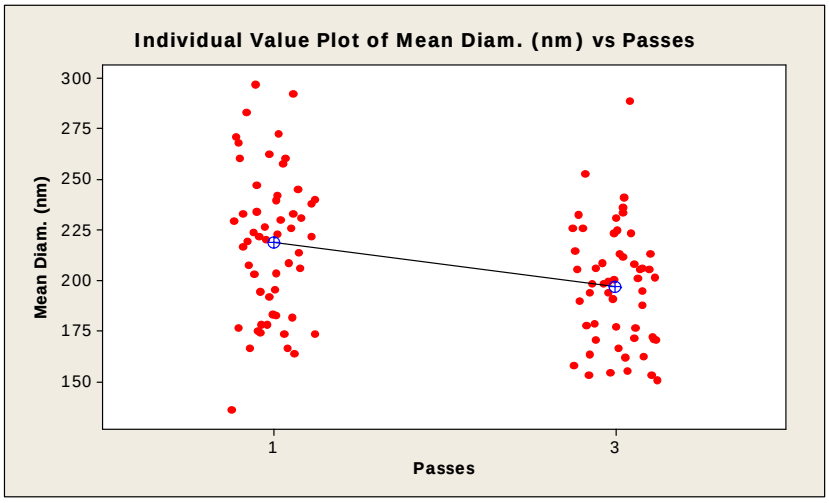

Figure 1. Three passes through the microfluidizing Processor makes smaller but more uniform liposomes. The liposomes prepared using M-110L Laboratory Microfluidizer® Processor; vesicle size distribution analyzed using the Model 380 Nicomp particle size analyzer.

Particle size distribution: Our results with respect to size distribution lead us to conclude that: (1) typical liposome preparation mostly contains vesicles with sizes distributed within 100-300 nm interval; (2) three passes through the homogenizer produces slightly smaller but more uniform liposomes (**Figure 1**), further increase of the number of passes dos not does not improve the vesicle size distribution; (3) encapsulation of a water-soluble antioxidant, such as NAC or GSH does not significantly alter the liposome size

distribution; (4) addition of a lipophilic antioxidant, such as α-tocopherol, in the liposome formulation slightly changes average particle size with high levels increasing and medium levels not having much of an effect (**Figure 2**).

Antioxidant content composition and stability: We measured the leakiness of GSH, a water-soluble encapsulated antioxidant, during prolonged storage (see **Figure 3).** In this experiment, GSH was encapsulated within the liposomes, and the external, non-encapsulated GSH removed by exhaustive dialysis. The liposomes were stored either at RT or at 4° C, and GSH concentration in the buffer monitored using Tietze's method [17] [18]. GSH leakage from the liposomes to the buffer is a measure of liposome membrane stability as charged GSH molecules cannot penetrate through an intact lipid bilayer. Our results show that the liposomes maintained high membrane stability within at least 1 month of storage. Only 3% of the GSH content was lost from the GSH or GSH/α-tocopherol containing liposomes.

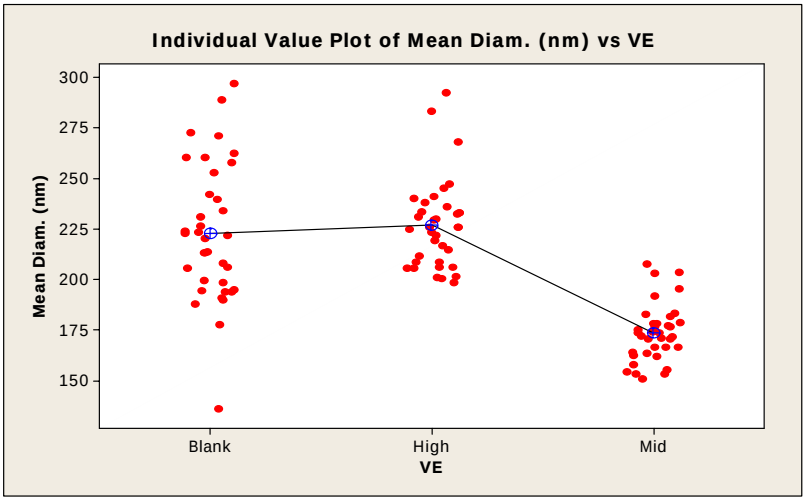

Figure 2. Vitamin E influences liposome size distribution. Blank: "Blank liposomes" (contain no antioxidants); High VE: "T-liposomes" (6.67% mol./mol. a-tocopherol); Mid. VE: "2x-T-liposomes" (13.33% mol./mol. a-tocopherol). The liposomes prepared using M-110L Laboratory Microfluidizer® Processor; vesicle size distribution analyzed using the Model 380 Nicomp particle size analyzer.

Table 1 Chemical and Physical Characterization of Liposomes

Type of Liposomes					
Composition	**Blank [B-L]**	**GSH [G-L]**	**αT (T-L)**	**GSH/ αT [GT-L]**	**NAC/T [NT-L]**
Lipid Components	**Mole Fractions/Concentration**				
PL/type	0.71/85G	0.71/85G	0.67/85G	0.67/85G	0.62/90H
PA	0	0	0	0	0.006
cholesterol	0.29	0.29	0.27	0.27	0.248
AT/mM	0/0	0/0	0.07/3.33	0.07/3.33	0.062/3.1
GT/mM	0/0	0/0	0/0	0/0	0.062/3.1
Aqueous Components	**Mole Fractions/Concentration**				
GSH/mM	0	75	0	75	0
NAC/mM	0	0	0	0	75
Size (nm)/% Peak 1	29.6±5.3 8%	90.2±16 23.5%	74.2±15.4 34.6%	78.6±13.4 37.2%	152.1±31.4 37.2%
Size (nm)/% Peak 2	141.8±28.5 92%	190.3±41.2 69.3%	248.5±45.8 65.4%	273.9±61.2 62.8	1326.3±292.6 68.6%

Also we have analyzed changes in lipid composition of vitamin E containing liposomes during prolonged storage. **Table 2** shows changes in vitamin E content of α- or γ-tocopherol containing liposome preparations stored for 4 weeks. Tocopherols were determined within the liposome samples using HPLC with electro-chemical detection. As we mentioned above, the liposome membrane is fairly stable physically, even at room temperature (leakage of a water-soluble compound from the inner space is minimal). However, addition of vitamin E to the lipid composition of liposomes influences the lipid bilayer organization. As we mentioned above vitamin E content of liposomes changes their vesicle size distribution (**Figure 2**). In addition, we found that liposomes containing α-tocopherol are less physically stable, in general, as compared

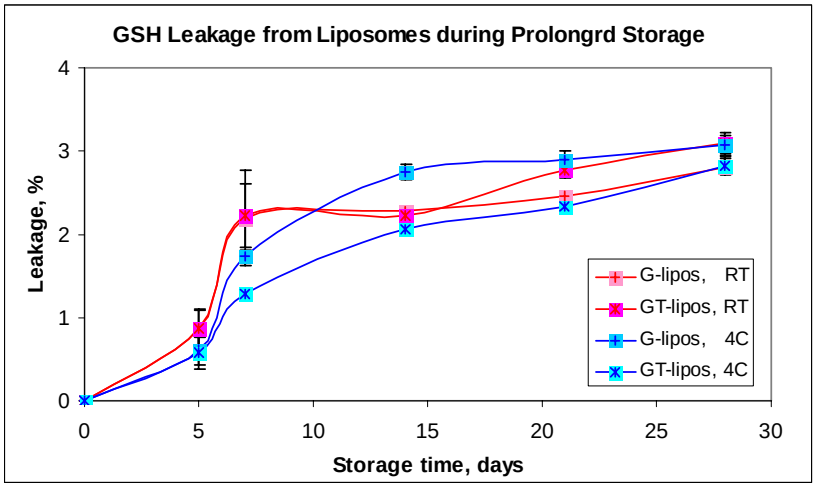

Figure 3. GSH-Liposome leakiness during pro-longed storage. 1 mL of "G-liposomes" or "G/T-liposomes" were put in sterile dialysis bag (8 kDa cut off) and dialyzed twice against 50 mL PBS. Dialyzed liposome samples were put in fresh PBS and incubated continuously at RT or at 4 C (fridge). GSH concentration within the each liposome sample and in the buffer was measured during 4 week incubation. Liposome leakiness was expressed as a percent of GSH in the buffer from the total GSH of each liposome sample.

with “Blank” or “G-liposomes”. Vitamin E containing liposomes, if stored at RT, completely loose their physical stability (phase separation was visually registered) during the 4th week of storage. We conclude that the inclusion of high amounts of vitamin E (more than 6% mol./mol.) reduces the physical stability of the liposomes due to the lipid bilayer perturbations. Liposomes stored at 4° C maintained their physical stability and average particle size but lost up to 60% of their vitamin E content due to its oxidation (Table 2). There were no significant differences in long-term stability between liposomes containing α-tocopherol or γ-tocopherol.

Table 2. Changes in vitamin E content of the liposomes during 4-week storage at 4° C

Description	“T-liposomes” (6.67% mol/mol) α -Tocopherol, mM	“2x-T-liposomes” (13.33% mol/mol) α -Tocopherol, mM
Day 1	2.98 ± 0.08	4.68 ± 0.10
Day 28	0.00 ± 0.01	0.00 ± 0.01
Day 28	0.68 ± 0.04	1.43 ± 0.15

In addition, we analyzed the chemical stability of the water-soluble content (GSH) encapsulated within the liposomes. **Figure 4** shows the loss of GSH due to oxidation to form GSSG (in GSH equivalents) as a function of storage time for the GSH-liposomes and the GSH/α-Tocopherol (G/T-) containing liposomes at RT or 4° C. These data show that GSH is oxidized rapidly at room temperature compared to 4° C. Moreover, the presence of α-tocopherol does not retard GSH oxidation. In addition, G/T-liposomes, similar to α-tocopherol containing liposomes, loose their physical stability (visible phase separation) during the 4th week of storage at RT.

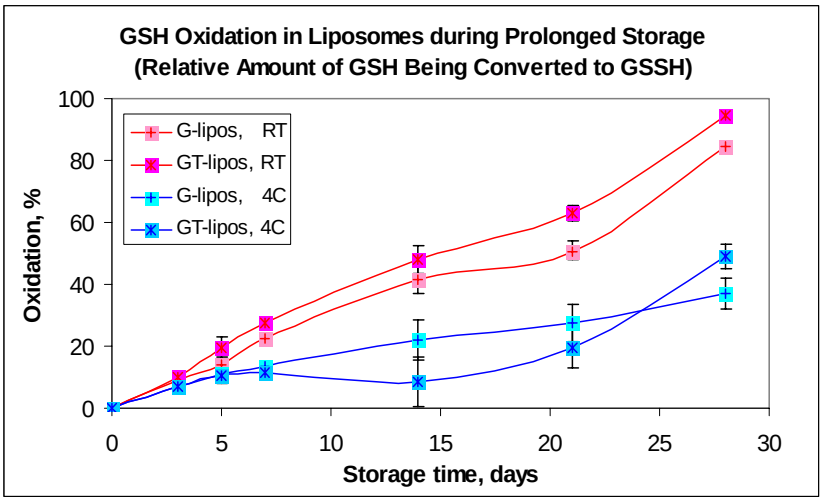

Figure 4. GSH oxidation (conversion to GSSG) within liposome fraction during pro-longed storage. “G-liposomes” or “G/T liposomes” were stored at room temperature (RT) or at 4 C. GSH and GSSG concentrations within the liposome samples was measured after 3, 5, 7, 14, 21 and 28 days of storage. Oxidation of GSH content of the liposomes was expressed as a percent of GSH converted to GSSG relatively to the total GSH/GSSG content of each sample.

The experiments describe above were done in the absence of a metal ion chelator. Chelators act as antioxidants by minimizing oxidation catalyzed by iron ions (a contaminant in all buffers). We have, therefore, analyzed the influence of metal ion chelators, such as ethylenediamine-tetraacetic acid (EDTA) and urate, on GSH chemical stability within the liposomes.

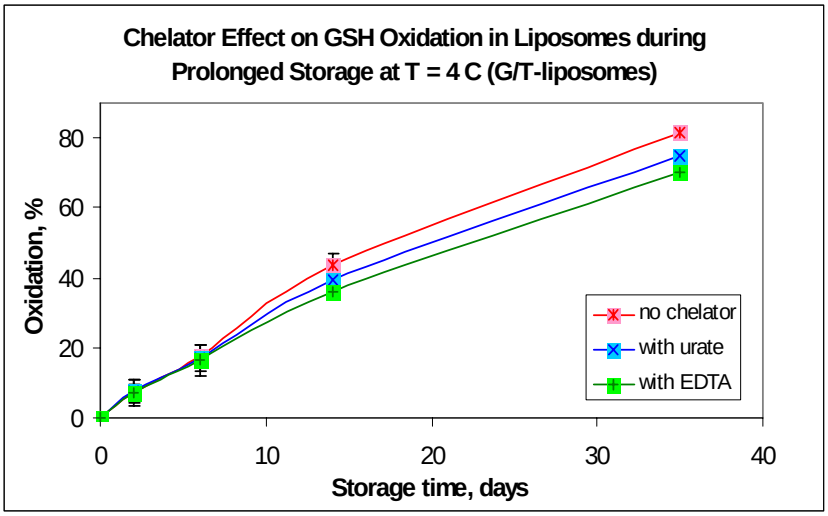

Figure 5. Chelator effect on GSH oxidation (conversion to GSSG) within liposome fraction during pro-longed storage. "G/T-liposomes" were stored at 4C (fridge). GSH and GSSG concentrations in the liposome samples was measured after 2, 6, 14, and 35 days of storage. Oxidation of GSH content of the liposomes was expressed as a percent of GSH converted to GSSG relatively to the total GSH/GSSG content of each liposome sample.

Figure 5 shows the effect of the chelators on GSH oxidation within the G/T-liposomes. Both urate and EDTA only slightly protect the GSH content of G/T-liposomes during storage at 4° C. GSH oxidation within G-liposomes showed similar rate at 4° C as for G/T-liposomes (**data not shown**). However, neither urate nor EDTA protected the GSH content of T-liposomes during storage at 4° C. Similar pattern was observed at both 4° C and RT: chelators slightly protected the GSH of G/T-liposomes but not that of the G-liposomes stored at RT (**Figure 6**).

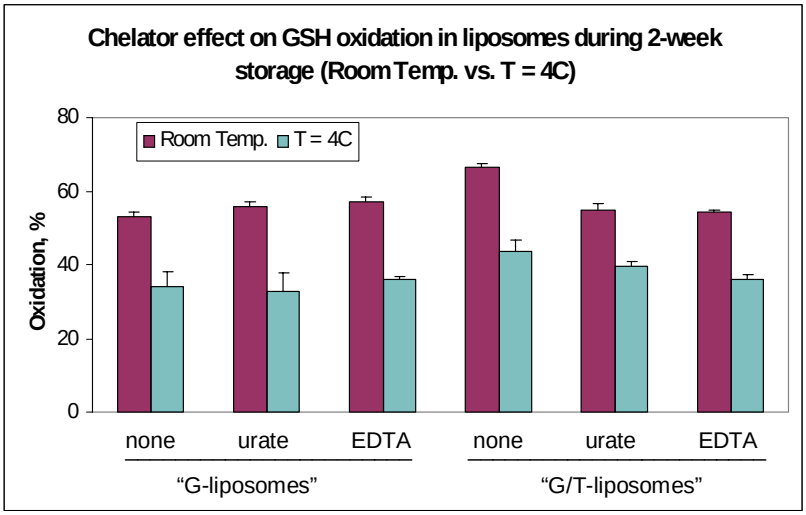

Figure 6. Chelator effect on GSH oxidation (conversion to GSSG) within liposome fraction during 2-week storage. "G-liposomes" or "G/T-liposomes" were stored at RT or 4 C (fridge). GSH and GSSG concentrations in the liposome samples was measured after 14 days of storage. Oxidation of GSH content of the liposomes was expressed as a percent of GSH converted to GSSG relatively to the total GSH/GSSG content of each liposome sample.

Based on the studies, we conclude that antioxidant liposomes posses a high degree of membrane stability even at RT. We found that the loss of antioxidative potency of the liposomes due to the chemical oxidation of the antioxidants is the major difficulty during long-term storage. Both lipid- and water-soluble antioxidant contents are being preserved much better if the liposomes are stored at 4° C. These data suggest that GSH and/or vitamin E containing liposomes would have to be either used relatively soon after being

formulated (perhaps within a week) or to be stored at 4° C for up to 4 weeks. Using lyophilized preparations is also a viable option.

Task 1 Investigate the cytotoxic effect of CEES on cultured human keratinocytes

Figure 7 shows the dose and time response of the NHEK keratinocytes exposed to CEES. In these experiments, the CEES was first dissolved in ethanol and then added to the culture medium with the final concentration of ethanol being no more than 2% by volume. **Figure 7** shows cell viability (as measured by the MTT assay) as a function of CEES dose after 16 or 48 hours of incubation. We found that NHEK cells were much more resistant to CEES induced inhibition of cell growth than other cell lines tested with a similar experimental design. As anticipated, higher doses and longer time of CEES incubation resulted in increased growth inhibition.

In order to determine if the addition of immuno-stimulators (LPS, PMA) and pro-inflammatory cytokines (TNF-α, IL-1β) could increase CEES toxicity to human keratinocytes, we performed experiments with NHEK cells exposed to various levels of CEES (**data not shown**). None of these immuno-stimulators enhanced toxicity of CEES as measured by the MTT assay. These results differ with our previous results obtained with murine macrophages simultaneously exposed to CEES and LPS [5].

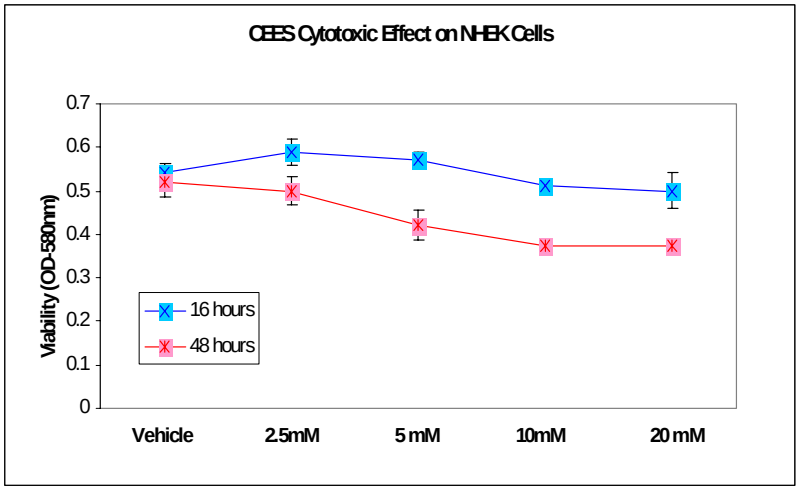

Figure 7. Cytotoxic effect of CEES on NHEK cells during long-time incubations. NHEK cells (Cambrex) were treated with various levels of CEES for up to 48 hours. CEES was applied as a stock solution in ethanol (final concentration of ethanol was no more than 2% vol.). Cell viability was measured as absorbance at 580nm (standard MTT assay).

The fact that LPS and other stimulators do not alter CEES toxicity in human keratinocytes possibly reflects a multi-step reaction to CEES/HD toxicity in human, which involves at least two major types of cells – skin cells and immune cells. We anticipate that, in the simplest case, CEES promotes cytokine release in keratinocytes which then induces the activation of macrophages and other immune cells (mast cells for instance), which in turn produce a feed-back reaction in keratinocytes stimulating apoptosis [12] [19] [20] [8] [21] [9] [22] [23] [24].

In the experiments described above we applied CEES in ethanol. According to the USAMRICD studies, human skin exposed to 300 µM concentration of HD will demonstrate oxidative stress, cytokine release, and massive apoptosis followed by necrosis. As a less toxic analog of HD, CEES would be expected to produce similar changes in keratinocytes at concentrations 3-4 times higher, i.e., 1 mM. [25] [21] [26].

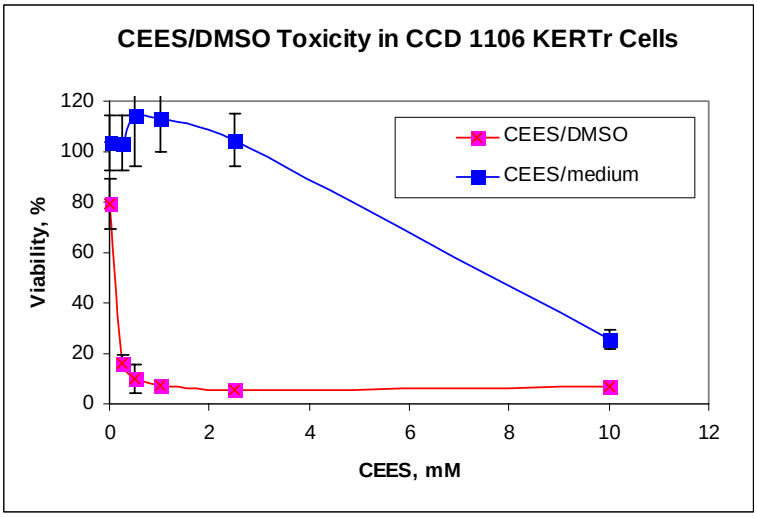

Figure 8. Cytotoxic effect of CEES/DMSO on NHEK cells during 24 h incubation. CCD 1106 KERTr cells were placed into 96-well plate in 0.25 ml/well of medium and treated with CEES applied either as pre-mixed solution in the media or as a stock solution in DMSO (final conc. 2% vol/vol). Cell viability was measured as absorbance at 580nm (standard MTT assay).

We, however, did not observe substantial cell death in human keratinocytes exposed to fairly high levels of CEES applied as a stock solution in ethanol. This method of CEES application appeared to result in a phase separation of the CEES from the cell culture medium thereby decreasing its effective concentration. We discussed this difficulty with a USAMRICD specialist Dr. R. Ray at the Bioscience Review 2006 Conference. Dr. R. Ray recommended two alternative methods of CEES application. The first method requires directly adding CEES to a plastic tube with the culture medium followed by extensive vortexing and immediately applying this mixture to cells in a multi-well plate. The second method requires preparation of a CEES stock solution in dimethyl sulfoxide (DMSO) which is then added to cells in a multi-well plate with gentle mixing. DMSO is known to be a very effective vehicle for a delivery of organic compounds to skin and enhances HD toxicity [27] [28].

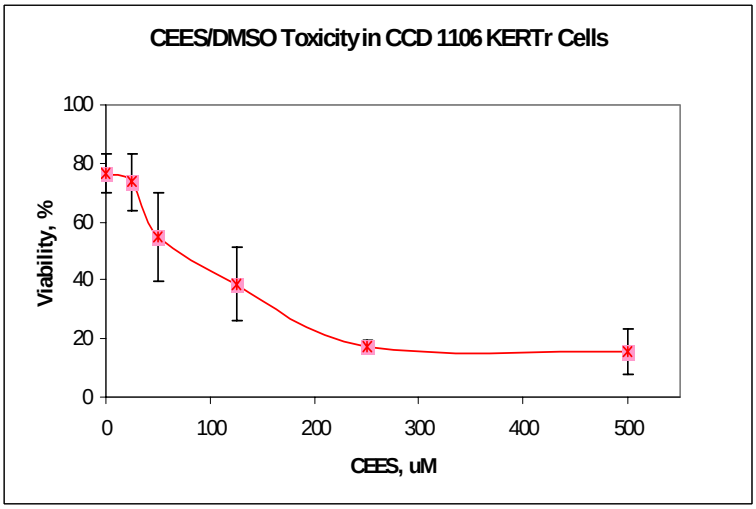

Figure 9. Cytotoxic effect of CEES/DMSO on NHEK cells during 24 h incubation. CCD 1106 KERTr cells were placed into 96-well plate in 0.25 ml/well of medium and treated with CEES applied as a stock solution in DMSO (final conc. 2% vol/vol). Cell viability was measured as absorbance at 580nm (standard MTT assay).

We tried both these methods of CEES application and the results as shown in **Figure 8**. CEES directly mixed with medium and applied to CCD 1106 KERTr keratinocytes showed moderate toxicity. In marked contrast, CEES in DMSO was much more toxic. **Figure 9** shows CEES/DMSO toxicity for low level of the toxicant.

The experiments above reported above utilized normal human NHEK cells. However, fully grown NHEK cells slowly, undergo terminal differentiation and are more resistant to genotoxic agents, such as CEES or HD, than actively proliferating cell cultures. Also, NHEK cells are expensive. In order to overcome such limitations we also utilized a continuously proliferating immortalized HaCaT human cell line (Cell-Lines-Service, Germany). We found that immortalized HaCaT human keratinocyte, unlike NHEK cells, have a higher susceptibility to CEES toxicity. Therefore, HaCaT keratinocytes were used for the majority of the experiments reported below.

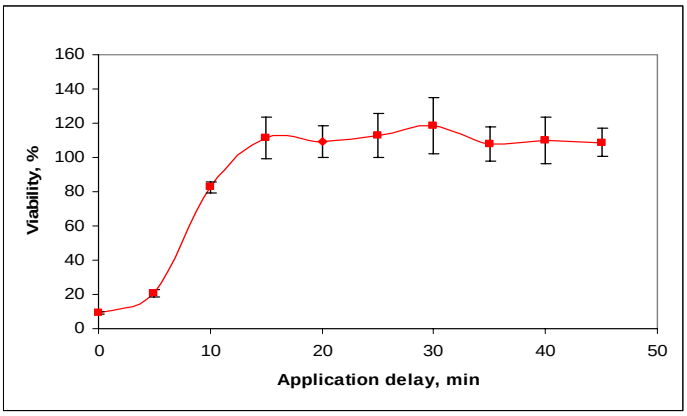

Figure 10. Influence of CEES Hydrolysis on Its Toxicity. 1.5 mM CEES in media was applied to HaCaT cells in 96-well plate after various time delays, as indicated. Cell viability was measured by the MTT assay after 24 hours.

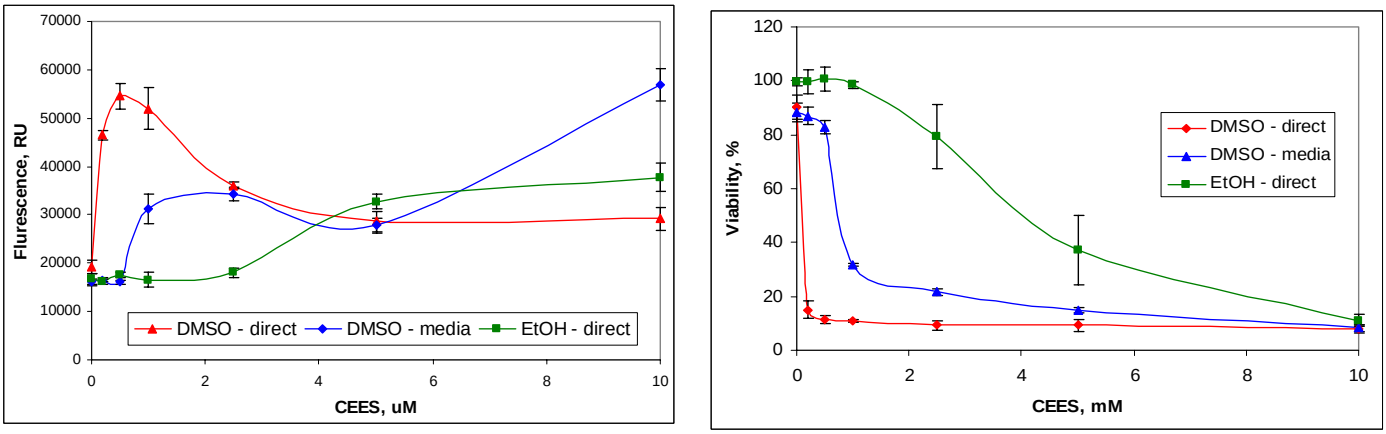

Figure 11- Influence of CEES Applications Technique on Cell Viability. CEES (0.2 – 10 mM) was applied to HaCaT cells in a 96-well plate: (1) directly as a stock solution in DMSO, (2) directly as a stock solution in EtOH, (3) as a stock solution pre-mixed in media. **Left:** Cell viability was measured by the MTT assay after 24 hours. **Right:** Amount of dead cells was measured by the PI assay after 24 hours.

As shown above, the technique for CEES application to our cell model systems is very important variable since CEES undergoes rapid hydrolysis in aqueous solutions [30, 31]. CEES/HD can be applied without any vehicle by direct mixing in the medium immediately prior the application. Although the latter method of CEES application is widely used, it allows hydrolysis to some extent. It takes a few minutes to pipette HD or CEES into the medium, and then into a multi-well plate. During this time hydrolysis will not only lower the "real" concentration of CEES but also make the effective CEES concentration different from the first to the last sample. Therefore, a more stable stock solution of CEES in a dry organic solvent would be preferable. Previously, we showed that DMSO was a very effective vehicle for CEES delivery to the cells. We found, also, that DMSO is a more effective vehicle than ethanol. CEES/DMSO stock solution provides a better application

model than direct dispersing of CEES in a large bolus of cell culture medium prior the experiment.

In order to determine if CEES hydrolysis in culture medium has an effect on its toxicity, we performed a simple time-course experiment. CEES (50 mM stock in DMSO) was mixed with appropriate volume of media to obtain a 1.5 mM final concentration, and then applied to HaCaT keratinocytes in a 96-well plate after various time delays. As shown in **Figure 10**, a quick drop in CEES toxicity was noted with only a 5 min delay. After 15 minutes, CEES was no longer toxic to the cells. These data support view that CEES hydrolysis is a critical experimental parameter in cellular toxicity studies.

Although we found that DMSO itself possesses a mild cytotoxic effect, such a drawback can be minimized by using a low vehicle concentration (1% (vol./vol.)). We have preformed a number of experiments to optimize the CEES application technique. Our results indicate that preparing a 100x stock solution in DMSO followed by quick mixing with media for only a limited number of repeated samples (up to 8) is very effective. We found that CEES hydrolysis is minimal with this technique (data not shown).

Figure 11 illustrates the effect of various application techniques on cell viability (MTT assay) or cell death (PI assay). The assay for cell viability is based on the reduction of 3-(4, 5-dimethylthiazolyl-2)-2,5-diphenyltetrazolium bromide (MTT) by mitochondrial dehydrogenase in viable cells yielding a purple formazan product. Cell viability was measured as the absorbance of the formazan product at 575 nm (monitored with a Molecular Devices microplate reader). The PI assay uses propidium iodide (PI) dye to differentiate live and dead cell. Cells that have lost membrane integrity cannot exclude PI, which emits a red fluoresce after binding to nuclear DNA or double stranded RNA. PI fluorescence was measured using a Fluostar Galaxy microplate reader using an excitation wavelength of 485 nm and an emission wavelength of 650 nm.

Applying CEES in DMSO directly to the well as cultured cells resulted in maximum loss of cell viability (**Figure 11, left**) and maximum cell death (**Figure 11, right**). This is due to minimizing CEES hydrolysis and exposing the cells to a transiently high level of CEES. The transiently high level of CEES is an uncontrolled variable and this fact minimizes the usefulness of direct application of stock CEES in DMSO. Adding the CEES in DMSO followed by rapid mixing in the media also produces marked loss of viability and increased cell death. This method has the advantage of not exposing the cells to a transiently high

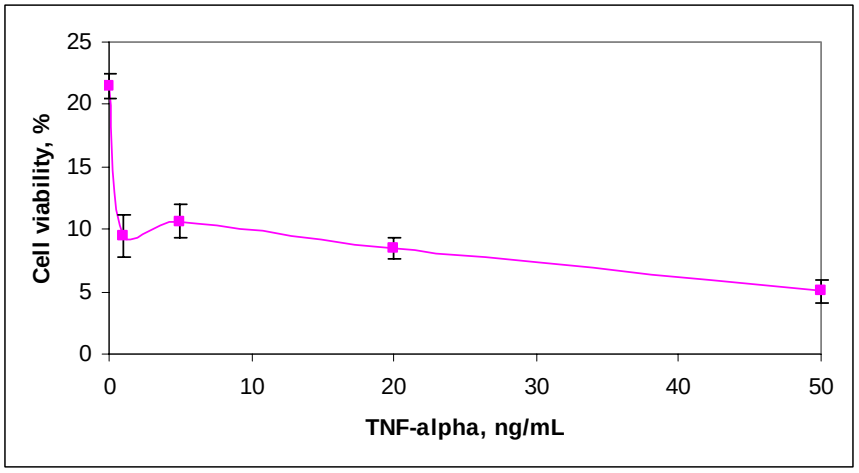

Figure 12. TNF Attenuates CEES Toxicity in Human Keratinocytes. HaCaT cells were treated with 1 mM CEES and various levels of TNF-alpha (simultaneously). Cell viability was measured by the CAM assay after 24 hours.

level of CEES and provides reproducible results with an IC_{50} of about 1 mM, which is in agreement with other studies [32-34]. Applying CEES directly in ethanol was less effective (than DMSO) at reducing cell viability and inducing cell death.

In order to determine if an addition of immuno-stimulators (LPS, PMA) and pro-inflammatory cytokines (TNF-α, IL-1β) increase CEES toxicity in immortalized HaCaT keratinocytes, we performed additional experiments with these cells exposed to various levels of CEES. None of these immuno-stimulators enhanced toxicity of CEES in NHEK keratinocytes as we reported previously for murine macrophages [5]. However, in proliferating HaCaT cells TNF-α did show a dose-dependent enhancement of CEES toxicity (**Figure 12)**, although LPS and IL-1β did not have any significant effect (data not shown)**.** The difference between NHEK and HaCaT cell reaction to the TNF-α treatment can be explained by the fact that HaCaT keratinocytes, unlike NHEK cells, proliferate continuously and do not undergo terminal differentiation. As a consequence, HaCaT cells are much more susceptible to the CEES/HD toxicity. The response of HaCaT cells to TNF-α is in agreement with our previous observations obtained with murine macrophages simultaneously exposed to CEES and various immuno-stimulators [5].

Using the direct CEES/DMSO application, we studied the cell death mechanisms in CCD 1106 KERTr keratinocytes. As a first step, we evaluated apoptosis as measured by the activation of caspase 3 activity in response to various levels of CEES after 24 hours (**Figure 13**). In this experiment CEES toxicity was relatively high, as we did not pre-mix the stock solution with media, but added it directly into a well which permits a transiently high local concentration of CEES/DMSO to exist before mixing is complete. We found that the low doses of CEES (50 - 100 μM) induced apoptosis but the higher doses did not. These data suggest that necrosis, rather than apoptosis, was the cause of cell death at the higher concentration. Staurosporin, a broad-spectrum kinase inhibitor, was used as a positive control since it is a well known caspase activator and apoptosis inducer.

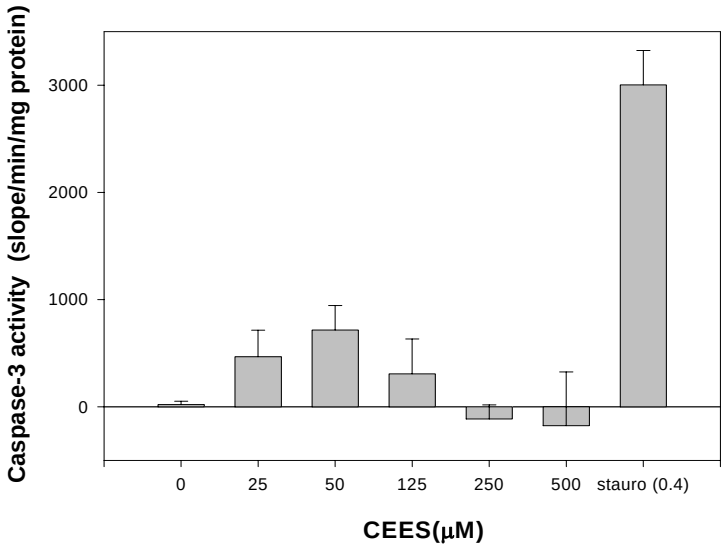

Figure 13. CEES-mediated Apoptosis in Human Keratinocytes. CEES (0.025 – 0.5 mM) was applied to CCD 1106 cells in a 96-well as a stock solution in DMSO. Apoptosis was measured after 24 hours as caspase-3 activity in cell lysates normalized to protein levels. Staurosporin (0.4 uM) was used as a positive control.

We next examined the time course for apoptosis at the low doses of CEES. As shown in **Figure 14,** we found that CEES induced activation of caspase 3 was maximal after 12 hours of incubation, which is in agreement with other reports regarding CEES or HD toxicity in human skin cells [29, 32, 35].

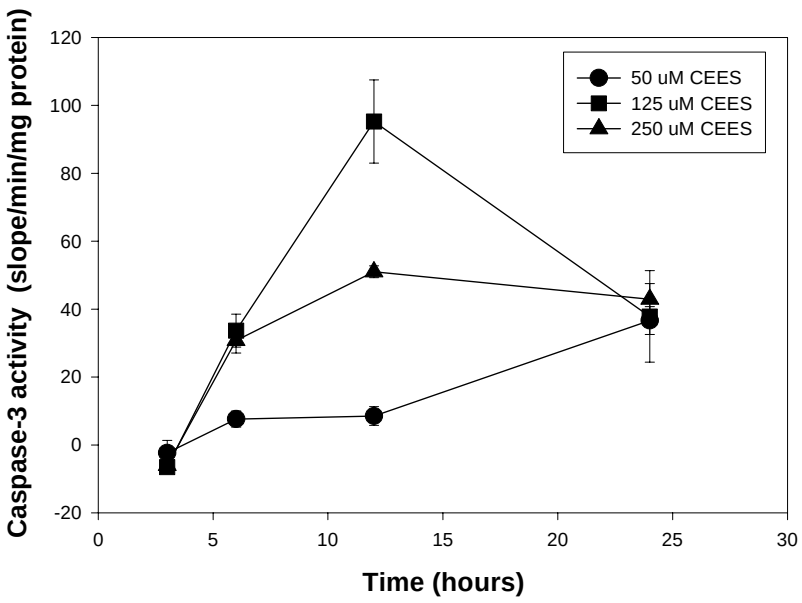

Figure 14. CEES-mediated Apoptosis in Human Keratinocytes. CEES (0.05 – 0.25 mM) was applied to CCD 1106 cells in a 96-well as a stock solution in DMSO. Apoptosis was measured after 24 hours as caspase-3 activity in cell lysates normalized to protein levels.

TASK 2 Determine the influence of CEES on various oxidative stress parameters

We monitored oxidative stress parameters in CEES/ethanol treated human keratinocytes. **Figure 15** shows the generation of intracellular superoxide anion (O_2*) in NHEK cells during 4 hours of incubation with 10 mM CEES. Superoxide levels were measured using specific fluorescent dye, dihydroethidium (HEt). Intracellular oxidation of HEt (measured as fluorescence of the product) reflects superoxide generation in cytoplasm. NHEK cells were loaded with 10 µM HEt for 1 h, then washed, and exposed to CEES. As was expected, 10 mM CEES induced high levels of superoxide production in NHEK cells. Interestingly, the production superoxide anion in NHEK cells appears to increase in a similar manner as CEES induced toxicity. HEt fluorescence increases with higher levels of CEES, whereas cell viability drops down (**Figure 15**). These data confirm that oxidative stress, and ROS generation in particular, is an important factor in CEES induced cell death.

We also measured intracellular production of hydrogen peroxide (H_2O_2) in CEES/ethanol treated NHEK cells (**Figure 16**). The cells were loaded with 20 µM dichloro-fluorescein diacetate (DCFH-DA) for 1 h, washed, and then exposed to CEES. In cytoplasm, DCFH-DA is rapidly being converted into dichlorofluorescein (DCFH) by esterases.

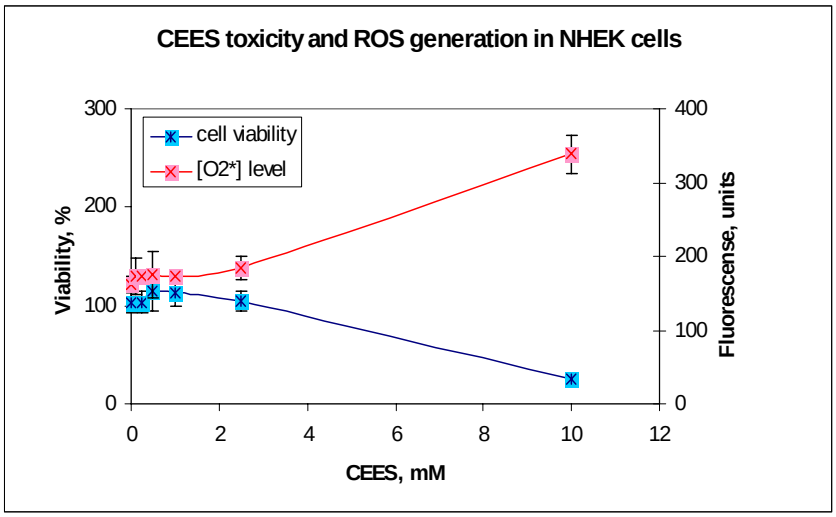

Figure 15. O_2* generation (measured as HEt intracellular oxidation) in NHEK cells after 4 h incubation was compared to CEES toxicity after 24 h. NHEK cells were loaded with 10 uM HEt for 1 h, washed by Hank's salt solution, and treated with CEES/ethanol. HEt oxidation was measured (end-point assay) as fluorescence at 360nm/410nm (ex./em.). Cell viability was measured as absorbance at 580nm (standard MTT assay).

H_2O_2 oxidizes DCFH yielding a highly fluorescent product. Surprisingly, CEES diminished hydrogen peroxide production in human keratinocytes. However, incubation of the cells with 50 µM H_2O_2 as a positive control did show an increase in intracellular levels of hydrogen peroxide (**data not shown**). We also explored if stimulation of the cells with LPS alter H_2O_2 production (**Figure 16**). HNEK cells stimulated with LPS showed similar response to CEES as non-stimulated cells.

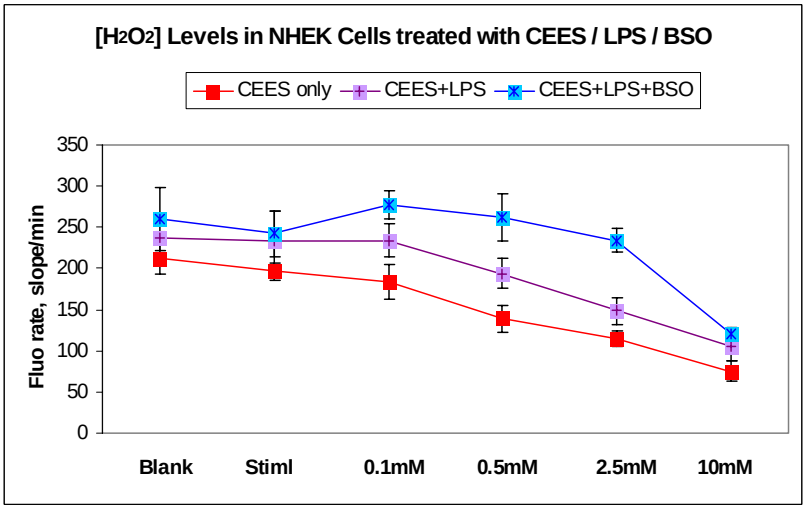

Figure 16. H_2O_2 generation (measured as DCFH-DA intracellular oxidation) in NHEK cells during 4 h incubation with CEES/ethanol. NHEK cells were loaded with 20 uM DCFH-DA for 1 h, washed by Hank's salt solution, and treated with CEES; or CEES and100 ug/mL LPS; or CEES and 100 ug/mL LPS, and 100 uM BSO (as indicated). DCFH-DA oxidation was continuously monitored (kinetic assay) as fluorescence at 485nm/520nm (ex./em.).

Pretreatment of the cells with buthionine-sulfoximine (BSO), which depletes intracellular GSH and thus alters CEES induced oxidative stress, slightly affected H_2O_2 production in LPS/CEES treated keratinocytes. However, DCFH-DA oxidation, in general, was still suppressed but not elevated in response to CEES treatments.

These results can be potentially explained by the fact that DCFH-DA also sensitive to intracellular NO. Previously, we have shown that CEES inhibits NO production in murine macrophages [5]. It is possible that a similar effect occurred in the human keratinocytes. Additional experiments to measure NO production in keratinocytes have also been performed.

Since CEES induces caspase-dependant apoptotic cell death in human keratinocytes it would be important to explore the relationship between apoptosis and oxidative stress in these cells. We stained HaCaT cells incubated with 2 mM CEES for 8 hours with carboxy-dichloroflurescin diaceatate (Car-DCFH DA), a membrane-permeable dye sensitive to reactive oxygen species (ROS) in the cytosol.

The cells were simultaneously stained with propidium iodide (PI), which is membrane-impermeable DNA sensitive dye capable of staining of nuclei of dead cells. **Figure 17B** shows cell death after CEES treatment as most of the nuclei are stained with PI; however, Car-DCFH DA staining did not reveal massive ROS production in these cells (**Figure 17A**). Figure 1C and D show a positive control: HaCaT cells incubated with 0.1 mM tert-butyl hydroperoxide (TBHP). In this case, Car-DCFH DA staining resulted in 4 fold higher fluorescence indicating massive generation of hydrogen peroxide and other ROS; however, cell survival was much greater in comparison with CEES treatment (**Figure 17C and D**, respectively). Although we did not detect oxidative stress changes in CEES treated keratinocytes in this experiment, we believe that the present data do not provide sufficient evidence to make a final conclusion. We will repeat similar experiments using other markers of oxidative stress, such as dihydroxyethidium and dihydrorhodamine 123.

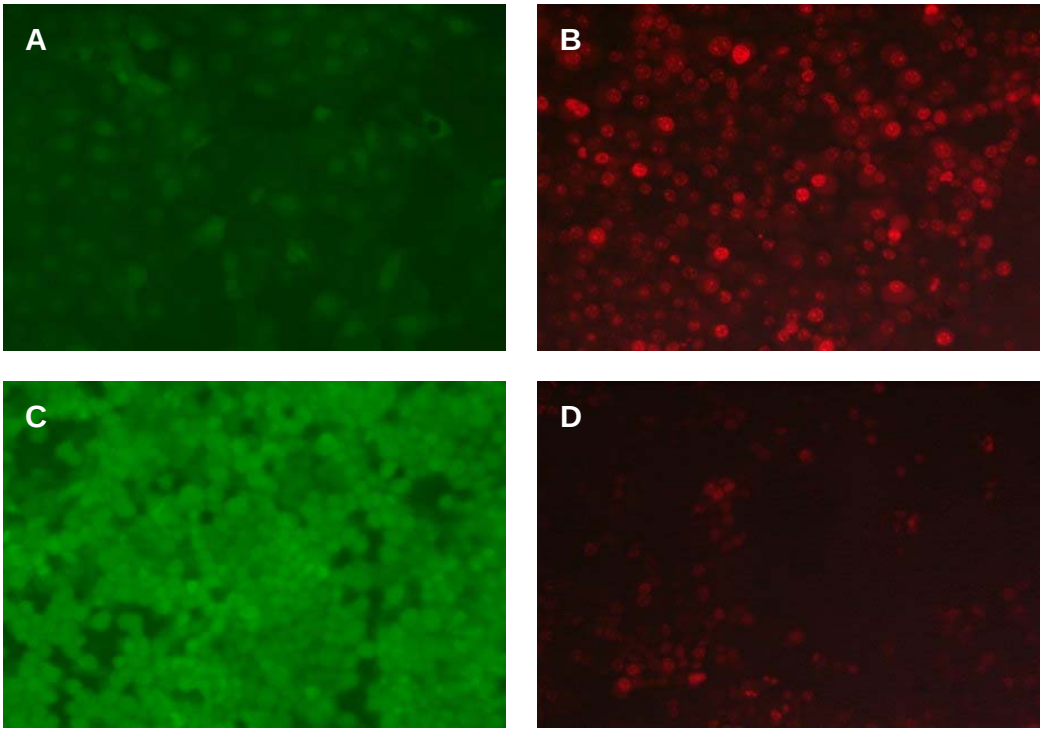

Figure 17. Oxidative Stress in Human Keratinocytes. HaCaT cells were incubated with 2 mM CEES (A, B) or 0.1 mM TBHP (C,D) for 8 hours in a 96-well plate. Oxidative stress was monitored by Car-DCFH DA staining (green fluorescence, on the left); cell death was monitored by PI staining (red fluorescence, on the right) under fluorescent microscope.

Although the direct measurement of ROS generation during CEES treatment was not yet successful in our experiments, we found indirect evidence for oxidative stress related changes in the experiments presented in the **Figure 18**. It is known that HD/CEES toxicity is associated with glutathione depletion, which is the major cytosolic antioxidant. Such depletion greatly reduces anti-oxidative potential of the cell, making it susceptible even to moderate oxidative changes. In order to explore the sensitivity of CEES treated cells to exogenous oxidative stimuli we examined CEES mediated toxicity in the presence or absence of TBHP, an agent promoting massive intracellular ROS generation.

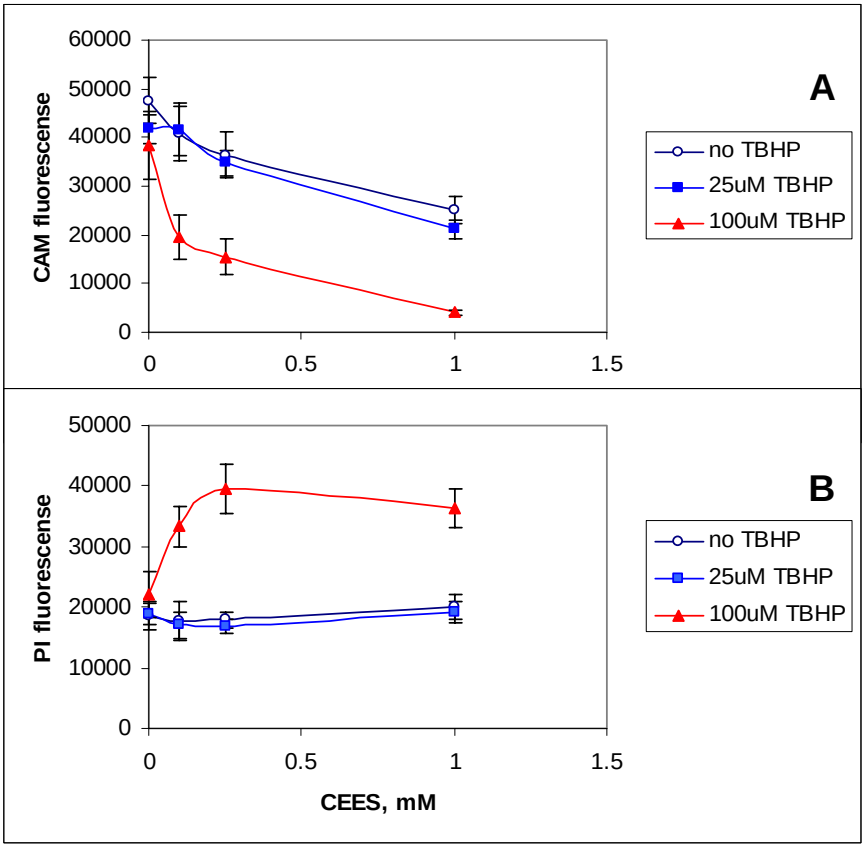

Figure 18. Oxidative Stress Enhances CEES Toxicity in Human Keratinocytes. HaCaT cells were incubated with CEES (as indicated) in the presence or absence of 25µM or 100 µM TBHP for 24 hours in a 96-well plate. Cell viability was monitored by calcein AM (CAM) staining (panel A), cell death was monitored by PI staining (panel B).

Interestingly, non-toxic doses of TBHP (up to 0.1 mM) significantly increased the toxic effect of CEES as measured via calcein AM (CAM) and PI staining (**Figure 18A and 18B**, respectively). CAM is a fluorescent marker of viable cells, whereas PI is a marker of dead cells. The data obtained with CAM staining were also confirmed with the MTT cell viability assay (data not shown). This effect of CEES is similar to our earlier observation in murine macrophages, where lipopolysaccaride (LPS) enhanced toxicity of the CEES. LPS is a potent inducer of oxidative stress in immune cells [5]. We believe that CEES mediated sensitivity to oxidative stress is important in HD/CEES toxicity *in vivo*.

Whether CEES directly induces ROS generation in keratinocytes is still unclear. We cannot find any evidence of such effect in the literature. However, HD is well known to induce ROS generation in endothelial and immune cells [36, 37]. Thus, oxidative stress may occur *in vivo* as a result of immune cell attack in response to keratinocyte-derived pro-inflammatory cytokines, such as TNF-α [9].

We also performed a series of experiments in order to monitor oxidative stress related changes in HaCaT keratinocytes treated with CEES. Using fluorescent dyes CMAC (7-amino-4-chloromethylcoumarin) and CMF-DA (5-chloromethylfluorescein diacetate) [42]

we attempted to compare intracellular GSH levels (CMAC staining) or levels of non-protein cellular thiols (CMF-DA staining) in keratinocytes treated for 16 h with 1) 1% DMSO (vehicle), 2) 2mM CEES, 3) 2mM CEES + 10mM NAC, 4) 0.1mM TBHP (tert-butyl hydroperoxide – oxidative stress positive control).

Figure 19 shows HaCaT cells stained with GSH-sensitive CMAC dye (*blue squares*), thiol-sensitive CMF-DA staining (*green squares*) and dead cells stained by PI (*red squares*) as examined under fluorescent microscope. Surprisingly, both GSH and thiol-sensitive dyes revealed that CEES-treated keratinocytes are not completely depleted of cellular thiols (*green*) and GSH in particular (*blue*) compared to TBHP-treated cells; although PI staining confirmed toxic effect for both CEES and TBHP treated cells (*red*). As expected NAC treatment increased thiol levels (*blue and green*) and viability (*red*) of CEES treated keratinocytes. These data are in agreement with our observation reported above showing as no free radical generation (carboxy-dichlorofluorescin diacetate (carDCFH-DA) staining) in CEES treated HaCaT cells after 8 hours. Combined together these findings suggest that oxidative stress in keratinocytes might be a relatively late event, which starts within 12-24 hours postexposure. At that time in HD-treated cells, cytokine release [9, 43] is maximal and the cell death pathway is being switched from apoptosis to necrosis [44].

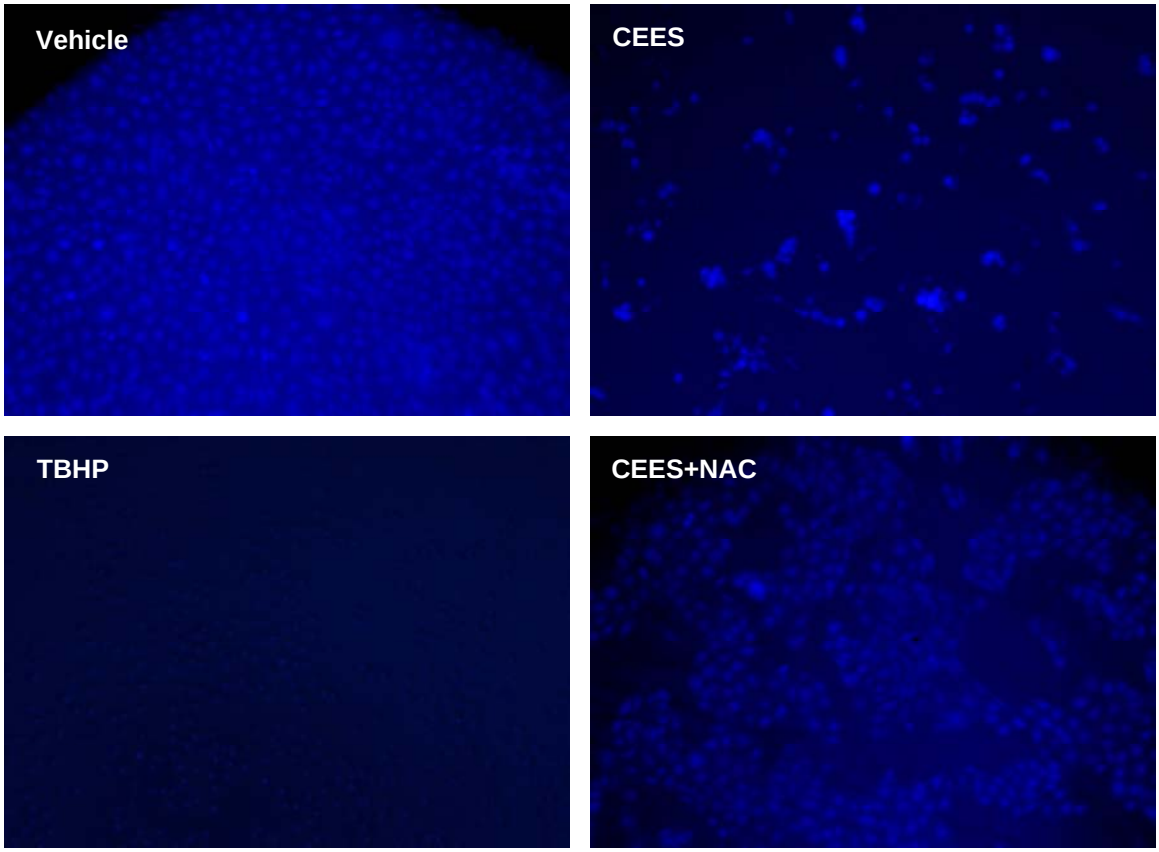

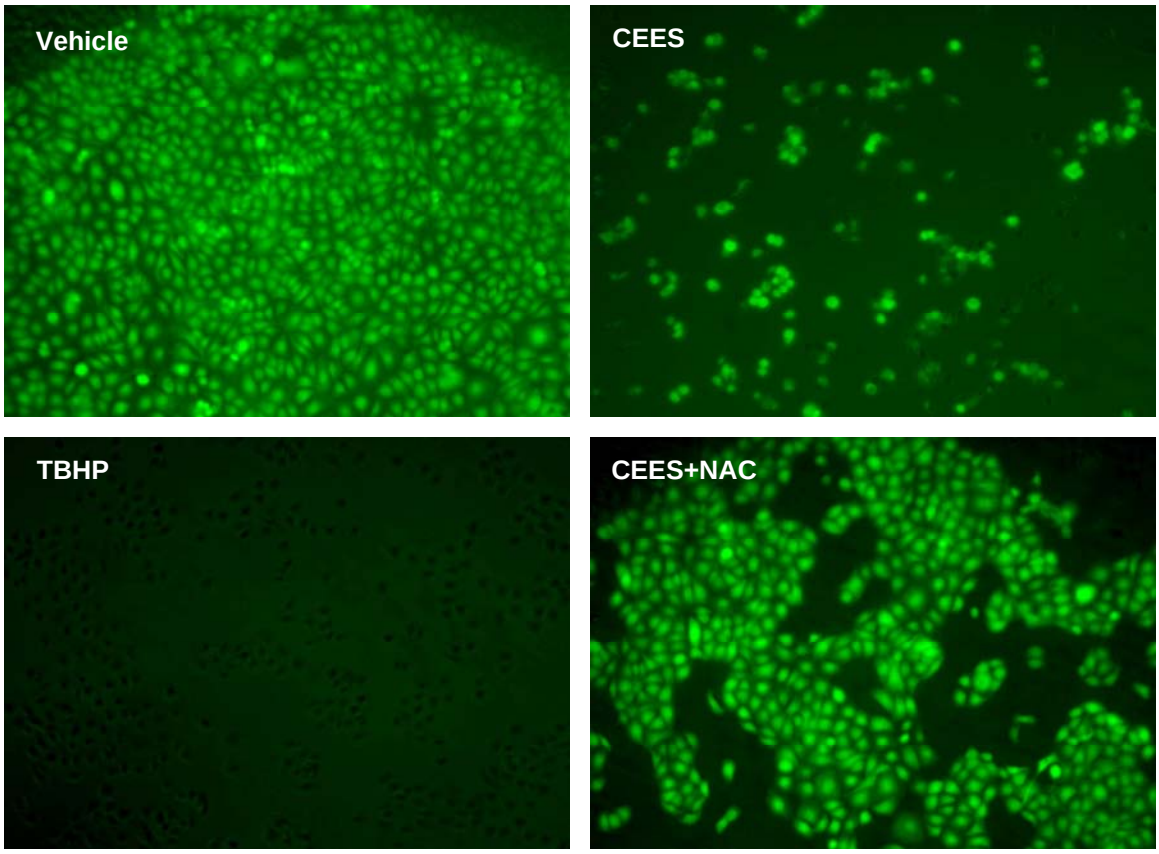
Vehicle
CEES
TBHP
CEES+NAC

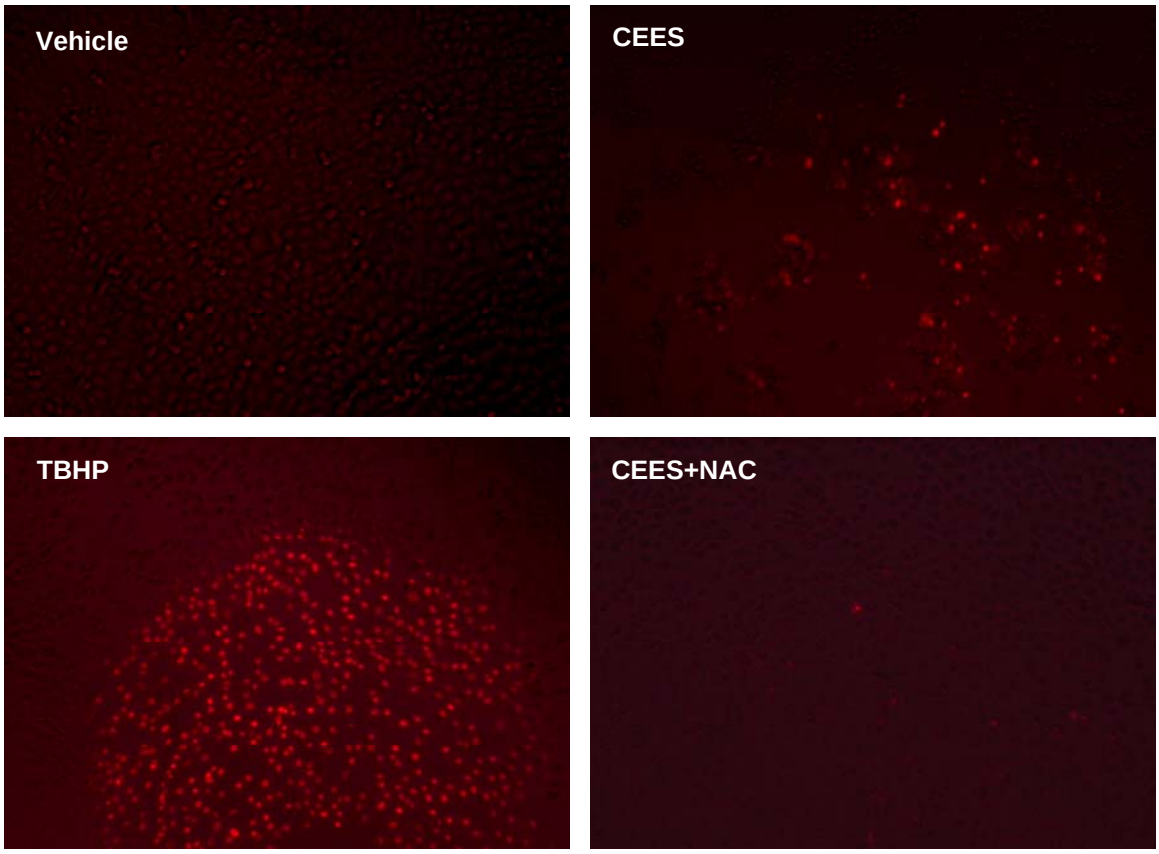

Figure 19. Oxidative stress related changes in human keratinocytes. HaCaT cells were incubated with 1% DMSO (vehicle), or 2 mM CEES, or 2mM CEES and 10mM NAC, or 0.1mM TBHP (as indicated) for 18 hours. Intracellular GSH levels were examined under a fluorescent microscope using 20 µM CMAC (*blue*); levels of non-protein cellular thiols were monitored using 20 µM CMF-DA (*green)* cell death was monitored by 2µM PI (*red*).

Another indirect evidence for the role of oxidative stress in HD/CEES toxicity is the protective effect of NAC. This potent antioxidant is capable of restoring intracellular GSH level, and has already been shown to be protective against CEES toxicity *in vivo* [38]. We have extensively studied the effect of NAC in CEES treated human keratinocytes. Using two independent caspase-3 assays we have shown that NAC effectively down-regulates CEES induced apoptosis in HaCaT cells. NAC (10 mM) reduces caspase-3 activity after 12 hour incubation (**Figure 20**). Caspase 3 activity was measured in cell lysates using the fluorescent substrate peptido (DEVD)-7-Amino-4-trifluoromethylcoumarin (DEVD-AFC) and normalized to the total cellular protein. We also performed Live Cell NucView 488 Caspase 3 assay, which allows detection of active caspase-3 in living cells. NucView 488 Caspase 3 substrate permeates the cell and undergoes specific enzymatic cleavage by caspase-3; the product is fluorescent and binds nuclear DNA. Thus, this method not only marks viable cells with activated caspase-3, but also reveals chromatin condensation in the apoptotic nuclei.

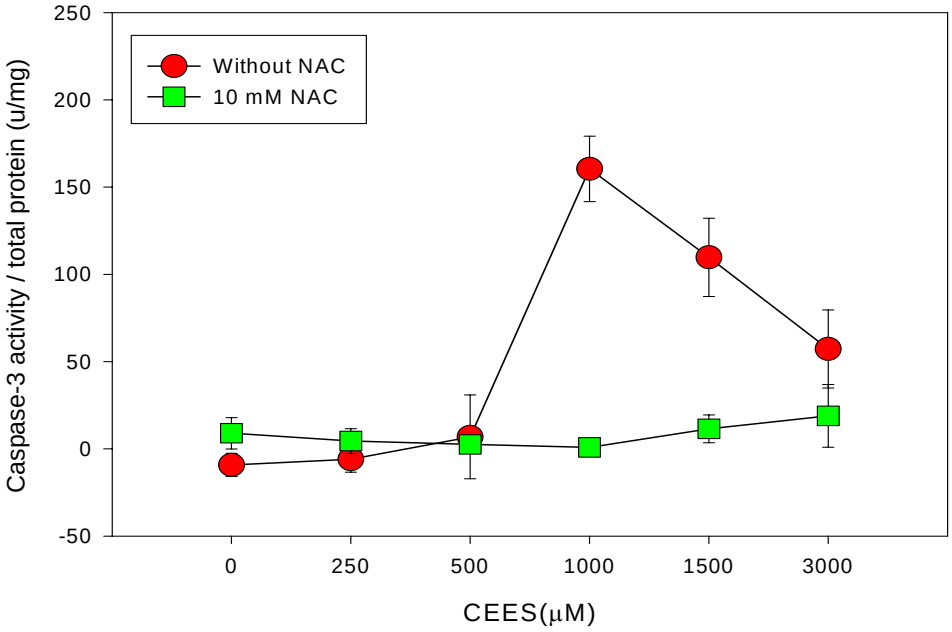

Figure 20. NAC Effect on CEES Induced Apoptosis in Human Keratinocytes. HaCaT cells were incubated with CEES (as indicated) in the presence or absence of 10 mM NAC for 24 h. Caspase-3 activity was measured in the cell lysates using DEVD-AFC substrate and normalized to the total protein.

Figure 21 shows CEES induced apoptosis in human keratinocytes. CEES (2 mM) promoted intensive green staining in HaCaT cells after 18 hours (**Figure 21C**); whereas similar incubation with 1% DMSO (vehicle) had no effect (**Figure 21A**). The green background reflects a phase-contrast view of the cells, which was merged with the fluorescent image. **Figure 21B and 21D** show positive (5 μM staurosporine) and negative controls (5 μM staurosporine with caspase-3 inhibitor), respectively.

Figure 22 shows the protective effect of NAC against CEES induced apoptosis in human keratinocytes. **Figure 22A and 22B** display CEES induced caspase-3 activation after 18 hours. Green fluorescence marks caspase-cleaved fluorescent product as it stains apoptotic nuclei; blue fluorescence (DAPI) stains nuclei of apoptotic cells. Markers at the pictures point to nuclei with clear visible chromatin condensation. Although NAC does not completely prevent CEES induced apoptosis (**Figure 22C and 22D**), it reduces the number of apoptotic cells as it can be seen with intense DAPI staining. Phase-contrast images of the same cells revealed dense confluent cell layers for both CEES and CEES/NAC treatments (not shown).

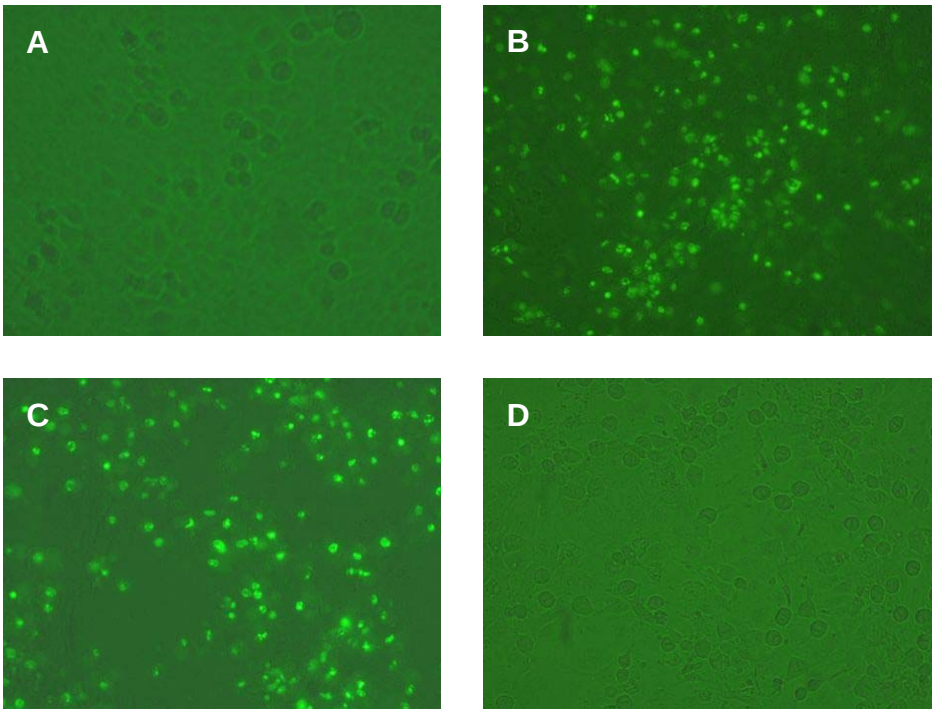

Figure 21. CEES-induced Apoptosis in Human Keratinocytes. HaCaT cells were incubated with vehicle (A), or 5µM staursporine (B), or 2 mM CEES (C), or 5µM staursporine with caspase-3 inhibitor (D) for 18 h. Caspase-3 activity was monitored using Live Cell NucView 488 Caspase-3 assay kit under fluorescent microscope.

We also measured the protective effect of NAC quantitatively using the MTT assay. **Figure 23A** shows that 5 mM NAC significantly increased cell viability if applied simultaneously with 2mM CEES. **Figure 23B** shows the increased cell viability of CEES treated keratinocytes as a function of NAC concentration. Notably, neither pre-treatment nor post-treatment of the CEES treated HaCaT cells with 10 mM NAC (cells were incubated 5 hours prior or after the CEES application) had any protective effect (data not shown).

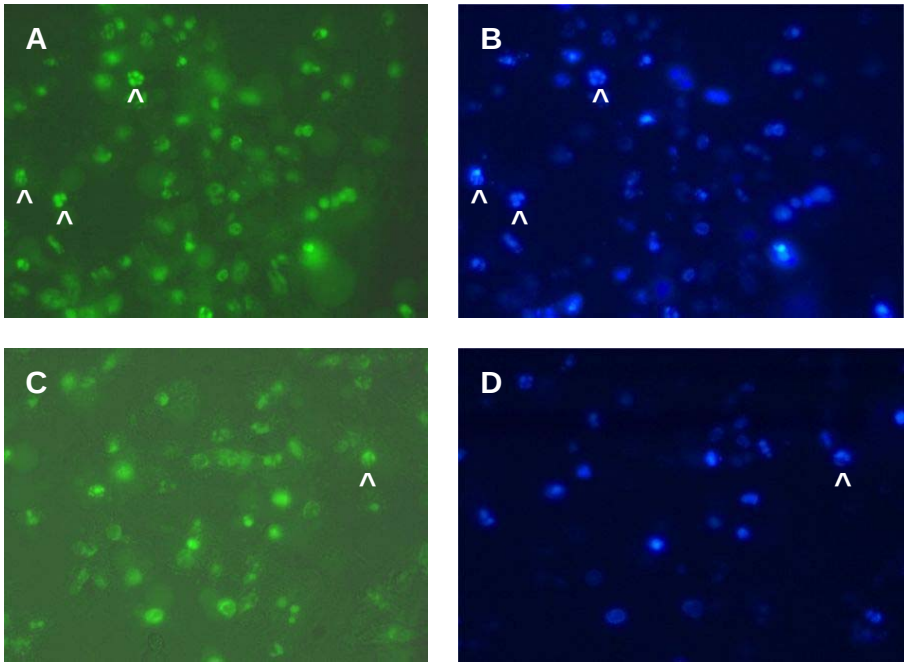

Figure 22. NAC Protects against CEES-induced Apoptosis in Human Keratinocytes. HaCaT cells were incubated with 2 mM CEES in the absence (A, B) or presence (C, D) of 10 mM NAC for 18 h. Caspase-3 activity was monitored using Live Cell NucView 488 Caspase-3 assay kit (green, left panels) under fluorescent microscope. Excessive DAPI staining (blue, right panels) shows apoptotic nuclei. Markers point to apoptotic nuclei with condensed chromatin.

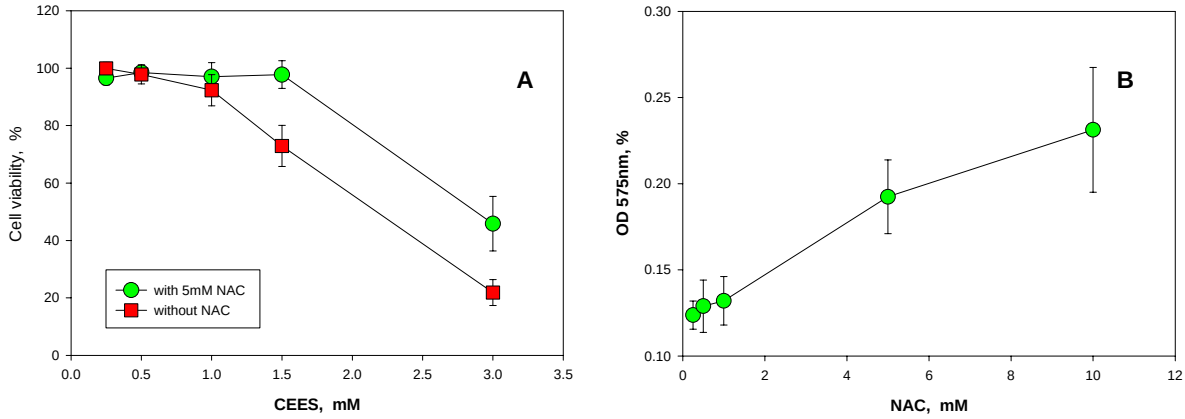

Figure 23. NAC Protects against CEES-induced Toxicity in Human Keratinocytes. HaCaT cells were incubated with CEES (as indicated) in the absence or presence of 5 mM NAC (panel A). HaCaT cells were incubated with 2 mM CEES in the presence of NAC (as indicated) (panel B). NAC was added to the media immediately after the CEES application. Cell viability was measured via standard MTT assay after 24 hours.

Task 4- The effectiveness of topical application of the optimal antioxidant liposome formulations

We performed experiments with four different types of antioxidant liposomes in order to test their protective abilities against CEES toxicity. **Figure 24** shows the effect of NAC/T-liposomes on NHEK cell viability when incubated for 24 hours with 10 mM CEES applied as a stock solution in ethanol. Interestingly, NAC/T-liposomes were not only protective, but also stimulated proliferation of NHEK cells both in the presence and in the absence of CEES. Blank liposomes not containing antioxidants did not show any protective effect, as was expected.

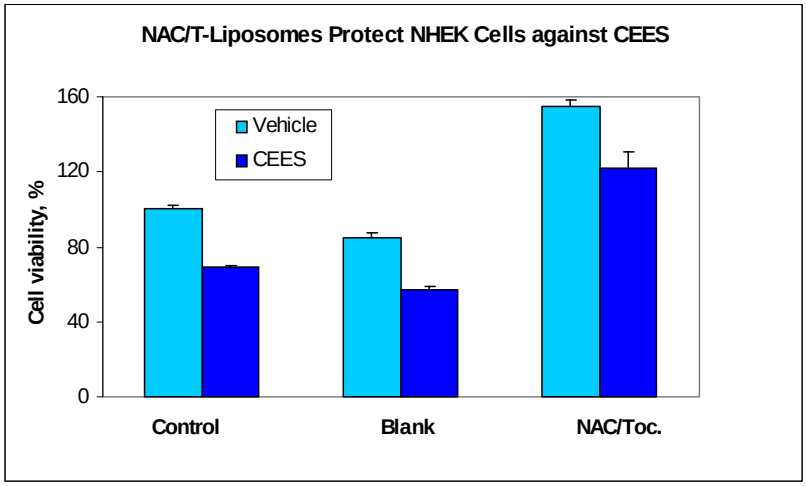

Figure 24. Protecting effect of NAC/T-liposomes (NAC/Toc) was compared to the effect of Blank liposomes (Blank) on NHEK cells treated with 10 mM CEES for 24 h. CEES was applied as a stock solution in ethanol. Control: cells treated with ethanol or CEES in the absence of liposomes. Cell viability was measured as absorbance at 580nm (standard MTT assay).

Figure 25 illustrates the influence of Blank liposomes, G-liposomes, G/T-liposomes, or T-liposomes on NHEK cell growth inhibition after 48 hr of incubation with 10 mM CEES/ethanol. After 48 hours blank-liposomes were not protective against CEES (67%) and decreased cell viability to 69% without CEES; GSH containing liposomes were also not protective against CEES (71%) and decreased cell viability to 71% without CEES; alpha-tocopherol containing liposomes were also not protective against CEES (72%) and decreased cell

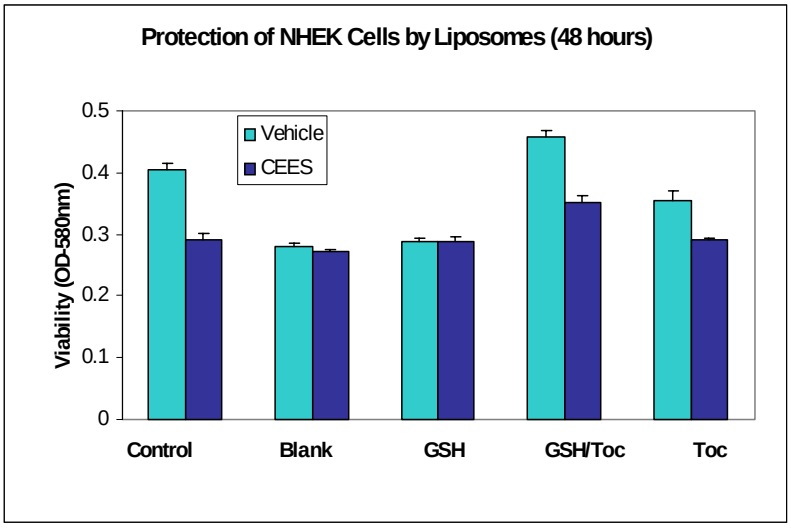

Figure 25. Protecting effect of antioxidant liposomes in NHEK cells treated with 10 mM CEES/ethanol for 48 hours. Control: cells treated with ethanol or CEES in the absence of liposomes; Blank: Blank liposomes; GSH: G-liposomes; GSH/Toc: G/T-liposomes; Toc: T-liposomes. Cell viability was measured as absorbance at 580 nm (standard MTT assay).

viability to 88% without CEES; only liposomes containing both GSH and alpha-tocopherol were protective against CEES (87%) and increased cell proliferation without CEES to 113%.

Interestingly, antioxidant liposomes not only showed protective effect against CEES-induced cell damage in keratinocytes, but also stimulate the cell growth and proliferation.

Using CEES/DMSO application, we tested five different types of antioxidant liposomes (see **Table 1**) for their ability to inhibit CEES toxicity in HaCaT keratinocytes. The liposomal formulations were: (1) **Blank liposomes** (no water- or lipid-soluble antioxidants); (2) glutathione containing **GSH-liposomes** (75 mM GSH); (3) alpha-tocopherol containing **AT-liposomes** (3.33 mM alpha-tocopherol); (4) alpha-tocopherol and GSH containing **GSH/T-liposomes** (3.33 mM alpha-tocopherol with 75 mM GSH); (5) alpha-tocopherol, gamma-tocopherol and NAC containing **NAC/T-liposomes** (3.1 mM alpha-tocopherol, 3.1 mM gamma-tocopherol with 75 mM NAC).

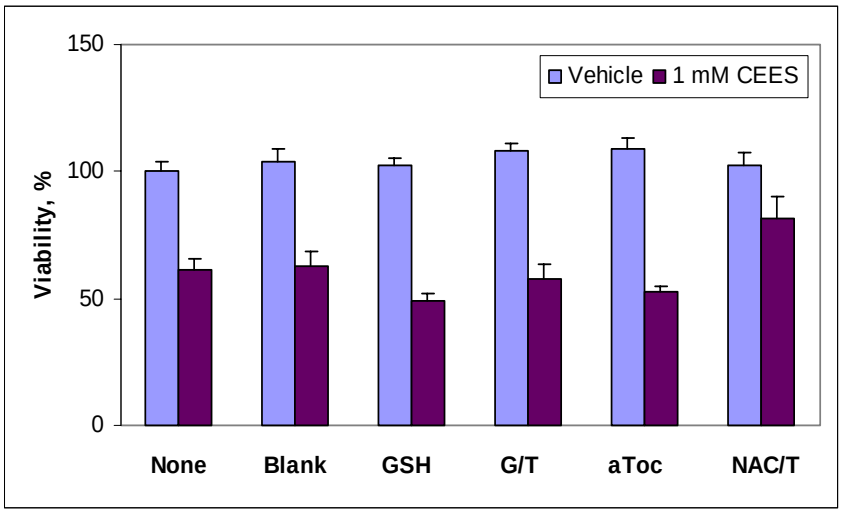

Figure 26. Antioxidant Liposome Protection against CEES Toxicity. CEES (1 mM) was applied as a stock solution in DMSO pre-mixed with media. Various liposomes were added immediately after the CEES application. Cell viability was measured by the MTT assay after 24 hours. **None:** cells treated with DMSO or CEES in the absence of liposomes; **Blank:** Blank liposomes; **GSH:** GSH-liposomes; **GSH/T:** GSH/alpha-tocopherol-liposomes; **AT:** alpha-tocopherol-liposomes; **NAC/T:** NAC/alpha-tocopherol-liposomes.

Figure 26 shows that the NAC/T liposomes partially prevented 1mM CEES-induced loss of cell viability, as measured by an MTT assay, whereas none of the other liposomal formulations were effective.

We later examined the protective abilities of NAC-containing liposomes against CEES toxicity in a series of separate experiments. We treated HaCaT cells with CEES and antioxidant liposomes simultaneously. **Figure 27** shows a protective effect of various concentrations of **NAC-liposomes** in comparison with blank liposomes in HaCaT cells. Both cell proliferation ability (CAM assay) and cell death (PI assay) were monitored after 24 hour of incubation with 2 mM CEES/DMSO. **NAC-liposomes (NL)** showed

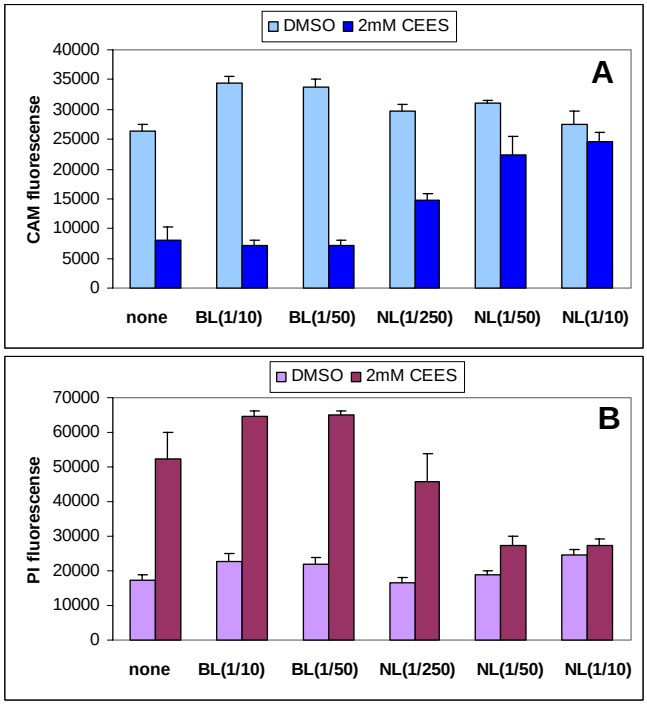

Figure 27. NAC Liposomes Protect against CEES-induced Toxicity in Human Keratinocytes. HaCaT cells were treated with 2 mM CEES; NAC liposomes (NL) or Blank liposomes (BL) were added simultaneously with CEES. Cell viability was monitored by CAM staining (panel A), cell death was monitored by PI staining (panel B) after 24 hours. None: cells treated with DMSO or CEES in the absence of liposomes; numbers show final dilutions of the liposomes.

a protective effect in HaCaT keratinocytes treated with CEES, which was dose-dependent. **Blank liposomes (BL)** made with lipids only (negative control) showed no protection, as expected. Liposome samples were diluted in media as indicated. Dilutions of 1:10, 1:50, and 1:250 gave 7.5 mM, 1.5 mM, and 0.3 mM final concentrations of NAC, respectively.

These data are particularly encouraging since they fully support our hypothesis that CEES (and HD) pathophysiology is mediated, at least in part, by oxidative stress and that antioxidant-liposomes represent an effective counter measure.

In addition, we found that mitochondria substrates, such as such as pyruvates, can be protective against CEES/HD mediated oxidative stress and cell death. A number of studies have shown that mitochondria substrates, attenuate mitochondria dysfunction and prevent cell death in various types of human cells exposed to alkylating agents, such as nitrogen mustard and N-methyl-N'-nitro-N-nitrosoguanidine (MNNG), chemical analogs of HD used as anti-cancer drugs[39-41]. Therefore, we initiated a series of experiments aimed to explore the possible protective effect of pyruvates (methyl pyruvate and ethyl pyruvate) on HaCaT keratinocytes exposed to HD.

Figure 28 shows the protective effect of methyl pyruvate (Panel A) or ethyl pyruvate (Panel B) in HaCaT cells exposed to 2 mM CEES or vehicle (DMSO). Hank's Balanced

Salt Solution (Sigma) supplied with 5% FBS was used instead of media in order to avoid pyruvate presence (Keratinocyte Media from Sigma, GibCo, or Cambrex contain 0.5 mM sodium pyruvate). The results revealed that simultaneous application of CEES and a low level of pyruvate (0.2 – 2 mM) could reduce the toxicity of CEES both in assays measuring cell viability (CAM assay) and the ones monitoring cell death (PI assay). These results will be further re-evaluated in order to find an optimal pyruvate concentration and possibly formulate antioxidant liposomes containing pyruvate for studies in the EpiDerm™ human skin model.

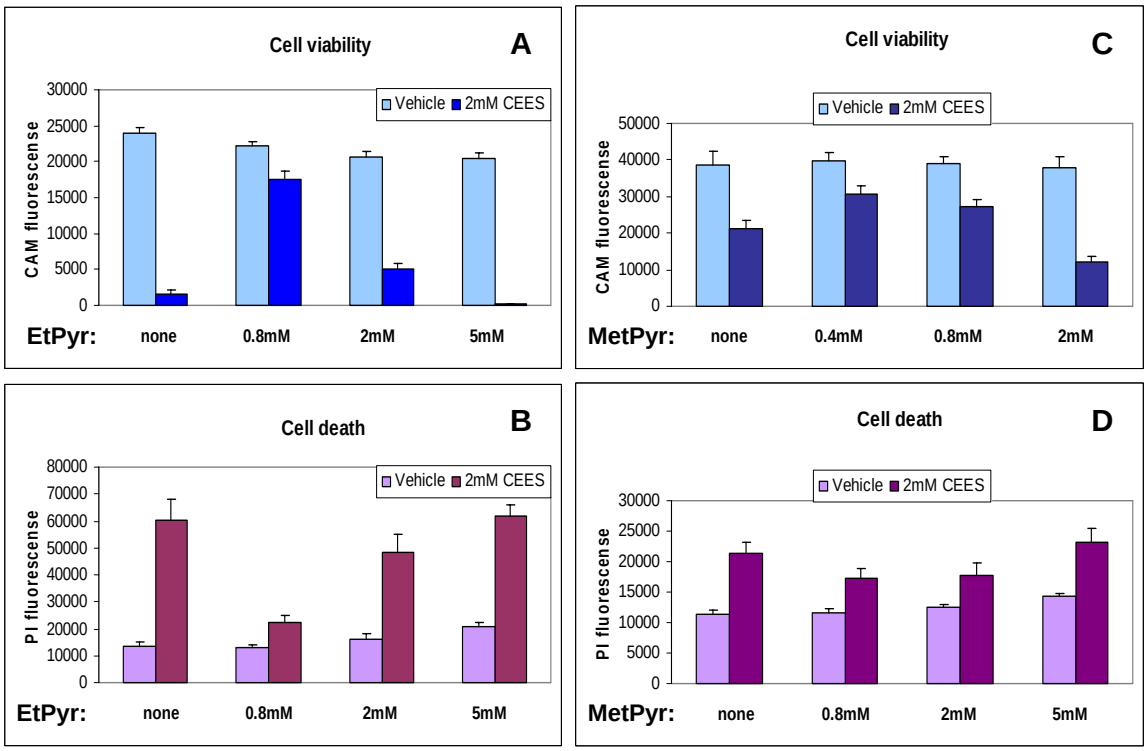

Figure 28. Alkyl Pyruvates Protect against CEES-induced Cell Death in Keratinocytes. HaCaT cells were incubated with 2 mM CEES or vehicle (DMSO) in the absence (none) or presence of methyl pyruvate (MetPyr; Panels A, B) or ethyl pyruvate (EtPyr; Panels C, D) (as indicated) for 24 h. Cell viability was monitored via CAM fluorescent staining; cell death was monitored via PI fluorescent staining.

We next carried out a series of experiments aimed to compare protective effects of various antioxidants in CEES-treated HaCaT cells. We compared the effects of 10mM N-acetylcysteine (NAC), 2mM ethyl pyruvate (EtPyr) and 0.1mM α-tocopherol (AT). Hank's Balansed Salt Solution (Sigma) supplied with 5% FBS was used instead of media as Keratinocyte Media from Sigma, GibCo, or Cambrex contain 0.5 mM sodium pyruvate.

Figure 29 shows that neither of the antioxidants had any protective effect on HaCaT keratinocytes treated with 2mM CEES in Hank's / FBS solution. However, our previous data showed that NAC does have a protective effect in CEES-treated HaCaT cells if used in the Keratinocyte Medium (Sigma). We have repeated the above described experiment

using the Keratinocyte Medium (**Figure 30**). As expected we were able to register the protective effect of NAC, however EtPyr and AT were still not protective. The fact that NAC was protective only in pyruvate containing medium possibly can be explained by combined effect of NAC and pyruvate. Notably, it has been shown earlier by other investigators that HD treated human cell lines undergo both apoptosis and necrosis, and NAC protects only from apoptotic cell death [45]. Thus, NAC would poorly protect keratinocytes if majority of the cells undergo necrosis, but would be protective when pyruvate switches the cell death pathway to apoptosis (see below). In case of lipophilic EtPyr and tocopherols we expect more protection with the liposome encapsulation of these agents. We will compare liposome-encapsulated antioxidants to the non-encapsulated agents in our future experiments.

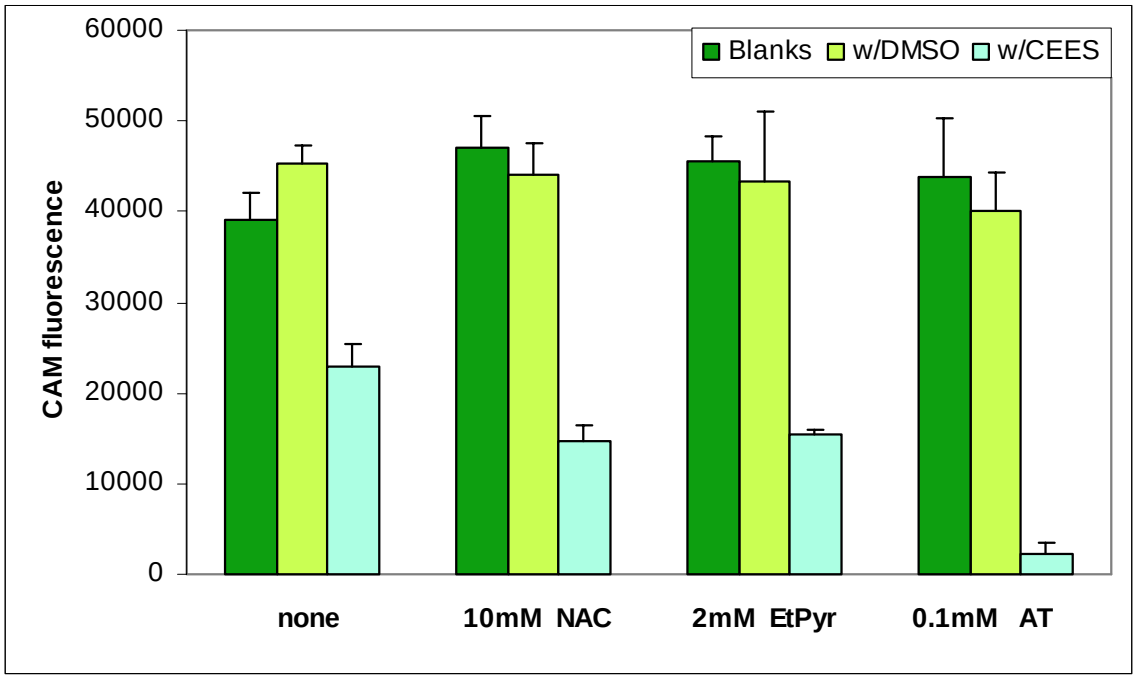

Figure 29. Antioxidant effects in human keratinocytes (CEES/Hank's). HaCaT cells were incubated in a 96-well plate with various antioxidants (as indicated) in **Hank's/FBS solution** (Blanks), with 1% DMSO (vehicle), or 2 mM CEES (as indicated) for 24 hours. Cell viability was monitored by 2μM CAM staining for 30 min using a fluorescent plate reader.

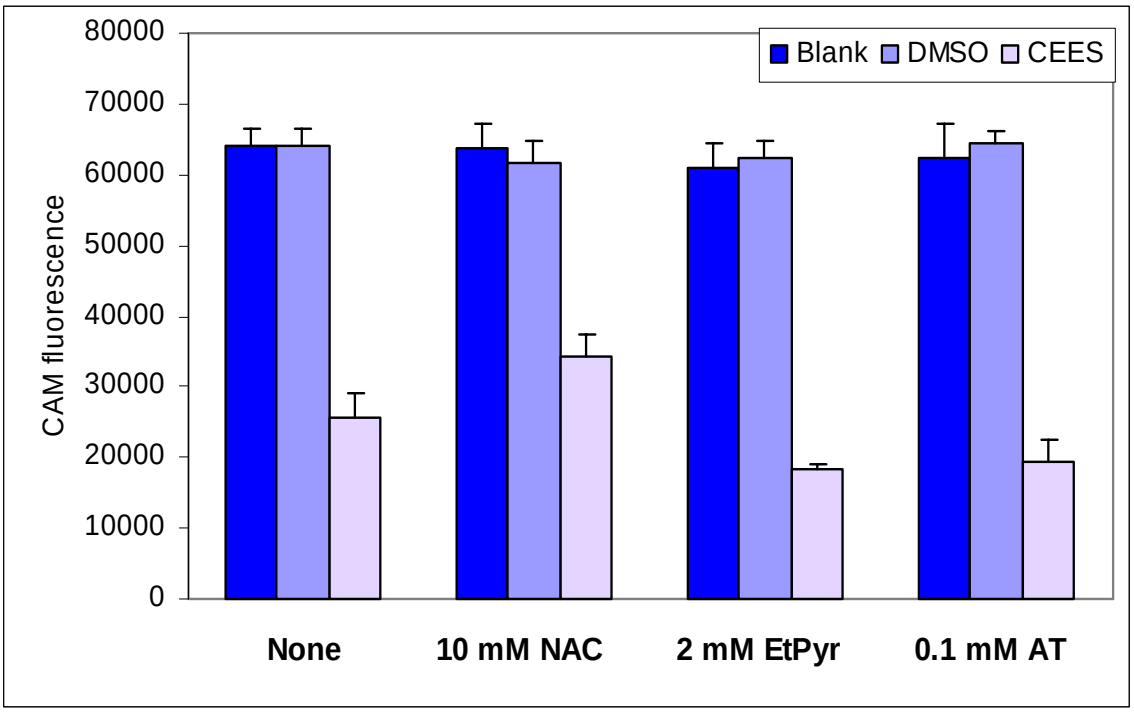

Figure 30. Antioxidant effects in human keratinocytes (CEES/Medium).). HaCaT cells were incubated in a 96-well plate with various antioxidants (as indicated) in **Keratinocyte Medium** (Blanks), with 1% DMSO (vehicle), or 2 mM CEES (as indicated) for 24 hours. Cell viability was monitored by 2μM CAM staining for 30 min using a fluorescent plate reader.

We continued experiments aimed at comparing the protective effects of various antioxidants in CEES-treated HaCaT cells. We also compared the effects of free antioxidants to the effects of liposome-encapsulated antioxidants. **Figure 31** shows the protective effects of 5 mM water-soluble antioxidants (NAC, GSH) or 50 μM lipophilic antioxidants (ALA, α-Toc, γ-Toc) in HaCaT keratinocytes treated with 1 mM CEES. As expected, both NAC and GSH increased cell viability as measured by the Alamar Blue fluorescence. GSH was the most protective as it increased cell viability from 28% up to 65%. Neither of the lipophilic antioxidants was protective. This fact can be explained by low solubility of these lipids in the tissue culture medium (lipophilic antioxidants were diluted in fresh media from EtOH stock solutions). Next, we explored the response of CEES-treated keratinocytes to various levels of GSH and NAC in media. **Figure 32** shows increase of the protective effect of GSH in dependence upon its concentration. Similar experiment with NAC had been done earlier (see Progress during second year).

In the following experiments, we compared the effects of free GSH or NAC to the effects of these antioxidants encapsulated in liposomes. **Figure 33** shows the protective effect of various levels of liposome-encapsulated GSH. **Figure 34** shows the same experiments done with liposome-encapsulated NAC. Both NAC and GSH established protection in HaCaT cells treated with 1 mM CEES, however, GSH was more effective at lower levels. Thus, 4 mM encapsulated GSH was as effective as 10 mM encapsulated NAC, but much more effective than 4 mM NAC. Surprisingly, 10 mM encapsulated GSH did not show any protection. This particular result is questionable as 10 mM non-encapsulated GSH was

protective (**Figure 32**). We believe that this result reflects statistical error as in many similar experiments, especially with EpiDerm tissues, 10 mM GSH showed highest protection (see below).

We also performed a series of experiments in order to find dose-response of the CEES-treated keratinocytes to both free and liposomal lipophilic antioxidants (ALA, α-Toc, γ-Toc). Unfortunately, neither free (diluted in fresh media from EtOH stock solutions) nor liposomal form of these lipid antioxidants did not establish any protective effect (**data not shown**). We also explored if a lipophilic antioxidant α-tocopherol would be protective if combined with 5 mM GSH (non-encapsulated). The experiment described in **Figure 35** shows that the presence of α-tocopherol does not increase the protective effect of free GSH. We suspect that the presence of tocopherols in the medium might quench fluorescence of Alamar Blue product and therefore affect the result of this experiment. This experiment also will be re-evaluated in future using the MTT assay.

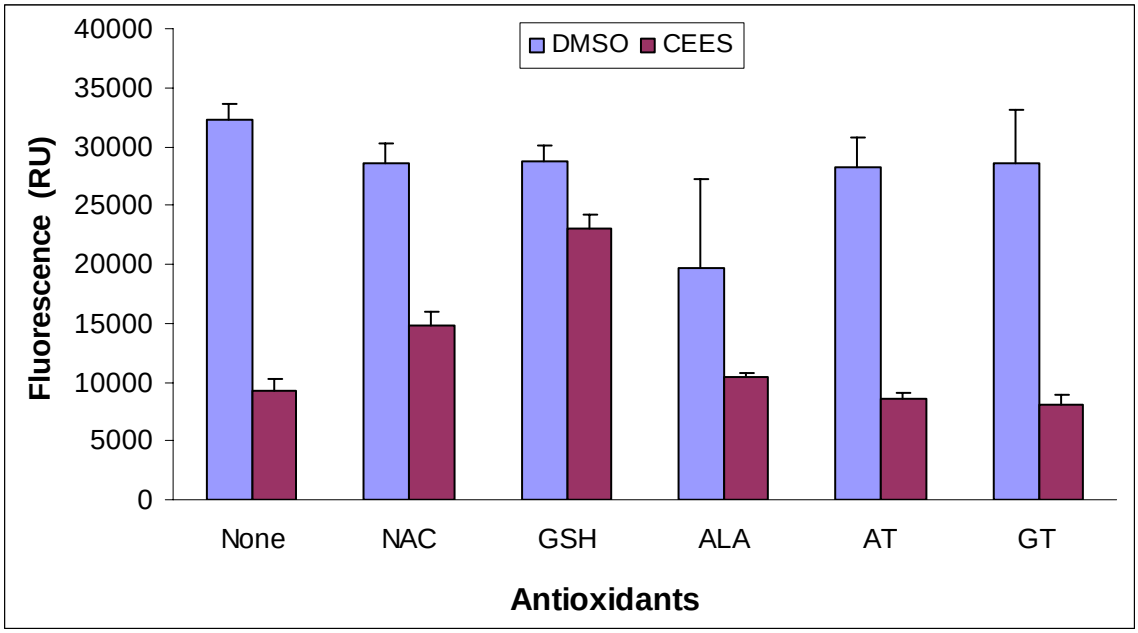

Figure 31. Protective effects of free antioxidants in human keratinocytes. HaCaT cells were incubated in a 96-well plate with various antioxidants (as indicated) applied simultaneously with 1% DMSO (vehicle), or 1 mM CEES (as indicated) for 20 hours. Cell viability was monitored by 5% Alamar Blue after 2 h using a fluorescent plate reader.

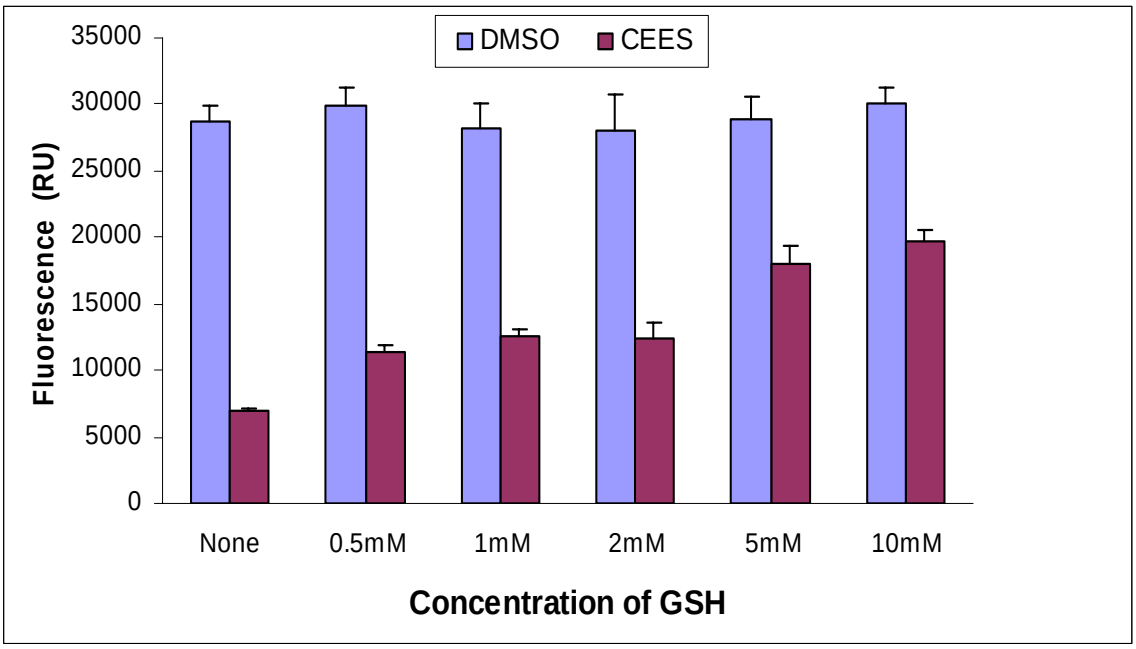

Figure 32. Protective effect of free GSH in human keratinocytes. HaCaT cells were incubated in a 96-well plate with various levels of GSH (as indicated) applied simultaneously with 1% DMSO (vehicle), or 1 mM CEES (as indicated) for 20 hours. Cell viability was monitored by 5% Alamar Blue after 2 h using a fluorescent plate reader.

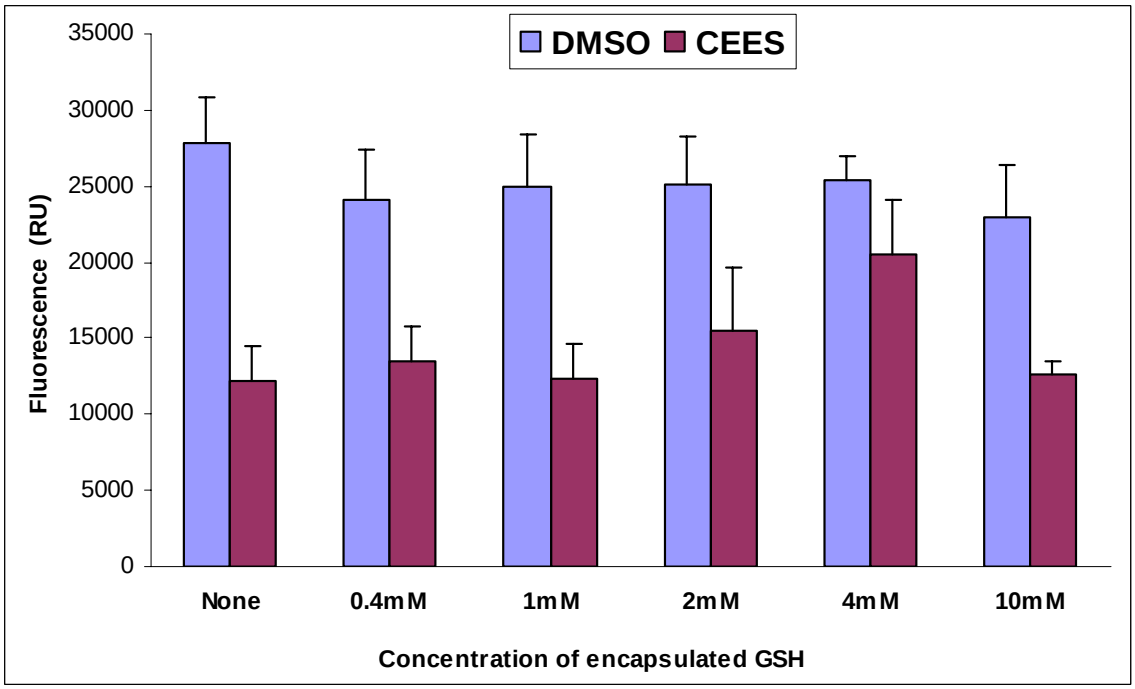

Figure 33. Protective effect of liposome-encapsulated GSH in human keratinocytes. HaCaT cells were incubated in a 96-well plate with various levels of liposomal GSH (as indicated) applied simultaneously with 1% DMSO, or 1 mM CEES (as indicated) for 20 hours. Cell viability was monitored by 5% Alamar Blue after 2 h using a fluorescent plate reader.

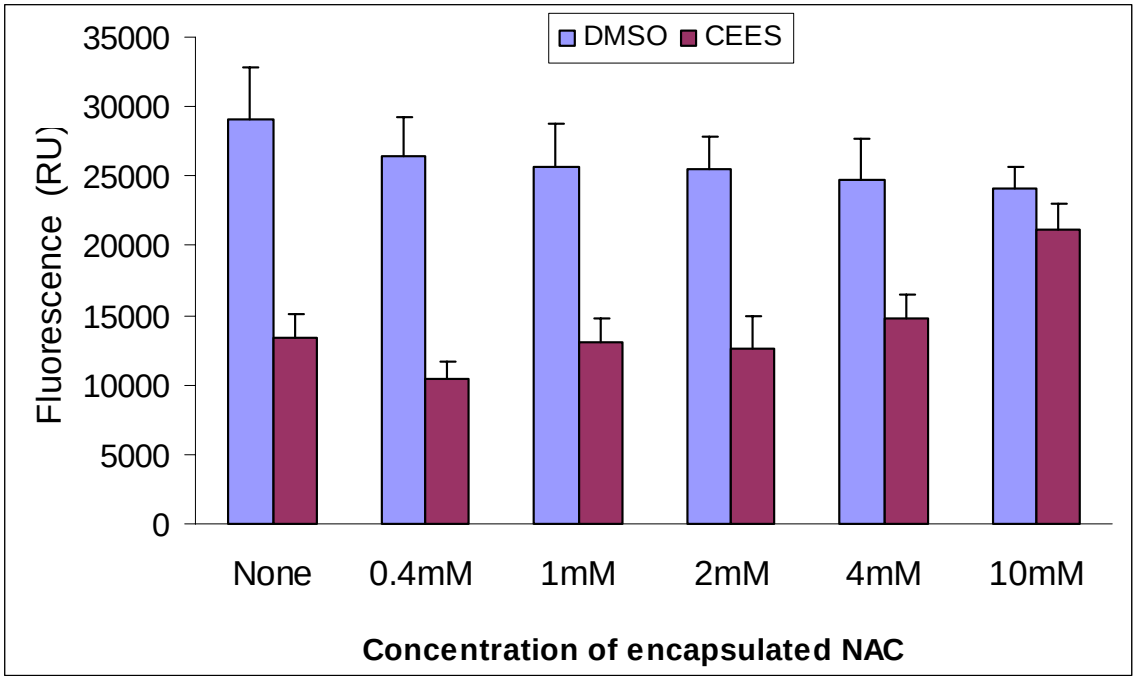

Figure 34. Protective effect of liposome-encapsulated NAC in human keratinocytes. HaCaT cells were incubated in a 96-well plate with various levels of liposomal NAC (as indicated) applied simultaneously with 1% DMSO, or 1 mM CEES (as indicated) for 20 hours. Cell viability was monitored by 5% Alamar Blue after 2 h using a fluorescent plate reader.

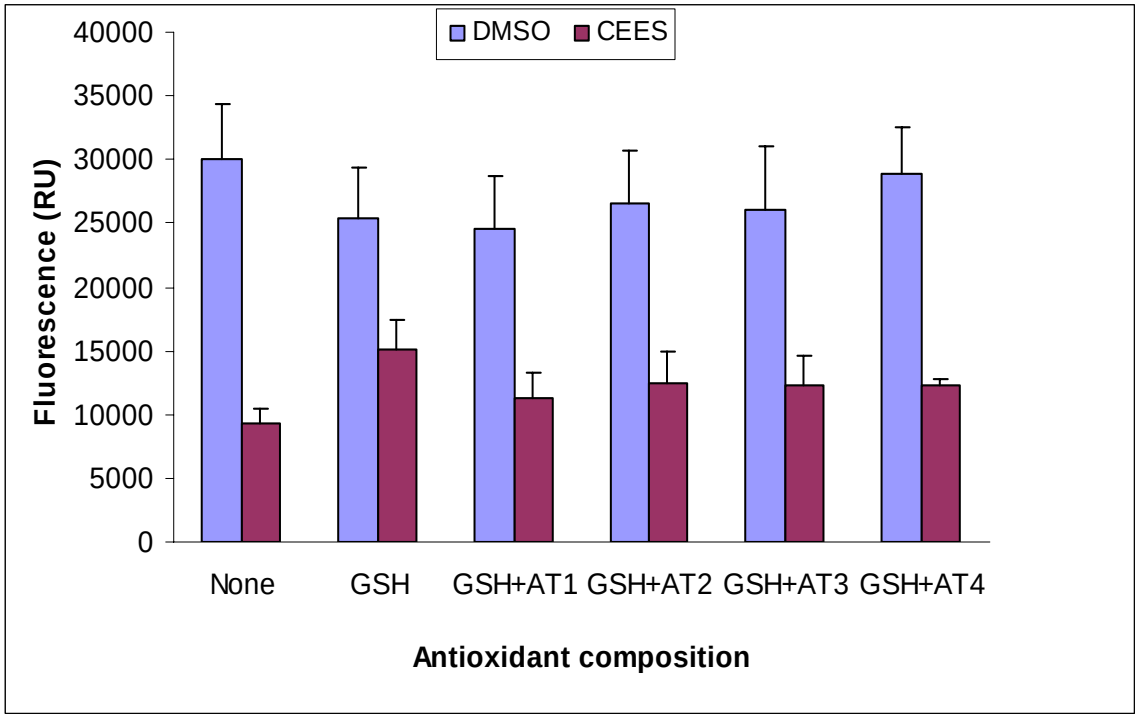

Figure 35. Protective effect of free GSH combined with alpha-tocopherol in human keratinocytes. HaCaT cells were incubated in a 96-well plate with 5 mM GSH combined with various levels of alpha-tocopherol (AT1, 1 µM; AT2, 5 µM; AT3, 10 µM; AT4, 25 µM) applied simultaneously with 1% DMSO, or 1 mM CEES (as indicated) for 20 hours. Cell viability was monitored by 5% Alamar Blue after 2 h using a fluorescent plate reader.

Final series of experiments in EpiDerm tissues

The ultimate aim of the Project was to develop an antioxidant liposome formulation to effectively protect human skin against HD/CEES toxicity. As detailed above, we tested various formulations of the liposomes containing both water-soluble (NAC, GSH) and lipid-soluble antioxidants (tocopherols, ALA) in HaCaT keratinocytes exposed to 1 mM CEES. The results of those studies provided data relevant to the choosing the most protective antioxidant liposome formulations and testing these formulations in CEES-treated human skin model. Finally, we performed a series of our experiments with the EpiDerm™ skin model. EpiDerm™ system consists of normal, human-derived epidermal keratinocytes (NHEK) which have been cultured to form a multilayered, highly differentiated model of the human epidermis (**Figure 36**). These "ready-to-use" tissues, which are cultured on specially prepared cell culture inserts (**Figure 37**) using serum free medium, attain levels of differentiation on the cutting edge of *in vitro* skin technology. Structurally, the EpiDerm Skin Model closely parallels human skin, thus providing a veryuseful *in vitro* means to assess toxicology.

EpiDerm is an established human epidermal model. It was successfully used to study CEES toxicity *in vitro* [32, 46]. At fist, we exposed EpiDerm tissues to various levels of CEES

(0.2 – 5 mM) to obtain dose-response. EpiDerm tissues were recovered from a transportation stress overnight in a clear 24-well plate in the supplied medium according to manufacturer's protocol. Fresh CEES stock solutions in DMSO were quickly mixed with the medium and applied topically (inside each insert) 250 μL per insert. As a control, we used vehicle - 1% DMSO (final conc.). Tissues were incubated at 37^0 C in the incubator for 18 hours. Cell viability was monitored via the MTS assay. MTS is a tetrazolium compound [3-(4,5-dimethyl-2-yl)-5-(3-carboxymethoxyphenyl)-2-(4-sulfophenyl)-2H-tetrazolium, inner salt], which is converted in a soluble formazan product by living cells. MTS assay allow us not only to measure cell viability by monitoring its product in the media, but also to save tissues for future proteomics analyses and microscopic examinations. **Figures 38 and Figure 39** show the dose response of EpiDerm tissues to topical exposure of CEES. MTS product was monitored both topically (on the top of the tissue - **Figure 38**) and apically (in the bottom media - **Figure 39**). High CEES levels (2.5 mM and higher) showed stable toxic effect in the EpiDerm tissues.

In the next experiment, we confirmed the protective effect of NAC and GSH containing antioxidant liposomes as those liposomal formulations were the most effective in HaCaT cells treated with CEES. **Figure 40** shows the protective effect of the antioxidant liposomes in EpiDerm tissues topically exposed to 2.5 mM CEES. Liposomes (contain 200 mM NAC or GSH encapsulated) were applied simultaneously with CEES and diluted in the medium (1:20). GSH containing liposomes were the most protective. Viability of the tissues treated with 2.5 mM CEES in the presence of GSH-liposomes was statistically not different from the control (tissues treated with vehicle alone). Notably, blank liposomes (consist of phospholipids and encapsulated PBS buffer) were not toxic, but not protective. We also monitored cellular ATP content of the keratinocytes within the tissues as ATP depletion is an important factor of cell death [40]. **Figure 41** shows that 2.5 mM CEES induced severe ATP depletion in the keratinocytes, whereas GSH-liposomes effectively restored cellular ATP almost up to the level of control (vehicle alone).

In the following experiment we compared the effects of GSH-liposomes in pre- and post-treatment settings. **Figure 42** shows the protective effect of GSH-liposomes in comparison with free (non-encapsulated) GSH. We also compared simultaneous application to 1 hour post-treatment. As expected, GSH-liposomes were highly protective in all the experimental settings. If applied simultaneously with CEES, GSH-liposomes fully restore viability of keratinocytes in the tissues; they were statistically more effective than free GSH. Notably, GSH or NAC (see above) show protective effect in CEES-treated keratinocytes only if sodium pyruvate (NaPyr) is present in the culture medium. The medium supplied by MatTek Company for EpiDerm tissues does contain 1 mM sodium pyruvate. Therefore, it is very likely that the protection that was documented in our experiments is due to the combined effect of GSH and NaPyr.

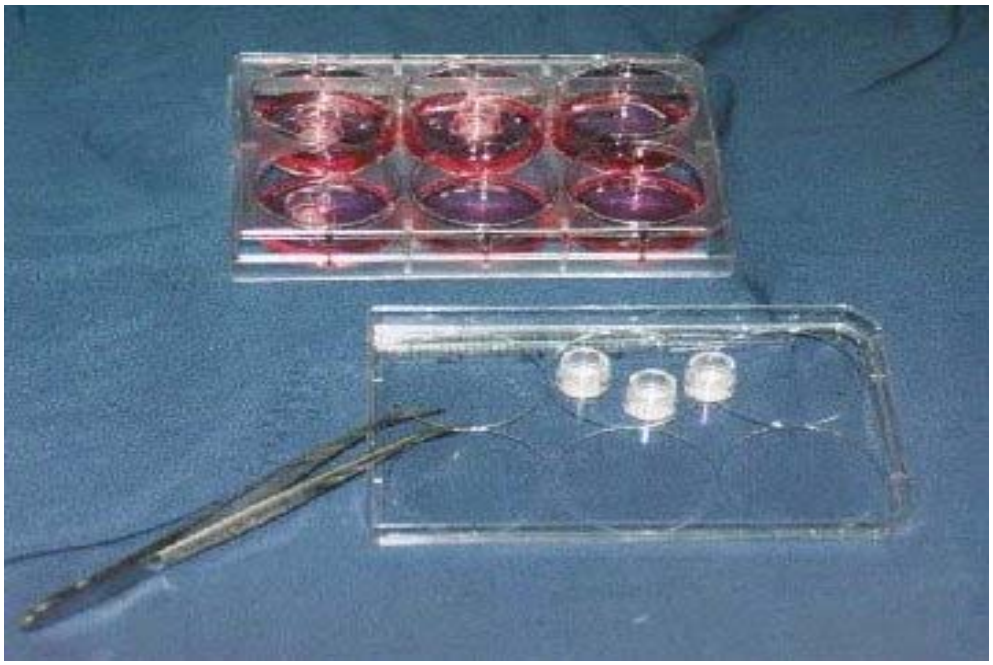

Figure 36. EpiDerm tissues from MatTek Company. Multilayer of normal human keratinocytes is grown on an air-liquid interface onto a membrane attached to the bottom of an insert. Empty inserts are shown separately. Although 6-well plate is shown, 24-well plates were used in our experiments.

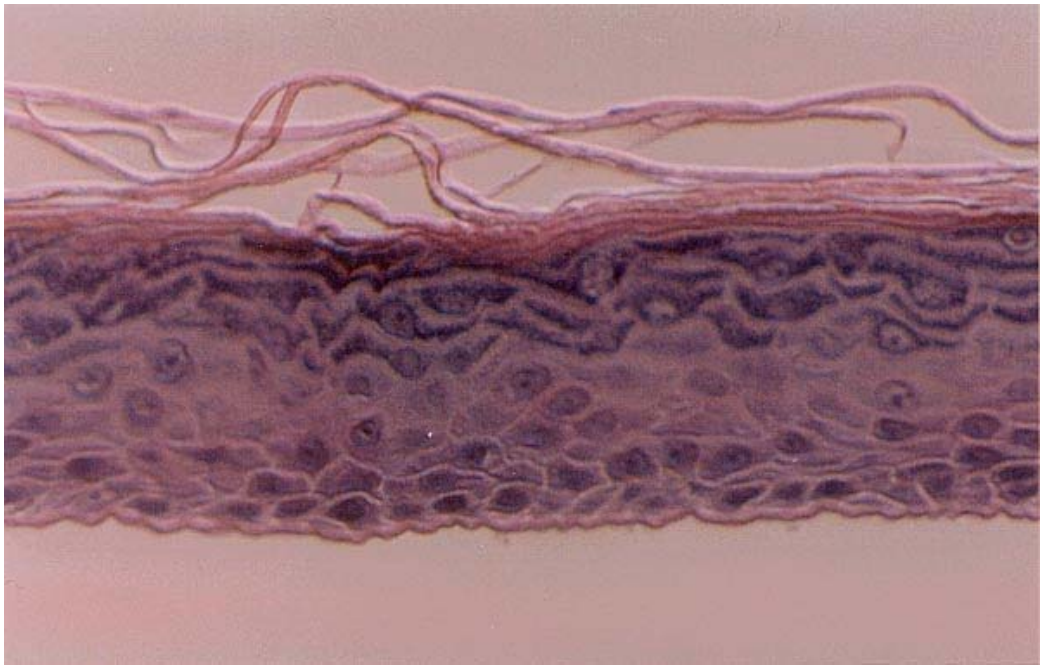

Figure 37. EpiDerm tissue EPI-200 under microscope. Typical microscopic image of an EpiDerm tissue section is shown (magnification x400). Proliferating keratinocytes are at the bottom, differentiated cells are on the top.

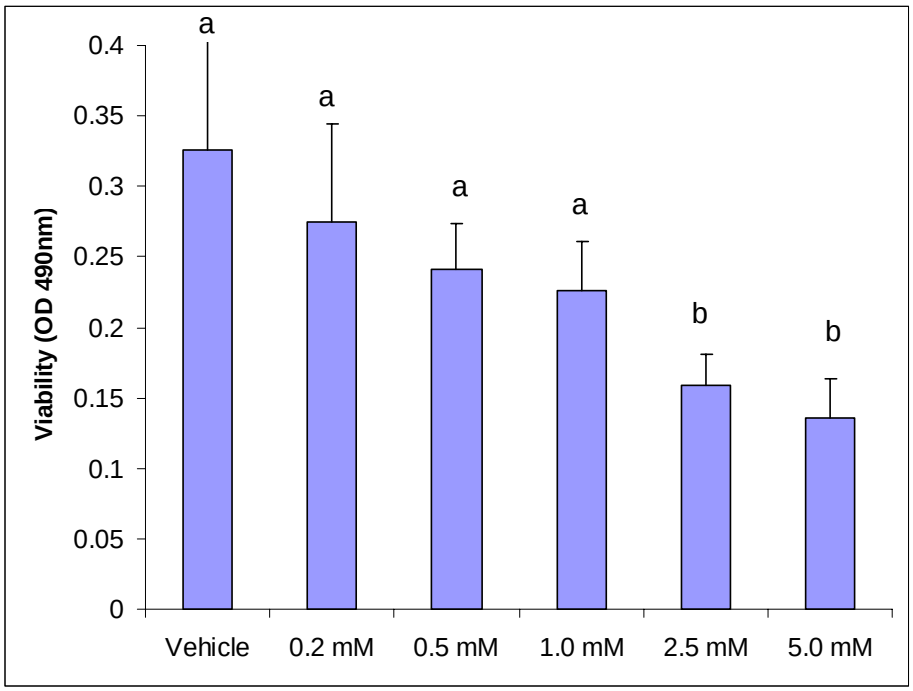

Figure 38. CEES toxicity in the EpiDerm tissues (monitored topically). EpiDerm tissues were exposed topically to CEES (as indicated) for 18 hours. Cell viability was monitored by the MTS assay in the topical liquids.

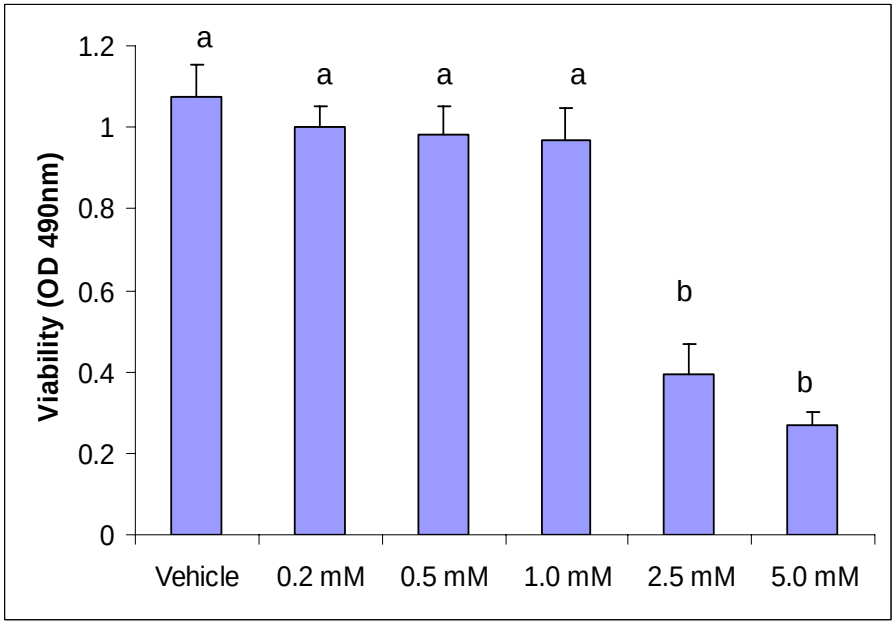

Figure 39. CEES toxicity in the EpiDerm tissues (monitored apically). EpiDerm tissues were exposed topically to CEES (as indicated) for 18 hours. Cell viability was monitored by the MTS assay in the bottom media.

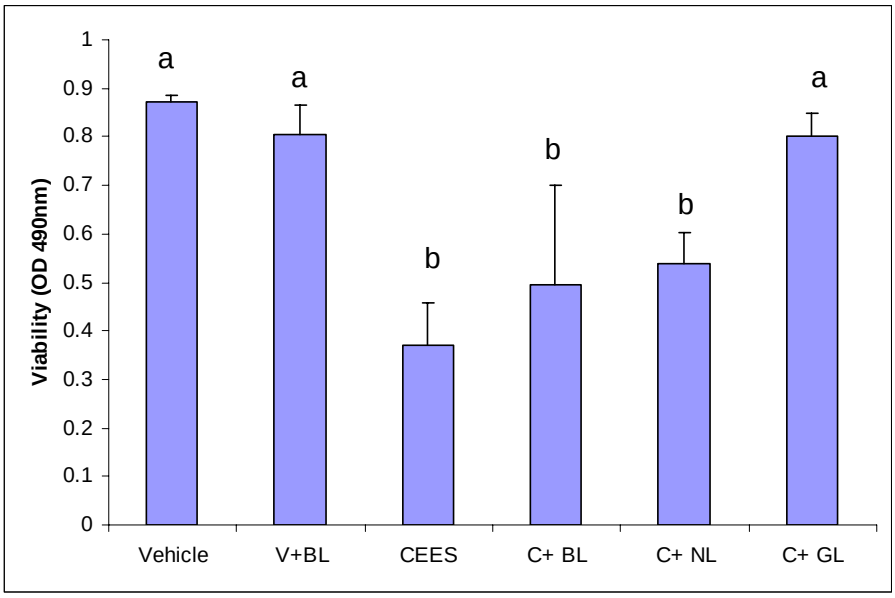

Figure 40. Protective effect of Antioxidant Liposomes in EpiDerm tissues. EpiDerm tissues were exposed topically to 2.5 mM CEES or vehicle (1% DMSO) in the absence or presence of Blank Liposomes (BL), NAC-Liposomes (NL), GSH-Liposomes (GL) [as indicated] for 18 hours. Cell viability was monitored by the MTS assay in the bottom media.

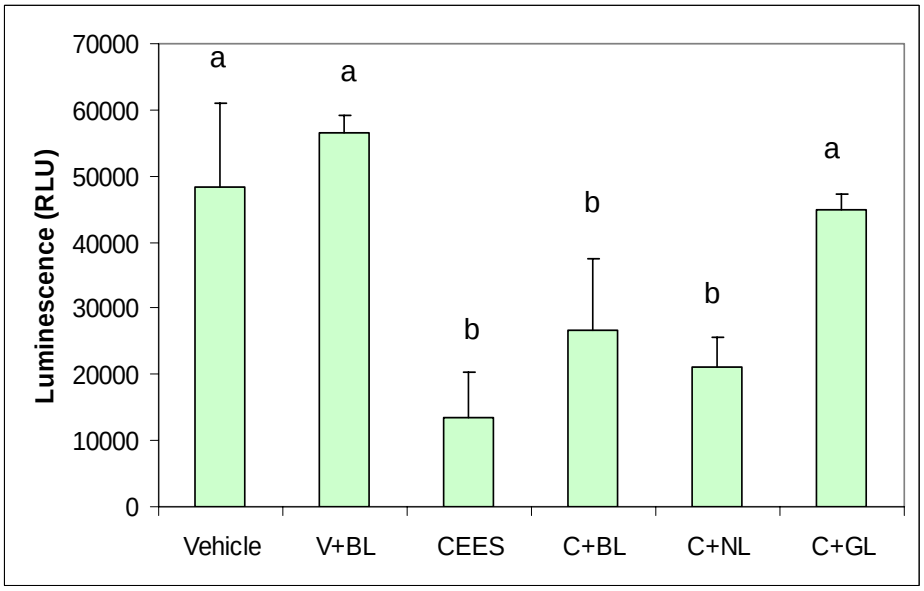

Figure 41. Antioxidant Liposomes restore cellular ATP in EpiDerm tissues. EpiDerm tissues were exposed topically to 2.5 mM CEES or vehicle (1% DMSO) in the absence or presence of Blank Liposomes (BL), NAC-Liposomes (NL), GSH-Liposomes (GL) [as indicated] for 18 hours. Cellular ATP was assayed in cell lysates by the ATP kit (Sigma).

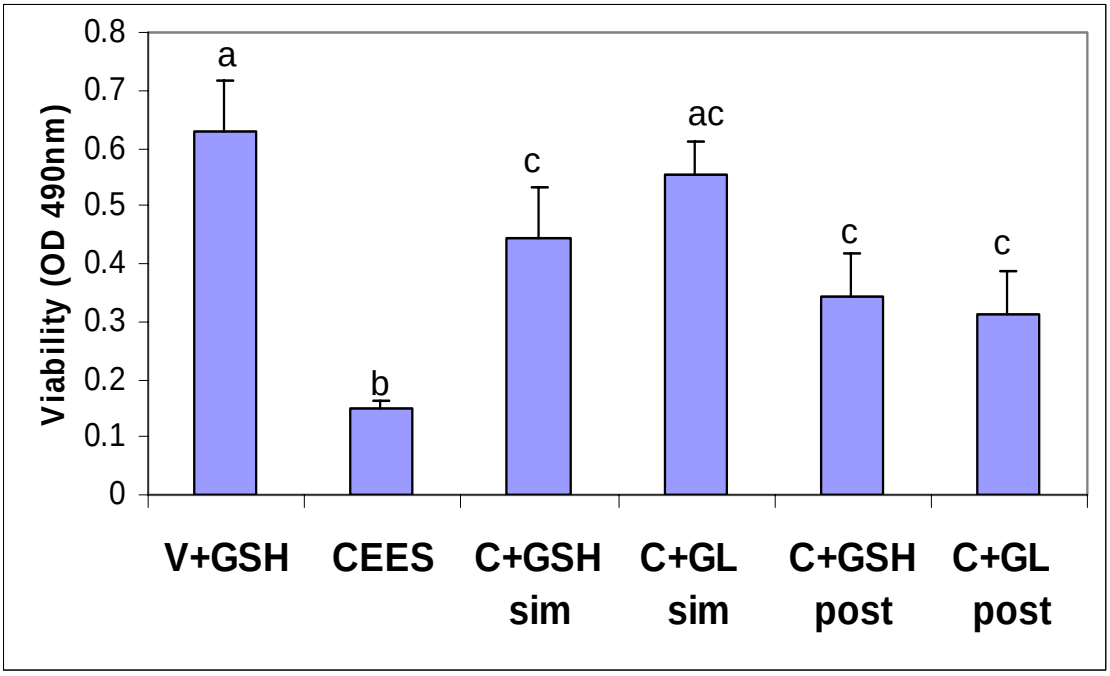

Figure 42. Protective effect of free GSH and GSH-Liposomes in EpiDerm: tissues were exposed topically to vehicle (1% DMSO) and 10 mM free GSH (V+GSH) or 2.5 mM CEES in the absence or presence of free GSH or GSH-Liposomes (GL) [sim, simultaneous application; post, 1 hour post-treatment]. Cell viability was monitored after 18 hours by the MTS assay.

We also explored if GSH-liposomes (or free GSH) influence apoptosis in keratinocytes within the EpiDerm tissues exposed to 2.5 mM CEES. We found that although GSH does protect the cells (increase viability and prevent ATP depletion) it does not reduce apoptosis as measured in the caspase-3 assay (**data not shown**). This finding allow us to speculate that keratinocytes exposed to relatively high levels of CEES or HD undergo necrosis to a much higher extent than apoptosis, which prevails at lower doses of the toxicants. This is in accordance with the recent findings that higher HD levels (more than 1 mM) induce ATP depletion and necrosis in HaCaT keratinocytes [47].

In order to further confirm the protective effect of GSH-liposomes we performed microscopic examinations of the EpiDerm tissues exposed to CEES. EpiDerm tissues were exposed to 2.5 mM CEES in the presence or absence of GSH-liposomes or Blank-liposomes; as a control tissues were exposed to vehicle (1% DMSO). After the MTS assay at the end of overnight incubation the tissues were quickly frozen and sectioned at -20^0C using a Cryostat device. 25 μm thick sections were observed and photographed under a phase-contrast microscope (x400 magnification). **Figure 43** shows the effect of GSH-liposomes on CEES-treated keratinocytes within the tissues. CEES exposure drastically reduces number of viable cells (blue colored cells acquired MTS stain), induces vesication (colorless voids) and fragmentation of extracellular matrix (not shown). Unlike Blank-

liposomes, GSH-liposomes (applied simultaneously with CEES) effectively restore number of viable cells, although their effect on vesication and fragmentation of extracellular matrix was negligible. Thus, the protective effect of GSH-liposomes was confirmed at the microscopic level.

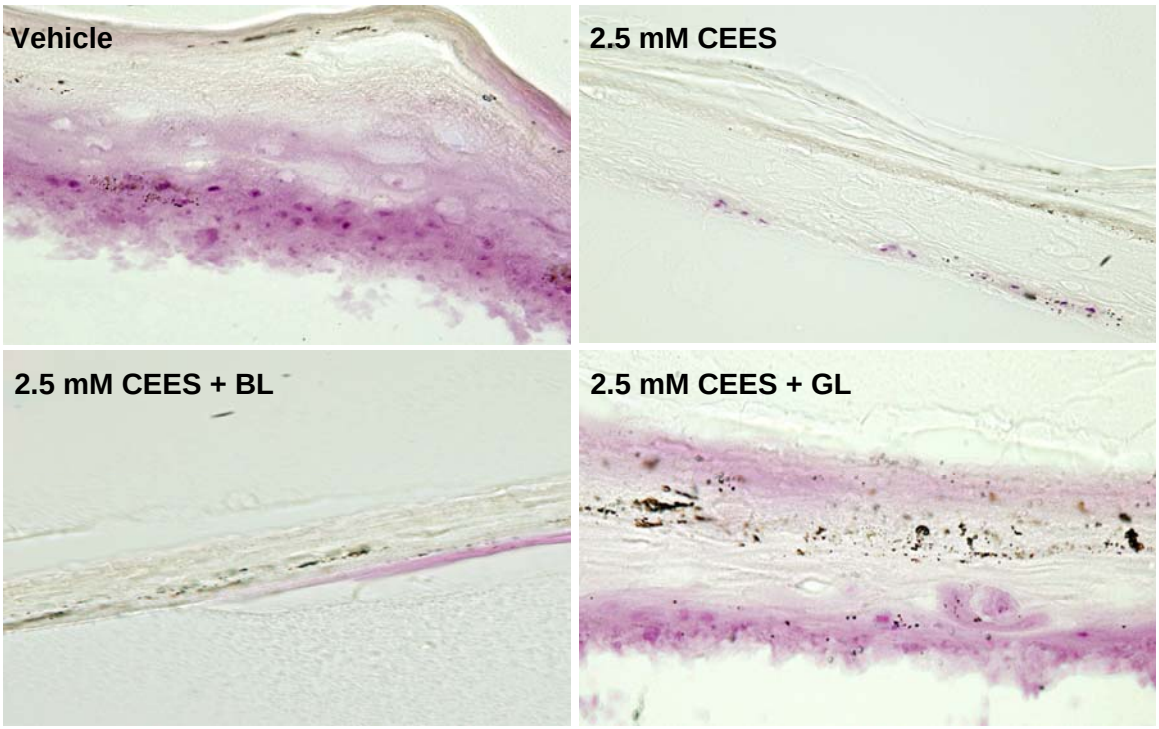

Figure 43. Protective effect of GSH-Liposomes in EpiDerm tissues: EpiDerm tissues were topically exposed to vehicle (1% DMSO) or 2.5 mM CEES in the absence or presence of GSH-Liposomes (GL). After the MTS assay EpiDerm tissues were frozen, dissected, and photographed under a light microscope with 400x magnification.

In addition, we performed proteomics studies aimed at identifying specific redox-sensitive proteins, expression of which might be affected by CEES/HD exposure, but restored by the GSH-liposomes. Relative expression of the proteins was accessed with 2D gel electrophoresis (2D-GE) technique. First, we compared protein mixtures obtained from cell lysates of EpiDerm tissues exposed to 2.5 mM CEES or vehicle (1% DMSO). In order to find statistically significant differences we ran three 2D gels per each sample. Proteins expressed differently in "CEES" and "Vehicle" tissue samples were found (see **Figure 44**). Next, we compared the same tissues exposed to CEES in the presence or absence of GSH-liposomes. We successfully selected proteins whose expression was by altered by CEES exposure but restored by the GSH-liposomes (see **Figure 44** and **Table 3**). In future studies we will identify these proteins utilizing LS/MS/MS analysis of in-gel digested target spots.

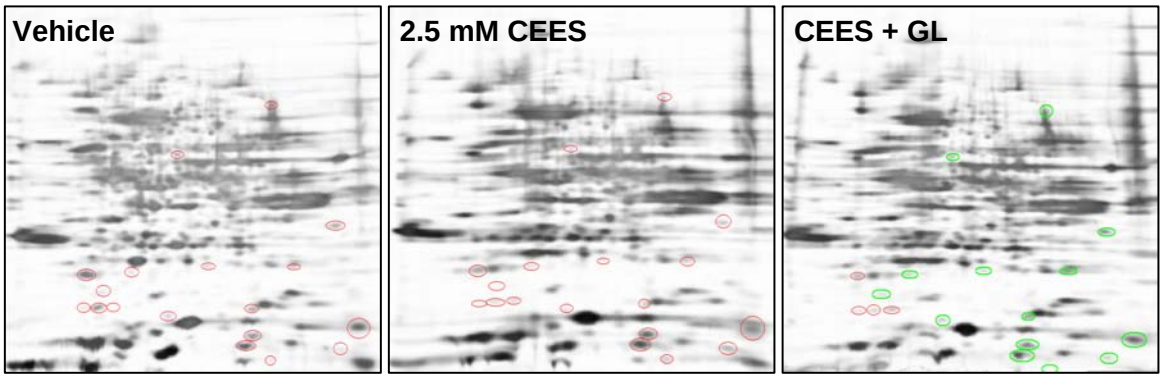

Figure 44. Proteomics Study of CEES toxicity and the effect of GSH-Liposomes in EpiDerm: tissues were exposed to vehicle or 2.5 mM CEES in the absence or presence of GSH-liposomes for 18 h. Cell lysates were separated by 2D gel electrophoresis, silver-stained and photographed (three gels per sample). Average differences in protein expression were quantified with Dymension-2 Software. The proteins differentially expressed after CEES exposure are marked with red circles. The proteins, which expression was partially reversed by GSH-liposomes are marked with green circles.

Table 1: Proteins expressed differentially in EpiDerm tissues.
Quantitative differences in protein expression are expressed as average 2D gel protein spot volume ratios normalized to "Vehicle" samples. (Positive values mean that the proteins are up-regulated, negative values mean that the proteins are down-regulated).

Spot	MW (kDa)		Volume Ratio	
		Vehicle	CEES	CEES + GL
1	50.6	1	-3.935	-1.322
2	34.1	1	-2.827	-1.049
3	28.3	1	-1.739	1.174
4	19.5	1	-2.92	-1.224
5	13.4	1	-3.186	-1.403
6	12.2	1	-2.02	1.068
7	11.7	1	1.657	-1.028
8	11.3	1	-1.591	-1.198
9	10.8	1	-2.095	-1.465
10	10.2	1	1.731	-1.219
11	9.3	1	1.761	-1.323

KEY RESEARCH ACCOMPLISHMENTS:

- Various aspects of CEES toxicity in human keratinocytes (inhibition of cell growth, oxidative stress parameters, influence of various immuno-stimulators) have been studied

- CEES application techniques to the cells have been optimized in order to provide a means of dealing with the rapid hydrolysis of CEES as an experimental variable

- Enhancement of CEES induced toxicity in HaCaT cells in the presence of TNF-α was documented

- We have confirmed that CEES induces apoptosis in human keratinocytes as measured by the caspase 3 assay; apoptotic changes were shown in living cells

- Oxidative stress related changes were studied in HaCaT cells using a fluorescent staining technique

- Enhancement of CEES induced toxicity in HaCaT cells was observed using an oxidative stress inducer TBHP

- The protective effect of NAC was studied in HaCaT cells. Effective concentrations of NAC have been shown to reduce CEES induced apoptosis and increase cell survival

- Major types of antioxidant liposomes have been tested in prevention of CEES-induced cell damage in human keratinocytes; protective effects have been documented

- GSH and NAC-containing liposomes have been found to be most effective in preventing CEES induced loss of keratinocyte viability and CEES induced cell death of keratinocytes

- Ethyl pyruvate and methyl pyruvate have been shown to protect HaCaT keratinocytes partially against CEES induced toxicity in dose-dependent manner

- Final series of experiments has been performed in human epidermal model (EpiDerm tissues); the protective effect of GSH-containing liposomes has been documented

- High levels of CEES (> 2 mM) significantly reduced the viability of human keratinocytes in EpiDerm tissues as measured by MTS assay and conformed by the tissue cryo-sectioning and microscopic examination

- GSH-containing liposomes in the presence of sodium pyruvate are effective in blocking CEES toxicity, but not in preventing apoptosis in EpiDerm tissues

- GSH-containing liposomes are effective in prevention of cellular ATP depletion in EpiDerm tissues

- Differentially expressed proteins in EpiDerm tissues exposed to CEES in the presence or absence GSH-Liposomes were characterized using 2D GE technique

- GSH-Liposomes in combination with pyruvates present a promising therapeutic strategy for the treatment of mustard toxicity in human skin

REPORTABLE OUTCOMES:

Publications:

Viktor Paromov, Milton Smith, and William L. Stone "Sulfur Mustard Toxicity in Human Skin: Role of Oxidative Stress, and Antioxidant Therapy" in: *Journal of Burns and Wounds* 2007, 7:e7

Viktor Paromov, Min Qui, Hongsong Yang, and Milton Smith, William L. Stone "The influence of N-acetyl-L-cysteine and Polymyxin B on oxidative stress and nitric oxide synthesis in stimulated macrophages treated with a mustard gas analog" in: *BMC Cell Biology* 2008, 9:33.

Min Qui, Viktor Paromov, Hongsong Yang, Milton Smith, and William L. Stone "Inhibition of inducible Nitric Oxide Synthase by a mustard gas analog in murine macrophages", in: *BMC Cell Biology* 2006, **7**:39

Suntres, Z, Stone, WL, and Smith, MG: Ricin-Induced Toxicity: The Role of Oxidative Stress, in: *J Med CBR Defense*, 3 (2005).

Smith, M, Das, S, Ward, P, Suntres, Z, Crawford, K and Stone, WL: Blister Agents and Oxidative Stress, In: *CHEMICAL WARFARE AGENTS: Chemistry, Pharmacology, Toxicology and Therapeutics*, CRC Press (submitted)

Presentations/Abstracts:

Hoesel, L.M., Pianko, M.J., Yang, H., Stone, W.L., Smith, M.G., Ward, P.A., Liposomes Containing Antioxidants Prevent Pulmonary Fibrosis in Half-Sulfur Mustard Gas Induced Lung Injury, Bioscience Review 2006, sponsored by the US Army Medical Research and Material Command and hosted by the US Army Medical Research Institute of Chemical Defense, June 4-9, 2006, Hunt Valley, invited platform presentation and abstract (page 109).

Stone, W.L., Li, Q., Paromov, V., Qui, M., Yang, H., Smith, M., Antioxidant Liposome Therapy for Exposure to a Sulfur Vesicating Agent, Bioscience Review 2006, sponsored by the US Army Medical Research and Material Command and hosted by the US Army Medical Research Institute of Chemical Defense, June 4-9, 2006, Hunt Valley, poster presentation and abstract (page 161).

Smith, M.G., Stone, W.L., Ward, P., Alibek, K., Wu, A., Das, S., Crawford, K., Anderson, D., Sciuto, A., Suntres, Z., Rest, R., A Multi-Threat and Diagnostic Countermeasure by the Advanced Medical Countermeasure Consortium, Bioscience Review 2006, sponsored by the US Army Medical Research and Material Command and hosted by the US Army Medical Research Institute of Chemical Defense, June 4-9, 2006, Hunt Valley, poster presentation and abstract (page 259).

Paromov, V., Kumari, S., Brannon, M., Muenyi C., Stone, W.L., The Protective Effect of Antioxidant Liposomes in a Human Epidermal Model Exposed to a Vesicating Agent, Bioscience Review 2008, sponsored by the US Army Medical Research and Material Command and hosted by the US Army Medical Research Institute of Chemical Defense, June 1-6, 2008, Hunt Valley, poster presentation and abstract (page 37).

Ward, P.A., Hoesel, L.M., Flierl, M.A., Rittirsch, D., Stone, W.L., Smith, M.G., Liposomal Blockade of Lung Injury after Exposure to 2-Chloroethyl Ethyl Sulfide, Bioscience Review 2008, sponsored by the US Army Medical Research and Material Command and hosted by the US Army Medical Research Institute of Chemical Defense, June 1-6, 2008, Hunt Valley, invited platform presentation and abstract (page 175).

Degrees obtained that are supported by this award: Mr. Christian Muenyi, graduate student in PI's lab has received MS degree from the Chemistry Department at East Tennessee State University as he initiated proteomic studies in order to complement the work funded by this application.

Funding applied for based on work supported by this award: NA

Employment or research opportunities applied for and/or received based on experience/training supported by this award: NA

Invited Presentations at International Meetings: The experiments described in this report have been presented as a poster at the Bioscience Review 2006 International Conference, Hunt Valley, Maryland (see attached abstract). In addition, Dr. Hongsong Yang has been invited to present our finding at the 6th International Workshop of Micronutrients, Oxidative Stress and the Environment held in Kuching, Malaysia, June 29th –July 2nd, 2006.

CONCLUSIONS:

Our experiments demonstrated CEES-induced oxidative stress and caspase-dependent apoptosis in human keratinocytes. Apoptotic changes were shown via fluorescent imaging in living cells at CEES levels less then 2 mM. We documented CEES-induced generation of ROS in human keratinocytes exposed to high levels of CEES only (Fig.15), in addition, we observed a dose-dependent enhancement of CEES toxicity by TBHP-induced oxidative stress. We also found that the pro-inflammatory cytokine, TNF-α, is able to enhance CEES-induced cytotoxicity in a dose-dependent manner. The latter results are in agreement with our previous observations obtained with murine macrophages simultaneously exposed to CEES and various immuno-stimulators [5]. In summary, these findings are in agreement with the concept that higher CEES/HD levels induce ATP depletion, oxidative stress, and necrosis in human keratinocytes, whereas lower levels induce apoptosis [47]. Our results suggest that the combination of antioxidants (GSH and pyruvates) not only increase cell viability, but also shift the cell death pathway from inflammation-inducing necrosis to less pathological form of apoptosis. However, this hypothesis needs more experimental evidence.

We studied the protective effect of free (non-encapsulated) and liposome-encapsulated antioxidants (NAC, GSH, tocopherols, ALA) in human keratinocytes. Effective concentrations of GSH and NAC have been shown to reduce CEES-induced apoptosis and increase cell survival in a dose-dependent manner. GSH-liposomes in the presence of sodium pyruvate were found to be the most protective.

We confirmed the protective effect of antioxidant liposomes against CEES-induced skin cell damage in human epidermal model (EpiDerm tissues exposed to 2.5 mM CESS). GSH-containing liposomes showed significant protective effect, and NAC-containing liposomes have been found to be partially protective in preventing CEES-induced loss of keratinocyte viability as measured by MTS assay and conformed by the tissue cryo-sectioning and microscopic examination. Interestingly, we found that GSH-containing liposomes in the presence of sodium pyruvate are effective in blocking CEES toxicity, but not in preventing apoptosis in EpiDerm tissues; GSH-containing liposomes are effective in prevention of cellular ATP depletion in EpiDerm tissues. These findings suggest that keratinocytes

exposed to higher CEES/HD levels mostly undergo necrosis with elevation of inflammation and oxidative stress; and GSH/pyruvate combination, especially if delivered by liposomes, is highly effective in reduction of such negative processes inside the cells.

We also initiated proteomics studies in CEES-exposed/GSH-liposome treated EpiDerm tissues. Differentially expressed proteins in EpiDerm tissues exposed to CEES in the presence or absence GSH-Liposomes were characterized using 2D GE technique. These proteins will be identified utilizing LS/MS/MS analysis of in-gel digested target spots. We would like continue these studies in the future as they would help to explore the molecular mechanisms of CEES/HD toxicity as well as the mechanisms of the antioxidant protective effect.

We believe that antioxidants, especially encapsulated in liposomes and applied topically, would be a highly effective therapeutic strategy against CEES-induced skin damage in humans. Further *in vivo* studies in an animal model will be needed in order to fully develop an effective treatment against HD toxicity.

REFERENCES:

1. Davreux CJ, Soric I, Nathens AB, Watson RW, McGilvray ID, Suntres ZE, Shek PN, Rotstein OD: **N-acetyl cysteine attenuates acute lung injury in the rat.** *Shock* 1997, **8:**432-438.
2. Fox ES, Brower JS, Bellezzo JM, Leingang KA: **N-acetylcysteine and alpha-tocopherol reverse the inflammatory response in activated rat Kupffer cells.** *J Immunol* 1997, **158:**5418-5423.
3. Fu Y, McCormick CC, Roneker C, Lei XG: **Lipopolysaccharide and interferon-gamma-induced nitric oxide production and protein oxidation in mouse peritoneal macrophages are affected by glutathione peroxidase-1 gene knockout.** *Free Radical Biology & Medicine* 2001, **31:**450-459.
4. Wang S, Leonard SS, Castranova V, Vallyathan V, Shi X: **The role of superoxide radical in TNF-alpha induced NF-kappaB activation.** *Ann Clin Lab Sci* 1999, **29:**192-199.
5. Stone WL, Qui M, Smith M: **Lipopolysaccharide enhances the cytotoxicity of 2-chloroethyl ethyl sulfide.** *BMC Cell Biol* 2003, **4:**1.
6. Mercurio F, Manning AM: **NF-kappaB as a primary regulator of the stress response.** *Oncogene* 1999, **18:**6163-6171.
7. Mercurio F, Manning AM: **Multiple signals converging on NF-kappaB.** *Curr Opin Cell Biol* 1999, **11:**226-232.
8. Downey JS, Han J: **Cellular activation mechanisms in septic shock.** *Front Biosci* 1998, **3:**d468-476.
9. Arroyo CM, Schafer RJ, Kurt EM, Broomfield CA, Carmichael AJ: **Response of normal human keratinocytes to sulfur mustard: cytokine release.** *Journal of Applied Toxicology : Jat* 2000, **20 Suppl 1:**S63-72.
10. Chatterjee D, Mukherjee S, Smith MG, Das SK: **Signal transduction events in lung injury induced by 2-chloroethyl ethyl sulfide, a mustard analog.** *J Biochem Mol Toxicol* 2003, **17:**114-121.
11. Atkins KB, Lodhi IJ, Hurley LL, Hinshaw DB: **N-acetylcysteine and endothelial cell injury by sulfur mustard.** *J Appl Toxicol* 2000, **20 Suppl 1:**S125-128.
12. Pathania V, Syal N, Pathak CM, Khanduja KL: **Vitamin E suppresses the induction of reactive oxygen species release by lipopolysaccharide, interleukin-1beta and tumor necrosis factor-alpha in rat alveolar macrophages.** *J Nutr Sci Vitaminol (Tokyo)* 1999, **45:**675-686.
13. Thirunavukkarasu V, Anuradha CV: **Influence of alpha-lipoic acid on lipid peroxidation and antioxidant defence system in blood of insulin-resistant rats.** *Diabetes Obes Metab* 2004, **6:**200-207.
14. Tsuchiya M, Kagan VE, Freisleben HJ, Manabe M, Packer L: **Antioxidant activity of alpha-tocopherol, beta-carotene, and ubiquinol in membranes: cis-parinaric acid-incorporated liposomes.** *Methods Enzymol* 1994, **234:**371-383.
15. Stone WL, Mukherjee S, Smith M, Das SK: **Therapeutic uses of antioxidant liposomes.** *Methods Mol Biol* 2002, **199:**145-161.
16. Gao R, Stone WL, Huang T, Papas AM, Qui M: **The uptake of tocopherols by RAW 264.7 macrophages.** *Nutr J* 2002, **1:**2.
17. Eyer P, Podhradsky D: **Evaluation of the micromethod for determination of glutathione using enzymatic cycling and Ellman's reagent.** *Anal Biochem* 1986, **153:**57-66.
18. Allen S, Shea JM, Felmet T, Gadra J, Dehn PF: **A kinetic microassay for glutathione in cells plated on 96-well microtiter plates.** *Methods Cell Sci* 2000, **22:**305-312.
19. Saccani A, Saccani S, Orlando S, Sironi M, Bernasconi S, Ghezzi P, Mantovani A, Sica A: **Redox regulation of chemokine receptor expression.** *Proc Natl Acad Sci U S A* 2000, **97:**2761-2766.
20. Giambartolomei GH, Dennis VA, Lasater BL, Philipp MT: **Induction of pro- and anti-inflammatory cytokines by Borrelia burgdorferi lipoproteins in monocytes is mediated by CD14.** *Infection and Immunity* 1999, **67:**140-147.

21. Ricketts KM, Santai CT, France JA, Graziosi AM, Doyel TD, Gazaway MY, Casillas RP: **Inflammatory cytokine response in sulfur mustard-exposed mouse skin.** *Journal of Applied Toxicology : Jat* 2000, **20 Suppl 1:**S73-76.
22. Smith ME, van_der_Maesen K, Somera FP: **Macrophage and microglial responses to cytokines in vitro: phagocytic activity, proteolytic enzyme release, and free radical production.** *Journal of Neuroscience Research* 1998, **54:**68-78.
23. Yamamoto T, Nakane T, Osaki T: **The mechanism of mononuclear cell infiltration in oral lichen planus: the role of cytokines released from keratinocytes.** *J Clin Immunol* 2000, **20:**294-305.
24. Arnold R, Seifert M, Asadullah K, Volk HD: **Crosstalk between keratinocytes and T lymphocytes via Fas/Fas ligand interaction: modulation by cytokines.** *J Immunol* 1999, **162:**7140-7147.
25. Arroyo CM, Schafer RJ, Kurt EM, Broomfield CA, Carmichael AJ: **Response of normal human keratinocytes to sulfur mustard (HD): cytokine release using a non-enzymatic detachment procedure.** *Human & Experimental Toxicology* 1999, **18:**1-11.
26. Ray P, Chakrabarti AK, Broomfield CA, Ray R: **Sulfur mustard-stimulated protease: a target for antivesicant drugs.** *J Appl Toxicol* 2002, **22:**139-140.
27. Wormser U, Green BS, Arad-Yellin R, Brodsky B, Shatz I, Nyska A: **In vivo and in vitro toxicity of newly synthesized monofunctional sulfur mustard derivatives.** *Toxicology* 1996, **108:**125-128.
28. Petrali JP, Hamilton, T.A., Benton, B.J., Anderson, D.R., Holmes, W.,, Kan RK, Tompkins,C.P., and Ray, R.: **Dimethyl Sulfoxide Accelerates Mustard Gas-induced Skin Pathology.** *Journal of Medical Chemical, Biological and Radiological Defense* 2005, **3:**1-7.
29. Rosenthal DS, Velena A, Chou FP, Schlegel R, Ray R, Benton B, Anderson D, Smith WJ, Simbulan-Rosenthal CM: **Expression of dominant-negative Fas-associated death domain blocks human keratinocyte apoptosis and vesication induced by sulfur mustard.** *J Biol Chem* 2003, **278:**8531-8540.
30. Kim YB, Lee YS, Choi DS, Cha SH, Sok DE: **Change in glutathione S-transferase and glyceraldehyde-3-phosphate dehydrogenase activities in the organs of mice treated with 2-chloroethyl ethyl sulfide or its oxidation products.** *Food Chem Toxicol* 1996, **34:**259-265.
31. Rohrbaugh DK, Yang YC, Ward JR: **Identification of degradation products of 2-chloroethyl ethyl sulfide by gas chromatography-mass spectrometry.** *J Chromatogr* 1988, **447:**165-169.
32. Blaha M, Kohl J, DuBose D, Bowers W, Jr., Walker J: **Ultrastructural and histological effects of exposure to CEES or heat in a human epidermal model.** *In Vitr Mol Toxicol* 2001, **14:**15-23.
33. Ray P, Ali ST: **Protease in normal human epidermal keratinocytes.** *Drug Chem Toxicol* 1998, **21:**319-327.
34. Chatterjee D, Mukherjee S, Smith MG, Das SK: **Evidence of hair loss after subacute exposure to 2-chloroethyl ethyl sulfide, a mustard analog, and beneficial effects of N-acetyl cysteine.** *J Biochem Mol Toxicol* 2004, **18:**150-153.
35. Ray R, Hauck S, Kramer R, Benton B: **A convenient fluorometric method to study sulfur mustard-induced apoptosis in human epidermal keratinocytes monolayer microplate culture.** *Drug Chem Toxicol* 2005, **28:**105-116.
36. Levitt JM, Lodhi IJ, Nguyen PK, Ngo V, Clift R, Hinshaw DB, Sweeney JF: **Low-dose sulfur mustard primes oxidative function and induces apoptosis in human polymorphonuclear leukocytes.** *Int Immunopharmacol* 2003, **3:**747-756.
37. Rappeneau S, Baeza-Squiban A, Jeulin C, Marano F: **Protection from cytotoxic effects induced by the nitrogen mustard mechlorethamine on human bronchial epithelial cells in vitro.** *Toxicol Sci* 2000, **54:**212-221.
38. Das SK, Mukherjee S, Smith MG, Chatterjee D: **Prophylactic protection by N-acetylcysteine against the pulmonary injury induced by 2-chloroethyl ethyl sulfide, a mustard analogue.** *J Biochem Mol Toxicol* 2003, **17:**177-184.
39. Ying W, Chen Y, Alano CC, Swanson RA: **Tricarboxylic acid cycle substrates prevent PARP-mediated death of neurons and astrocytes.** *J Cereb Blood Flow Metab* 2002, **22:**774-779.
40. Zong WX, Ditsworth D, Bauer DE, Wang ZQ, Thompson CB: **Alkylating DNA damage stimulates a regulated form of necrotic cell death.** *Genes Dev* 2004, **18:**1272-1282.
41. Ying W, Alano CC, Garnier P, Swanson RA: **NAD+ as a metabolic link between DNA damage and cell death.** *J Neurosci Res* 2005, **79:**216-223.

42. Sebastia J, Cristofol R, Martin M, Rodriguez-Farre E, Sanfeliu C: **Evaluation of fluorescent dyes for measuring intracellular glutathione content in primary cultures of human neurons and neuroblastoma SH-SY5Y.** *Cytometry A* 2003, **51:**16-25.
43. Arroyo CM, Burman DL, Kahler DW, Nelson MR, Corun CM, Guzman JJ, Smith MA, Purcell ED, Hackley BE, Jr., Soni SD, Broomfield CA: **TNF-alpha expression patterns as potential molecular biomarker for human skin cells exposed to vesicant chemical warfare agents: sulfur mustard (HD) and Lewisite (L).** *Cell Biol Toxicol* 2004, **20:**345-359.
44. Meier HL, Millard CB: **Alterations in human lymphocyte DNA caused by sulfur mustard can be mitigated by selective inhibitors of poly(ADP-ribose) polymerase.** *Biochim Biophys Acta* 1998, **1404:**367-376.
45. Dabrowska MI, Becks LL, Lelli JL, Jr., Levee MG, Hinshaw DB: **Sulfur mustard induces apoptosis and necrosis in endothelial cells.** *Toxicol Appl Pharmacol* 1996, **141:**568-583.
46. Blaha M, Bowers W, Kohl J, DuBose D, Walker J, Alkhyyat A, Wong G: **Effects of CEES on inflammatory mediators, heat shock protein 70A, histology and ultrastructure in two skin models.** *Journal of Applied Toxicology : Jat* 2000, **20 Suppl 1:**S101-108.
47. Kehe K, Raithel K, Kreppel H, Jochum M, Worek F, Thiermann H: **Inhibition of poly(ADP-ribose) polymerase (PARP) influences the mode of sulfur mustard (SM)-induced cell death in HaCaT cells.** *Arch Toxicol* 2007.

Appendices:

- Published papers
- Poster Presentations

JOURNAL OF BURNS AND WOUNDS WWW.JOURNALOFBURNSANDWOUNDS.COM

Sulfur Mustard Toxicity Following Dermal Exposure

Role of Oxidative Stress, and Antioxidant Therapy

Victor Paromov,[a] *Zacharias Suntres,*[b] *Milton Smith,*[c] *and William L. Stone*[a]

[a]Department of Pediatrics, East Tennessee State University, Johnson City; [b]Northern Ontario School of Medicine, Advanced Technology and Academic Centre, 955 Oliver Road Thunder Bay, ON P7B 5E1; and [c]AMAOX, Ltd., #208, 6300 N. Wickham Rd, Melbourne, Fla.

Correspondence: stone@etsu.edu

Published August 20, 2007

Objective: Sulfur mustard (bis-2-(chloroethyl) sulfide) is a chemical warfare agent (military code: HD) causing extensive skin injury. The mechanisms underlying HD-induced skin damage are not fully elucidated. This review will critically evaluate the evidence showing that oxidative stress is an important factor in HD skin toxicity. Oxidative stress results when the production of reactive oxygen (ROS) and/or reactive nitrogen oxide species (RNOS) exceeds the capacity of antioxidant defense mechanisms. **Methods:** This review will discuss the role of oxidative stress in the pathophysiology of HD skin toxicity in both in vivo and in vitro model systems with emphasis on the limitations of the various model systems. Evidence supporting the therapeutic potential of antioxidants and antioxidant liposomes will be evaluated. Antioxidant liposomes are effective vehicles for delivering both lipophilic (incorporated into the lipid bilayers) and water-soluble (encapsulated in the aqueous inner-spaces) antioxidants to skin. The molecular mechanisms interconnecting oxidative stress to HD skin toxicity are also detailed. **Results:** DNA repair and inflammation, in association with oxidative stress, induce intracellular events leading to apoptosis or to a programmable form of necrosis. The free radical, nitric oxide (NO), is of considerable interest with respect to the mechanisms of HD toxicity. NO signaling pathways are important in modulating inflammation, cell death, and wound healing in skin cells. **Conclusions:** Potential future directions are summarized with emphasis on a systems biology approach to studying sulfur mustard toxicity to skin as well as the newly emerging area of redox proteomics.

SULFUR MUSTARD: A CENTURY OF THREAT

Sulfur mustard (SM) or mustard gas (bis-2-(chloroethyl) sulfide, military code: HD) is a chemical warfare agent classified as a weapon of mass destruction. Mustard gas was one of the first chemical weapons deployed against troops on a battlefield during World War I, almost hundred years ago. Since then, the military use of mustard gas has been documented in a number of situations. In 1988, HD was used with devastating results

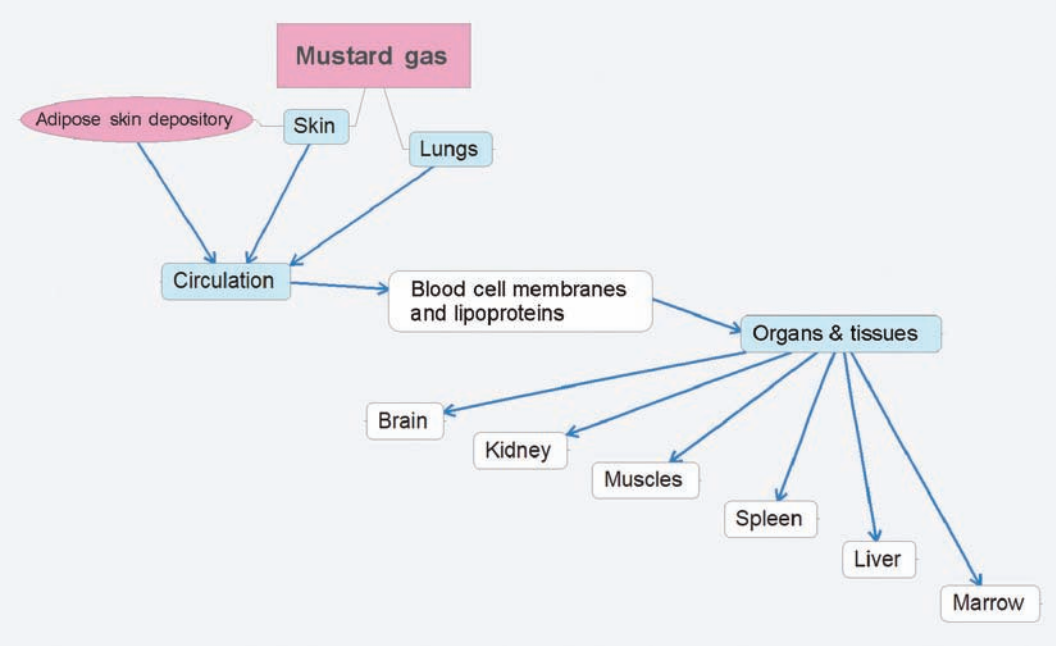

Figure 1. Distribution and accumulation of HD via circulation after dermal/inhalation exposure.

by Saddam Hussein's military forces against civilian targets in Halabja and later during the Iran-Iraq war. Mustard gas produces casualties in the battlefield and forces opposing troops to wear full protective equipment thus slowing the tempo of military operations. It is highly probable that mustard gas could be used by terrorists since it is a simple chemical compound readily synthesized without elaborate technology. Moreover, as a "persistent agent" (US Army classification) aerosolized mustard gas presents a threat for up to 1 week under dry and warm weather conditions because it remains in the environment until fully hydrolyzed. Along with nerve agents, mustard gas presents a major threat as a potential and effective chemical weapon. The possibility of low technology production, easy stockpiling, and difficulty in verifying its storage makes mustard gas a continuing worldwide threat. Presently, there is no antidote or effective treatment for mustard gas intoxication.

PATHOPHYSIOLOGY OF SULFUR MUSTARD ON SKIN

Clinical and physiological characteristics

Mustard gas is lethal in high doses and causes severe damage to the interface organs, that is, skin, lungs, respiratory tract, and eyes. The most prominent toxic effects of HD are on skin where it produces severe damage including extremely slow healing lesions and blisters which can ulcerate, vesicate, and promote secondary infections. Because of its hydrophobic nature, mustard gas easily penetrates and accumulates in the lipid component of exposed tissues. Upon contact with the skin, about 80% of HD evaporates and only about 20% is absorbed by the skin. Skin not only accumulates but also distributes HD to other tissues. Only about 10%–12% of the initially absorbed HD is retained in the skin, whereas up to 90% of HD enters circulation as indicated in Figure 1[1] Extractable skin reservoirs of HD

can be found in the dermis and epidermis even 24 to 48 hours postexposure.[2] In the case of a lethal poisoning, HD concentration in skin blisters remains very high even 7 days after exposure.[3] Consequently, even after the initial exposure skin reservoirs continue to distribute HD via circulation to the body tissues thereby increasing damage to several organs. Figure 1 schematically shows the distribution pathway of HD toxicity throughout the human body. We would like to point that, although skin is the initial accumulator of HD, its toxic effect is also prominent in distal organs. Therefore, the effect of HD after dermal exposure is not limited only to skin tissues

While the epidermis contains no blood vessels, both the dermis and the subcutaneous regions are rich in blood vessels. Adipose cells in the subcutaneous skin layer are likely to be a depository for HD due to their high lipid content (as indicated in Figure 1). Moreover, HD solublized in adipose cells would be out of contact with water and thereby resistant to hydrolysis. After acute skin exposure, HD would be systemically delivered to various tissues in the body via lipid rich blood cell membranes and plasma lipoproteins and accumulate in lipid rich tissues (adipose tissues, brain, and skin). Chemical analyses following acute HD exposure show a high accumulation in thigh fat, brain, abdominal skin, kidney, and muscle tissues, in decreasing order.[3] In addition, HD can be found in the spleen, liver, and bone marrow.[4] The organs acquiring the most damage after dermal and/or respiratory exposure are indicated in Figure 1.

Skin damage caused by aerosolized HD appears after a latent period of up to 24 hours. First symptoms, such as itching, burning, and erythema, are followed by hyperpigmentation, tissue necrosis, and blister formation in warm moist areas of the body. When a large skin area is exposed to HD, medical conditions can be complicated by fluid imbalance, general inflammation, systemic intoxication, and secondary infection. At high doses, HD can also produce systemic effects with gastrointestinal symptoms (nausea and vomiting), respiratory distress due to the bronchospasm, temporary blindness as well as corneal damage. In most lethal cases, massive skin burns and wounds, as well as lung damage, are the primary causes of death. Since it damages DNA, mustard gas promotes mutagenesis and carcinogenesis.[1,5–7] Acute and severe exposures to HD have been shown to produce skin cancers.[8,9]

A few limited cases of HD exposure in humans provide some evidence for oxidative stress. HD metabolites derived from hydrolysis (thiodiglycol, thiodiglycol sulphoxide), as well as HD metabolites from glutathione (GSH) conjugates by the beta-lyase pathway, can be found in human urine after HD exposure.[10,11] Both thiodiglycol sulphoxide and beta-lyase metabolites can be detected indicating GSH conjugation. Thiodiglycol has also been detected in urine samples from individuals not exposed to HD and is therefore not useful as a definitive marker for HD exposure.[11] In contrast, HD metabolites from the glutathione (GSH)/beta-lyase pathway are specific for HD exposure.[10,11] These observations suggest that GSH depletion occurs in humans, and that GSH-HD/beta-lyase pathway metabolites provide a specific and useful biomarker for diagnosing HD exposure. GSH is a key intracellular antioxidant and its depletion by HD would be expected to increase oxidative stress.

The effects of HD in humans are very complicated and not fully elucidated. Figure 2 summarizes some of the key potential molecular mechanisms for HD toxicity in skin cells (as discussed in more detail below). Macromolecular damage and thiol depletion are primary and presumably the most dangerous intracellular events following HD exposure to skin

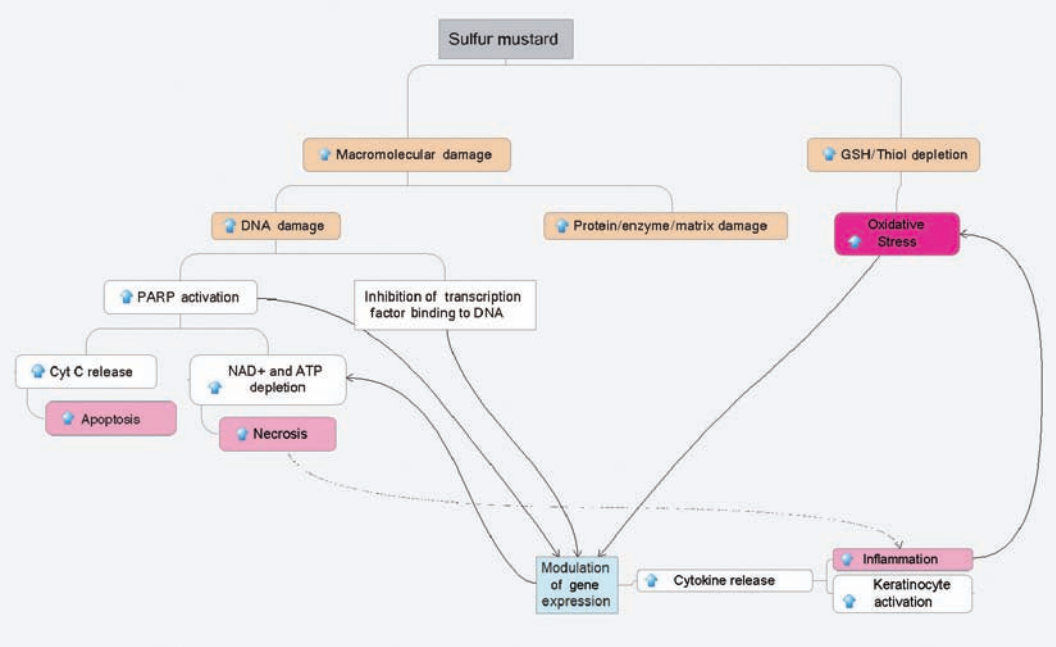

Figure 2. Schematic representation of the hypothesized molecular mechanisms of HD toxicity in skin cells.

cells. Macromolecular damage includes DNA damage as well as covalent modification of proteins and inactivation of enzymes. HD can affect cellular proteins both directly or indirectly by influencing expression and thereby altering the function of various enzymes, causing fragmentation of the extracellular matrix and cell detachment. GSH and total cellular thiol depletion is considered to be the major source of the oxidative stress. These primary damaging events modulate gene expression and induce inflammation and oxidative stress, which finally leads to apoptosis and/or necrosis (see Fig 2).

GENERAL COUNTERMEASURES

Presently, elimination of contact, decontamination, and supportive therapies are the only primary treatments for the vesicant exposure. Respirators and protective masks are effective in preventing inhalation, and special protective clothing can be used to eliminate skin exposure. Various decontaminating agents can eliminate or effectively reduce the toxic effect of HD if used immediately after the exposure. Ambergard XE-555 Resin reactive powder, hypochlorite neutralizing solutions, reactive skin lotions, and absorbent powders can be used to remove HD from human skin. Substantial HD reservoirs can be found in human skin even 24 hours after exposure.[12] These reservoirs can account for up to 35% of the total dose, and it is important, therefore, to develop decontaminating techniques capable of the removing such reservoirs thereby reducing further skin and systemic damage. Graham et al[13] have provided an excellent review of the strategies and current therapies for treating

cutaneous HD toxicity and promoting wound healing. An optimal therapeutic approach is, however, still lacking.

In this review, we will focus on the potential role of antioxidant therapy; we will review the data from in vivo and in vitro models, suggesting that oxidative stress is an important molecular mechanism underlying HD toxicity and that antioxidants can be therapeutically useful. The strengths and limitations of the in vivo and in vitro models will be detailed.

MUSTARD GAS/ANALOG-INDUCED OXIDATIVE STRESS IN ANIMAL MODELS AND THE EFFECTS OF ANTIOXIDANTS

Detailed information about HD toxicity to human skin, especially at the molecular level, is very limited. Animal models are, therefore, the major source of information about the pharmacokinetics and the molecular mechanisms of HD skin toxicity. Unfortunately, there is no animal model that exactly mimics the development of HD injury in human skin. Young swine and miniature swine skin are, however, considered to be the best models since they have a similar skin structure (epidermis, dermis, and subcutaneous tissue) and barrier function. Furred animals are poor models probably because their skin is not as well keratinized as human skin, thereby permitting more rapid penetration of drugs or toxins.

Despite limitations, the mouse ear model, the rabbit, the hairless guinea pig, the nude mouse, and the weanling swine have all been useful for studying the (1) pathophysiology, (2) molecular mechanism of action, and (3) efficacy of countermeasures for HD injury. Studies on the Yucatan mini-pig have demonstrated that laminin in the dermo-epithelial junction is a target for partial protease degradation following HD exposure. The protease cleavage of laminin networks may account for the blistering effect of HD.[14] The logistics of dealing with even miniature swine has, however, limited their use in HD studies.

In 2002, Naghii[15] reviewed much of the existing literature connecting HD toxicity and oxidative stress and suggested that further studies in animal models were well justified. Direct evidence for free radical formation in rat lung lavage following inhalation of HD vapor has been obtained by using electron paramagnetic resonance (EPR) and spin trapping techniques.[16] These studies show a rapid formation of ascorbyl radicals followed by the formation of carbon-centered radicals.[16]

Elsayed et al[17,18] have demonstrated that subcutaneous injections of either a butyl 2-chloroethyl sulfide (a monofunctional mustard analog) or 2-chloroethyl 4-chlorobutyl sulfide (a bifunctional mustard gas analog) in animal models caused an elevation in lung tissue lipid peroxidation as assayed by the thiobarbituric acid (TBA) assay. The TBA assay is, however, not very specific: rather then directly measuring levels of lipid hydroperoxide, this assay is generally considered a measure of total "thiobarbituric acid reactive substances" (TBARS). Total (GSH+GSSG) and oxidized (GSSG) glutathione contents in lung tissue were found to increase 1 hour and 24 hours after subcutaneous injection of butyl 2-chloroethyl sulfide.[18] Subcutaneous injection of 2-chloroethyl 4-chlorobutyl sulfide was associated with increased GSSG and decreased GSH at 1 hour postexposure. The increased formation of GSSG and TBARS in lung tissues following subcutaneous injection of mustard analogs is consistent with oxidative stress and suggests that dermal exposure can impact distal organs. This notion is supported by the work of Vijayaraghavan et al,[19] who found that dermally applied HD induces hepatic lipid peroxidation and GSH depletion in mice. In

this study, the generation of malondialdehyde (MDA) was used as an indirect measure of lipid peroxidation Vitamin E or flavonoids, while not influencing hepatic GSH depletion, did reduce MDA levels, suggesting a therapeutic potential.[19]

The effects of topically applied HD on key antioxidant enzymes has been measured but with conflicting results. For example, Husain et al[20] found that HD decreased the levels of glutathione peroxidase in white blood cells, spleen, and liver compared to control. Elsayed et al,[18] however, found an increased level of glutathione peroxidase compared to controls. Elsayed[17] interpreted the increased level of glutathione peroxidase (and other antioxidant enzymes) as an upregulation in response to oxidative stress, whereas Husain et al[20] interpreted the decreased levels of glutathione peroxidase as a potential cause of oxidative stress. Careful in vitro work with purified enzymes may help clarify these issues.

Despite the importance of skin itself as a primary target for HD toxicity, this organ has not been extensively studied with respect to oxidative stress. Yourick et al,[21] using the hairless guinea pig model, analyzed the skin NAD+ and NADP+ content as a function of time after HD exposure. Skin NAD+ content was found to decrease to a minimum after 16 hours (20% of control) whereas NADP+ levels increased (260%) between 1 and 2 hours and returned to control levels at 4 hours. This marked increase in NADP+ levels was thought to be an early marker of oxidative stress and a contributory factor for HD toxicity.[21] Increased NADP+ levels are a result of increased NADPH consumption: NADPH is a major source of reducing equivalents for key antioxidant enzymes such as glutathione reductase/peroxidase and thioredoxine reductase/peroxidase and lack of NADPH would be a source of oxidative stress.

The data present above support the view that diminished antioxidant protective mechanisms are a consequence of HD exposure. It is less clear, however, whether or not the resulting oxidative stress is a direct contributing factor to mustard toxicity or a secondary effect due to inflammation. In any event, the ability of exogenous antioxidants (as discussed below) to decrease HD toxicity supports the hypothesis that decreasing oxidative stress and/or inflammation is a viable therapeutic strategy.

Antioxidant protection in animal models

As early as 1985, work by Vojvodic et al[22] demonstrated that vitamin E was very effective in extending the survival time of rats acutely poisoned by HD. Vitamin E is, however, a generic term referring to at least 4 different tocopherols (alpha-, beta-, gamma-, and delta-) and 4 tocotrienols (alpha-, beta-, gamma-, and delta-). The particular form of vitamin E used in the Vojvodic et al experiments was not specified.[22] Vitamin E is generally considered to be the primary lipid soluble antioxidant but it is now recognized that vitamin E has important "nonantioxidant" roles in modulating various signal transduction and gene regulation pathways.[23–25] Moreover, the different chemical forms of vitamin E are now known to have distinct chemical and biological properties.[26,27] It is important, therefore, to specify the particular chemical and stereochemical form of vitamin E used in a given experiment.

Superoxide dismutase (SOD, EC 1.15.1.1) is a key antioxidant enzyme that catalyzes the dismutation of superoxide radicals into oxygen and hydrogen peroxide. Eldad et al[28] studied the therapeutic role of both Cu-Zn-SOD (cytosolic form) and Mn-SOD (mitochondrial form) in HD skin damage, using the Hartley guinea pig model. Pretreatment of the animals

by intraperitoneal injection with either form of SOD resulted in a dramatically reduced skin lesion area induced by HD.[28] Treatment with SOD was, however, not effective when given 1 hour after HD poisoning.[28] These data strongly suggest that superoxide radicals play a key role in HD-induced skin toxicity. Superoxide radicals alone are not a particularly damaging form of free radicals but they rapidly react with nitric oxide radicals to form peroxynitrite, which is a potent oxidant capable of causing tissue damage.[29–31]

HD and its analogs are alkylating agents that chemically react with and deplete biological thiols such as GSH, which is a key intracellular antioxidant. By promoting ROS generation and lipid peroxidation (as discussed above), HD will also promote the consumption of GSH and a reduced level of NADPH (see above) will inhibit the regeneration of GSH from GSSG. It is reasonable, therefore, that exogenous GSH or *N*-acetyl-L-cysteine (NAC) would help minimize oxidative stress induced by HD or its analogs. Kumar et al[32] tested the potential protective effect of GSH given to Swiss albino female mice following acute exposure to HD by either inhalation or percutaneous routes. GSH was administered by intraperitoneal injection and the dose was 400 mg/kg of body weight, which translates into about a 20 mM concentration in blood. Survival time following inhalation exposure to HD was increased by GSH administration as well as 2 other antioxidants: trolox (6-hydroxy-2,5,7,8-tetramethylchroman-2-carboxylic acid), which is a water-soluble derivative of alpha-tocopherol, and quercetin, which a flavonoid.[32] Inhalation exposure to HD depleted hepatic GSH levels, and increased hepatic and lung lipid peroxidation (as indirectly measured by MDA levels), and exogenous GSH was able to reduce lung and hepatic lipid peroxidation as well as prevent GSH depletion in these tissues.[32] None of the 3 antioxidants tested were able to significantly increase survival time following percutaneous exposure to HD but exogenous GSH was effective in preventing GSH depletion in blood and liver. Surprisingly, lung levels of GSH were not altered by percutaneous HD exposure.[32] The data present in work by Kumar et al[32] show that the potential effectiveness of antioxidant therapy is dependent on the route of HD exposure.

The role of GSH and NAC (and other antioxidants) in attenuating acute lung injury by 2-chloroethyl ethyl sulfide (CEES) has recently been studied in a rat model in which lung damage was quantitatively measured by the extravasation of.^{125}-I-bovine serum albumin into the extravascular compartment.[33,34] CEES is a monofunctional analog of HD that has proven very useful in mimicking HD exposure. When the experimental animals were depleted of either complement or neutrophils prior to CEES exposure (by intrapulmonary injection) lung damage was significantly decreased.[34] Neutrophil depletion was accomplished by IP injection of rabbit anti-serum to rat polymorphonuclear neutrophils and complement depletion by IP injections cobra venom factor.[34] Antioxidants such as catalase, dimethyl sulfoxide, dimethyl urea, resveratrol, and NAC all provided significant protection in this animal model.[34] NAC (an acetylated form of L-cysteine) can directly function as free radical scavenger and its metabolites are capable of stimulating GSH synthesis.[35] NAC was found to be the most effective antioxidant among those tested[33,34] and was effective even when given up to 90 minutes after lung exposure to CEES.

In the work of McClintock et al,[33] NAC was superior to GSH. In vitro by Gross et al[36] found that pretreatment of human peripheral blood lymphocytes (PBL) with 10 mM NAC elevated GSH level to 122% of untreated control but caused only a partial protective effect on HD-induced cytotoxicity. These researches also noted work by Meister and Anderson, suggesting[37] that exogenously added GSH does not appear to enter the cell very **[AQ1]**

effectively. This may help explain why NAC is superior to GSH in the work by McClintock et al.[33]

Bhat et al[38] have studied the potential therapeutic use of lipoic acid to decrease oxidative stress and mustard gas toxicity in a rat model. Lipoic acid is a disulphide derivative of octanoic acid, and it is known to be a crucial prosthetic group for various cellular enzymatic complexes. Lipoic acid has been identified as a potent antioxidant and a potential therapeutic agent for the prevention or treatment of pathological conditions mediated via oxidative stress, as in the case of ischemia-reperfusion injury, diabetes, radiation injury, and oxidative damage of the central nervous system.[39–43] Lipoic acid is taken up and reduced by cells to dihydrolipoate, a more powerful antioxidant than the parent compound, which is also exported to the extracellular medium; hence, protection is affected in both extracellular and intracellular environments. Both lipoic acid and dihydrolipoate, in addition to their direct antioxidant properties, have been shown to regenerate, through redox cycling, other antioxidants such as vitamin C and vitamin E, and to raise intracellular glutathione levels.[44,45] Bhat et al[38] found that lipoic acid pretreatment decreased the levels of lipid peroxidation (measured as MDA) in lung, skin, and eyes in HD treated rats but was not effective posttreatment.

Antioxidant liposomes as a potential countermeasure

Antioxidant liposomes may represent an optimal means of treating HD-induced skin lesions. The authors' laboratory is currently testing this hypothesis. The term "antioxidant liposome" is relatively new and refers to liposomes containing lipid soluble chemical antioxidants, water-soluble chemical antioxidants, enzymatic antioxidants, or combinations of these various antioxidants. Antioxidant liposomes hold great promise in the treatment of many diseases and conditions in which oxidative stress plays a prominent role.[46,47] The relative ease of incorporating hydrophilic and lipophilic therapeutic agents into liposomes; the possibility of directly delivering liposomes to an accessible body site; and the relative nonimmunogenicity and low toxicity of liposomes have rendered this system highly attractive for drug delivery. Moreover, several studies have clearly indicated that the liposomal antioxidant formulations, compared to that of the free nonencapsulated antioxidants, exert a far superior protective effect against oxidative stress-induced tissue injuries.[48]

Experimental studies have shown that liposomes and their constituents effectively penetrate skin.[49,50] Topical application of antioxidant-liposomes is likely, therefore, to be particularly effective in enhancing the antioxidant status of skin. Work by Kirjavainen et al[49] suggests that liposomes containing dioleylphosphatidyl ethanolamine (DOPE) are better able to penetrate into the stratum corneum than liposomes without DOPE. Similarly, ultradeformable liposomes, lipid vesicles with special membrane flexibility due to incorporation of an edge activator such as sodium cholate, have been shown to be superior in comparison to ordinary phosphatidylcholine liposomes (see http://www.skinforum.org.uk/abstracts/ebtassam-essa.php).

At present there are no data on the potential use of antioxidant liposomes in treating HD-induced skin lesions but McClintock et al[33] have found that liposomes containing pegylated (PEG) catalase, PEG-SOD, or the combination were very effective in reducing

CEES-induced lung injury in a rat model. Similarly, liposomes containing NAC, GSH, or resveratrol also were effective according to this study.

In vitro studies using human skin models

Keratinocyte cell lines

In vivo models are essential for testing countermeasures to HD or its analogs, however, in vitro models are also critical for rapid screening of potential therapeutic agents and for detailed studies at the molecular level. Skin is the largest organ of the human body with a complicated multilayer multicell type structure. As mentioned above, there is no model system perfectly mimicking human skin. Normal or immortalized human keratinocytes cultured on plastic as a monolayer represent the simplest and least inexpensive model and are suitable for an initial approach for HD toxicity studies. Normal human epidermal keratinocytes (NHEK) isolated from adult or infant fetal skin tissue are available commercially. These cells are easy to handle, can be frozen for long-term storage but require special medium containing a mixture of growth factors.[51] Even then, NHEK cells spontaneously transform after 3–5 passages as they continuously undergo terminal differentiation.

Nevertheless, NHEK remains the only commercially available normal cell line possessing all of the structural and functional features of normal skin keratinocytes and is being used by many investigators to study mustard gas toxicity.[52] However, the requirement of special growth medium and a short lifespan make this model more expensive than immortalized human keratinocytes such as human pappiloma virus (HPV)–immortalized cell lines or spontaneously immortalized HaCaT cells. There are also a number of commercially available human keratinocyte cell lines immortalized via transfection with DNA coding E6 and/or E7 viral oncoproteins. All of these cell lines still require special medium with growth factors and, like NHEK, have a limited lifespan since they spontaneously transform after 10 to 15 passages.[53]

The HaCaT cell line, originating in Germany, has recently become commercially available; it represents spontaneously immortalized adult human keratinocytes.[54] HaCaT cells are extremely easy to handle and do not require special medium. Theoretically, HaCaT cells have an unlimited lifespan but they do show morphological changes after 10 to 20 passages. Despite the altered growth potential, HaCaT cells still express differentiation-specific markers[54] and unlike HPV-immortalized cell lines, HaCaT cells are not tumorigenic when transplanted into nude mice.[54]

It is well known that HD, like UV radiation, affects mostly proliferating keratinocytes within the lower dermis and basement membrane. Differentiating keratinocytes of the epidermis are much less susceptible to toxicity since they do not undergo apoptosis and respond weakly to inflammatory stimuli. Normal keratinocytes undergo terminal differentiation (so-called "cornification") in response to a high (1 mM) exogenous Ca^{++} concentration.[51] Normal keratinocytes in vivo start to differentiate when they detach from the basement membrane and migrate to the suprabasal layers.[55] Thus, NHEK and HPV-immortalized keratinocytes, unlike HaCaT cells, spontaneously differentiate when subcultured in response to the cell detachment. Therefore, only the first passages of NHEK cells are truly proliferating, whereas every passage of HaCaT culture consists of proliferating cells. On the other hand, HaCaT cells show impaired production and release of IL-1[56] which is crucial for normal

keratinocyte proliferation and also plays an important role in keratinocyte activation and keratinocyte/fibroblast crosstalk in normal skin.[57]

As previously acknowledged, HD-induced depletion of intracellular glutathione (GSH) is a triggering event for oxidative stress in skin. Smith et al[58] have shown that pretreatment of the human keratinocyte cell line, SVK-14, with GSH markedly increases the resistance to HD-induced cytotoxicity. Conversely, pretreatment with buthionine sulfoximine (BSO) increases the sensitivity of G361, SVK14, HaCaT, and NCTC 2544 human keratinocytes to HD toxicity.[59] BSO lowers intracellular GSH by irreversibly inhibiting the rate-limiting GSH synthesis enzyme γ-glutamylcysteine synthetase. Surprisingly, there is no reported direct evidence to date for the enhanced generation of ROS and/or RNOS in HD-treated keratinocytes.

As pointed out earlier, HD and its chemical analogs cause massive leukocyte infiltration in animal skin and lungs[60,61] It is likely that lymphocytes and macrophages, attracted to the burned area by cytokines released from keratinocytes/fibroblasts, could be a major source of oxidative stress to skin cells. It has been demonstrated that HD-exposed NHEK cells express chemoattractants such as TNF-α, IL-1β, IL-8, and GM-CSF.[62–64] Moreover, an enhanced ability of NHEK cells to attract lymphocytes in vitro was demonstrated in an experiment in which the media from HD-treated keratinocytes was tested for chemoattractant activity to polymorphonuclear leukocytes purified from human blood.[65]

Multilayer keratinocyte tissues

Multilayer skin tissues (so-called "3D skin models") are a more realistic model for toxicological studies. The simplest models of this class consist only of keratinocytes such as the commercially available Epiderm, which is a few millimeters thick structure of human NHEK cells grown on top of a wet membrane. Epiderm provides the possibility of applying HD (or other gaseous agents) in vapor or aerosol form which closely simulates a real HD attack. However, this model represents differentiating keratinocytes on a collagen matrix and practically all of the cells within the tissue start to cornify at the moment they are fully grown. Blaha et al[66–68] have characterized the ultrastructural, histological, and molecular response of the Epiderm model to CEES. The Epiderm system not only has great potential for identifying and developing sulfur mustard therapeutic agents but also has limitations. In vivo, skin damage would be accompanied by the rapid leakage of serum, leukocyte infiltration, and perhaps mast cell degranulation (see below) but these events will not occur in any of the available in vitro skin models.

More advanced tissue models, like EpidermFT full thickness skin tissue model, consist of 2 cell types: a bottom layer of human fibroblasts imbedded in gelatin and an upper multilayer of human keratinocytes. This particular model is particularly valuable for studies involving paracrine signaling (keratinocyte/fibroblast interactions). HaCaT cells, with normal human or mouse fibroblasts, have also been used to construct 3D models of human skin. However, the impaired IL-1 production in these cells presents some technical difficulties that can be overcome with the addition of human growth factors.[56] These multilayer skin models morphologically mimic the dermis and epidermis of human skin including the cuboidal appearance of the basal cell layer, the presence of the stratum spinosum and stratum granulosum with typical stellate-shaped keratohyalin granules, and the presence of numerous lamellar bodies that are extruded at the stratum granulosum–stratum corneum interface.

In a key experiment, Blaha et al[67] compared the effects of CEES on the secretion of key inflammatory mediators using 2 model human skin systems, the Epiderm system (from MatTek Corporation) and the Skin2 system (a 3D skin model) from Advanced Tissue Sciences, which consists of differentiating keratinocytes on a fibroblast-collagen matrix. In the Skin2 system, the proinflammatory cytokine IL-1alpha increased in response to CEES but the proinflammatory cytokine IL-6 decreased: the Epiderm showed undetectable levels of IL-6 and the levels of IL-1alpha did not change in response to CEES.[67] These data show that the presence of fibroblasts in the Skin2 model dramatically changes the cytokine secretion response to CEES.

More recently, Hayden et al[69] evaluated the effects of HD on the EpiDermFT skin model which has a 3D, highly differentiated human skin-like structure with an epidermis and a dermis. This in vitro model permits the study of dermal phenomena in which fibroblast-keratinocyte cell interactions are important as appears to be the case for CEES-induced skin injury (see above). Hayden et al[69] treated the EpiDerm-FT model with HD for 8 minutes and evaluated the structural effects at 6 and 12 hours postexposure. Histological analyses showed typical HD targeting of basal keratinocytes (cytopathology, condensed chromatin, pyknotic nuclei, and increased eosinophilia) and epidermal cleavage at the dermal/epidermal junction. Transmission electron microscopy showed that lamina densa of the basement membrane to be largely intact. The EpiDerm-FT model represents a major advance in the development of human skin models and its use in studying the molecular mechanisms/proteomics for HD/CEES toxicity is just beginning to be exploited.

Human skin allografts in immunodeficient mice

A third class of human skin model is provided by the use of human skin allografts in immunodeficient mice. Human skin cells, either genetically modified[70] or normal,[71] were grafted onto nude mice and successfully used to examine HD-induced biochemical alterations in skin. In 1995, Rosenthal et al[70] described an engineered human skin model, in which human keratinocyte clones, with some genetic modifications, were grafted onto nude mice, where they formed histologically normal human skin. Later, the same group reported an advanced model developed in immunodeficient nude mice, where a pellet of cells containing human keratinocytes and fibroblasts were placed on top of the muscular layer at the graft site and grown for 1 week.[71] Glass bulbs filled with HD can be directly applied to the sections of mouse skin containing the human skin allograft. Although these in vivo models are expensive and complicated, they possess a number of advantages over any of the in vitro cultured skin models. Grafted human skin models make it possible to obtain a detailed picture of HD-induced morphological, ultrastructural, and inflammatory alterations in various layers of skin cells possessing the realistic complexity of multiple cell–cell interactions. Recently, 3D human skin allografts in mice have allowed investigators to identify distinctive prevesication and postvesication phases and to monitor both dermal-epidermal separation and basal membrane alterations in response to HD exposure.[72,73] However, a limitation of this model is the lack of a functional immune response in the recipient mice.

In spite of the ever higher degrees of physiological complexity, there is not a single model that reflects all the features of human skin. The choice of a particular model may, therefore, be dictated by the particular experimental design and goals. Wound healing studies, for example, would require an in vivo system with an intact immune system since

immune cells are known to contribute to skin regeneration. Moreover, immune cells are thought to play important roles both in HD-induced skin inflammation and in postexposure wound healing through the expression of proinflammatory cytokines (such as Il-1β, TNF-α, IL-6, and GM-CSF) within the first hour after exposure and proceeding through vesication and blister formation.[64] Leukocyte infiltration always starts shortly after HD treatment in mice, rabbits, or guinea pigs. In wound healing, leukocytes and macrophages provide many of the molecular signals regulating fibroblast and keratinocyte proliferation.

The effects of HD on all of the various cell types that come in contact with skin, including macrophages and mast cells, are also important in understanding the overall effects of HD on skin in vivo. Rikimaru et al[74] have used full-thickness human skin explants to study inflammatory mediators in response to topically applied HD. These investigators found that culture fluids from the HD-treated skin contained increased levels of histamine, plasminogen-activating activity, and prostaglandin E2 compared to control explants. It was concluded that both mast cells and epidermal cells were apparently involved in early mediation of the inflammatory response to HD.[74] In contrast, Inoue et al[75] found that the inflammatory response of the mouse ear to HD did not differ in mast cell deficient mice compared to normal mice. At present, there is no obvious explanation for the differences observed between the work of Rikimaru et al[74] and that of Inoue et al[75] It may well be that the mouse ear is not an optimal model for human skin. It is critically important to determine whether HD, or other toxic vesicants, degranulate mast cells since this process could be a major source of inflammatory mediators and, therefore, a major factor in modulating the immune response to HD. In particular, mast cell degranulation would release large amounts of TNF-alpha, which is an inflammatory cytokine.

We have previously reported that lipopolysaccharide (LPS) as well as other inflammatory factors such as TNF-alpha and IL-1-beta amplify the toxicity of CEES[76] and that CEES is a potent inhibitor of nitric oxide production from inducible nitric oxide synthase (iNOS).[77] LPS is a major component of the cell wall of gram-negative bacteria and is known to trigger a variety of inflammatory reactions in macrophages and other cells having CD14 receptors.[78,79] In particular, LPS is known to stimulate the macrophage secretion of nitric oxide[80] and inflammatory cytokines such as tumor TNF-alpha and IL-1-beta[81] Figure 3 shows that RAW 264.7 macrophages stimulated with LPS at 100 ng/mL are markedly more susceptible ($P < .05$) to CEES cytotoxicity (24 hours with 500 μM) than resting macrophages as indicated by a dramatic drop in dehydrogenase activity as measured by the MTT ((3-(4,5-dimethylthiazol-2-yl)-2,5-diphenyltetrazolium bromide) assay. In the absence of LPS, CEES at a level of 500 μM did not significantly affect cell viability.[76] Figure 4 shows that CEES (100–500 μM for 24 hours) inhibits the secretion of nitric oxide into the cell medium by LPS stimulated macrophages in a dose-dependent manner[77] In these experiments, nitrite secretion into the cell culture medium was used as a measure of nitric oxide synthesis. Macrophages (and mast cells) are both present in dermal tissues.

IgE-mediated mast cell degranulation is known to be inhibited by nitric oxide production.[82] NO is a powerful antioxidant[83] and increased intracellular levels of NO are known to inhibit mast cell degranulation.[84] Significantly, mast cell degranulation and histamine release are stimulated by membrane lipid peroxidation and inhibited by antioxidants such as alpha-tocopherol.[85] Collectively, the information presented above suggests that HD/CEES could induce mast cell degranulation by increasing oxidative stress and/or

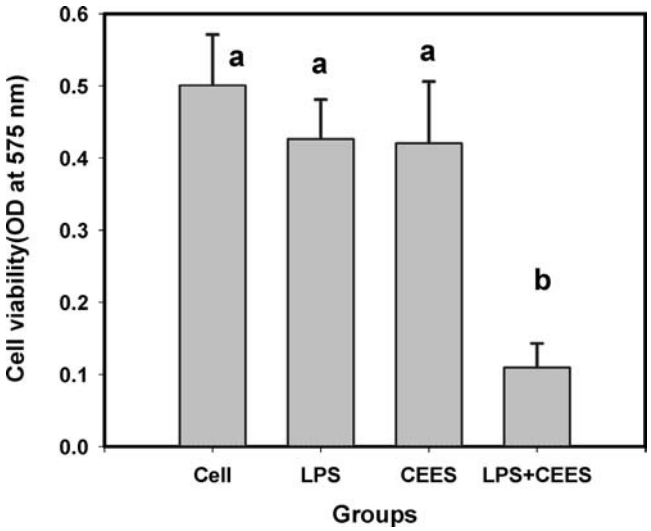

Figure 3. LPS (100 ng/mL) enhances the cytotoxicity of CEES (500 μM). Means not sharing a common letter are significantly different ($P < .05$). Cytotoxicity was measured after 24 hours by the MTT assay.

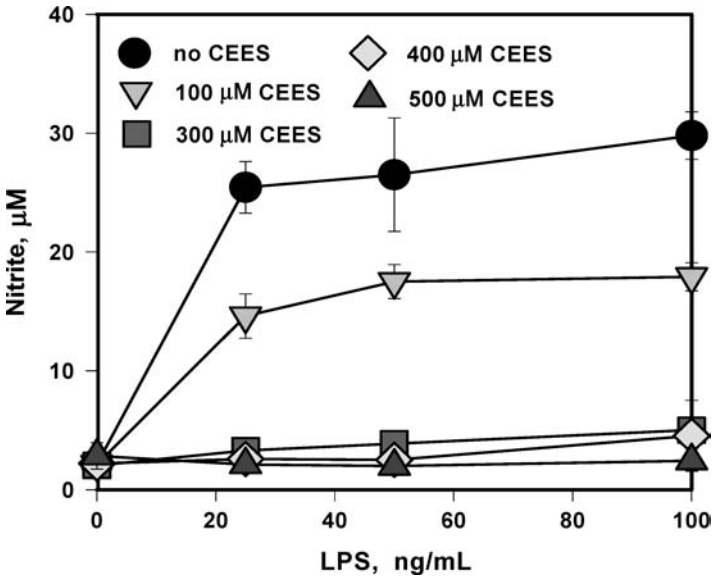

Figure 4. CEES inhibits NO production in LPS stimulated RAW 264.7 macrophages. Cells were simultaneously treated with various levels of CEES (as indicated) and low doses of LPS (as indicated). NO production was monitored as the concentration of nitrite in the culture media after 24 hours.

decreasing nitric oxide production. The subsequent release of TNF-alpha could enhance the cellular toxicity of HD/CEES.

NO generation, mediated by iNOS, is also crucial for the rapid healing of human skin wounds. Although, keratinocytes are known to express iNOS and generate NO in wound healing, it is likely that macrophages, known for their ability to express iNOS and generate high levels of NO, also contribute to the healing stimuli. Thus, it is tempting to suggest that the development of a 3-cell-type (macrophages/fibroblasts/keratinocytes) model would provide a unique and optimal model for studying skin vesication, blistering, and wound healing under very reproducible experimental conditions.

MOLECULAR MECHANISMS FOR MUSTARD TOXICITY

The molecular mechanisms of HD skin toxicity are complex and not yet fully understood. We will focus on 3 major types of interrelated events: primary macromolecule damage, oxidative stress, and inflammation. All of these processes are tightly interconnected and play central roles in HD toxicity. The hypothesized mechanisms of HD toxic effect in skin cells are summarized in Figure 2. In addition, we will discuss the importance of NO signaling modulation in HD toxicity since it is likely to be important for the postexposure wound healing process in skin.

Primary macromolecule damage

HD easily penetrates both cellular and nuclear membranes due to its hydrophobic nature. In the cytosol, it reacts with water forming a highly electrophilic ethylene episulfonium derivative that is the ultimate alkylating agent. DNA alkylation and crosslinking are well-documented primary intracellular damaging reactions of HD. Extensive DNA damage, due to alkylating agents, activates and overloads the DNA repair machinery. In particular, DNA damage induces expression of poly (ADP-ribose) polymerase (PARP), the key regulatory enzyme involved in DNA repair and hypothesized to regulate cell fate by modulating death and survival transcriptional programs.[86] HD induces PARP expression in normal human keratinocytes and the possible involvement of this nuclear enzyme in the regulation of HD cell death mechanisms has been extensively studied.[87–91]

PARP-1 is the most abundant member of the of PARP protein family. PARP-1 binds to DNA structures that have single- and double-strand breaks, crossovers, cruciforms, or supercoils[92]; it signals DNA rupture and facilitates base-excision repair.[93,94] Normally, the intracellular level of PARP-1 is very low, and this enzyme can be detected in the cytosol only under stressful conditions. Upon binding to the damaged DNA sites, PARP-1 metabolizes β-nicotinamide adenine dinucleotide (NAD^+) into branched polymers of ADP-ribose that are transferred to a set of nuclear proteins. This process also results in a very large decrease in the pyridine nucleotide pool. Poly(ADP-ribosyl)ation is thought to be beneficial for genome repair since modifications of proteins proximal to the DNA breaks facilitate multiple local openings of the condensed chromatin structure allowing the binding of the repair protein complex.[93,95]

Despite the beneficial effect, PARP can induce apoptosis or necrosis in skin cells treated with HD[91] or other alkylating agents.[86,96] Thus, limited expression of PARP proteins helps in DNA repair and promotes cell survival but its overexpression (as in case of massive DNA damage) can induce cell death.[97] PARP overproduction, especially in cells utilizing aerobic glycolysis, can lead to the depletion of cellular NAD^+ and ATP (see Fig 2) which rapidly promotes general intracellular bioenergetic collapse and oxidative stress resulting in a regulated form of necrosis.[86,96,98–100] HD is cytotoxic to both dermal fibroblasts and epidermal keratinocytes. It has been suggested that PARP determines the mode of HD-induced cell death in skin fibroblast but not in keratinocytes.[91] In mouse skin fibroblast the absence of PARP shifts the mode of HD-induced cell death shifts from necrosis to apoptosis,[91] whereas keratinocytes, with or without PARP, primarily express an apoptotic form of cell death.[91] HD-treated human keratinocytes show a PARP activation, an upregulation of proapoptotic p53 accompanied by a downregulation of antiapoptotic Bcl-2, and, finally, to caspase activation and apoptosis.[87,90] This pathway was found to be Ca^{++} and calmodulin dependent.[90]

Necrosis due to PARP-induced depletion of NAD^+ and ATP exhaustion during aerobic glycolysis is thought to be the main mechanism of cell death induced by DNA damaging agents, especially in proliferating cells.[96] However, these observations may vary with the dose of alkylating agent, with cell type and perhaps the particular composition of the culture medium (see below) in the case of in vitro studies. HD promotes apoptosis in HeLa cells (10–100 μM),[101] peripheral blood lymphocytes (6–300 μM),[102] keratinocytes (50–300 μM),[53,87] and endothelial cells (<250 μM).[103] A time-dependent shift to necrosis was observed in HD-treated lymphocytes.[102] but a shift toward necrosis is observed at higher levels of HD in endothelial cells (>500 μM)[103] and HeLa (1 mM)[101] Interestingly, human fibroblasts undergo necrosis even at lower concentrations of HD (100–500 μM).[91] In most human cell types, apoptosis predominates within 6–12 hours of postexposure time, whereas necrotic events markedly increase after 12–24 hours.

Countermeasures capable of preventing rapid ATP depletion and mitochondrial dysfunction could be protective against HD-induced necrosis. Unfortunately, this approach would not eliminate cell death completely since apoptosis would likely proceed. However, a shift from necrosis to the less inflammatory apoptotic pathway could possibly be beneficial by helping eliminate secondary infections and improving wound healing. PARP activation causes NAD^+ depletion and NAD+ is required for glycolysis and pyruvate synthesis.[104] In the absence of pyruvate, mitochondrial respiration fails causing bioenergetic collapse and cell death via necrosis.[86] Therefore, the addition of a mitochondria substrate, such as pyruvate, glutamate, or glutamine, to the cell medium could be protective against necrosis.[104] A protective effect of pyruvate treatment has, indeed, been documented in genotoxic stress caused by nitrogen mustard or *N*-methyl-*N*′-nitro-*N*-nitrosoguanidine (MNNG), a chemical analog of HD used as anticancer drugs.[96,100,104]

Alkyl pyruvates, such as methyl pyruvate and ethyl pyruvate, are excellent alternative mitochondrial substrates since they (unlike pyruvate) are stable in solution. In aqueous solutions, pyruvate spontaneously undergoes a series of chemical reactions yielding 2, 4-dihydroxy-2-methylglutarate, which is a mitochondrial poison.[105] In addition, alkyl pyruvates also function as effective and potent scavengers of free radicals. Pyruvates are capable of scavenging hydrogen peroxide (H_2O_2) and the hydroxyl radical (OH&rad;$^-$).[106,107] Administration of pyruvates was shown to protect against various types of oxidant-mediated

cellular and organ injuries in numerous in vitro and in vivo studies.[108,109] These data further suggest that HD activation of PARP and the subsequent depletion of pyruvate is also a contributing factor for HD-induced oxidative stress.

In preliminary results, the authors' laboratory has observed that methyl pyruvate provides protection to human keratinocytes (HaCaT cell line) treated with CEES and a similar effect was observed with ethyl pyruvate (unpublished data). It is worth noting that commercially available serum-free media, formulated to culture NHEK cells, contains 0.5 mM sodium pyruvate. Keratinocyte media from Gibco, Sigma, and Cambrex all contain 0.5 mM pyruvate. It is possible, therefore, that necrosis has not been observed in HD-treated NHEK cells due to the protective effect of sodium pyruvate in the culture media.

In our experiments (unpublished data), however, we used immortalized HaCaT keratinocytes, which proliferate continuously but do not differentiate. Actively proliferating cells utilizes aerobic glycolysis and are more susceptible to mitochondrial dysfunction and necrosis.[86,96,100] After limited number of passages NHEK cells, unlike HaCaT cells, undergo terminal differentiation which is a form of cell death different from either apoptosis or necrosis.[55] This difference between HaCaT and NHEK cells theoretically could cause discrepancies in the cell death pathway caused by HD. Parallel experiments are now being done with NHEK and HaCaT cells to further characterize the protective effect of pyruvate to HD/CEES.

Inflammation

HD-treated normal human keratinocytes release proinflammatory TNF-α, IL-6, IL-1β in a dose-dependent manner[62] but the particular cytokine profiles observed differ depending on the skin model used and the dose of HD.[63,64,110] Cytokine production and responses are known to be regulated by the activation of nuclear transcription factor-kappaB (NF-kappaB) and this activation also plays a key role in determining the fate of a damaged cell. There are numerous activators of NF-kappaB such as bacterial and viral infections, chemical damage, radiation, and oxidative stress. In response to these stimuli, an active NF-kappaB protein complex is liberated in the cytoplasm and it subsequently translocates to the nucleus and triggers selective gene expression. Among the genes regulated by NF-kappaB are adhesion molecules, pro-inflammatory mediators (IL-1 beta, TNF-alpha, interleukin 6), chemokines, IL-8, iNOS, E-selectin, vascular cell adhesion molecule 1 (ICAM-1), and granulocyte-macrophage colony stimulating factor (GM-CSF).[34,111–114] In general, NF-kappaB activation also triggers antiapoptotic genes and promotes cell survival.

Although the precise mechanism(s) of HD-induced gene expression has not yet been fully described in skin cells, it is very likely connected to the DNA damaging effect of HD (see Fig 2) and could, therefore, be PARP-dependent. PARP-1 is known to be a coactivator of NF-kappaB.[115]; however, this pathway has not been fully explored in HD-treated keratinocytes or fibroblasts. It is also possible that HD modulates NF-kappaB and other nuclear factors by covalently modifying DNA binding sequences for transcription factors. Grey et al[116] have shown that HD inhibits the in vitro binding of transcription factor activating protein-2 (AP-2) via alkylating the AP-2 DNA consensus binding sequence rather than by direct damage to the AP-2 protein.

In addition, it is highly possible that HD-induced oxidative stress also can stimulate inflammatory responses via transcription factors. Many of the activators of NF-kappaB can

be blocked with the use of antioxidants.[117,118] Transcription factors AP-1,[119,120] MAF and NRL,[121,122] and NF-IL6[123,124] are regulated by oxygen-dependent mechanisms, and sensitive to ROS. Interestingly, chemical compounds indirectly disrupting NF-kappaB activation induce apoptosis in cancer cells,[125–130] whereas inhibitors of NF-kappaB activation protect HD-treated human keratinocytes.[131,132]

It is also unclear how exactly the proinflammatory cytokines, such as IL-6, contribute to the HD-induced skin damage. It is known, however, that inflammatory processes contribute to the skin damage. In animal models, both skin and lung exposure to HD or CEES causes massive leukocyte infiltration, which starts shortly after the exposure and builds up continuously.[60,61] The fact that skin burns and blistering have a latent period also suggests that secondary responses in skin cells/immune cells also contribute to the mechanisms of HD toxicity. HD treatment is known to induce NF-kappaB activation and release of inflammatory cytokines in both keratinocytes and macrophages.[63,110,133–135] TNF-alpha, in general, induces apoptosis in keratinocytes and treatment with anti-TNF-alpha antibodies is protective against UV-induced skin lesions.[136] However, the effect of TNF-alpha in HD-treated skin is complex and an attempt to reduce cell death in normal human keratinocytes by blocking TNFR1, the major cell receptor for TNH-alphas was not successful.[71]

It is likely that keratinocyte activation (see Fig 2) plays an important role in HD toxicity. Activation of keratinocytes is a multistep pathway induced in response to skin injury. Activated keratinocytes are hyperproliferative and able to migrate to the site of injury in order to form layers of fresh cells in the dermis and epidermis. Activation is regulated by various cell signaling pathways including TNF-alpha.[57,137] Since HD-treated keratinocytes release high levels of TNF-alpha in the medium,[133] we suggest that HD promotes keratinocyte activation, subsequent hyperproliferation, and an enhanced susceptibility to the PARP-mediated bioenergetic collapse. This series of molecular events would cause a shift from apoptosis to necrosis. Although a time- or concentration-dependent shift from apoptosis to necrosis has been well documented for HD-treated lymphocytes,[102] endothelial cells,[103] and HeLa cells,[101] such changes have not been noted for human keratinocytes. As discussed above, this may be due to the fact that NHEK cells are always protected from necrosis by pyruvate-containing media. The recently documented protective effect of NF-kappaB inhibitors in NHEK and HaCaT cells treated with HD[131,132] also supports our speculation since these inhibitors downregulate TNF-alpha which would impair keratinocyte activation.

WOUND HEALING

NO signaling plays a key role in the inflammation and wound healing.[138–140] Animal studies[141] have shown that in iNOS knockout mice, wound healing is impaired but restored by iNOS gene transfer. Lack of NO and impaired expression of iNOS after the HD exposure are thought to be important events promoting skin burns and blistering. We have shown that HD treatment inhibits iNOS expression and NO synthesis (see Fig 4) in LPS-stimulated murine macrophages.[77] Suppression of iNOS expression and several protein activators of wound healing have also been found in human keratinocytes treated with HD.[142]

In keratinocytes, the beginning stage of the wound healing process is determined by the activation process. Under conditions of physical injury, the keratinocyte cell cycle is activated and the cells become hyperproliferative and migrate to the site of injury in response to chemokines.[57,137] Activation of keratinocytes, as well as their return to the healthy basal phenotype, is controlled by cytokines and growth factors produced by various cutaneous cell types, including keratinocytes and lymphocytes infiltrated at the wound site. Various intracellular signaling pathways are involved at the different stages of activation. Interestingly, NF-kappaB activation and consequent autocrine TNF-alpha production occur at the initial stages of the activation and allow keratinocytes to become hyperproliferative and migratory.[57,137] Activation is terminated when lymphocytes, present at the wound site, release interferon-gamma (IFN-gamma), which induces the activation of STAT-1 and makes keratinocytes contract newly deposit fibronectin-rich basement membrane. Finally, transforming growth factor-beta (TGF-beta) secreted by fibroblasts induces the expression of K5 and K14, fully reverting the keratinocytes to a healthy basal phenotype and making them responsive to differentiation stimuli.[57]

In human cells, expression of iNOS, which is the main NO-generating protein in keratinocytes,[143] is regulated synergistically by 2 major pathways: NF-kappaB and STAT-1.[144] As pointed above, both HD and its chemical analog CEES downregulate iNOS expression in murine macrophages[77]and human keratinocytes.[142] Since NF-kappaB activation is well documented in NHEK cells,[131–133] it is possible that the impaired expression of iNOS in HD-treated cells could be attributed to a STAT-1-dependent mechanisms. In addition, the possible STAT-1 inhibition by HD could disrupt the IFN-gamma signaling pathway resulting in keratinocytes unable to terminate their wound healing state.[57] Thus, simultaneous HD-induced NF-kappaB activation and STAT-1 inhibition could alter necrosis, inhibit NO generation, prevent wound healing, and possibly affect vesication and blistering.

The molecular mechanisms whereby HD alters transcription factors activation are not fully elucidated. However, it is highly possible that the ability of mustards to alkylate DNA is involved. As pointed above, HD is capable of chemically modifying both proteins (via crosslinking of Cys residues) and DNA (via alkylation of guanine rich sequences, and crosslinking). It seems likely that HD would more effectively damage "more exposed" regions of DNA with accessibility to transcription factors. Interestingly, Gray[116] had shown that HD inhibits the in vitro binding of transcription factor AP-2 via alkylation of the guanine-rich consensus DNA sequences but not by directly damaging the AP-2 protein. It is tempting to assume that other transcription factor functions could be affected by HD in a similar manner. However, the effects of HD on NF-kappaB and STAT-1α have not been elucidated and AP-2 remains the only transcription factor studied in relation to HD toxicity.

Since some transcription factors are sensitive to ROS and to the redox state of the cell in general, it is likely that oxidative stress, inflammation, and NO signaling are tightly interconnected in skin and its dynamic responses to toxic agents. Soneja et al[145] have suggested that wound healing could be accelerated under the circumstances in which oxidative stress is minimized but NO production remains elevated. On the other hand, under conditions elevating oxidative stress, the toxicity of mustards can be greatly enhanced. For instance, the HD analog CEES shows much higher toxicity in cells stimulated by LPS, TNF-alpha, or IL-1beta, which enhance inflammation and oxidative stress.[76]

FUTURE DIRECTIONS

A systems biology approach to mustard toxicity

As discussed above, HD toxicity in skin results from a multistep complex mechanism involving a number of signaling cascades and various cell types. It is extremely difficult to follow each step in this mechanism even in a simple in vitro model. A systems biology approach would view HD toxicity as time-dependent disruption of an integrated and interacting network of genes, proteins, and biochemical reactions. This approach would emphasize integrating data obtained from transcriptomics, metabolomics, and proteomics with the purpose of constructing and validating a comprehensive model of HD toxicity. The computational tools for this task would include network mapping as well as correlation, logical, and kinetic modeling.[146] This comprehensive model would be the best way to address the question: "how relevant to the HD-induced cell death pathways are the direct chemical alterations caused by HD to various cellular proteins (oxidation, cross-linking, and fragmentation) and the indirect chemical protein alterations caused by ROS and RNOS?"

A transcriptomic approach to studying HD toxicity is already yielding useful results. In NHEK cells, DNA array techniques have been applied to studying HD-altered gene expression,[147,148] and mRNA differential display has been used to examine HD-induced transcriptional modulations in human epidermal keratinocytes.[149] Microarray analyses of gene expression in CEES- or HD-exposed mouse skin in vivo have also been accomplished.[147,150] These studies are providing a deeper insight into the mechanism of HD toxicity since they have identified a number of genes upregulated at the early (0.5–4 hours) and intermediate (24 hours) stages of postexposure. DNA array analyses are capable of providing crucial information regarding the changes in transcriptional activity in the cell and are useful in the search for "the key" signaling pathways involved in HD toxicity. These studies will help in the design of evermore effective countermeasures and help identify key biomarkers for therapeutic efficacy. Proteomic data on HD toxicity are currently very limited but this approach would complement the previously accumulated microarray data by helping identify all the key proteins involved in HD toxicity at different stages.

Collectively, the literature reviewed here supports the notion that oxidative stress, free radical damage to biomolecules, and alterations in redox sensitive signaling pathways are key factors in understanding vesicant toxicology. It is likely, therefore, that the newly emerging area of redox proteomics would be particularly useful in understanding HD damage to skin. Redox proteomics is focused on characterizing (1) the chemical modifications of specific proteins induced by ROS and RNOS; (2) alterations in specific proteins induced by changes in redox sensitive transcription factors; and (3) alterations in the function/structure of specific proteins caused by redox sensitive posttranslational modifications.[151–153] In this regard, small thiols, like GSH, are no longer viewed just as protective antioxidants but as redox regulators of proteins via glutathionylation or by oxidation of protein cysteine residue.[152] Redox proteomics is rapidly emerging as a very powerful tool for characterizing and identifying proteins based on their redox state.[153] This approach has recently been used to specifically identify oxidized proteins in Alzheimer's disease and this information has proven useful in identifying new therapeutic targets and in providing new molecular insights into disease etiology.[154]

Multicomponent antioxidant liposomes

HD, due to its hydrophobic nature, effectively penetrates deep into the skin and affects mostly proliferating cells within basement membrane, that is, the lowest layer of proliferating keratinocytes. These growing cells would be highly susceptible to the PARP-mediated bioenergetic collapse since they actively utilize aerobic glycolysis. HD is likely, therefore, to induce necrosis rather than apoptosis in these cells, which would subsequently promote severe inflammation, skin blistering, and vesication. Thus, it is critically important to provide fast and efficient delivery of the desired drugs to the deeper skin layers and liposomes hold promise in this regard. By encapsulating a lipid soluble thiol, antioxidant liposomes could also effectively diminish (by direct covalent reaction) the stores of HD in skin lipid depots. Although this review has emphasized antioxidants, there is practically no limit to the possible encapsulated agents that can be incorporated into liposomes and delivered to the skin cells. These agents could include PARP inhibitors, protease inhibitors, anti-inflammatory agents, and chemical or enzymatic antioxidants. Currently, we are testing novel formulations of multiagent antioxidant liposomes containing both antiapoptotic (NAC) and antinecrotic (ethyl pyruvate) agents. Liposomes can also be formulated with agents designed to accelerate wound healing such as epidermal growth factor, transforming growth factor-β, platelet-derived growth factor, insulin-like growth factor, keratinocyte growth factor, and fibroblast growth factor.

REFERENCES

1. Somani SM, Babu SR. Toxicodynamics of sulfur mustard. *Int J Clin Pharmacol Ther Toxicol*. 1989;27:419–435.
2. Sinclair DC. Disability produced by exposure of skin to mustard-gas vapour. *Br Med J*. 1950;1:346–349.
3. Drasch G, Kretschmer E, Kauert G, von Meyer L. Concentrations of mustard gas [bis(2-chloroethyl)sulfide] in the tissues of a victim of a vesicant exposure. *J Forensic Sci*. 1987;32:1788–1793.
4. Vijayaraghavan R, Kulkarni A, Pant SC, et al. Differential toxicity of sulfur mustard administered through percutaneous, subcutaneous, and oral routes. *Toxicol Appl Pharmacol*. 2005;202:180–188.
5. Papirmeister B, Gross CL, Meier HL, Petrali JP, Johnson JB. Molecular basis for mustard-induced vesication. *Fundam Appl Toxicol*. 1985;5:S134–S149.
6. Langenberg JP, van der Schans GP, Spruit HE, et al. Toxicokinetics of sulfur mustard and its DNA-adducts in the hairless guinea pig. *Drug Chem Toxicol*. 1998;21(suppl 1):131–147.
7. Wormser U. Toxicology of mustard gas. *Trends Pharmacol Sci*. 1991;12:164–167.
8. Hay A. Effects on health of mustard gas. *Nature*. 1993;366:398.
9. Pearson GS. Veterans at risk: the health effects of mustard gas and lewisite. *Nature*. 1993;365:218.
10. Black RM, Read RW. Biological fate of sulphur mustard, 1,1′-thiobis(2-chloroethane): identification of beta-lyase metabolites and hydrolysis products in human urine. *Xenobiotica*. 1995;25:167–73.
11. Boyer AE, Ash D, Barr DB, et al. Quantitation of the sulfur mustard metabolites 1,1′-sulfonylbis[2-(methylthio)ethane] and thiodiglycol in urine using isotope-dilution Gas chromatography-tandem mass spectrometry. *J Anal Toxicol*. 2004;28:327–332.
12. Chilcott RP, Jenner J, Carrick W, Hotchkiss SA, Rice P. Human skin absorption of bis-2-(chloroethyl)sulphide (sulphur mustard) in vitro. *J Appl Toxicol*. 2000;20:349–355.
13. Graham JS, Chilcott RP, Rice P, Milner SM, Hurst CG, Maliner BI. Wound healing of cutaneous sulfur mustard injuries: strategies for the development of improved therapies. *J Burns Wounds*. 2005;4:e1.
14. Lindsay CD, Rice P. Changes in connective tissue macromolecular components of Yucatan mini-pig skin following application of sulphur mustard vapour. *Hum Exp Toxicol*. 1995;14:341–348.
15. Naghii MR. Sulfur mustard intoxication, oxidative stress, and antioxidants. *Mil Med*. 2002;167:573–575.

16. Anderson DR, Yourick JJ, Arroyo CM, Young GD, Harris LW. Use of EPR spin-trapping techniques to detect radicals from rat lung lavage fluid following sulfur mustard vapor exposure. *Med Defense Biosci Rev Proc*. 1993;1:113–121.
17. Elsayed NM, Omaye ST. Biochemical changes in mouse lung after subcutaneous injection of the sulfur mustard 2-chloroethyl 4-chlorobutyl sulfide. *Toxicol*. 2004;199:195–206.
18. Elsayed NM, Omaye ST, Klain GJ, Korte DW Jr. Free radical-mediated lung response to the monofunctional sulfur mustard butyl 2-chloroethyl sulfide after subcutaneous injection. *Toxicol*. 1992;72:153–165.
19. Vijayaraghavan R, Sugendran K, Pant SC, Husain K, Malhotra RC. Dermal intoxication of mice with bis(2-chloroethyl)sulphide and the protective effect of flavonoids. *Toxicol*. 1991;69:35–42.
20. Husain K, Dube SN, Sugendran K, Singh R, Das Gupta S, Somani SM. Effect of topically applied sulphur mustard on antioxidant enzymes in blood cells and body tissues of rats. *J Appl Toxicol*. 1996;16:245–248.
21. Yourick JJ, Dawson JS, Benton CD, Craig ME, Mitcheltree LW. Pathogenesis of 2,2′-dichlorodiethyl sulfide in hairless guinea pigs. *Toxicol*. 1993;84:185–197.
22. Vojvodic V, Milosavljevic Z, Boskovic B, Bojanic N. The protective effect of different drugs in rats poisoned by sulfur and nitrogen mustards. *Fundam Appl Toxicol*. 1985;5:160–168.
23. Azzi A, Gysin R, Kempna P, et al. Vitamin E mediates cell signaling and regulation of gene expression. *Ann N Y Acad Sci*. 2004;1031:86–95.
24. Ricciarelli R, Zingg JM, Azzi A. Vitamin E: protective role of a Janus molecule. *Faseb J*. 2001;15:2314–2325.
25. Zingg JM, Azzi A. Non-antioxidant activities of vitamin E. *Curr Med Chem*. 2004;11:1113–1133.
26. Cooney RV, Franke AA, Harwood PJ, Hatch-Pigott V, Custer LJ, Mordan LJ. Gamma-tocopherol detoxification of nitrogen dioxide: superiority to alpha-tocopherol. *Proc Natl Acad Sci U S A*. 1993;90:1771–1775.
27. Samandari E, Visarius T, Zingg JM, Azzi A. The effect of gamma-tocopherol on proliferation, integrin expression, adhesion, and migration of human glioma cells. *Biochem Biophys Res Commun*. 2006;342:1329–1333.
28. Eldad A, Ben Meir P, Breiterman S, Chaouat M, Shafran A, Ben-Bassat H. Superoxide dismutase (SOD) for mustard gas burns. *Burns*. 1998;24:114–119.
29. Alvarez MN, Trujillo M, Radi R. Peroxynitrite formation from biochemical and cellular fluxes of nitric oxide and superoxide. *Methods Enzymol*. 2002;359:353–366.
30. Beckman JS, Koppenol WH. Nitric oxide, superoxide, and peroxynitrite: the good, the bad, and ugly. *Am J Physiol*. 1996;271:1424–1437.
31. Fukuyama N, Nakazawa H. [Superoxide, nitric oxide and peroxynitrite]. *Nippon Yakurigaku Zasshi*. 1998;112:169–176.
32. Kumar O, Sugendran K, Vijayaraghavan R. Protective effect of various antioxidants on the toxicity of sulphur mustard administered to mice by inhalation or percutaneous routes. *Chem Biol Interact*. 2001;134:1–12.
33. McClintock SD, Hoesel LM, Das SK, et al. Attenuation of half sulfur mustard gas-induced acute lung injury in rats. *J Appl Toxicol*. 2006;26:126–131.
34. McClintock SD, Till GO, Smith MG, Ward PA. Protection from half-mustard-gas-induced acute lung injury in the rat. *J Appl Toxicol*. 2002;22:257–262.
35. Kelly GS. Clinical applications of *N*-acetylcysteine. *Altern Med Rev*. 1998;3:114–127.
36. Gross CL, Innace JK, Hovatter RC, Meier HL, Smith WJ. Biochemical manipulation of intracellular glutathione levels influences cytotoxicity to isolated human lymphocytes by sulfur mustard. *Cell Biol Toxicol*. 1993;9:259–267.
37. Meister A, Anderson ME. Glutathione. *Annu Rev Biochem*. 1983;52:711–760.
38. Bhat S, Gulati S, Husain K, Milner SM. Lipoic acid decreases oxidative stress in sulphur mustard toxicity. Proceedings of American Burn Association, 38th Annual Meeting, S139. Las Vegas, Nevada: *J Burn Care Res*, 27(2, suppl):S139, 2006.
39. Bast A, Haenen GR. Lipoic acid: a multifunctional antioxidant. *Biofactors*. 2003;17:207–213.
40. Dincer Y, Telci A, Kayali R, Yilmaz IA, Cakatay U, Akcay T. Effect of alpha-lipoic acid on lipid peroxidation and anti-oxidant enzyme activities in diabetic rats. *Clin Exp Pharmacol Physiol*. 2002;29:281–284.
41. Ernst A, Stolzing A, Sandig G, Grune T. Antioxidants effectively prevent oxidation-induced protein damage in OLN 93 cells. *Arch Biochem Biophys*. 2004;421:54–60.

42. Maritim AC, Sanders RA, Watkins JB, III. Effects of alpha-lipoic acid on biomarkers of oxidative stress in streptozotocin-induced diabetic rats. *J Nutr Biochem*. 2003;14:288–294.
43. Wollin SD, Jones PJ. Alpha-lipoic acid and cardiovascular disease. *J Nutr*. 2003;133:3327–3330.
44. Busse E, Zimmer G, Schopohl B, Kornhuber B. Influence of alpha-lipoic acid on intracellular glutathione in vitro and in vivo. *Arzneimittelforschung*. 1992;42:829–831.
45. Han D, Handelman G, Marcocci L, et al. Lipoic acid increases de novo synthesis of cellular glutathione by improving cystine utilization. *Biofactors*. 1997;6:321–338.
46. Stone WL, Mukherjee S, Smith M, Das SK. Therapeutic uses of antioxidant liposomes. *Methods Mol Biol*. 2002;199:145–161.
47. Stone WL, Smith M. Therapeutic uses of antioxidant liposomes. *Mol Biotechnol*. 2004;27:217–230.
48. Fan J, Shek PN, Suntres ZE, Li YH, Oreopoulos GD, Rotstein OD. Liposomal antioxidants provide prolonged protection against acute respiratory distress syndrome. *Surg*. 2000;128:332–338.
49. Kirjavainen M, Urtti A, Jaaskelainen I, et al. Interaction of liposomes with human skin in vitro—the influence of lipid composition and structure. *Biochim Biophys Acta*. 1996;1304:179–189.
50. Kirjavainen M, Urtti A, Valjakka-Koskela R, Kiesvaara J, Monkkonen J. Liposome-skin interactions and their effects on the skin permeation of drugs. *Eur J Pharm Sci*. 1999;7:279–286.
51. Boyce ST, Ham RG. Calcium-regulated differentiation of normal human epidermal keratinocytes in chemically defined clonal culture and serum-free serial culture. *J Invest Dermatol*. 1983;81:33s–40s.
52. Smith WJ, Gross CL, Chan P, Meier HL. The use of human epidermal keratinocytes in culture as a model for studying the biochemical mechanisms of sulfur mustard toxicity. *Cell Biol Toxicol*. 1990;6:285–291.
53. Stoppler H, Stoppler MC, Johnson E, et al. The E7 protein of human papillomavirus type 16 sensitizes primary human keratinocytes to apoptosis. *Oncogene*. 1998;17:1207–1214.
54. Boukamp P, Petrussevska RT, Breitkreutz D, Hornung J, Markham A, Fusenig NE. Normal keratinization in a spontaneously immortalized aneuploid human keratinocyte cell line. *J Cell Biol*. 1988;106:761–771.
55. Lippens S, Denecker G, Ovaere P, Vandenabeele P, Declercq W. Death penalty for keratinocytes: apoptosis versus cornification. *Cell Death Differ*. 2005;12(suppl 2):1497–1508.
56. Maas-Szabowski N, Starker A, Fusenig NE. Epidermal tissue regeneration and stromal interaction in HaCaT cells is initiated by TGF-alpha. *J Cell Sci*. 2003;116:2937–2948.
57. Freedberg IM, Tomic-Canic M, Komine M, Blumenberg M. Keratins and the keratinocyte activation cycle. *J Invest Dermatol*. 2001;116:633–640.
58. Smith CN, Lindsay CD, Upshall DG. Presence of methenamine/glutathione mixtures reduces the cytotoxic effect of sulphur mustard on cultured SVK-14 human keratinocytes in vitro. *Hum Exp Toxicol*. 1997;16:247–253.
59. Simpson R, Lindsay CD. Effect of sulphur mustard on human skin cell lines with differential agent sensitivity. *J Appl Toxicol*. 2005;25:115–128.
60. Wormser U, Sintov A, Brodsky B, Nyska A. Topical iodine preparation as therapy against sulfur mustard-induced skin lesions. *Toxicol Appl Pharmacol*. 2000;169:33–39.
61. Das SK, Mukherjee S, Smith MG, Chatterjee D. Prophylactic protection by *N*-acetylcysteine against the pulmonary injury induced by 2-chloroethyl ethyl sulfide, a mustard analogue. *J Biochem Mol Toxicol*. 2003;17:177–184.
62. Arroyo CM, Schafer RJ, Kurt EM, Broomfield CA, Carmichael AJ. Response of normal human keratinocytes to sulfur mustard: cytokine release. *J Appl Toxicol. Jat*. 2000;20(suppl 1):S63–S72.
63. Ricketts KM, Santai CT, France JA, et al. Inflammatory cytokine response in sulfur mustard-exposed mouse skin. *J Appl Toxicol. Jat*. 2000;20(suppl 1):73–76.
64. Sabourin CL, Petrali JP, Casillas RP. Alterations in inflammatory cytokine gene expression in sulfur mustard-exposed mouse skin. *J Biochem Mol Toxicol*. 2000;14:291–302.
65. Vavra AK, Laurent CJ, Ngo V, Sweeney JF, Levitt JM. Sulfur mustard primes phagocytosis and degranulation in human polymorphonuclear leukocytes. *Int Immunopharmacol*. 2004;4:437–445.
66. Blaha M, Bowers W, Kohl J, DuBose D, Walker J. Il-1-related cytokine responses of nonimmune skin cells subjected to CEES exposure with and without potential vesicant antagonists. 2000;13:99–111.
67. Blaha M, Bowers W, Kohl J, et al. Effects of CEES on inflammatory mediators, heat shock protein 70A, histology and ultrastructure in two skin models. *J Appl Toxicol. Jat*. 2000;20(suppl 1):S101–S108.

68. Blaha M, Kohl J, DuBose D, Bowers W Jr, Walker J. Ultrastructural and histological effects of exposure to CEES or heat in a human epidermal model. *In Vitr Mol Toxicol*. 2001;14:15–23.
69. Hayden PJ, Petrali JP, Hamilton TA, Kubilus J, Smith WJ, Klausner M. Development of a full thickness in vitro human skin equivalent (EpiDerm-FT) for sulfur mustard research, SID Abstract #174. 2005 Society for Investigative Dermatology Annual Meeting, 2005.
70. Rosenthal DS, Shima TB, Celli G, De Luca LM, Smulson ME. Engineered human skin model using poly(ADP-ribose) polymerase antisense expression shows a reduced response to DNA damage. *J Invest Dermatol*. 1995;105:38–43.
71. Rosenthal DS, Velena A, Chou FP, et al. Expression of dominant-negative Fas-associated death domain blocks human keratinocyte apoptosis and vesication induced by sulfur mustard. *J Biol Chem*. 2003;278:8531–8540.
72. Greenberg S, Margulis A, Garlick JA. In vivo transplantation of engineered human skin. *Methods Mol Biol*. 2005;289:425–430.
73. Greenberg S, Kamath P, Petrali J, Hamilton T, Garfield J, Garlick JA. Characterization of the initial response of engineered human skin to sulfur mustard. *Toxicol Sci*. 2006;90:549–557.
74. Rikimaru T, Nakamura M, Yano T, et al. Mediators, initiating the inflammatory response, released in organ culture by full-thickness human skin explants exposed to the irritant, sulfur mustard. *J Invest Dermatol*. 1991;96:888–897.
75. Inoue H, Asaka T, Nagata N, Koshihara Y. Mechanism of mustard oil-induced skin inflammation in mice. *Eur J Pharmacol*. 1997;333:231–240.
76. Stone WL, Qui M, Smith M. Lipopolysaccharide enhances the cytotoxicity of 2-chloroethyl ethyl sulfide. *BMC Cell Biol*. 2003;4:1.
77. Qui M, Paromov VM, Yang H, Smith M, Stone WL. Inhibition of inducible nitric oxide synthase by a mustard gas analog in murine macrophages. *BMC Cell Biol*. 2006;7:39.
78. Wright SD, Ramos RA, Tobias PS, Ulevitch RJ, Mathison JC. CD14, a receptor for complexes of lipopolysaccharide (LPS) and LPS binding protein. *Sci*. 1990;249:1431–1433.
79. Downey JS, Han J. Cellular activation mechanisms in septic shock. *Front Biosci*. 1998;3:d468–d476.
80. Tepperman BL, Chang Q, Soper BD. Protein kinase C mediates lipopolysaccharide- and phorbol-induced nitric-oxide synthase activity and cellular injury in the rat colon. *J Pharmacol Exp Ther*. 2000;295:1249–1257.
81. Shapira L, Takashiba S, Champagne C, Amar S, Van Dyke TE. Involvement of protein kinase C and protein tyrosine kinase in lipopolysaccharide-induced TNF-alpha and IL-1 beta production by human monocytes. *J Immunol*. 1994;153:1818–1824.
82. Eastmond NC, Banks EM, Coleman JW. Nitric oxide inhibits IgE-mediated degranulation of mast cells and is the principal intermediate in IFN-gamma-induced suppression of exocytosis. *J Immunol*. 1997;159:1444–1450.
83. Wink DA, Miranda KM, Espey MG, et al. Mechanisms of the antioxidant effects of nitric oxide. *Antioxid Redox Signal*. 2001;3:203–213.
84. McCauley SD, Gilchrist M, Befus AD. Nitric oxide: a major determinant of mast cell phenotype and function. *Mem Inst Oswaldo Cruz*. 2005;100(suppl 1):11–14.
85. Masini E, Palmerani B, Gambassi F, et al. Histamine release from rat mast cells induced by metabolic activation of polyunsaturated fatty acids into free radicals. *Biochem Pharmacol*. 1990;39:879–889.
86. Chiarugi A. Poly(ADP-ribose) polymerase: killer or conspirator? The "suicide hypothesis" revisited. *Trends Pharmacol Sci*. 2002;23:122–129.
87. Rosenthal DS, Simbulan-Rosenthal CM, Iyer S, et al. Sulfur mustard induces markers of terminal differentiation and apoptosis in keratinocytes via a Ca^{2+}-calmodulin and caspase-dependent pathway. *J Invest Dermatol*. 1998;111:64–71.
88. Hinshaw DB, Lodhi IJ, Hurley LL, Atkins KB, Dabrowska MI. Activation of poly [ADP-Ribose] polymerase in endothelial cells and keratinocytes: role in an in vitro model of sulfur mustard-mediated vesication. *Toxicol Appl Pharmacol*. 1999;156:17–29.
89. Bhat KR, Benton BJ, Rosenthal DS, Smulson ME, Ray R. Role of poly(ADP-ribose) polymerase (PARP) in DNA repair in sulfur mustard-exposed normal human epidermal keratinocytes (NHEK). *J Appl Toxicol*. 2000;20(suppl 1):S13–S17.

90. Rosenthal DS, Simbulan-Rosenthal CM, Iyer S, Smith WJ, Ray R, Smulson ME. Calmodulin, poly(ADP-ribose)polymerase and p53 are targets for modulating the effects of sulfur mustard. *J Appl Toxicol*. 2000;20(suppl 1):S43–S49.
91. Rosenthal DS, Simbulan-Rosenthal CM, Liu WF, et al. PARP determines the mode of cell death in skin fibroblasts, but not keratinocytes, exposed to sulfur mustard. *J Invest Dermatol*. 2001;117:1566–1573.
92. Kim MY, Zhang T, Kraus WL. Poly(ADP-ribosyl)ation by PARP-1: "PAR-laying" NAD+ into a nuclear signal. *Genes Dev*. 2005;19:1951–1967.
93. D'Amours D, Desnoyers S, D'Silva I, Poirier GG. Poly(ADP-ribosyl)ation reactions in the regulation of nuclear functions. *Biochem J*. 1999;342(Pt 2):249–268.
94. Herceg Z, Wang ZQ. Functions of poly(ADP-ribose) polymerase (PARP) in DNA repair, genomic integrity and cell death. *Mutat Res*. 2001;477:97–110.
95. Shall S, de Murcia G. Poly(ADP-ribose) polymerase–1: what have we learned from the deficient mouse model? *Mutat Res*. 2000;460:1–15.
96. Zong WX, Ditsworth D, Bauer DE, Wang ZQ, Thompson CB. Alkylating DNA damage stimulates a regulated form of necrotic cell death. *Genes Dev*. 2004;18:1272–1282.
97. Burkle A. PARP-1: a regulator of genomic stability linked with mammalian longevity. *Chembiochem*. 2001;2:725–728.
98. Bouchard VJ, Rouleau M, Poirier GG. PARP-1, a determinant of cell survival in response to DNA damage. *Exp Hematol*. 2003;31:446–454.
99. Decker P, Muller S. Modulating poly (ADP-ribose) polymerase activity: potential for the prevention and therapy of pathogenic situations involving DNA damage and oxidative stress. *Curr Pharm Biotechnol*. 2002;3:275–283.
100. Ying W, Alano CC, Garnier P, Swanson RA. NAD+ as a metabolic link between DNA damage and cell death. *J Neurosci Res*. 2005;79:216–223.
101. Sun J, Wang YX, Sun MJ. Apoptosis and necrosis induced by sulfur mustard in Hela cells. *Zhongguo Yao Li Xue Bao*. 1999;20:445–448.
102. Meier HL, Millard CB. Alterations in human lymphocyte DNA caused by sulfur mustard can be mitigated by selective inhibitors of poly(ADP-ribose) polymerase. *Biochim Biophys Acta*. 1998;1404:367–376.
103. Dabrowska MI, Becks LL, Lelli JL Jr, Levee MG, Hinshaw DB. Sulfur mustard induces apoptosis and necrosis in endothelial cells. *Toxicol Appl Pharmacol*. 1996;141:568–583.
104. Ying W, Chen Y, Alano CC, Swanson RA. Tricarboxylic acid cycle substrates prevent PARP-mediated death of neurons and astrocytes. *J Cereb Blood Flow Metab*. 2002;22:774–779.
105. Willems JL, de Kort AF, Vree TB, Trijbels JM, Veerkamp JH, Monnens LA. Non-enzymic conversion of pyruvate in aqueous solution to 2,4-dihydroxy-2-methylglutaric acid. *FEBS Lett*. 1978;86:42–44.
106. O'Donnell-Tormey J, Nathan CF, Lanks K, DeBoer CJ, de la Harpe J. Secretion of pyruvate. An antioxidant defense of mammalian cells. *J Exp Med*. 1987;165:500–514.
107. Dobsak P, Courderot-Masuyer C, Zeller M, et al. Antioxidative properties of pyruvate and protection of the ischemic rat heart during cardioplegia. *J Cardiovasc Pharmacol*. 1999;34:651–659.
108. Das UN. Pyruvate is an endogenous anti-inflammatory and anti-oxidant molecule. *Med Sci Monit*. 2006;12:RA79–RA84.
109. Mallet RT, Sun J, Knott EM, Sharma AB, Olivencia-Yurvati AH. Metabolic cardioprotection by pyruvate: recent progress. *Exp Biol Med (Maywood)*. 2005;230:435–443.
110. Sabourin CL, Danne MM, Buxton KL, Casillas RP, Schlager JJ. Cytokine, chemokine, and matrix metalloproteinase response after sulfur mustard injury to weanling pig skin. *J Biochem Mol Toxicol*. 2002;16:263–272.
111. Akira S, Kishimoto T. NF-IL6 and NF-kappa B in cytokine gene regulation. *Adv Immunol*. 1997;65:1–46.
112. Brennan P, O'Neill LA. Effects of oxidants and antioxidants on nuclear factor kappa B activation in three different cell lines: evidence against a universal hypothesis involving oxygen radicals. *Biochim Biophys Acta*. 1995;1260:167–175.
113. Barnes PJ, Adcock IM. Transcription factors and asthma. *Eur Respir J*. 1998;12:221–234.
114. Rahman I, MacNee W. Role of transcription factors in inflammatory lung diseases. *Thorax*. 1998;53:601–612.

115. Martin-Oliva D, O'Valle F, Munoz-Gamez JA, et al. Crosstalk between PARP-1 and NF-kappaB modulates the promotion of skin neoplasia. *Oncog*. 2004;23:5275–5283.
116. Gray PJ. Sulphur mustards inhibit binding of transcription factor AP2 in vitro. *Nucleic Acids Res*. 1995;23:4378–4382.
117. Schulze-Osthoff K, Bauer MK, Vogt M, Wesselborg S. Oxidative stress and signal transduction. *Int J Vitam Nutr Res*. 1997;67:336–342.
118. Schwager J, Schulze J. Influence of ascorbic acid on the response to mitogens and interleukin production of porcine lymphocytes. *Int J Vitam Nutr Res*. 1997;67:10–16.
119. Xanthoudakis S, Miao GG, Curran T. The redox and DNA-repair activities of Ref-1 are encoded by nonoverlapping domains. *Proc Natl Acad Sci U S A*. 1994;91:23–27.
120. Yao KS, Xanthoudakis S, Curran T, O'Dwyer PJ. Activation of AP-1 and of a nuclear redox factor, Ref-1, in the response of HT29 colon cancer cells to hypoxia. *Mol Cell Biol*. 1994;14:5997–6003.
121. Kerppola TK, Curran T. A conserved region adjacent to the basic domain is required for recognition of an extended DNA binding site by Maf/Nrl family proteins. *Oncogene*. 1994;9:3149–3158.
122. Kerppola TK, Curran T. Maf and Nrl can bind to AP-1 sites and form heterodimers with Fos and Jun. *Oncogene*. 1994;9:675–684.
123. Klampfer L, Lee TH, Hsu W, Vilcek J, Chen-Kiang S. NF-IL6 and AP-1 cooperatively modulate the activation of the TSG-6 gene by tumor necrosis factor alpha and interleukin-1. *Mol Cell Biol*. 1994;14:6561–6569.
124. Hsu W, Kerppola TK, Chen PL, Curran T, Chen-Kiang S. Fos and Jun repress transcription activation by NF-IL6 through association at the basic zipper region. *Mol Cell Biol*. 1994;14:268–276.
125. Crispen PL, Uzzo RG, Golovine K, et al. Vitamin E succinate inhibits NF-kappaB and prevents the development of a metastatic phenotype in prostate cancer cells: implications for chemoprevention. *Prostate*. 2007. **[AQ2]**
126. Campbell SE, Stone WL, Lee S, et al. Comparative effects of RRR-alpha- and RRR-gamma-tocopherol on proliferation and apoptosis in human colon cancer cell lines. *BMC Cancer*. 2006;6:13.
127. Smirnov AS, Ruzov AS, Budanov AV, Prokhortchouk AV, Ivanov AV, Prokhortchouk EB. High constitutive level of NF-kappaB is crucial for viability of adenocarcinoma cells. *Cell Death Differ*. 2001;8:621–630.
128. Dhanalakshmi S, Singh RP, Agarwal C, Agarwal R. Silibinin inhibits constitutive and TNFalpha-induced activation of NF-kappaB and sensitizes human prostate carcinoma DU145 cells to TNFalpha-induced apoptosis. *Oncogene*. 2002;21:1759–1767.
129. Ma Z, Otsuyama K, Liu S, et al. Baicalein, a component of Scutellaria radix from Huang-Lian-Jie-Du-Tang (HLJDT), leads to suppression of proliferation and induction of apoptosis in human myeloma cells. *Blood*. 2005;105:3312–3318.
130. Taguchi T, Takao T, Iwasaki Y, Nishiyama M, Asaba K, Hashimoto K. Suppressive effects of dehydroepiandrosterone and the nuclear factor-kappaB inhibitor parthenolide on corticotroph tumor cell growth and function in vitro and in vivo. *J Endocrinol*. 2006;188:321–331.
131. Minsavage GD, Dillman 3d JF. Protective role of CAPE on bi-functional alkylating agent-induced toxicity in keratinocytes via modulation of NF-kappaB, p53 and ARE/EpRE signaling. *Biosci 2006 Med Defense Rev*, 2006;94–94. **[AQ3]**
132. Minsavage GD, Dillman Iii JF. Bifunctional alkylating agent-induced p53 and nonclassical nuclear factor-kappa b (nf-{kappa}b) responses and cell death are altered by caffeic acid phenethyl ester (cape): A potential role for antioxidant/electrophilic response element (ARE/EpRE) signaling. *J Pharmacol Exp Ther*. 2007. **[AQ4]**
133. Arroyo CM, Burman DL, Kahler DW, et al. TNF-alpha expression patterns as potential molecular biomarker for human skin cells exposed to vesicant chemical warfare agents: sulfur mustard (HD) and Lewisite (L). *Cell Biol Toxicol*. 2004;20:345–359.
134. Atkins KB, Lodhi IJ, Hurley LL, Hinshaw DB. *N*-acetylcysteine and endothelial cell injury by sulfur mustard. *J Appl Toxicol*. 2000;20(suppl 1):S125–S128.
135. Chatterjee D, Mukherjee S, Smith MG, Das SK. Signal transduction events in lung injury induced by 2-chloroethyl ethyl sulfide, a mustard analog. *J Biochem Mol Toxicol*. 2003;17:114–121.
136. Duthie MS, Kimber I, Dearman RJ, Norval M. Differential effects of UVA1 and UVB radiation on Langerhans cell migration in mice. *J Photochem Photobiol B*. 2000;57:123–131.

137. Steffensen B, Hakkinen L, Larjava H. Proteolytic events of wound-healing–coordinated interactions among matrix metalloproteinases (MMPs), integrins, and extracellular matrix molecules. *Crit Rev Oral Biol Med*. 2001;12:373–398.
138. Schwentker A, Billiar TR. Nitric oxide and wound repair. *Surg Clin North Am*. 2003;83:521–530.
139. Weller R. Nitric oxide: a key mediator in cutaneous physiology. *Clin Exp Dermatol*. 2003;28:511–514.
140. Witte MB, Barbul A. Role of nitric oxide in wound repair. *Am J Surg*. 2002;183:406–412.
141. Yamasaki K, Edington HD, McClosky C, et al. Reversal of impaired wound repair in iNOS-deficient mice by topical adenoviral-mediated iNOS gene transfer. *J Clin invest*. 1998;101:967–971.
142. Ishida H, Ray R, Cao Y, Ray P. Role of nitric oxide (NO) in wound healing. *Biosci 2006 Med Defense Rev.* 2006;1:112.
143. Arany I, Brysk MM, Brysk H, Tyring SK. Regulation of inducible nitric oxide s ynthase mRNA levels by differentiation and cytokines in human keratinocytes. *Biochem Biophys Res Commun*. 1996;220:618–622.
144. Kleinert H, Schwarz PM, Forstermann U. Regulation of the expression of inducible nitric oxide synthase. *Biol Chem*. 2003;384:1343–1364.
145. Soneja A, Drews M, Malinski T. Role of nitric oxide, nitroxidative and oxidative stress in wound healing. *Pharmacol Rep*. 2005;57(suppl):108–119.
146. Perkel JM. What can systems biology do for you? Four computational modeling strategies and the data that build them. *Scientist*. 2007;21:68.
147. Rogers JV, Choi YW, Kiser RC, et al. Microarray analysis of gene expression in murine skin exposed to sulfur mustard. *J Biochem Mol Toxicol*. 2004;18:289–299.
148. Sabourin CL, Rogers JV, Choi YW, et al. Time- and dose-dependent analysis of gene expression using microarrays in sulfur mustard-exposed mice. *J Biochem Mol Toxicol*. 2004;18:300–312.
149. Platteborze PL. Effects of sulfur mustard on transcription in human epidermal keratinocytes: analysis by mRNA differential display. *J Appl Toxicol*. 2003;23:249–254.
150. Dillman JF, III, Hege AI, Phillips CS, et al. Microarray analysis of mouse ear tissue exposed to bis-(2-chloroethyl) sulfide: gene expression profiles correlate with treatment efficacy and an established clinical endpoint. *J Pharmacol Exp Ther*. 2006;317:76–87.
151. Sultana R, Boyd-Kimball D, Poon HF, et al. Redox proteomics identification of oxidized proteins in Alzheimer's disease hippocampus and cerebellum: an approach to understand pathological and biochemical alterations in AD. *Neurobiol Aging*. 2005.
152. Ghezzi P, Bonetto V, Fratelli M. Thiol-disulfide balance: from the concept of oxidative stress to that of redox regulation. *Antioxid Redox Signal*. 2005;7:964–972.
153. Ghezzi P, Bonetto V. Redox proteomics: identification of oxidatively modified proteins. *Proteomics*. 2003;3:1145–1153.
154. Butterfield DA. Proteomics: a new approach to investigate oxidative stress in Alzheimer's disease brain. *Brain Res*. 2004;1000:1–7.

[AQ5]

Author Queries

Title: Sulfur Mustard Toxicity Following Dermal Exposure Role of Oxidative Stress, and Antioxidant Therapy

Authors: Victor Paromov, Zacharias Suntres, Milton Smith, and William L. Stone

AQ1: Note that the sentence (In vitro by. . . cytotoxicity.) is not clear.
AQ2: Provide the volume number and the page range.
AQ3: Check the second author surname and provide volume number if any.
AQ4: Provide the volume number and the page range.
AQ5: Provide the volume number and the page range.

BMC Cell Biology

Research article

Inhibition of inducible Nitric Oxide Synthase by a mustard gas analog in murine macrophages

Min Qui[†1], Victor M Paromov*[†1], Hongsong Yang[†1], Milton Smith[2] and William L Stone[†1]

Address: [1]Department of Pediatrics, East Tennessee State University, Johnson City, TN, USA and [2]Amox Ltd., Lawton, MI 49605, USA

Email: Min Qui - qui@etsu.edu; Victor M Paromov* - paromov@etsu.edu; Hongsong Yang - yangh@etsu.edu; Milton Smith - mgsmithmd@isp01.net; William L Stone - stone@etsu.edu

* Corresponding author †Equal contributors

Published: 30 November 2006

BMC Cell Biology 2006, **7**:39 doi:10.1186/1471-2121-7-39

Received: 22 September 2006
Accepted: 30 November 2006

This article is available from: http://www.biomedcentral.com/1471-2121/7/39

Abstract

Background: 2-Chloroethyl ethyl sulphide (CEES) is a sulphur vesicating agent and an analogue of the chemical warfare agent 2,2'-dichlorodiethyl sulphide, or sulphur mustard gas (HD). Both CEES and HD are alkylating agents that influence cellular thiols and are highly toxic. In a previous publication, we reported that lipopolysaccharide (LPS) enhances the cytotoxicity of CEES in murine RAW264.7 macrophages. In the present investigation, we studied the influence of CEES on nitric oxide (NO) production in LPS stimulated RAW264.7 cells since NO signalling affects inflammation, cell death, and wound healing. Murine macrophages stimulated with LPS produce NO almost exclusively via inducible nitric oxide synthase (iNOS) activity. We suggest that the influence of CEES or HD on the cellular production of NO could play an important role in the pathophysiological responses of tissues to these toxicants. In particular, it is known that macrophage generated NO synthesised by iNOS plays a critical role in wound healing.

Results: We initially confirmed that in LPS stimulated RAW264.7 macrophages NO is exclusively generated by the iNOS form of nitric oxide synthase. CEES treatment inhibited the synthesis of NO (after 24 hours) in viable LPS-stimulated RAW264.7 macrophages as measured by either nitrite secretion into the culture medium or the intracellular conversion of 4,5-diaminofluorescein diacetate (DAF-2DA) or dichlorofluorescin diacetate (DCFH-DA). Western blots showed that CEES transiently decreased the expression of iNOS protein; however, treatment of active iNOS with CEES *in vitro* did not inhibit its enzymatic activity

Conclusion: CEES inhibits NO production in LPS stimulated macrophages by decreasing iNOS protein expression. Decreased iNOS expression is likely the result of CEES induced alteration in the nuclear factor kappa B (NF-κB) signalling pathway. Since NO can act as an antioxidant, the CEES induced down-regulation of iNOS in LPS-stimulated macrophages could elevate oxidative stress. Since macrophage generated NO is known to play a key role in cutaneous wound healing, it is possible that this work has physiological relevance with respect to the healing of HD induced skin blisters.

Background

HD is a chemical weapon that can produce casualties in military situations and has been used with devastating results against civilian populations [1]. Extensive and slow healing lesions following exposure to HD can place a heavy burden on the medical services of military and public health organizations. The design of effective countermeasures to HD depends upon a detailed understanding of the molecular mechanisms for its toxicity. Important mechanisms of HD induced skin injury are alkylation of DNA and other macromolecules, accompanied by enhanced reactive oxygen species (ROS) generation and depletion of intracellular glutathione (GSH) [2-5]. Depletion of GSH by HD and its metabolites is known to shift the intracellular redox milieu toward a more oxidized state with a subsequent loss of protection against oxidative free radicals and an activation of inflammatory responses[6,7].

It has been shown that HD induces a vast "spectrum" of inflammatory cytokines released from keratinocytes [8,9]. It is likely that CEES cause similar changes in macrophages and leukocytes. We previously found that LPS, as well as inflammatory cytokines, such as tumor necrosis factor-alpha (TNF-α) and interleukin one-beta (IL-1β), significantly amplify the toxicity of CEES in RAW264.7 macrophages [10]. In macrophages, stimulation by LPS, as well as by pro-inflammatory cytokines, leads to the activation and nuclear translocation of NF-κB [11]. One of the major consequences of such activation in macrophages is an induction of iNOS expression with subsequent elevation of intracellular NO [12]. The effect of CEES on NO generation and on the NF-κB pathway is potentially significant since NO signalling plays an important role in inflammation, the mechanisms of cell death NF-κB [13,14], and wound healing [15,16]. The present work describes the inhibition of NO production and iNOS expression in LPS stimulated macrophages treated with CEES.

Results

CEES transiently suppresses NO production and iNOS expression in LPS stimulated cells

In Figure 1a, we examined nitrite secretion into the cell culture medium by RAW 264.7 murine macrophages after 24 hours of treatment with CEES and various levels of LPS. Nitrite level in the cell culture medium, as measured by the Griess reagent, is a reliable indicator of nitric oxide secretion. These data show that CEES (100–500 μM) inhibited the secretion of NO into the cell medium by LPS stimulated macrophages in a dose-dependent manner. Low levels of CEES (≤ 100 μM) only partially inhibited NO production, whereas levels higher than 300 μM completely inhibited NO production. Although CEES does decrease the viability of LPS stimulated macrophages [10], the decreased generation of NO cannot be accounted simply for the loss of viable cells. Figure 1b shows that in case nitrite levels in the culture medium (as measured by OD at 532 nm) are normalized to the amount of viable cells (OD at 580 nm, MTT assay, measured separately) there is still a significant CEES dose dependent inhibition of NO formation.

In order to determine if CEES influenced cellular levels of iNOS, we performed Western blot analyses (Figure 1c) of the cell lysates using highly selective anti-iNOS antibodies with equal amounts of total protein applied to each lane. Control RAW 264.7 macrophages had no detectable iNOS protein, CEES treatment alone did not induce any iNOS protein but LPS (10 ng/ml for 24 hours) produced a marked induction of iNOS protein. When simultaneously treated with LPS (10 ng/ml) and CEES (300 μM) there was a marked reduction in the LPS induction of iNOS protein.

We then examined the influence of 300 μM CEES on the time course of NO production in macrophage stimulated with 10 ng/ml LPS. Figure 2a shows that CEES delays, but does not prevent, the production of NO (as measured by nitrite formation) in LPS-stimulated macrophages. In fact, after 12 hours the rate of NO production is about the same in cells treated with LPS alone compared with cells treated with both LPS and CEES. Western blot data (Figure 2b) from the cells used in Figure 2a show a similar pattern: LPS alone induces robust iNOS protein expression which is completely inhibited by CEES for up to 6 hours. After 12 hours, however, the cells incubated with both CEES and LPS show a rebound in the expression of iNOS and after 24 hours the iNOS protein level in cells treated with both CEES and LPS is very similar to that observed in cells treated with LPS alone. These data show that the influence of CEES on both nitric oxide synthesis and iNOS expression is transient.

CEES does not inhibit iNOS enzymatic activity in vitro

In order to evaluate the possible direct inhibitory effect of CEES on iNOS activity *in vitro*, we measured the intracellular rates of 4,5-diaminofluorescein (DAF-2) or dichlorofluorescin (DCFH) oxidation in intact macrophages. Dichlorofluorescin diacetate (DCFH-DA) is permeable to the cell plasma membrane and intracellular esterases convert it into a membrane impermeable (DCFH) form which is can be oxidized to highly fluorescent dichlorofluorescein (DCF) by free radicals. In macrophages, the oxidation of DCFH has been shown to be a sensitive and relatively selective probe for monitoring intracellular NO formation by iNOS [17].

Using DCFH-DA and DAF-2DA, we were able to continuously monitor NO formation in intact macrophages under a variety of conditions. Previously, we [18] and oth-

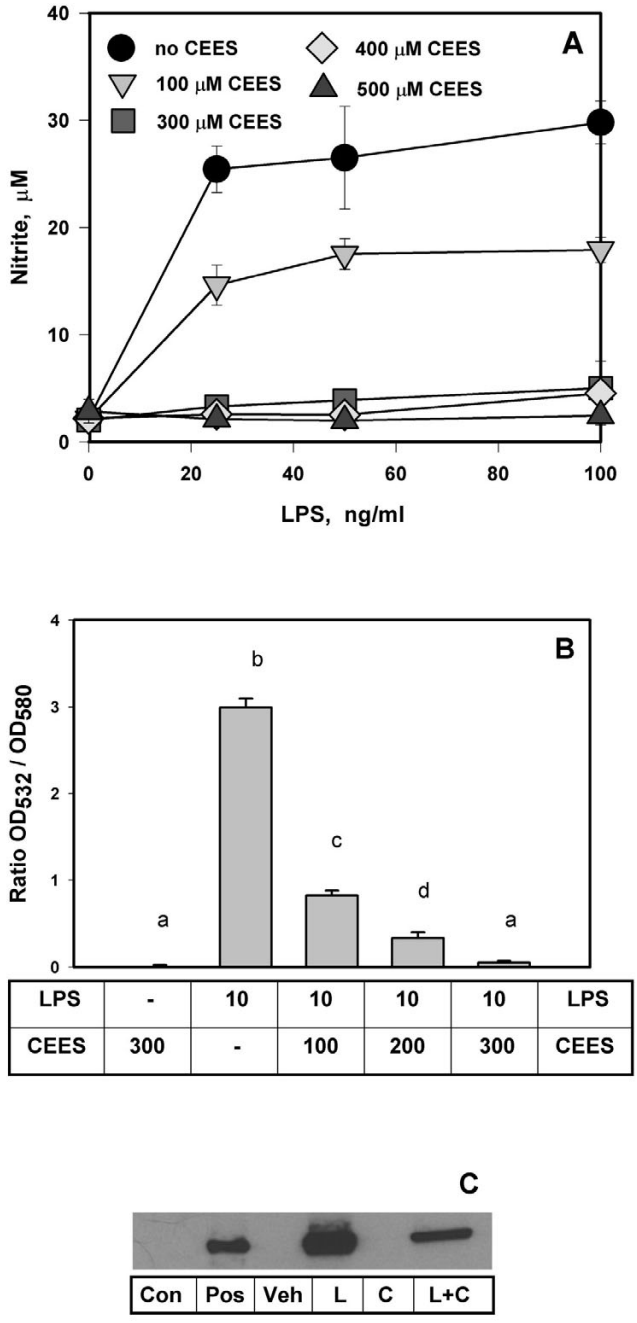

Figure 1

CEES inhibits NO production and iNOS expression in LPS stimulated RAW264.7 macrophages. *Panel A*: Macrophages were simultaneously treated with various levels of CEES (as indicated) and low doses of LPS (as indicated). NO production was monitored as the concentration of nitrite in the culture medium after 24 h. *Panel B*: Cells were treated similarly as for *Panel A*; LPS, 10 ng/ml; CEES, 100, 200, or 300 μM (as indicated). Means not sharing a common letter are significantly different ($p < 0.05$). Nitrite levels in the culture medium (OD at 532 nm) were normalized to the amount of viable cells (OD of the MTT product at 580 nm). *Panel C*: Western blot analysis of iNOS protein from cells simultaneously incubated with 300 μM CEES and/or 10 ng/ml LPS for 24 h; cell lysates were prepared as described in Materials and Methods: Con, control cells; Pos, iNOS protein for positive control; Veh, vehicle; L, 10 ng/ml LPS stimulated cells; C, 300 μM CEES treated cells; L+C, LPS/CEES treated cells.

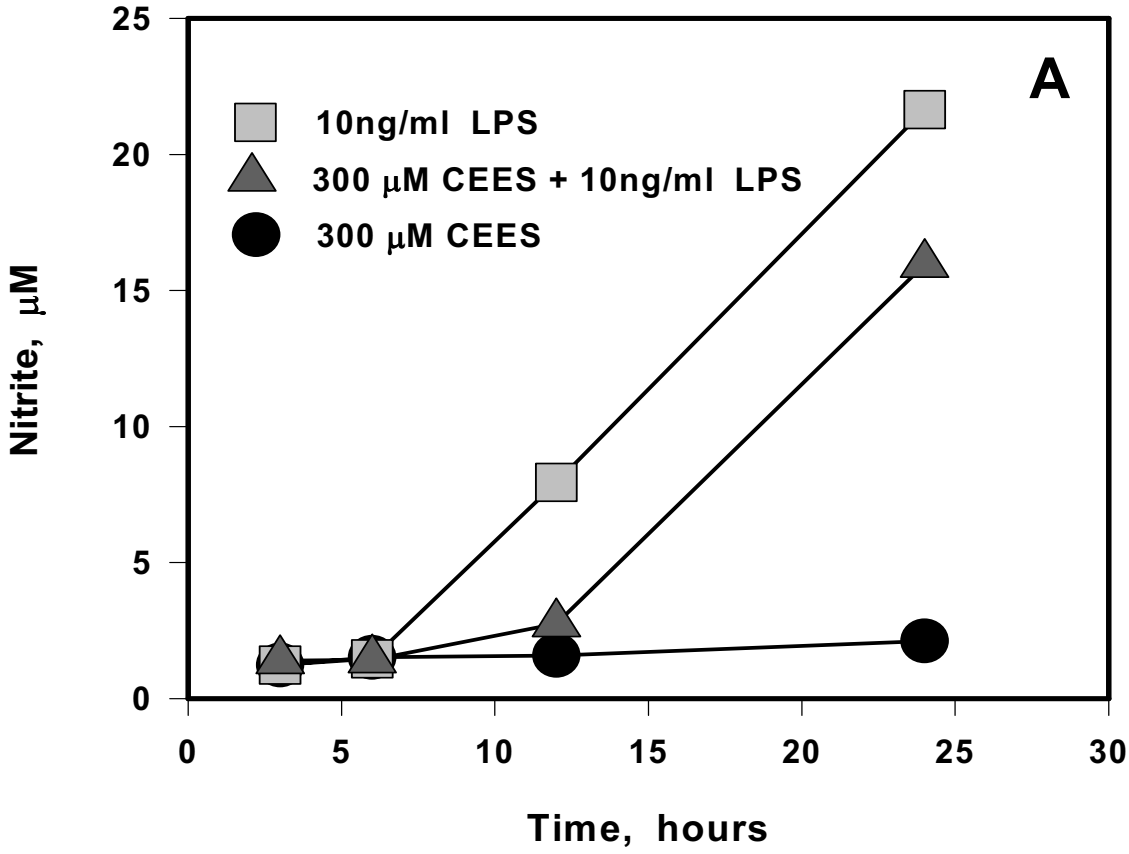

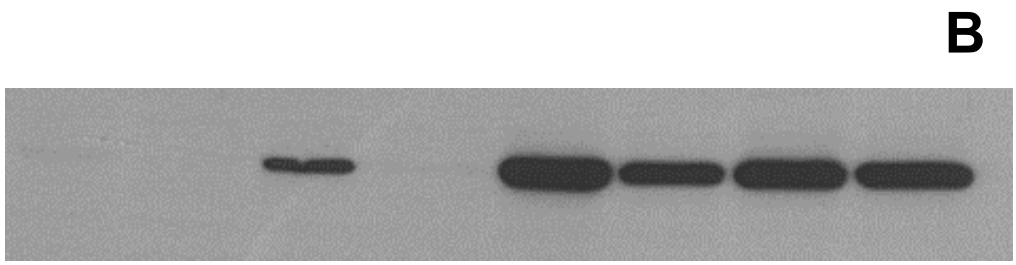

3h	3h	6h	6h	12h	12h	24h	24h
L	L+C	L	L+C	L	L+C	L	L+C

Figure 2
Time course of NO production and iNOS expression in LPS stimulated RAW264.7 macrophages incubated with CEES. *Panel A*: Macrophages were incubated with 10 ng/ml LPS alone, 300 μM CEES alone or simultaneously with both 300 μM CEES 10 ng/ml LPS for various time intervals (as indicated). NO production measured as concentration of nitrite in culture medium. *Panel B*: Western blot analysis of iNOS protein from the cells incubated with 300 μM CEES with or without 10 ng/ml LPS; cell lysates were prepared after 3, 6, 12, or 24 hour incubation (as indicated) as described in Materials and Methods; L, LPS; C, CEES.

ers [19] have shown that LPS exclusively induces the iNOS form of nitric oxide synthase in murine macrophages. Figure 3a shows DCFH oxidation in RAW 264.7 cells stimulated with different levels of LPS for 24 hours. In the absence of LPS, the rate of DCFH oxidation was extremely low but increased with increasing exposure to LPS; however, this effect was nearly saturated at LPS levels above 15 ng/ml.

We then measured the rates of DAF-2 oxidation in RAW 264.7 macrophages stimulated with 20 ng/ml LPS in the presence or absence of 500 μM CEES during 24 hour incubations (Figure 3b). In the absence of LPS or CEES, minimal DAF-2 oxidation was observed. As expected, LPS alone induced a marked increase in DAF-2 oxidation. Next, macrophages incubated with LPS for 24 hours were then exposed (post-treatment) to 500 μM CEES and the rate of DAF-2 oxidation immediately measured. As shown in Figure 3b, there was no change in rate of DAF-2 oxidation compared to cells treated with LPS alone. These data strongly support the notion that CEES does not directly inhibit iNOS enzymatic activity. Similar results were obtained with DCFH-DA staining (data not shown). As expected, macrophages simultaneously treated with both LPS and CEES for 24 hours show a marked decrease in either DAF-2 or DCFH oxidation.

To further confirm that DCFH oxidation is overwhelmingly due to iNOS, we incubated LPS-stimulated macrophages with ebselen (see Figure 3c). Ebselen is a selenoorganic compound that can inhibit both the activity of iNOS [20] and its induction by LPS [21]. Ebselen (25 μM) almost completely inhibited the DCFH oxidation in RAW 264.7 cells treated with 10 ng/ml or 20 ng/ml LPS. Ebselen was not cytotoxic at the levels used in Figure 3 (data not shown).

Discussion

Overall, the experiments detailed in this work show that CEES treatment in LPS-stimulated RAW264.7 murine macrophages transiently inhibits intracellular NO generation by interfering with iNOS expression rather than by direct inhibition of iNOS enzymatic activity. CEES (as well as HD) undergo rapid hydrolysis in aqueous solutions and this may account, in part, for the transitory nature of its inhibiting effect on iNOS induction [22]. LPS is a major component of the cell wall of gram-negative bacteria and is known to trigger a variety of inflammatory reactions in macrophages and other cells expressing CD14 receptors [23,24]. LPS is ubiquitous and is present in serum, tap water, and dust. Military and civilian personnel would, indeed, always have some degree of exposure to environmental LPS.

LPS stimulation of macrophages is known to involve the activation of protein phosphorylation by kinases as well as the activation of nuclear transcription factors such as NF-κB [25-28]. An important consequence of NF-κB activation in macrophages is the induction of iNOS expression followed with highly elevated NO production [12]. Nitric oxide has been demonstrated to have an important role in promoting cell death; however, the precise nature of this role varies with cell type and the dose. Low levels of nitric oxide protect RAW 264.7 macrophages from hydrogen peroxide induced apoptosis [29], however, nitric oxide has also been reported to induce apoptosis in J774 macrophages [14]. Nitric oxide can induce cell death through energy depletion-induced necrosis and oxidant-induced apoptosis.

We are currently exploring the potential molecular mechanism(s) whereby CEES interferes with iNOS expression in LPS stimulated macrophages. It is possible that GSH depletion caused by CEES determines iNOS expression. There are strong evidences suggesting that thiol depletion and iNOS expression are interrelated [30-32]. For example, LPS stimulated macrophages depleted of GSH exhibit a decreased level of iNOS protein and nitrite production [32]. Similarly, both *in vitro* [30] and *in vivo* [31] studies show that hepatocytes depleted of GSH have a diminished production of nitric oxide which is primarily due to a decreased level of iNOS mRNA. Vos et al. [31] have also presented evidence showing that GSH modulation of iNOS expression in hepatocytes is correlated with NF-kB activation, i.e., GSH depletion is associated with a lack of NF-kB activation. The influence of GSH depletion is not, however, consistent in all cell types. Glucose induced reduction of GSH in intestinal epithelial cells is associated with NF-kB activation and upregulation of iNOS gene expression [33].

It is also possible that CEES decreases iNOS expression by interfering with the LPS-induced activation of transcription factor NF-κB and/or signal transducer and activator of transcription-1α (STAT-1α). It is interesting, therefore, that Gray [34] has found that both CEES and HD inhibit the *in vitro* binding of transcription factor activating protein-2 (AP-2) via alkylating the AP-2 DNA consensus binding sequence rather than by direct damage to the AP-2 protein. Furthermore, it is significant that neither CESS nor its hydrolysis products were found to damage the AP-2 transcription factoring in a manner that prevented its DNA binding [35]. Similar experiments have yet to be done with NF-κB. Chen et al. [36] have also found that nitrogen mustard (bis(2-chloroethul) methylamine) similarly inhibits the binding of AP-2 to its consensus sequence. Nitrogen mustard also was shown to inhibit the binding of NF-κB to the GC-rich consensus sequence due to the interactions with DNA [37]. It is possible, therefore,

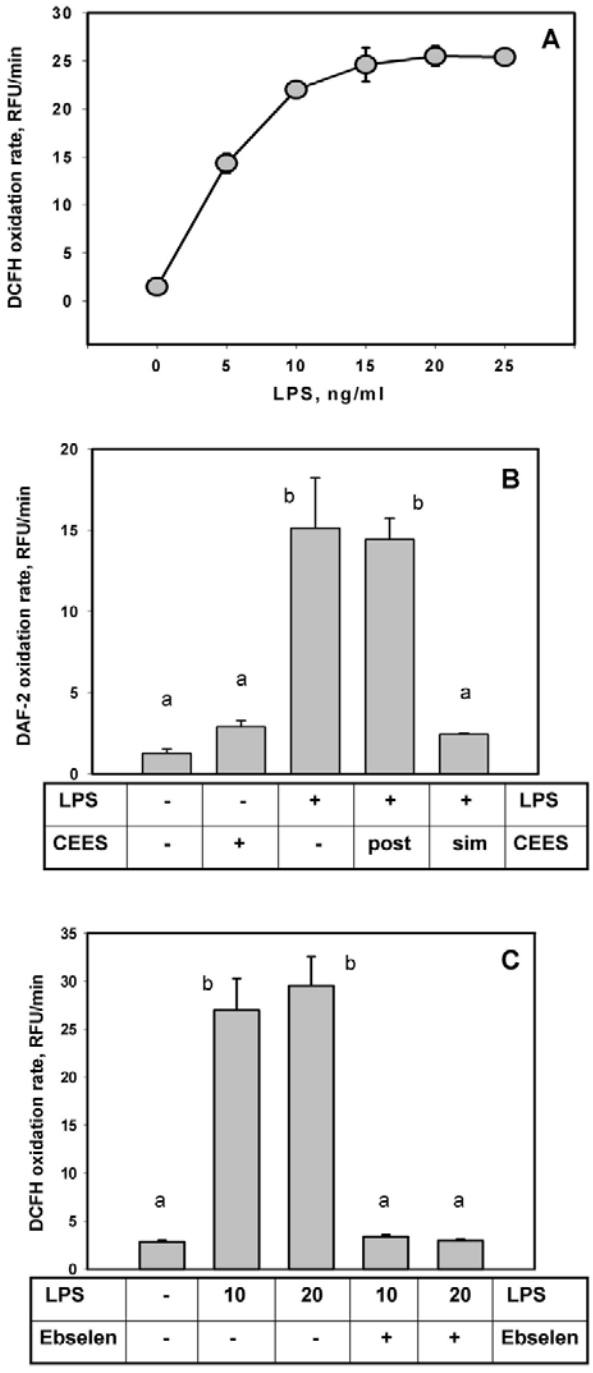

Figure 3

CEES reduces intracellular NO in LPS stimulated RAW264.7 macrophages. *Panel A*: Intracellular DCFH (20 μM) oxidation in LPS stimulated macrophages (as indicated) incubated for 2 h. Fluorescence (excitation 485 nm, emission 520 nm) was measured in Relative Fluorescence Units (RFU); the oxidation rate was expressed as RFU/min. *Panel B*: Macrophages stimulated with 20 ng/ml LPS, were incubated in the presence or absence of 500 μM CEES (as indicated) for 24 h. Post, CEES was applied after the 24 hours of LPS stimulation; Sim, CEES was applied simultaneously with LPS. *Panel C*: LPS stimulated cells were incubated in the presence or absence of 25 μM ebselen, a selective iNOS inhibitor (as indicated). 10, 10 ng/ml LPS; 20, 20 ng/ml LPS. Mean values not sharing a common letter are significantly different ($p < 0.05$).

that CEES also alkylates the NF-κB consensus sequence thereby preventing the binding of the NF-κB to the iNOS promoter. LPS and/or cytokine-inducible NF-κB binding elements of the murine iNOS promoter have been identified [38], and they are rich of guanine, which is the major alkylation site for HD or CEES. The possible effect of CEES on iNOS promoter regulation is currently being explored.

Although the activation of NF-κB due to mustard or CEES exposure have been shown in various cell lines [7,37,39], the detailed mechanism of this event is still unclear. Recent report [39] showed that NF-κB-driven gene expression has maximum at 9 hours in HD treated keratinocytes. In contrast, in a guinea pig model, Chatterjee et al. [40] have shown that NF-κB activation in lung tissues occurs shortly after CEES expose (1 hour), then disappears within 2 hours completely. However, in our experiments we did not observe any short term stimulating effect of CEES on NO production or iNOS expression (data not shown). Notably, the electrophoretic mobility shift assays used by Chatterjee et al. to measure NF-κB activation show only the state of NF-κB protein complex and provide no information regarding its binding to the DNA consensus sequences.

The physiological significance of potentially decreased iNOS expression by exposure to CEES or HD is not known. Considerable evidence, however, supports the view that nitric oxide production via iNOS plays a key role in wound healing [41-43]. Animal studies [16] have shown that the iNOS knockout mice have impaired wound healing that is reversed by iNOS gene transfer. Soneja et al. [44] have suggested that wound healing could be accelerated under circumstances where oxidative stress is minimized and nitric oxide production enhanced. We have initiated work to explore the role of antioxidants in preventing HD induced pathology in skin.

Conclusion

Our results show that CEES transiently inhibits NO production in LPS stimulated macrophages by inhibiting the expression of iNOS protein and not by modulating the enzymatic activity of iNOS. The decreased iNOS expression induced by CEES suggests that this alkylating agent inhibits the LPS stimulated activation of NF-κB and/or STAT-1α transcription factors, and this possibility is being investigated. We cannot directly address the physiological significance of our *in vitro* results, however, both decreased expression of iNOS and decreased production of nitric oxide are associated with impaired wound healing [16,41,43,44]. It is likely that the CEES or HD toxicity is modulated by a complex balance between nitric oxide production, thiol depletion and oxidative stress.

Methods

Materials

RPMI-1640 medium without phenol red and fetal bovine serum with a low endotoxin level were purchased from Life Technologies (Gaithersburg, MD). Rabbit anti-mouse iNOS antibody was obtained from Transduction Laboratory (Lexington, KY). Horseradish peroxidase conjugated anti-rabbit polyclonal antibodies, Escherichia coli lipopolysaccharide serotype 0111:B4, 3-(4,5-dimethylthiazolyl-2)-2,5-diphenyltetrazolium bromide (MTT), and 2-chloroethyl ethyl sulphide were obtained from Sigma Chemical Company (St. Louis, MO).

Cell culture and treatments

RAW264.7 murine macrophage-like cells (American Type Culture Collection, Rockville, MD) were cultured at 37°C in a humidified incubator with 5% CO_2 in RPMI-1640 medium with 10% fetal bovine serum, 50 U/ml penicillin and 50 mg/ml streptomycin (GiBcoBRL Grand Island, NY). CEES was used as a fresh (2 week old or less) 50 mM stock solution in dried ethanol. LPS was prepared as a 1 mg/ml stock solution in PBS and stored at -20°C for up to 3 months.

MTT assay

The MTT (3-(4,5-dimethylthiazool-2yl)-2,5-diphenyltetrazolium bromide) assay was performed by a slight modification of the method described by Wasserman et al. [45,46]. Briefly, at the end of each experiment, cultured cells in 96 well plates (with 200 μl of medium per well) were incubated with MTT (20 μl of 5 μg/ml per well) at 37°C for 4 hours. The formazan product was solubilized by addition of 100 μl of dimethyl sulfoxide (DMSO) and 100 μl of 10% SDS in 0.01 M HCl and the OD measured at 575 nm (Molecular Devices SPECTRAmax Plus microplate reader).

Western blot analysis

Cellular protein lysates were prepared as described in the protocol from Transduction Laboratory (Lexington, KY). Briefly, about 10^6 adherent cells were rinsed once with cold PBS and solublized by boiling in 0.1 ml of SDS-PAGE sample buffer for 5 min. Protein concentration was determined by the BCA protein assay (Pierce Chemical Co., Rockford, IL). A 30 μg aliquot of protein was separated via 8% SDS-PAGE and electrotransferred onto a nitrocellulose membrane. Western blotting was performed with a rabbit polyclonal antiserum against the C-terminal (961 to 1144 amino acids) sequence of mouse iNOS (Transduction Lab, Lexington, KY). The protein was detected using an enhanced chemiluminescence kit from Amersham Life Science (Arlington Heights, IL). Murine iNOS (Calbiochem, CA) was used as a positive control.

Determination of NO production

The production of NO, reflecting cellular NO synthase activity, was estimated from the accumulation of nitrite (NO_2^-), a stable breakdown product of NO, in the medium. Nitrite was measured using the Griess reagent according to the method of Green et al. [47]. Briefly, an aliquot of cell culture medium was mixed with an equal volume of Greiss reagent which reacts with nitrite to form an azo-product. Absorbance of the reaction product was determined at 532 nm using a microplate reader (Molecular Devices Microplate Reader). Sodium nitrite was used as a standard to calculate nitrite concentrations.

Intracellular NO measurement

Assays were performed using 96-well tissue culture plates as described by Imrich and Kobzik [17]. The cell density was adjusted to 2×10^5/ml, and a 100 μl aliquot of the cell suspension in media was placed put in each well. CEES and LPS solutions to achieve desired concentrations were added and the plate incubated for 24 h at 37°C in 5% CO_2. Following the removal of media, serum free 1640 RPMI supplemented with 10 mM HEPES containing 20 μM DCFH-DA or 10 μM DAF-2DA (final concentration) was added, and the plates incubated for 2 h at 37°C. Fluorescence intensity (relative fluorescence unit, RFU) was continuously monitored using 485 nm for excitation and 520 nm emission in a florescence microplate reader (FluoStar Microplate Reader, BMG).

Statistical analyses

Data were analyzed by followed with the Scheffe test for significance with $p < 0.05$. Results were expressed as the mean ± SD. In all the Figures, mean values not sharing a common letter are significantly different ($p < 0.05$). Mean values sharing a common letter are not significantly different. The mean values and standard deviations of at least three independent experiments are provided in all the Figures.

Abbreviations

HD, sulphur mustard gas

CEES, 2-chloroethyl ethyl sulphide

LPS, lipopolysaccharide

NO, nitric oxide

iNOS, inducible nitric oxide synthase

NF-κB, nuclear factor kappa B

STAT-1α, signal transducer and activator of transcription-1α

DCF, dichlorofluorescein

DCFH, dichlorofluorescin

DCFH-DA, dichlorofluorescin diacetate

TNF-α, tumor necrosis factor-alpha

IL-1β, interleukin-1 beta

AP2, activating protein 2

MTT, 3-(4,5-dimethylthiazool-2yl)-2,5-diphenyltetrazolium bromide

DMSO, dimethyl sulfoxide

DEM, diethylmaleate

BSO, buthionine sulfoximine

DAF-2DA, 4,5-diaminofluorescein diacetate

Authors' contributions

WLS supervised the overall conduct of the research, which was performed in his laboratory. MQ and HY carried out all of the experimental work in this study and performed the statistical analyses. WLS and VP analyzed the data and drafted the manuscript. MS (along with WLS) conceived of the study, participated in the study design, and provided continuous evaluation of the experimental data. All authors read and approved the final manuscript.

Acknowledgements

This research was supported by two United States Army Medical Research Command Grants: "The Influence of Antioxidant Liposomes on Macrophages Treated with Mustard Gas Analogues", USAMRMC Grant No. 98164001, and "Topical Application of Liposomal Antioxidants for Protection against CEES Induced Skin Damage", USAMRMC Grant No. W81XWH-05-2-0034.

References

1. Smith KJ, Skelton H: **Chemical warfare agents: their past and continuing threat and evolving therapies. Part I of II.** *Skinmed* 2003, **2(4):**215-221.
2. Yourick JJ, Dawson JS, Benton CD, Craig ME, Mitcheltree LW: **Pathogenesis of 2,2'-dichlorodiethyl sulfide in hairless guinea pigs.** *Toxicology* 1993, **84(1-3):**185-197.
3. Elsayed NM, Omaye ST, Klain GJ, Korte DW Jr.: **Free radical-mediated lung response to the monofunctional sulfur mustard butyl 2-chloroethyl sulfide after subcutaneous injection.** *Toxicology* 1992, **72(2):**153-165.
4. Elsayed NM, Omaye ST: **Biochemical changes in mouse lung after subcutaneous injection of the sulfur mustard 2-chloroethyl 4-chlorobutyl sulfide.** *Toxicology* 2004, **199(2-3):**195-206.
5. Kadar T, Turetz J, Fishbine E, Sahar R, Chapman S, Amir A: **Characterization of acute and delayed ocular lesions induced by sulfur mustard in rabbits.** *Curr Eye Res* 2001, **22(1):**42-53.
6. Gross CL, Innace JK, Hovatter RC, Meier HL, Smith WJ: **Biochemical manipulation of intracellular glutathione levels influences**

cytotoxicity to isolated human lymphocytes by sulfur mustard. *Cell Biol Toxicol* 1993, **9(3):**259-267.
7. Atkins KB, Lodhi IJ, Hurley LL, Hinshaw DB: **N-acetylcysteine and endothelial cell injury by sulfur mustard.** *J Appl Toxicol* 2000, **20 Suppl 1:**S125-8.
8. Arroyo CM, Schafer RJ, Kurt EM, Broomfield CA, Carmichael AJ: **Response of normal human keratinocytes to sulfur mustard (HD): cytokine release using a non-enzymatic detachment procedure.** In *Hum Exp Toxicol Volume 18*. Issue 1 ENGLAND ; 1999:1-11.
9. Sabourin CL, Petrali JP, Casillas RP: **Alterations in inflammatory cytokine gene expression in sulfur mustard-exposed mouse skin.** *J Biochem Mol Toxicol* 2000, **14(6):**291-302.
10. Stone WL, Qui M, Smith M: **Lipopolysaccharide enhances the cytotoxicity of 2-chloroethyl ethyl sulfide.** *BMC Cell Biol* 2003, **4(1):**1.
11. Li YH, Yan ZQ, Brauner A, Tullus K: **Activation of macrophage nuclear factor-kappa B and induction of inducible nitric oxide synthase by LPS.** *Respiratory research* 2002, **3:**23.
12. Kleinert H, Pautz A, Linker K, Schwarz PM: **Regulation of the expression of inducible nitric oxide synthase.** *European journal of pharmacology* 2004, **500(1-3):**255-266.
13. Borutaite V, Brown G: **What else has to happen for nitric oxide to induce cell death?** *Biochem Soc Trans* 2005, **33(Pt 6):**1394-1396.
14. Borutaite V, Brown GC: **Nitric oxide induces apoptosis via hydrogen peroxide, but necrosis via energy and thiol depletion.** *Free Radic Biol Med* 2003, **35(11):**1457-1468.
15. Nakai K, Kubota Y, Kosaka H: **Inhibition of nuclear factor kappa B activation and inducible nitric oxide synthase transcription by prolonged exposure to high glucose in the human keratinocyte cell line HaCaT.** *The British journal of dermatology* 2004, **150(4):**640-646.
16. Yamasaki K, Edington HD, McClosky C, Tzeng E, Lizonova A, Kovesdi I, Steed DL, Billiar TR: **Reversal of impaired wound repair in iNOS-deficient mice by topical adenoviral-mediated iNOS gene transfer.** *J Clin Invest* 1998, **101(5):**967-971.
17. Imrich A, Kobzik L: **Fluorescence-based measurement of nitric oxide synthase activity in activated rat macrophages using dichlorofluorescin.** *Nitric Oxide* 1997, **1(4):**359-369.
18. Huang A, Li C, Kao RL, Stone WL: **Lipid hydroperoxides inhibit nitric oxide production in RAW264.7 macrophages.** *Free Radic Biol Med* 1999, **26:**526-537.
19. Schmidt HH, Warner TD, Nakane M, Forstermann U, Murad F: **Regulation and subcellular location of nitrogen oxide synthases in RAW264.7 macrophages.** *Molecular pharmacology* 1992, **41(4):**615-624.
20. Hattori R, Inoue R, Sase K, Eizawa H, Kosuga K, Aoyama T, Masayasu H, Kawai C, Sasayama S, Yui Y: **Preferential inhibition of inducible nitric oxide synthase by ebselen.** *Eur J Pharmacol* 1994, **267(2):**R1-2.
21. Zhang N, Weber A, Li B, Lyons R, Contag PR, Purchio AF, West DB: **An inducible nitric oxide synthase-luciferase reporter system for in vivo testing of anti-inflammatory compounds in transgenic mice.** In *J Immunol Volume 170*. Issue 12 United States ; 2003:6307-6319.
22. Gray PJ: **Sulphur mustards inhibit binding of transcription factor AP2 in vitro.** In *Nucleic Acids Res Volume 23*. Issue 21 ENGLAND ; 1995:4378-4382.
23. Wright SD, Ramos RA, Tobias PS, Ulevitch RJ, Mathison JC: **CD14, a receptor for complexes of lipopolysaccharide (LPS) and LPS binding protein.** *Science* 1990, **249(4975):**1431-1433.
24. Downey JS, Han J: **Cellular activation mechanisms in septic shock.** *Front Biosci* 1998, **3:**d468-76.
25. Chen CC, Wang JK, Lin SB: **Antisense oligonucleotides targeting protein kinase C-alpha, -beta I, or -delta but not -eta inhibit lipopolysaccharide-induced nitric oxide synthase expression in RAW 264.7 macrophages: involvement of a nuclear factor kappa B-dependent mechanism.** In *J Immunol Volume 161*. Issue 11 UNITED STATES ; 1998:6206-6214.
26. Fujihara M, Connolly N, Ito N, Suzuki T: **Properties of protein kinase C isoforms (beta II, epsilon, and zeta) in a macrophage cell line (J774) and their roles in LPS-induced nitric oxide production.** In *J Immunol Volume 152*. Issue 4 UNITED STATES ; 1994:1898-1906.
27. Shapira L, Takashiba S, Champagne C, Amar S, Van Dyke TE: **Involvement of protein kinase C and protein tyrosine kinase in lipopolysaccharide-induced TNF-alpha and IL-1 beta production by human monocytes.** *J Immunol* 1994, **153(4):**1818-1824.
28. Shapira L, Sylvia VL, Halabi A, Soskolne WA, Van Dyke TE, Dean DD, Boyan BD, Schwartz Z: **Bacterial lipopolysaccharide induces early and late activation of protein kinase C in inflammatory macrophages by selective activation of PKC-epsilon.** *Biochem Biophys Res Commun* 1997, **240(3):**629-634.
29. Yoshioka Y, Kitao T, Kishino T, Yamamuro A, Maeda S: **Nitric oxide protects macrophages from hydrogen peroxide-induced apoptosis by inducing the formation of catalase.** *J Immunol* 2006, **176(8):**4675-4681.
30. Harbrecht BG, Di Silvio M, Chough V, Kim YM, Simmons RL, Billiar TR: **Glutathione regulates nitric oxide synthase in cultured hepatocytes.** *Ann Surg* 1997, **225(1):**76-87.
31. Vos TA, Van Goor H, Tuyt L, De Jager-Krikken A, Leuvenink R, Kuipers F, Jansen PL, Moshage H: **Expression of inducible nitric oxide synthase in endotoxemic rat hepatocytes is dependent on the cellular glutathione status.** *Hepatology* 1999, **29(2):**421-426.
32. Buchmuller-Rouiller Y, Corrandin SB, Smith J, Schneider P, Ransijn A, Jongeneel CV, Mauel J: **Role of glutathione in macrophage activation: effect of cellular glutathione depletion on nitrite production and leishmanicidal activity.** *Cell Immunol* 1995, **164(1):**73-80.
33. Powell LA, Warpeha KM, Xu W, Walker B, Trimble ER: **High glucose decreases intracellular glutathione concentrations and upregulates inducible nitric oxide synthase gene expression in intestinal epithelial cells.** *J Mol Endocrinol* 2004, **33(3):**797-803.
34. Gray PJ: **Sulphur mustards inhibit binding of transcription factor AP2.** *Nucleic Acids Research* 1995, **23(Vol. 23):**4378-4382.
35. Gray PJ: **Sulphur mustards inhibit binding of transcription factor AP2 in vitro.** *Nucleic Acids Res* 1995, **23(21):**4378-4382.
36. Chen XM, Gray PJ, Cullinane C, Phillips DR: **Differential sensitivity of transcription factors to mustard-damaged DNA.** *Chemico-biological interactions* 1999, **118(1):**51-67.
37. Fabbri S, Prontera C, Broggini M, D'Incalci M: **Differential inhibition of the DNA binding of transcription factors NF kappa B and OTF-1 by nitrogen mustard and quinacrine mustard: transcriptional implications.** *Carcinogenesis* 1993, **14(9):**1963-1967.
38. Spink J, Cohen J, Evans TJ: **The cytokine responsive vascular smooth muscle cell enhancer of inducible nitric oxide synthase. Activation by nuclear factor-kappa B.** *The Journal of biological chemistry* 1995, **270(49):**29541-29547.
39. Minsavage GD, Dillman 3d JF: **Protective role of CAPE on bifunctional alkylating agent-induced toxicity in keratinocytes via modulation of NF-kappaB, p53 and ARE/EpRE signaling .** In *Bioscience 2006 Medical Defense Review* ; 2006:94-94.
40. Chatterjee D, Mukherjee S, Smith MG, Das SK: **Signal transduction events in lung injury induced by 2-chloroethyl ethyl sulfide, a mustard analog.** *J Biochem Mol Toxicol* 2003, **17(2):**114-121.
41. Schwentker A, Billiar TR: **Nitric oxide and wound repair.** *Surg Clin North Am* 2003, **83(3):**521-530.
42. Weller R: **Nitric oxide: a key mediator in cutaneous physiology.** *Clin Exp Dermatol* 2003, **28(5):**511-514.
43. Witte MB, Barbul A: **Role of nitric oxide in wound repair.** *Am J Surg* 2002, **183(4):**406-412.
44. Soneja A, Drews M, Malinski T: **Role of nitric oxide, nitroxidative and oxidative stress in wound healing.** *Pharmacol Rep* 2005, **57 Suppl:**108-119.
45. Wasserman TH, Twentyman P: **Use of a colorimetric microtiter (MTT) assay in determining the radiosensitivity of cells from murine solid tumors.** *Int J Radiat Oncol Biol Phys* 1988, **15(3):**699-702.
46. Twentyman PR, Luscombe M: **A study of some variables in a tetrazolium dye (MTT) based assay for cell growth and chemosensitivity.** *Br J Cancer* 1987, **56(3):**279-285.
47. Green LC, Wagner DA, Glogowski J, Skipper PL, Wishnok JS, Tannenbaum SR: **Analysis of nitrate, nitrite, and [15N]nitrate in biological fluids.** In *Anal Biochem Volume 126*. Issue 1 UNITED STATES ; 1982:131-138.

BMC Cell Biology

BioMed Central

The influence of N-acetyl-L-cysteine on oxidative stress and nitric oxide synthesis in stimulated macrophages treated with a mustard gas analogue

BMC Cell Biology 2008, **9**:33 doi:10.1186/1471-2121-9-33

Victor Paromov (paromov@etsu.edu)
Min Qui (qui@etsu.edu)
Hongsong Yang (yangh@etsu.edu)
Miltorn Smith (mgsmithmd@gmail.com)
William L Stone (stone@etsu.edu)

ISSN 1471-2121

Article type Research article

Submission date 14 January 2008

Acceptance date 20 June 2008

Publication date 20 June 2008

Article URL http://www.biomedcentral.com/1471-2121/9/33

The influence of N-acetyl-L-cysteine on oxidative stress and nitric oxide synthesis in stimulated macrophages treated with a mustard gas analogue

Victor Paromov [1], Min Qui[1], Hongsong Yang[1], Milton Smith [2], William L Stone[1§]

[1] Department of Pediatrics, College of Medicine, East Tennessee State University, Johnson City, TN 37614, USA
[2] AMAOX, Ltd., #208, 6300 N. Wickham Road, Melbourne, FL 32944, USA

[§]Corresponding author

Email addresses:

VP: paromov@etsu.edu

HY: yangh@etsu.edu

MQ: qui@etsu.edu

MS: mgsmithmd@gmail.com

WLS: stone@etsu.edu

Abstract

Background

Sulphur mustard gas, 2, 2'-dichlorodiethyl sulphide (HD), is a chemical warfare agent. Both mustard gas and its monofunctional analogue, 2-chloroethyl ethyl sulphide (CEES), are alkylating agents that react with and diminish cellular thiols and are highly toxic. Previously, we reported that lipopolysaccharide (LPS) significantly enhances the cytotoxicity of CEES in murine RAW 264.7 macrophages and that CEES transiently inhibits nitric oxide (NO) production via suppression of inducible NO synthase (iNOS) protein expression. NO generation is an important factor in wound healing. In this paper, we explored the hypotheses that LPS increases CEES toxicity by increasing oxidative stress and that treatment with N-acetyl-L-cysteine (NAC) would block LPS induced oxidative stress and protect against loss of NO production. NAC stimulates glutathione (GSH) synthesis and also acts directly as a free radical scavenger. The potential therapeutic use of the antibiotic, polymyxin B, was also evaluated since it binds to LPS and could thereby block the enhancement of CEES toxicity by LPS and also inhibit the secondary infections characteristic of HD/CEES wounds.

Results

We found that 10 mM NAC, when administered simultaneously or prior to treatment with 500 μM CEES, increased the viability of LPS stimulated macrophages. Surprisingly, NAC failed to protect LPS stimulated macrophages from CEES induced loss of NO production. Macrophages treated with both LPS and CEES show increased oxidative stress parameters (cellular thiol depletion and increased protein carbonyl levels). NAC effectively protected RAW 264.7 cells simultaneously treated with CEES and LPS from GSH loss and oxidative stress. Polymyxin B was found to partially block nitric oxide production and diminish CEES toxicity in LPS-treated macrophages.

Conclusion

The present study shows that oxidative stress is an important mechanism contributing to CEES toxicity in LPS stimulated macrophages and supports the notion that antioxidants could play a therapeutic role in preventing mustard gas toxicity. Although NAC reduced oxidative stress in LPS stimulated macrophages treated with CEES, it did not reverse CEES-induced loss of NO production. NAC and polymyxin B were found to help prevent CEES toxicity in LPS-treated macrophages.

Background

Mustard gas (HD) is a chemical weapon that can easily and inexpensively be produced and used against military or civilian populations with both acute and devastating long-term effects [1-3]. It produces rapid damage to eyes, skin and pulmonary tissues as well as subsequent damage to many internal organ systems [1, 4]. Despite its long history of use, starting in World War I, the molecular mechanisms for HD toxicity are not fully understood and there is continuing research on the design of optimal countermeasures. Mustard gas acts as an alkylating agent covalently modifying DNA, proteins and other

macromolecules. There is increasing evidence that HD or CEES toxicity is due, in part, to an enhanced production of inflammatory cytokines [5-9], increased oxidative stress [10] and the generation of damaging reactive oxygen species (ROS) [8, 9, 11]. HD and CEES have been shown to shift the intracellular redox milieu toward a more oxidized state by reacting with and depleting the intracellular antioxidant GSH with a subsequent loss of protection against ROS and an activation of inflammatory responses [12-14].

In a previous publication, we showed that the cytotoxicity of CEES towards murine RAW 264.7 macrophages was markedly enhanced by the presence of low levels of LPS (25 ng/ml), or pro-inflammatory cytokines, i.e., 50 ng/ml IL-1ß or 50 ng/ml TNF-α [15]. LPS is part of the cell wall of gram negative bacteria: it is ubiquitous and is found in serum, tap water and dust. Both civilian and military personnel would always have some degree of exposure to environmental LPS. HD induced skin lesions often have secondary infections which could markedly increase LPS levels. In macrophages, stimulation by LPS, as well as by pro-inflammatory cytokines, leads to the activation and nuclear translocation of transcription factor NF-κB (nuclear factor-kappa B). One of the major consequences of such activation in macrophages is an induction of iNOS expression with subsequent elevation of intracellular NO [16, 17]. In addition to NF-κB activation, the binding of transcription factor STAT-1 (signal transducer and activator of transcription-1) to the inducible nitric oxide synthase (iNOS) promoter is required for optimal induction of the iNOS gene by LPS [17].

In a recent publication, we found that CEES transiently inhibits nitric oxide (NO) production by suppressing iNOS protein expression in LPS stimulated macrophages [18]**.** NO production is an important factor in promoting wound healing [19, 20] and iNOS deficiency impairs wound healing in animal models [21]. RAW 264.7 macrophages have undetectable levels of iNOS or NO production in the absence of LPS and in the presence of LPS they show a marked induction of iNOS and NO production [18].

In the present study, we tested the hypothesis that the synergistic cytotoxic effect of CEES with LPS is due to increased oxidative stress with a subsequent depletion of intracellular GSH levels and an increase in protein carbonyls. In some cell types, GSH has also been found to regulate NO generation with decreased GSH levels associated with decreased NO production [22-24]. Vos et al. [25] found that GSH depletion in hepatocytes prevented iNOS induction by cytokines but this effect could be reversed by the addition of NAC. We, therefore, hypothesized that the addition of NAC to stimulated macrophages would reverse the loss of NO production caused by CEES. We also reasoned that polymyxin B, by binding to LPS, would diminish CEES toxicity in LPS treated macrophages.

Results

The influence of NAC on cell viability and NO production in CEES/LPS treated macrophages

Figure 1a shows the effect of NAC treatment on RAW 264.7 macrophages treated with LPS and/or 500 μM CEES for 24 h. In this experiment, NAC was added simultaneously with LPS and CEES. In the absence of NAC, LPS, at either 50 ng/ml or 100 ng/ml level, markedly decreased cell viability in CEES treated cells compared to cells treated with LPS or CEES alone. This is similar to our previous observations in which cell viability was measured by both the MTT assay and the propidium iodide exclusion assay; the assays were well correlated with each other [15]. The addition of 10 mM NAC increased the viability of macrophages treated with both CEES and LPS (50 ng/ml or 100 ng/ml) to the same level observed for control cells (treated with vehicle alone). It is likely that the differences in the viability of cells treated with NAC and different levels of LPS represent experimental variability since these differences are marginal.

Figure 1b shows NO release, measured as the nitrite levels in the cell culture medium, for the identical cells/treatments used in Figure 1a. As expected, LPS treatment alone resulted in a marked increase of NO generation, and LPS-stimulated macrophages treated with CEES showed a marked reduction in NO production. Surprisingly, NAC treatment did not prevent the decrease in NO production caused by CEES. In cells treated with LPS alone, NAC treatment actually resulted in a decreased production of NO (up to 40% reduction).

In order to further evaluate NAC as a potential protective agent for CEES toxicity in stimulated macrophages, we did two additional experiments in which NAC was added to macrophages 5 h prior to CEES application or 5 h after CEES application. These additional experiments provide a measure of the potential time frame during which NAC could be therapeutically useful. Similar to the previous experiment, LPS and CEES were added simultaneously (as indicated). As shown in Figure 2a, NAC had a substantial protective effect on cell viability when added 5 h before CEES/LPS; however NAC did not protect against loss of NO production in CEES/LPS-treated cells (Figure 2b). When added 5 h after CEES treatment (Figure 3a), NAC was much less effective in protecting the macrophages but still resulted in at least a doubling of the cell viability compared to the cells not treated with NAC. As shown in Figure 3b, NAC added 5 h after CEES/LPS, also failed to restore NO production.

We believe that the difference in viability of cells stimulated with LPS in the absence or in the presence of NAC (Figure 2A) could represent experimental variation since relatively small differences are being compared. In the contrast, the protective effect of NAC on CEES+LPS treated macrophages is robust and over seven fold. This point is further reinforced by the data shown in Figure 3A, where viability of cells stimulated with LPS in the absence or in the presence of NAC was not significantly different.

The influence of NAC on oxidative stress and NO production, intracellular GSH and thiols in CEES/LPS treated macrophages by fluorescence microscopy

The influence of NAC on macrophages treated with CEES/LPS was also examined by fluorescent microscopy using three fluorescent probes: a) carboxy-dichlorofluorescin

diacetate (carDCFH-DA), a sensor for combined ROS and reactive nitrogen oxide species (RNOS) generation [26-28]; b) 7-amino-4-chloromethylcoumarin (CMAC), an indicator of intracellular GSH [29], and; c) 5-chloromethylfluorescein diacetate (CMF-DA), a probe for total non-protein cellular thiol levels that lacks specificity for GSH [29, 30].

Figure 4a shows the results using the lipid soluble carDCFH-DA probe. This probe enters cells and is trapped after being converted to a nonfluorescent polar derivative by cellular esterases. CarDCFH can then be oxidized by either ROS [26, 28] or reactive nitrogen oxide species (RNOS) [26, 27] to the fluorescent product carboxydichlorofluorescein (car-DCF) and thereby provide a qualitative index of oxidation stress. As expected, treatment with LPS alone (50 ng/ml for 12 h) induced a marked generation of ROS plus RNOS in macrophages. We and others have shown that car-DCF fluorescence in activated macrophages is almost entirely from NO generation rather than ROS generation [18, 27]. Figure 4a also shows that a 12 h treatment with CEES alone (500 μM) or simultaneous treatment with 500 μM CEES and 50 ng/ml LPS (CEES+LPS) induces a higher level of car-DCF fluorescence than observed in control cells treated with vehicle alone. We previously reported that CEES markedly reduces NO generation in LPS stimulated cells by reducing the expression of inducible iNOS [18]. The car-DCF fluorescence observed in CEES treated cells or CEES+LPS cells is likely, therefore, to be due to an enhanced generation of ROS alone with a minimal contribution from RNOS.

Simultaneous treatment with 10 mM NAC reduced the car-DCF fluorescence observed in LPS stimulated cells, as well as in CEES or CEES+LPS treated RAW 264.7 macrophages (Figure 4a, compare top row to bottom row). These data qualitatively suggest that CEES and CEES+LPS treatments induce oxidative stress in RAW 264.7 macrophages that can be diminished by NAC treatment.

As a next step we examined intracellular levels of GSH using the CMAC probe (Figure 4b, top row) and levels of total intracellular thiols using the CMF-DA probe (Figure 4c, top row). Both the CMAC and CMF probes revealed similar qualitative patterns: CEES or CEES+LPS treatment for 12 h caused cellular GSH and thiol depletion but treatment with LPS alone did not. These data reinforce the notion that treatment with either CEES alone or treatment with CEES+LPS induces sufficient oxidative stress to reduce intracellular GSH and thiol levels. LPS alone, however, did not induce GSH or thiol depletion. NAC application was found to inhibit the loss of GSH and thiol levels caused by CEES or CEES+LPS treatment (see Figures 4b and 4c, bottom rows).

The microscopic data (Figure 4) show merged visible/fluorescent images, thus allowing cell counting and the monitoring of cell morphology changes. The counts of live (morphologically unchanged) cells under conditions described above (Figure 4) confirmed the major observations from the MTT- derived data (Figure 1a): (1) NAC treatment enhance (3-fold) the viability of CEES+LPS treated macrophages; (2) CEES+LPS is more toxic than CEES alone. The cells count (as percentage of untreated control cells ± SEM) were 57% ± 7, 76% ± 10, 18% ± 4, 84% ± 8, 75% ± 9, 67% ± 6,

54% ± 10, respectively for macrophages treated with CEES (500 μM), LPS (50 ng/ml), CEES+LPS, NAC (10 mM), NAC+CEES, NAC+LPS and NAC+CEES+LPS.

Quantitative effects of CEES on GSH status and protein carbonyl levels in LPS-stimulated RAW 264.7 macrophages

Since the fluorescence microscopy data presented above are primarily qualitative, we wanted to confirm our results by a more quantitative approach. We, therefore, determined the effect of 500 μM CEES on the GSH/GSSG status of RAW 264.7 macrophage treated or untreated with 50 ng/ml LPS for 12 h. Total GSH (GSH+GSSG) and GSSG concentrations were measured in cell lysates using a quantitative GSH assay kit and the values normalized to total protein content of the lysate (see Materials and Methods). Figure 5 shows that both total GSH and GSSG levels in macrophages treated with either vehicle alone or LPS were not significantly different, i.e., similar to our fluorescent microscopy data. However, cells treated with CEES alone showed a depletion in total GSH as well as an increase in GSSG levels; cells treated with both CEES and LPS were further depleted in total GSH and the percentage of GSSG in these cells was the highest (40%). These results show that LPS alone does not induce a significant oxidative stress, CEES alone induces a moderate oxidative stress but the combination of both CEES and LPS induces the highest observed level of oxidative stress.

In addition, we measured the protein carbonyl levels in control cells, cells treated with CEES (500 μM) alone or cells simultaneously treated with both LPS (50 ng/ml) and CEES (500 μM) for 12 h. Protein carbonyls are stable protein oxidation products. The combination of CEES and LPS produced about 1.5 fold increase in protein carbonyl levels, however cells treated with CEES alone were not significantly different from control cells treated with vehicle alone (data not shown). Cells treated with LPS alone were not assayed in this experiment since both our qualitative (Figure 4b and 4c) and quantitative data (Figure 5) showed no evidence of oxidative stress with this treatment.

The inability of NAC to reverse NO loss in CEES/LPS treated cells is not GSH dependent

The data in Figure 1b show that NAC has almost no ability to restore NO production in LPS-stimulated macrophages treated with CEES. An inability of NAC to prevent the depletion of GSH in LPS-stimulated cells treated with CEES could possibly explain these results. In order to explore this possibility, we examined the ability of 5 mM NAC to prevent GSH depletion in LPS (50 ng/ml) stimulated and CEES treated (500 μM for 4 h) RAW 264.7 cells. Figure 6 shows that CEES treatment alone decreased intracellular GSH by only about 10% compared to LPS stimulated cells in the absence NAC. As expected, the decrease in GSH levels was quite large in cells treated with both CEES+LPS (in the absence of NAC) but treatment with 5 mM NAC was effective in preventing this loss. The data shown in Figure 6 were obtained by HPLC analyses of the cell lysates but

similar results were obtained by using a fluorometric assay for GSH [31] (data not shown). Despite the fact that NAC can increase the GSH level by three fold in CEES+LPS treated cells it does almost nothing to increase NO production (Figure 1a). These data suggest that the loss of NO production in CEES treated stimulated macrophages is not GSH dependent as has been observed in some other cell lines [22-25].

Polymyxin B diminishes CEES toxicity in LPS-treated macrophages and partially blocks LPS induced NO production.

Polymyxin B is an antibiotic drug, which selectively binds and neutralizes LPS. Since LPS enhances CEES toxicity, we tested the ability of polymyxin B to reduce CEES toxicity (500 μM) and decrease NO generation in LPS (50 ng/ml) stimulated macrophages. Figure 7a shows that polymyxin B (10 μg/ml) had no cytotoxic effect on RAW 264.7 macrophages but partially reduced the cytotoxicity of CEES+LPS treated cells (18 h). Nevertheless, polymyxin B produced at least a six fold increase in cell viability compared to cell treated with both LPS and CEES for 18 h. As shown in Figure 7b, polymyxin B effectively blocked the production of NO (measured as nitrite levels) in LPS (50 ng/ml for 18 h) treated macrophages as would be expected if it bound and blocked the action of LPS.

Discussion

The cytotoxic effect of HD, and its analogue CEES, is believed to involve an increased generation of damaging free radicals and ROS [8, 11-13, 32]. The data presented here show that LPS in combination with CEES induces intracellular GSH and thiol depletion as well as increased levels of protein carbonyls. In experiments with various human cell lines we have found that GSH depletion is relatively rapid as it occurs within first hour of incubation (data not shown). Thus, it is likely that this depletion is due, in large part, by a direct reaction of CEES with GSH. The measurement of protein carbonyls is one of the best indices for oxidative stress due to the stability of protein carbonyls and sensitivity of the measurement [33]. Cellular thiols are important markers of the redox state of the cell. In particular, GSH is one of the major components of the intracellular redox system and a key intracellular antioxidant that functions as a substrate for glutathione peroxidase which detoxifies both hydrogen peroxide and lipid hydroperoxides [34, 35]. Depletion of intracellular stores of GSH plays an important role in the development of oxidative stress [12, 13, 36]. Recent work also suggests that the anti-apoptotic protein Bcl-2 directly interacts with GSH to regulate an important mitochondrial GSH pool that influences mitochondrial oxidative stress and subsequent apoptosis [37]. It is highly possible that both sulphur and nitrogen mustards possess a similar ability to deplete cellular thiols and induce protein oxidation.

Taken together, our data strongly suggest that CEES induces oxidative stress in stimulated macrophages. Moreover, the pattern of oxidative stress parallels the pattern observed for CEES cytotoxicity, i.e., cytotoxicity and oxidative stress are amplified in cells treated with both CEES and LPS. The addition of 5-10 mM NAC, a well

characterized water-soluble antioxidant, was found to be very effective in minimizing CEES toxicity in stimulated macrophages and in preventing GSH depletion. Our data suggests that NAC can be added five hours before or even five hours after CEES and still exert a cytoprotective effect. Das et al. [9] recently found that NAC in drinking water was effective in reducing CEES-induced lung toxicity to Guinea pigs. Fan et al. [38] have shown that liposomal encapsulated NAC delivered intratracheally was more effective than free NAC against acute respiratory distress syndrome in a rat model. It is interesting, therefore, that McClintock et al. [39] have shown that reducing agents (NAC or GSH), as well as some anti-oxidant enzymes, delivered via liposomes, can substantially diminish CEES-induced injury in rat lungs. We are currently formulating an optimal antioxidant liposome preparation for treating either lung or skin induced CEES/HD injury.

We previously reported that CEES induces a transient loss of iNOS protein expression in LPS stimulated RAW 264.7 macrophages but does not inhibit the enzymatic activity of iNOS. Based of the work of others [22-25], we hypothesized that NAC treatment would not only be protective against CEES toxicity but would also restore NO production in LPS stimulated macrophages treated with CEES. Our results indicate, however, that this was not the case. Our data did, however, show that NAC effectively increases cell viability, increases GSH levels and reduces oxidative stress in LPS stimulated macrophages treated with CEES.

CEES could inhibit iNOS protein synthesis by a number of possible molecular mechanisms which we are currently exploring [18]. It is generally accepted that both the transcription factor NF-κB and STAT-1 play central roles in the LPS induction of iNOS [17, 40]. It is possible that CEES/HD could inhibit the NF-κB and/or the STAT-1 pathways in RAW 264.7 macrophages and consequently block iNOS gene expression. For instance, CEES could alkylate the NF-κB consensus nucleotide binding sequences thereby preventing the binding of activated NF-κB to the iNOS promoter and block the subsequent production of iNOS mRNA and protein expression. Previous studies *in vitro* have shown that DNA alkylation by CEES [41, 42] or by nitrogen mustard [43] can inhibit the DNA binding of transcription factor AP2 or NF-κB.

Alternatively, the DNA binding ability of the NF-κB and/or STAT-1 transcription factors could be reduced by direct covalent modification by CEES or as an indirect result of GSH depletion, i.e., redox regulation. Nishi et al. [44] have found, for example, that the cysteine-62 (Cys-62) residue of the p50 NF-κB protein subunit is oxidized in the cytoplasm but reduced in the nucleus, and that the reduced form is essential for NF-κB DNA binding. It is possible that CEES could rapidly react with Cys-62 of the p50 NF-κB subunit and prevent its DNA binding. However, since NAC was found to restore GSH levels without restoring iNOS activity (see Figures 1 and 7), it is unlikely that a GSH redox modulation of the p50 Cys-62 is the molecular mechanism for CEES induced loss of iNOS protein in LPS-stimulated macrophages. This cannot, however, be completely ruled out based on our current data.

Moreover, there is evidence suggesting that alkylating agents do not inhibit but rather promote NF-κB activation. It is known that CEES or HD treated cells release elevated levels of TNF-α and also show NF-κB activation both *in vitro* and *in vivo* as measured by electrophoretic mobility shift assays (EMSAs)[7, 45, 46]. Minsavage and Dillman recently demonstrated that NF-κB is activated by HD treatment in human cell lines via nonclassical p53-dependent pathway [47]. Collectively, these data suggest that the inhibition of iNOS expression by CEES or HD could be due to downregulation of the STAT-1 and/or classical NF-κB pathway. We are currently exploring these various molecular mechanisms.

In the work presented here, we also tested the ability of polymyxin B to block the effect of LPS. Polymyxin B binds to the lipid A domain of LPS and neutralizes its activity. Our data show that polymyxin B effectively inhibits CEES toxicity in LPS stimulated cells. *In vivo*, LPS could directly enhance CEES/HD toxicity in cells with functional CD14 receptors or by triggering the release of pro-inflammatory cytokines, such as TNF-α and IL-1ß, by immune cells. We have previously demonstrated that inflammatory cytokines also enhance CEES cytotoxicity [15].

Conclusions

Our *in vitro* work presents novel evidence supporting the view that oxidative stress is an important component of CEES/HD toxicity and that antioxidants have therapeutic potential. We anticipated that NAC would prevent GSH depletion and restore the loss of iNOS activity in CEES treated macrophages stimulated with LPS. Although NAC was effective in preventing both CEES toxicity and GSH depletion, it failed to restore iNOS expression. Our results to date indicate that CEES causes a transient decrease in iNOS protein syntheses rather than a direct inhibition of iNOS activity due to covalent modification(s) by CEES. We are currently investigating the molecular mechanism(s) for the down regulation of iNOS expression by CEES.

Inhibition of iNOS and NO production could be an important element in the slow wound healing observed subsequent to CEES/HD injury. Considerable evidence suggests that iNOS is an important component of wound healing [19, 20, 48]. Although NAC maybe effective at reducing CEES/HD toxicity it is not effective at elevating NO production due to iNOS inhibition by CEES/HD. A more detailed understanding of the molecular mechanism(s) responsible for iNOS inhibition by CEES/HD could, therefore, be useful in the design of more effective countermeasures.

The fact that LPS was found to enhance CEES toxicity highlights the potential importance of preventing secondary infection in the treatment of HD toxicity. LPS is a component of gram negative bacteria and a ubiquitous environmental contaminant. Its presence at very low levels (ng/ml) amplifies the toxicity of CEES. Polymyxin B, a topically applied antibiotic that binds LPS, was shown to block the iNOS inducing ability of LPS and to reduce CEES toxicity in LPS stimulated cells. Polymyxin B could, therefore, be useful as a supportive treatment in order to prevent secondary

infections and to reduce HD toxicity, since it both neutralizes LPS and prevents the growth of gram-negative bacteria in healing wounds.

The path to an optimal countermeasure to CEES/HD exposure may lie in a poly-drug formulation that minimizes oxidative stress, prevents inflammation and secondary infections, and, also, protects iNOS activity. Antioxidant liposomes are currently being investigated as they have unique ability for targeted delivery of both water-soluble and lipid soluble antioxidants [49] or other drugs, for instance, polymyxin B (personal communications, Dr. Zach Suntres) as well as anti-inflammatory agents.

Methods

Materials

RPMI-1640 medium without phenol red and fetal bovine serum with a low endotoxin level were purchased from Life Technologies (Gaithersburg, MD). *Escherichia coli* lipopolysaccharide serotype 0111:B4, 3-(4,5-dimethylthiazolyl-2)-2,5-diphenyltetrazolium bromide (MTT), CEES, NAC, Greiss reagent, GSH, BHT, EDTA, and all organic solvents used were obtained from Sigma Chemical Company (St. Louis, MO). Fluorescent dyes carDCFH-DA, CMAC, and CMF-DA were purchased from Molecular Probes (Invitrogen Corp., Carlsbad, CA).

Cell culture and treatments

RAW264.7 murine macrophage-like cells (American Type Culture Collection, Rockville, MD) were cultured at 37^{o}C in a humidified incubator with 5% CO_2 in RPMI-1640 medium with 10% fetal bovine serum, 100 U/ml penicillin and 100 mg/ml streptomycin (GiBcoBRL Grand Island, NY). Adherent cells were subcultured in 96 well Costar tissue culture plates and treated with CEES and/or LPS in the presence or absence of various concentrations of NAC as indicated in the Figure legends. CEES was used only as a fresh 50 mM stock solution in anhydrous ethanol. LPS was prepared as a 0.5 μg/ml stock solution in PBS, filter-sterilized and stored at -20^{0} C for up to 6 months. NAC was prepared as a 0.5 M stock solution in PBS (pH adjusted to 7.4), filter-sterilized and stored at 4^{0} C for up to two weeks.

MTT assay

MTT assay was performed by a slight modification of the method described by Wasserman et al. [50, 51]. Briefly, at the end of each experiment, cultured cells in 96 well plates (with 200 μl of medium per well) were incubated with MTT (20 μl of 5 μg/ml per well) at 37^{o}C for 4 h. The formazan product was solubilized by addition of 100 μl of dimethyl sulfoxide (DMSO) and the OD measured at 575 nm with a Spectramax Plus 384 microplate reader (Molecular Devices Corp, Sunnyvale, CA)

NO generation in RAW264.7 macrophages

The production of NO, reflecting cellular NO synthase activity, was estimated from the accumulation of nitrite (NO_2^-), a stable breakdown product of NO, in the medium. NO_2^- was assayed by the method of Green et al. [52]. Briefly, an aliquot of cell culture medium was mixed with an equal volume of Greiss reagent which reacts with NO_2^- to form an azo-product. Absorbance of the reaction product was determined at 532 nm using a Spectramax Plus 384 microplate reader (Molecular Devices Corp, Sunnyvale, CA). Sodium nitrite was used as a standard to calculate NO_2^- concentrations.

Quantitative GSH analyses

RAW264.7 macrophages incubated in 96-well plate (~10^6 adherent cells/well) and treated with LPS/CEES/NAC as indicated in the Figure legends was assayed for total GSH (GSH plus GSSG) using the GSH assay kit (World Precision Instruments, Sarasota, FL) according to the company's protocol. This assay uses the Tietze's enzymatic recycling method [53]. In order to measure just GSSG, 2-vinylpyridine was first used to derivatize GSH alone [54]. Total GSH and GSSG levels were normalized to the total protein (as determined by the standard BCA assay). Alternatively, GSH analyses of the cell lysates were analyzed by isocratic HPLC with electrochemical detector composed of Coulochem II model 5200A and a Coulochem 5011 analytical cell (ESA Inc, Chelmsford, MA) as described by [55]. Since the cell lysates contained no measurable levels of homocysteine, this aminothiol was used as an internal standard.

Protein carbonyl measurement

Protein carbonyl levels were measured by an enzyme immunoassay kit from Cell Biolabs (San Diego, CA) according to the manufacture's instructions. In this assay, the protein samples are derivatized by making use of the reaction between 2,4-dinitrophenylhydrazine (DNPH) and protein carbonyls to form a DNP hydrazone which is assayed using an anti-DNP antibody and a HRP conjugated secondary antibody. A standard curve from the oxidized BSA standards was run with each microplate. This kit assay is essentially a modification [56] of the method described by Buss et al. [57].

Fluorescent microscopic analyses

The cell density was adjusted to 2×10^5/ml, and a 100 µl aliquot of the cell suspension in media was placed in each well of an 8-well Lab-Tek chamber glass slide (Nunc, Rochester, NY). Vehicle alone, CEES alone (500 µM), CEES+LPS (50 ng/ml) in the presence or absence of NAC (10 mM) were simultaneously added to chamber slides and incubated for 12 h at 37°C in 5% CO_2. At the end of the treatment a stock solution of desired fluorescent probe in DMSO was added and the slides incubated for an additional 30 min at 37°C. The cells were washed with fresh PBS twice, observed and digitally photographed using a MOTIC inverted phase contrast fluorescence microscope equipped with a Nikon Coolpix E4300 4-megapixel camera (Martin Microscope, Easley, SC). A 20 µM carDCFH-DA and a standard FITC filter were used to monitor combined ROS

and RNOS generation; a 20 μM CMAC and a standard DAPI filter were used to monitor intracellular GSH; a 20 μM CMF-DA and a standard FITC filter were used to monitor cellular thiol levels. All the optical filters were obtained from Chroma Technology Corp (Rockingham, VT).

Statistical analyses

Data were analyzed ANOVA followed with the Scheffe test for significance with $p < 0.05$ using SPSS 14.0 for Windows (Chicago, IL). Results were expressed as the mean ± SD. In all the Figures, mean values not sharing a common letter are significantly different ($p<0.05$). Mean values sharing a common letter are not significantly different. The mean values and standard deviations of at least three independent experiments are provided in all the Figures.

Abbreviations

AP2, activating protein 2; CEES, 2-chloroethyl ethyl sulphide; carDCFH-DA, carboxy-dichlorofluorescin diacetate; CMAC, 7-amino-4-chloromethylcoumarin; CMF-DA, 5-chloromethylfluorescein diacetate; DNPH, 2,4-dinitrophenylhydrazine; GSH, reduced glutathione; GSSG, oxidized glutathione; HD, sulphur mustard gas; IL-1ß, interleukin-1 beta ; LPS, lipopolysaccharide; MTT, 3-(4,5-dimethylthiazool-2yl)-2,5-diphenyltetrazolium bromide; NAC, N-acetyl-L-cysteine ; NO, nitric oxide; iNOS, inducible nitric oxide synthase; NF-κB, nuclear factor kappa B; RNOS, reactive nitrogen oxide species; ROS, reactive oxygen species; STAT-1, signal transducer and activator of transcription-1; TNF-α, tumor necrosis factor-alpha

Authors' contributions

VP and WLS analyzed the data and drafted the manuscript. WLS supervised the overall conduct of the research, which was performed in his laboratory. VP, MQ and HY carried out the experimental work in this study and performed the statistical analyses. MS (along with WLS) conceived of the study, participated in the study design, and provided continuous evaluation of the experimental data. All authors read and approved the final manuscript.

Acknowledgements

This research was supported by three United States Army Medical Research Command (USAMRMC) Grants: “The Influence of Antioxidant Liposomes on Macrophages Treated with Mustard Gas Analogues”, Grant No. 98164001; “Topical Application of Liposomal Antioxidants for Protection against CEES Induced Skin Damage”, Contract

No. W81XWH-05-2-0034 and; “A Proteomic Approach for Studying the Therapeutic Use of Antioxidant Liposomes”, Contract No. W81XWH-06-2-044.

References

1. Paromov V, Suntres Z, Smith M, Stone WL: Sulfur mustard toxicity following dermal exposure: role of oxidative stress, and antioxidant therapy. *Journal of burns and wounds* 2007, 7:e7.

2. Balali-Mood M, Hefazi M: The pharmacology, toxicology, and medical treatment of sulphur mustard poisoning. *Fundam Clin Pharmacol* 2005, 19(3):297-315.

3. Smith KJ, Casillas R, Graham J, Skelton HG, Stemler F, Hackley BE, Jr.: Histopathologic features seen with different animal models following cutaneous sulfur mustard exposure. *Journal of dermatological science* 1997, 14(2):126-135.

4. Dacre JC, Goldman M: Toxicology and pharmacology of the chemical warfare agent sulfur mustard. *Pharmacological reviews* 1996, 48(2):289-326.

5. Arroyo CM, Burman DL, Kahler DW, Nelson MR, Corun CM, Guzman JJ, Smith MA, Purcell ED, Hackley BE, Jr., Soni SD *et al*: TNF-alpha expression patterns as potential molecular biomarker for human skin cells exposed to vesicant chemical warfare agents: sulfur mustard (HD) and Lewisite (L). *Cell biology and toxicology* 2004, 20(6):345-359.

6. Arroyo CM, Schafer RJ, Kurt EM, Broomfield CA, Carmichael AJ: Response of normal human keratinocytes to sulfur mustard (HD): cytokine release using a non-enzymatic detachment procedure. *Human & experimental toxicology* 1999, 18(1):1-11.

7. Arroyo CM, Schafer RJ, Kurt EM, Broomfield CA, Carmichael AJ: Response of normal human keratinocytes to sulfur mustard: cytokine release. *Journal of Applied Toxicology : Jat* 2000, 20 Suppl 1:S63-72.

8. Arroyo CM, Von Tersch RL, Broomfield CA: Activation of alpha-human tumour necrosis factor (TNF-alpha) by human monocytes (THP-1) exposed to 2-chloroethyl ethyl sulphide (H-MG). *Human and Experimental Toxicology* 1995, 14(7):547-553.

9. Das SK, Mukherjee S, Smith MG, Chatterjee D: Prophylactic protection by N-acetylcysteine against the pulmonary injury induced by 2-chloroethyl ethyl sulfide, a mustard analogue. *Journal of biochemical and molecular toxicology* 2003, 17(3):177-184.

10. Mukhopadhyay S, Rajaratnam V, Mukherjee S, Smith M, Das SK: Modulation of the expression of superoxide dismutase gene in lung injury by 2-chloroethyl ethyl sulfide, a mustard analog. *Journal of biochemical and molecular toxicology* 2006, 20(3):142-149.

11. Elsayed NM, Omaye ST, Klain GJ, Korte DW, Jr.: Free radical-mediated lung response to the monofunctional sulfur mustard butyl 2-chloroethyl sulfide after subcutaneous injection. *Toxicology* 1992, 72(2):153-165.

12. Elsayed NM, Omaye ST: Biochemical changes in mouse lung after subcutaneous injection of the sulfur mustard 2-chloroethyl 4-chlorobutyl sulfide. *Toxicology* 2004, 199(2-3):195-206.

13. Han S, Espinoza LA, Liao H, Boulares AH, Smulson ME: Protection by antioxidants against toxicity and apoptosis induced by the sulphur mustard analog 2-chloroethylethyl sulphide (CEES) in Jurkat T cells and normal human lymphocytes. *British journal of pharmacology* 2004, 141(5):795-802.

14. Naghii MR: Sulfur mustard intoxication, oxidative stress, and antioxidants. *Mil Med* 2002, 167(7):573-575.

15. Stone WL, Qui M, Smith M: Lipopolysaccharide enhances the cytotoxicity of 2-chloroethyl ethyl sulfide. *BMC cell biology* 2003, 4(1):1.

16. Ganster RW, Taylor BS, Shao L, Geller DA: Complex regulation of human inducible nitric oxide synthase gene transcription by Stat 1 and NF-kappa B. *Proceedings of the National Academy of Sciences of the United States of America* 2001, 98(15):8638-8643.

17. Gao J, Morrison DC, Parmely TJ, Russell SW, Murphy WJ: An interferon-gamma-activated site (GAS) is necessary for full expression of the mouse iNOS gene in response to interferon-gamma and lipopolysaccharide. *The Journal of biological chemistry* 1997, 272(2):1226-1230.

18. Qui M, Paromov VM, Yang H, Smith M, Stone WL: Inhibition of inducible Nitric Oxide Synthase by a mustard gas analog in murine macrophages. *BMC cell biology* 2006, 7:39.

19. Schwentker A, Billiar TR: Nitric oxide and wound repair. *The Surgical clinics of North America* 2003, 83(3):521-530.

20. Witte MB, Kiyama T, Barbul A: Nitric oxide enhances experimental wound healing in diabetes. *The British journal of surgery* 2002, 89(12):1594-1601.

21. Yamasaki K, Edington HD, McClosky C, Tzeng E, Lizonova A, Kovesdi I, Steed DL, Billiar TR: Reversal of impaired wound repair in iNOS-deficient mice by topical adenoviral-mediated iNOS gene transfer. *The Journal of clinical investigation* 1998, 101(5):967-971.

22. Duval DL, Sieg DJ, Billings RE: Regulation of hepatic nitric oxide synthase by reactive oxygen intermediates and glutathione. *Archives of biochemistry and biophysics* 1995, 316(2):699-706.

23. Harbrecht BG, Di Silvio M, Chough V, Kim YM, Simmons RL, Billiar TR: Glutathione regulates nitric oxide synthase in cultured hepatocytes. *Ann Surg* 1997, 225(1):76-87.

24. Tirmenstein MA, Nicholls-Grzemski FA, Schmittgen TD, Zakrajsek BA, Fariss MW: Glutathione-dependent regulation of nitric oxide production in isolated rat hepatocyte suspensions. *Antioxidants & redox signaling* 2000, 2(4):767-777.

25. Vos TA, Van Goor H, Tuyt L, De Jager-Krikken A, Leuvenink R, Kuipers F, Jansen PL, Moshage H: Expression of inducible nitric oxide synthase in endotoxemic rat hepatocytes is dependent on the cellular glutathione status. *Hepatology* 1999, 29(2):421-426.

26. Myhre O, Andersen JM, Aarnes H, Fonnum F: Evaluation of the probes 2',7'-dichlorofluorescin diacetate, luminol, and lucigenin as indicators of reactive species formation. *Biochemical pharmacology* 2003, 65(10):1575-1582.

27. Imrich A, Kobzik L: Fluorescence-based measurement of nitric oxide synthase activity in activated rat macrophages using dichlorofluorescin. *Nitric Oxide* 1997, 1(4):359-369.

28. LeBel CP, Ischiropoulos H, Bondy SC: Evaluation of the probe 2',7'-dichlorofluorescin as an indicator of reactive oxygen species formation and oxidative stress. *Chemical research in toxicology* 1992, 5(2):227-231.

29. Sebastia J, Cristofol R, Martin M, Rodriguez-Farre E, Sanfeliu C: Evaluation of fluorescent dyes for measuring intracellular glutathione content in primary cultures of human neurons and neuroblastoma SH-SY5Y. *Cytometry A* 2003, 51(1):16-25.

30. Poot M, Kavanagh TJ, Kang HC, Haugland RP, Rabinovitch PS: Flow cytometric analysis of cell cycle-dependent changes in cell thiol level by combining a new laser dye with Hoechst 33342. *Cytometry* 1991, 12(2):184-187.

31. Kamencic H, Lyon A, Paterson PG, Juurlink BH: Monochlorobimane fluorometric method to measure tissue glutathione. *Analytical biochemistry* 2000, 286(1):35-37.

32. Elsayed NM, Omaye ST, Klain GJ, Inase JL, Dahlberg ET, Wheeler CR, Korte DW, Jr.: Response of mouse brain to a single subcutaneous injection of the monofunctional sulfur mustard, butyl 2-chloroethyl sulfide (BCS)*. *Toxicology* 1989, 58(1):11-20.

33. Berlett BS, Stadtman ER: Protein oxidation in aging, disease, and oxidative stress. *The Journal of biological chemistry* 1997, 272(33):20313-20316.

34. Stone WL, Smith M: Therapeutic uses of antioxidant liposomes. *Mol Biotechnol* 2004, 27(3):217-230.

35. Droge W: Free radicals in the physiological control of cell function. *Physiological reviews* 2002, 82(1):47-95.

36. Kadar T, Turetz J, Fishbine E, Sahar R, Chapman S, Amir A: Characterization of acute and delayed ocular lesions induced by sulfur mustard in rabbits. *Current eye research* 2001, 22(1):42-53.

37. Zimmermann AK, Loucks FA, Schroeder EK, Bouchard RJ, Tyler KL, Linseman DA: Glutathione binding to the Bcl-2 homology-3 domain groove: a molecular basis for Bcl-2 antioxidant function at mitochondria. *The Journal of biological chemistry* 2007, 282(40):29296-29304.

38. Fan J, Shek PN, Suntres ZE, Li YH, Oreopoulos GD, Rotstein OD: Liposomal antioxidants provide prolonged protection against acute respiratory distress syndrome. *Surgery* 2000, 128(2):332-338.

39. McClintock SD, Hoesel LM, Das SK, Till GO, Neff T, Kunkel RG, Smith MG, Ward PA: Attenuation of half sulfur mustard gas-induced acute lung injury in rats. *J Appl Toxicol* 2006, 26(2):126-131.

40. Kleinert H, Pautz A, Linker K, Schwarz PM: Regulation of the expression of inducible nitric oxide synthase. *Eur J Pharmacol* 2004, 500(1-3):255-266.

41. Chen XM, Gray PJ, Cullinane C, Phillips DR: Differential sensitivity of transcription factors to mustard-damaged DNA. *Chemico-biological interactions* 1999, 118(1):51-67.

42. Gray PJ: Sulphur mustards inhibit binding of transcription factor AP2 in vitro. *Nucleic Acids Res* 1995, 23(21):4378-4382.

43. Fabbri S, Prontera C, Broggini M, D'Incalci M: Differential inhibition of the DNA binding of transcription factors NF kappa B and OTF-1 by nitrogen mustard and quinacrine mustard: transcriptional implications. *Carcinogenesis* 1993, 14(9):1963-1967.

44. Nishi T, Shimizu N, Hiramoto M, Sato I, Yamaguchi Y, Hasegawa M, Aizawa S, Tanaka H, Kataoka K, Watanabe H *et al*: Spatial redox regulation of a critical cysteine residue of NF-kappa B in vivo. *The Journal of biological chemistry* 2002, 277(46):44548-44556.

45. Atkins KB, Lodhi IJ, Hurley LL, Hinshaw DB: N-acetylcysteine and endothelial cell injury by sulfur mustard. *J Appl Toxicol* 2000, 20 Suppl 1:S125-128.

46. Chatterjee D, Mukherjee S, Smith MG, Das SK: Signal transduction events in lung injury induced by 2-chloroethyl ethyl sulfide, a mustard analog. *Journal of biochemical and molecular toxicology* 2003, 17(2):114-121.

47. Minsavage GD, Dillman JFr: Bifunctional alkylating agent-induced p53 and nonclassical nuclear factor kappaB responses and cell death are altered by caffeic acid phenethyl ester: a potential role for antioxidant/electrophilic response-element signaling. *J Pharmacol Exp Ther* 2007, 321(1):202-212.

48. Soneja A, Drews M, Malinski T: Role of nitric oxide, nitroxidative and oxidative stress in wound healing. *Pharmacol Rep* 2005, 57 Suppl:108-119.

49. Stone WL, Mukherjee S, Smith M, Das SK: Therapeutic uses of antioxidant liposomes. *Methods in molecular biology (Clifton, NJ* 2002, 199:145-161.

50. Wasserman TH, Twentyman P: Use of a colorimetric microtiter (MTT) assay in determining the radiosensitivity of cells from murine solid tumors. *Int J Radiat Oncol Biol Phys* 1988, 15(3):699-702.

51. Twentyman PR, Luscombe M: A study of some variables in a tetrazolium dye (MTT) based assay for cell growth and chemosensitivity. *Br J Cancer* 1987, 56(3):279-285.

52. Green LC, Wagner DA, Glogowski J, Skipper PL, Wishnok JS, Tannenbaum SR: Analysis of nitrate, nitrite, and [15N]nitrate in biological fluids. *Analytical biochemistry* 1982, 126(1):131-138.

53. Tietze F: Enzymic method for quantitative determination of nanogram amounts of total and oxidized glutathione: applications to mammalian blood and other tissues. *Analytical biochemistry* 1969, 27(3):502-522.

54. Griffith OW: Determination of glutathione and glutathione disulfide using glutathione reductase and 2-vinylpyridine. *Analytical biochemistry* 1980, 106(1):207-212.

55. Houze P, Gamra S, Madelaine I, Bousquet B, Gourmel B: Simultaneous determination of total plasma glutathione, homocysteine, cysteinylglycine, and methionine by high-performance liquid chromatography with electrochemical detection. *Journal of clinical laboratory analysis* 2001, 15(3):144-153.

56. Alamdari DH, Kostidou E, Paletas K, Sarigianni M, Konstas AG, Karapiperidou A, Koliakos G: High sensitivity enzyme-linked immunosorbent assay (ELISA) method for measuring protein carbonyl in samples with low amounts of protein. *Free radical biology & medicine* 2005, 39(10):1362-1367.

57. Buss H, Chan TP, Sluis KB, Domigan NM, Winterbourn CC: Protein carbonyl measurement by a sensitive ELISA method. *Free radical biology & medicine* 1997, 23(3):361-366.

Figure legends

Figure 1 – NAC effect on viability and NO production in CEES/LPS treated RAW 264.7 cells (simultaneous NAC/CEES/LPS application)

Panel A: Macrophages incubated with 50 or 100 ng/ml of LPS or/and 500 µM CEES were simultaneously treated with or without 10 mM NAC (as indicated) for 24 hours. Cell viability was measured using the MTT assay (see Materials and Methods) and expressed as OD at 575 nm. *Panel B:* Macrophages were incubated as described above and NO production measured as the concentration of nitrite in the culture media as described in Materials and Methods. Mean values not sharing a common letter are significantly different ($p<0.05$).

Figure 2 – NAC effect on viability and NO production in CEES/LPS incubated RAW 264.7 cells (NAC pre-treatment)

Panel A: Macrophages were pre-treated with or without 10 mM NAC for 5 hours and then incubated with 50 or 100 ng/ml of LPS or/and 500 µM CEES (as indicated) for 24 hours. Cell viability was measured using the MTT assay (see Materials and Methods) and expressed as OD at 575 nm. *Panel B:* Macrophages were incubated as described above and NO production measured as concentration of nitrite in the culture media as described in Materials and Methods. Mean values not sharing a common letter are significantly different ($p<0.05$).

Figure 3 – NAC effect on viability and NO production in CEES/LPS treated RAW 264.7 cells (NAC post-treatment)

Panel A: Macrophages were incubated with 50 or 100 ng/ml of LPS or/and 500 µM CEES (as indicated) for 24 hours and 10 mM NAC was added to the cell culture medium 5 hours after the CEES/LPS application. Cell viability was measured using the MTT assay (see Materials and Methods) and expressed as OD at 575 nm. *Panel B:* Macrophages were incubated as described above and NO production measured as concentration of nitrite in the culture media as described in Materials and Methods. Mean values not sharing a common letter are significantly different ($p<0.05$).

Figure 4- Fluorescent microscopy probes for oxidative stress, GSH and total thiols in RAW 264.7 cells

Panel A: Combined generation of ROS and RNOS were monitored using 20 μM carDCFH-DA; *Panel B*: Intracellular GSH levels were examined using 20 μM CMAC; *Panel C*: Levels of non-protein cellular thiols were monitored using 20 μM CMF-DA under a fluorescent microscope. Macrophages were treated with CEES (500 μM) and/or LPS (50 ng/mL) and incubated in the absence of NAC (top row in each panel) or in the presence of 10 mM NAC for 12 h.

Figure 5 – Glutathione status in RAW 264.7 cells incubated with CEES/LPS

Macrophages were incubated with 50 ng/ml LPS or/and 500 μM CEES for 12 h. Total GSH (GSH+GSSG) and GSSG levels were measured using a GSH assay kit (see Materials and Methods section) in cell lysates and normalized to total protein. Numbers show the percentage of GSSG in total GSH. Mean values not sharing a common letter are significantly different ($p<0.05$).

Figure 6 – NAC restores intracellular GSH in RAW 264.7 cells incubated with CEES/LPS

Macrophages incubated with 50 ng/ml LPS or/and 500 μM CEES were simultaneously treated with or without 5 mM NAC (as indicated). Cell lysates were measured for reduced GSH after 4 hour incubation using the HPLC technique described in Materials and Methods. The GSH levels were normalized to an internal homocysteine standard. Mean values not sharing a common letter are significantly different ($p<0.05$).

Figure 7 – Polmyxin B partially protects LPS stimulated RAW 264.7 cells from CEES toxicity and blocks NO production

Panel A: Macrophages incubated with 50 ng/ml LPS or/and 500 μM CEES were simultaneously treated with or without 10 μg/mL polymyxin B (as indicated) for 18 hours. Cell viability was measured using the MTT assay (see Materials and Methods) and expressed as OD at 575 nm. *Panel B:* Macrophages were incubated as described above. NO production was measured as nitrite concentration in the culture media as described in Materials and Methods. Mean values not sharing a common letter are significantly different ($p<0.05$).

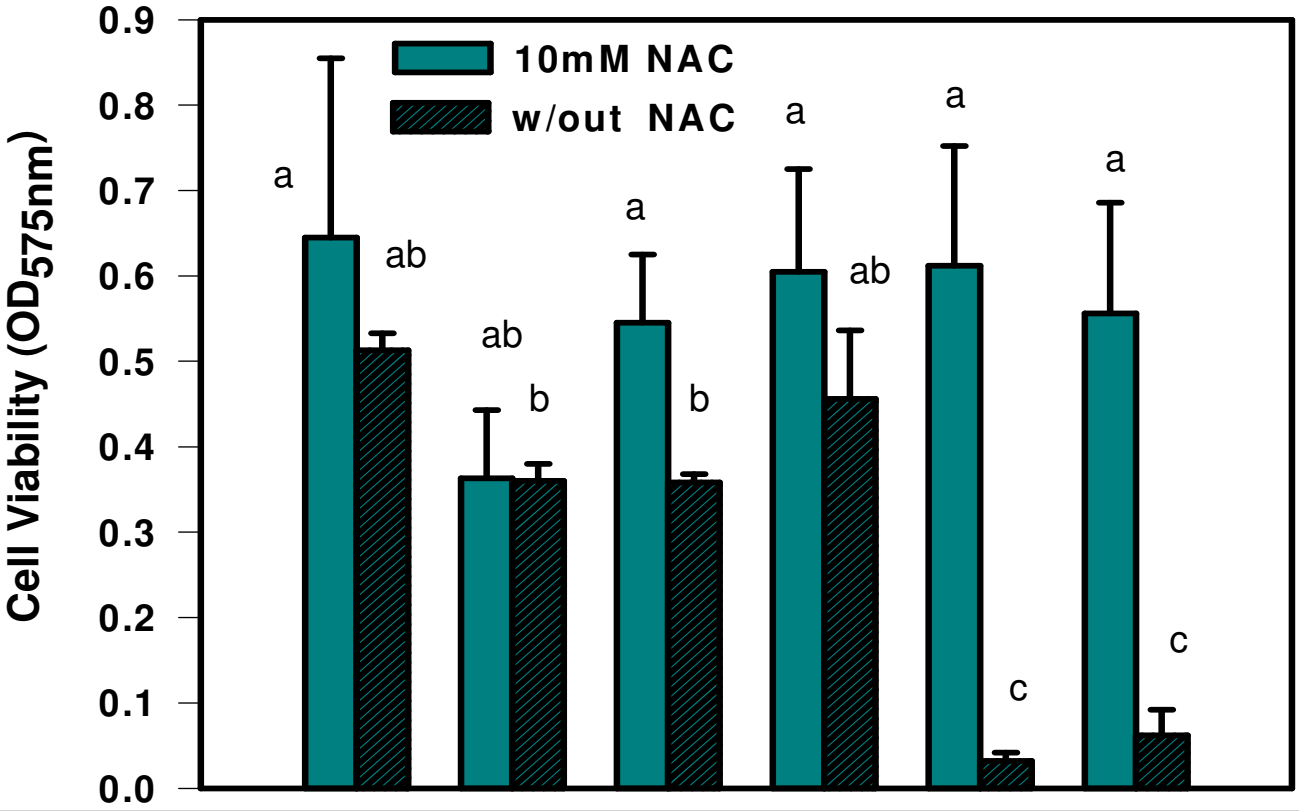

LPS 50 ng/mL	-	+	-	-	-	+	LPS 50ng/mL
LPS 100 ng/mL	-	-	+	-	+	-	LPS 100 ng/m
CEES 500 µM	-	-	-	+	+	+	CEES 500 µM

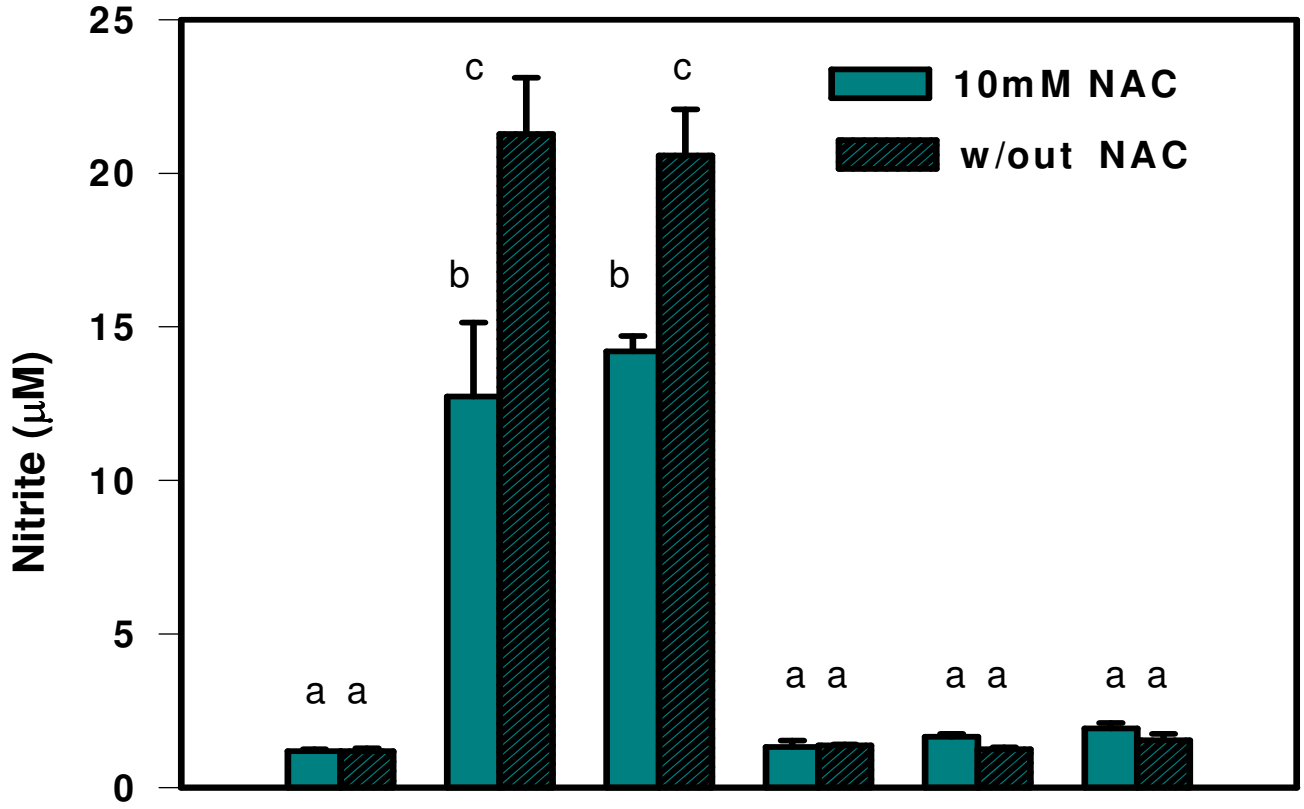

LPS 50 ng/mL	-	+	-	-	-	+	LPS 50ng/mL
LPS 100 ng/mL	-	-	+	-	+	-	LPS 100 ng/m
CEES 500 µM	-	-	-	+	+	+	CEES 500 µM

Figure 1

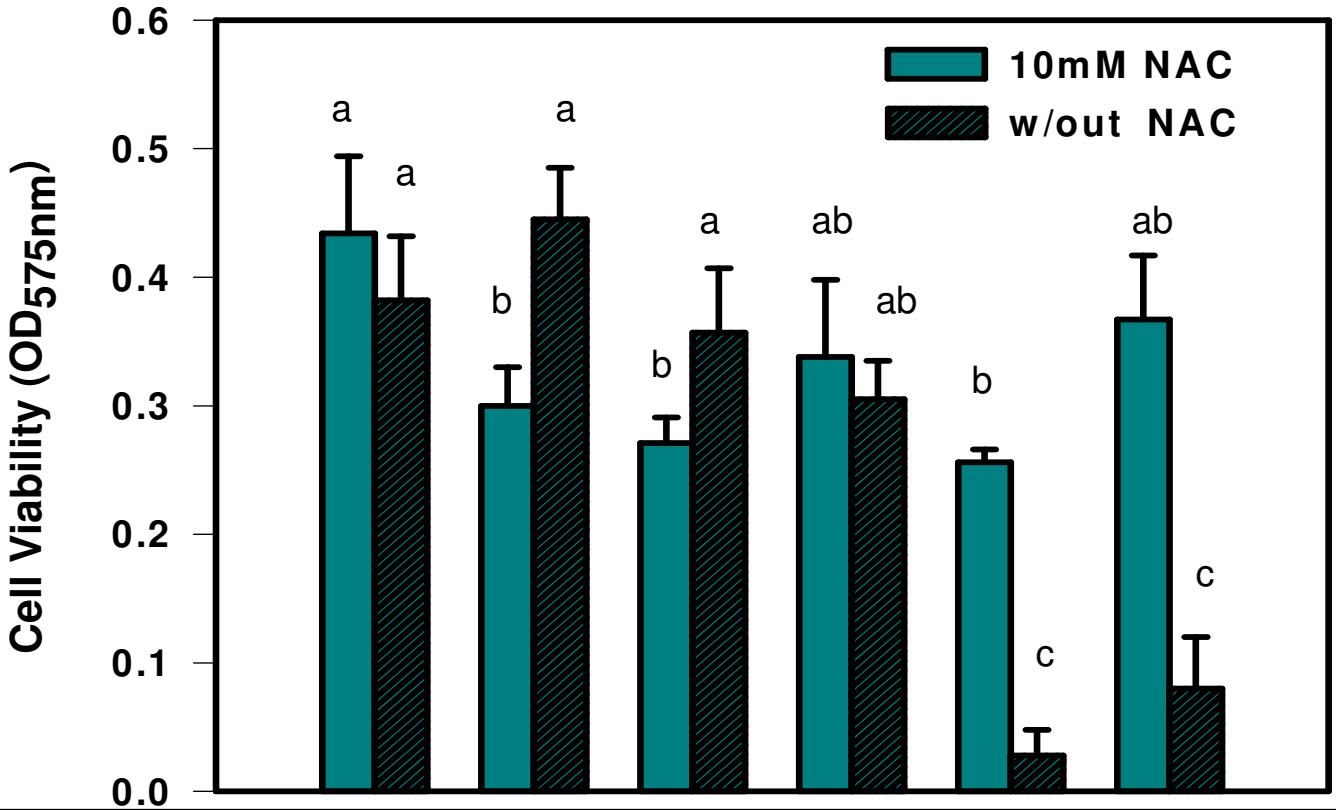

LPS 50 ng/mL	-	+	-	-	-	+	LPS 50ng/mL
LPS 100 ng/mL	-	-	+	-	+	-	LPS 100 ng/mL
CEES 500 µM	-	-	-	+	+	+	CEES 500 µM

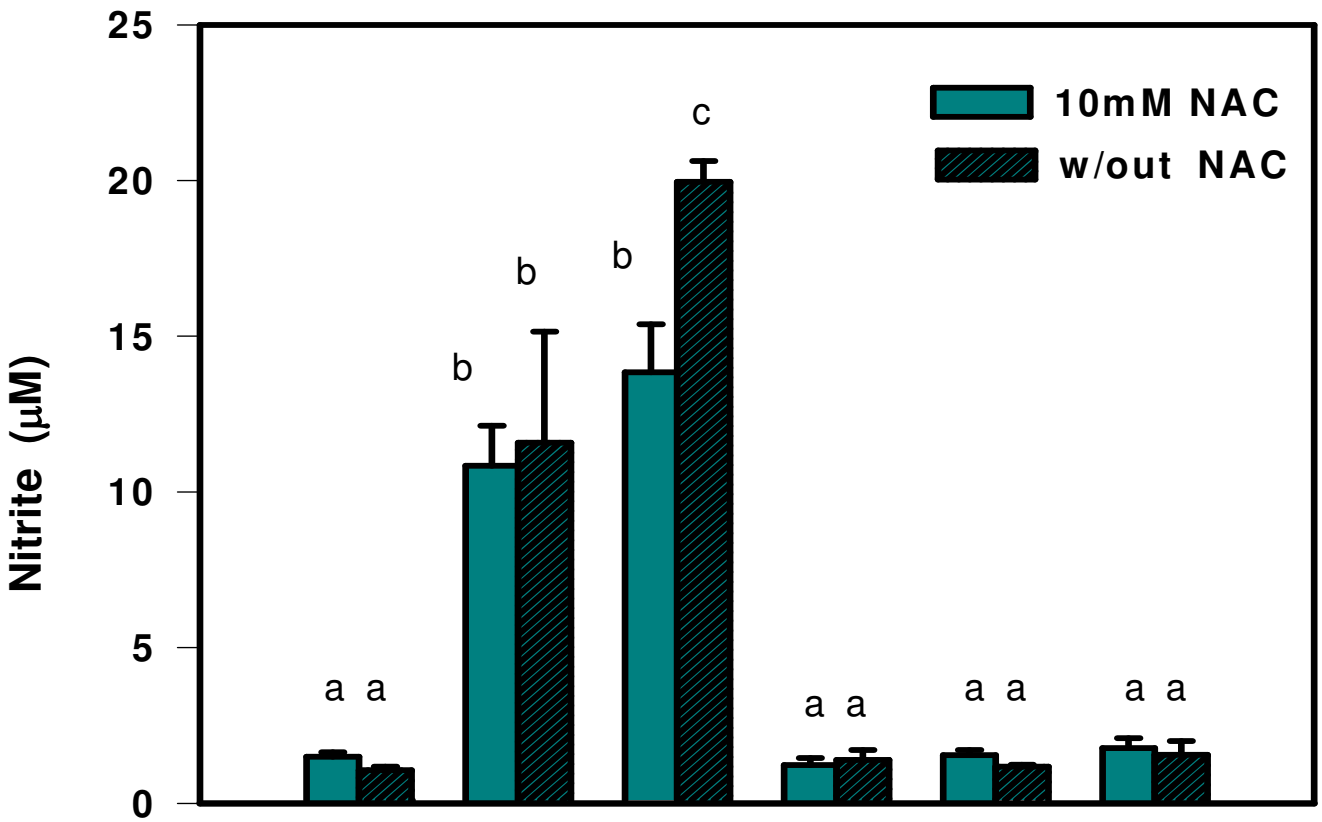

LPS 50 ng/mL	-	+	-	-	-	+	LPS 50ng/mL
LPS 100 ng/mL	-	-	+	-	+	-	LPS 100 ng/mL
CEES 500 µM	-	-	-	+	+	+	CEES 500 µM

Figure 2

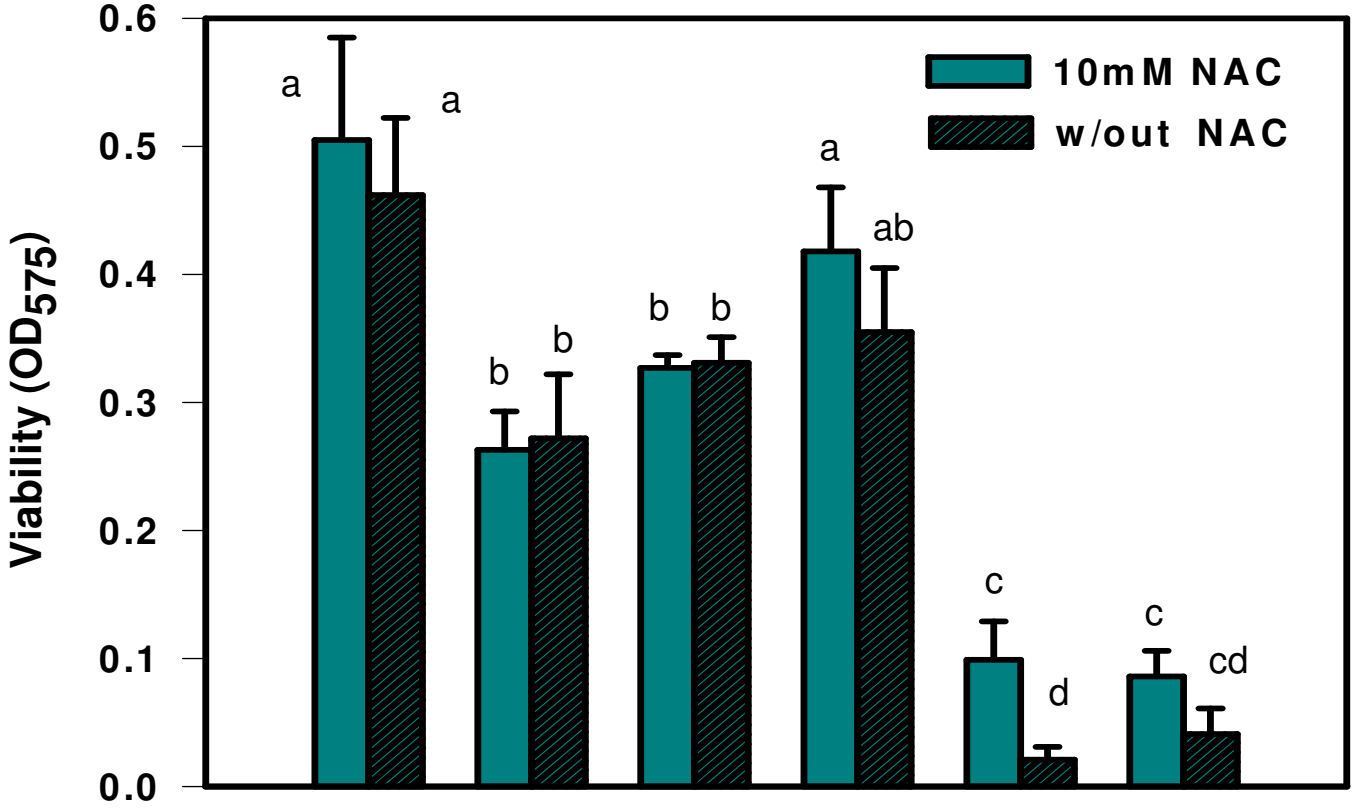

LPS 50 ng/mL	-	+	-	-	-	+	LPS 50ng/m
LPS 100 ng/mL	-	-	+	-	+	-	LPS 100 ng/m
CEES 500 µM	-	-	-	+	+	+	CEES 500 µM

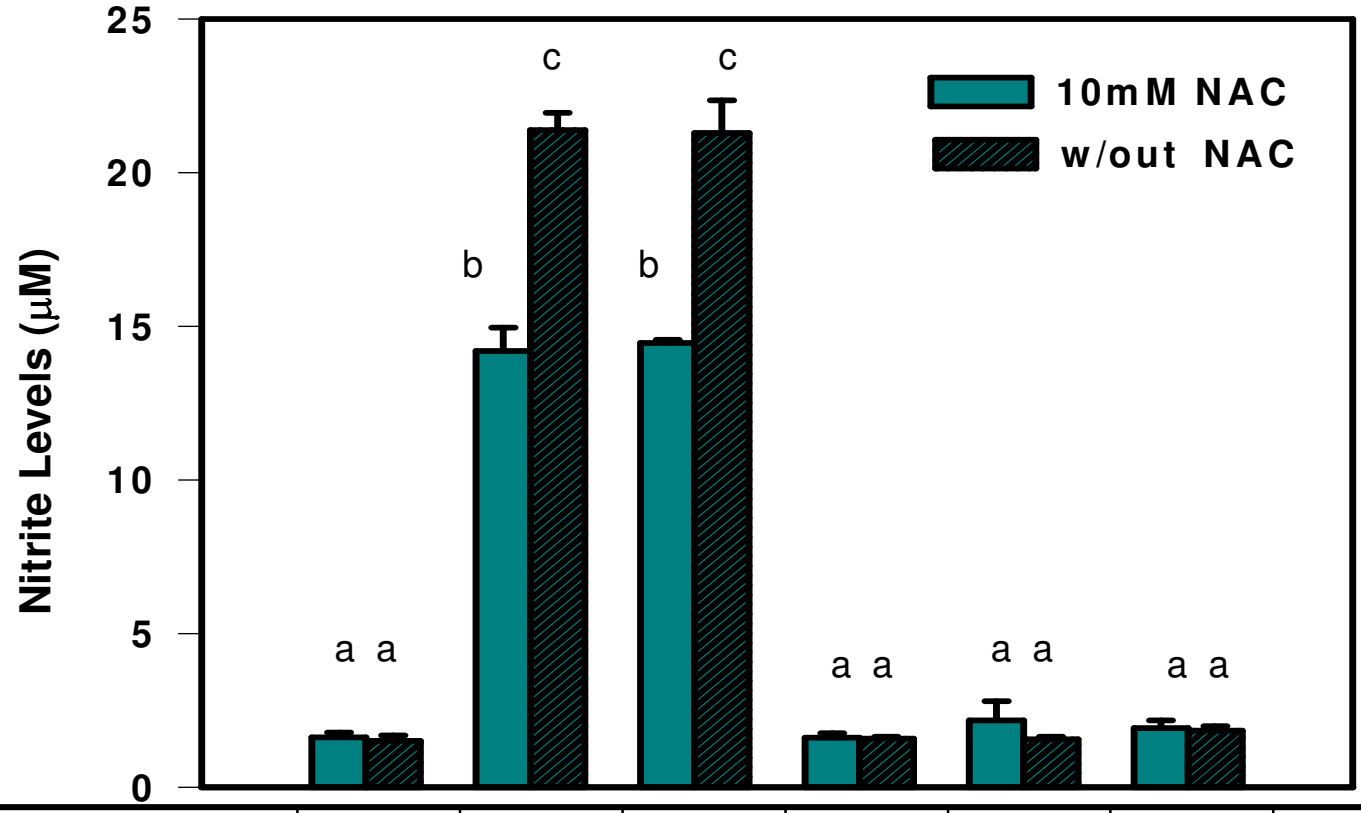

LPS 50 ng/mL	-	+	-	-	-	+	LPS 50ng/m
LPS 100 ng/mL	-	-	+	-	+	-	LPS 100 ng/m
CEES 500 µM	-	-	-	+	+	+	CEES 500 µM

Figure 8

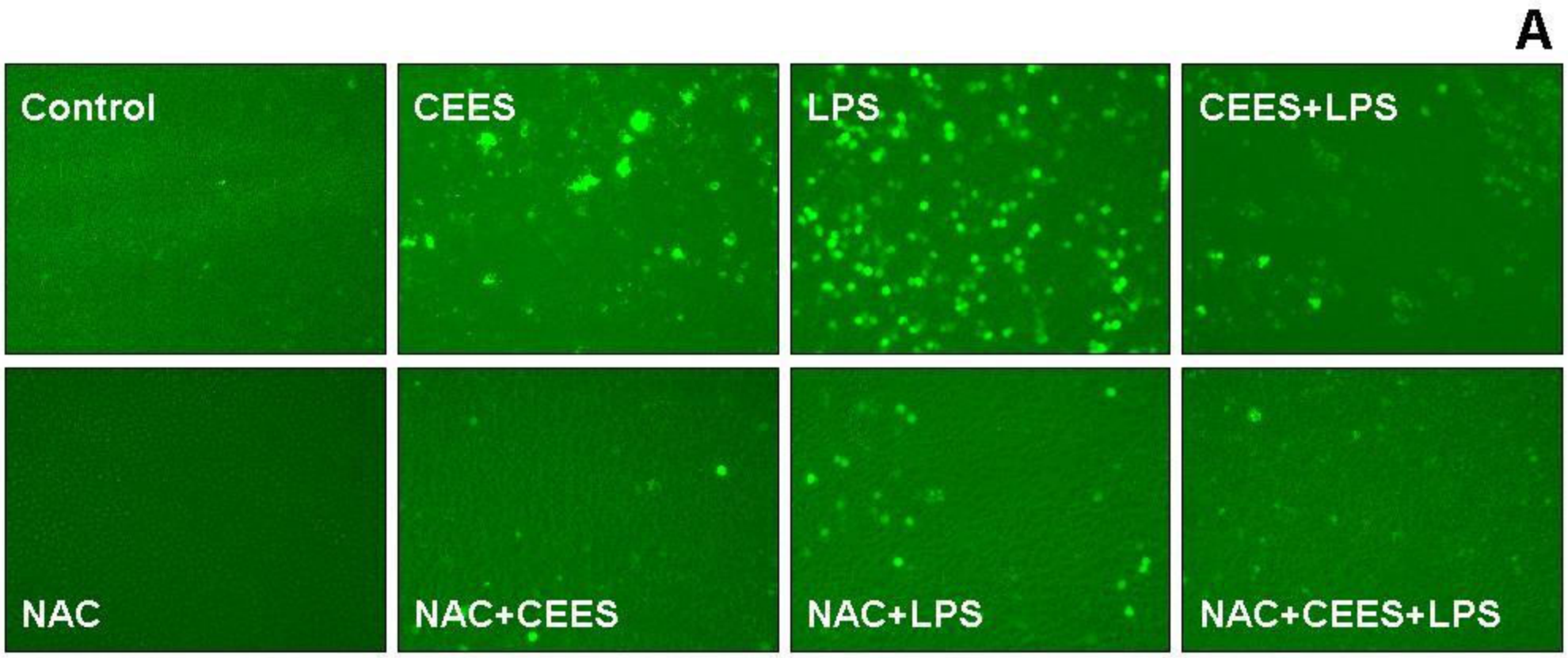
A
Control
CEES
LPS
CEES+LPS
NAC
NAC+CEES
NAC+LPS
NAC+CEES+LPS

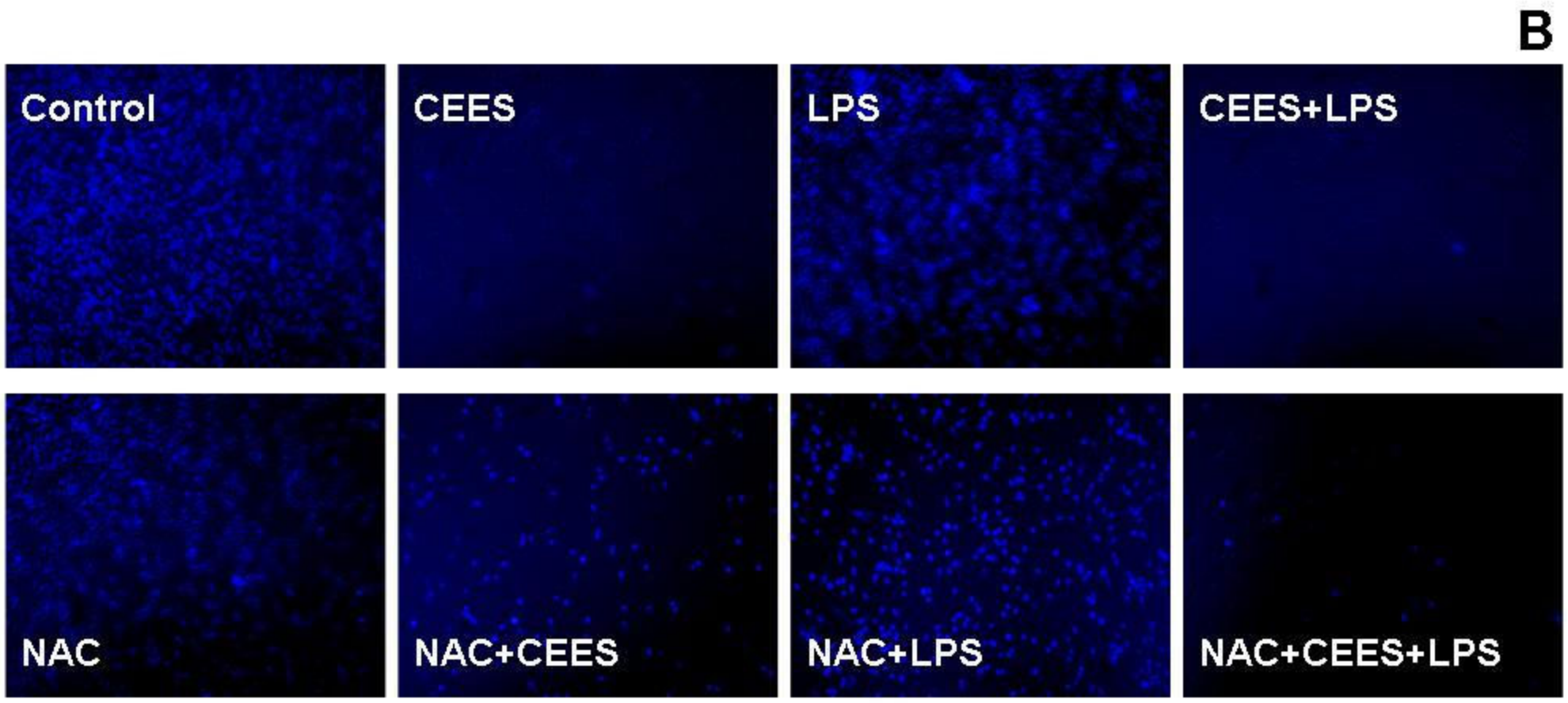
B
Control
CEES
LPS
CEES+LPS
NAC
NAC+CEES
NAC+LPS
NAC+CEES+LPS

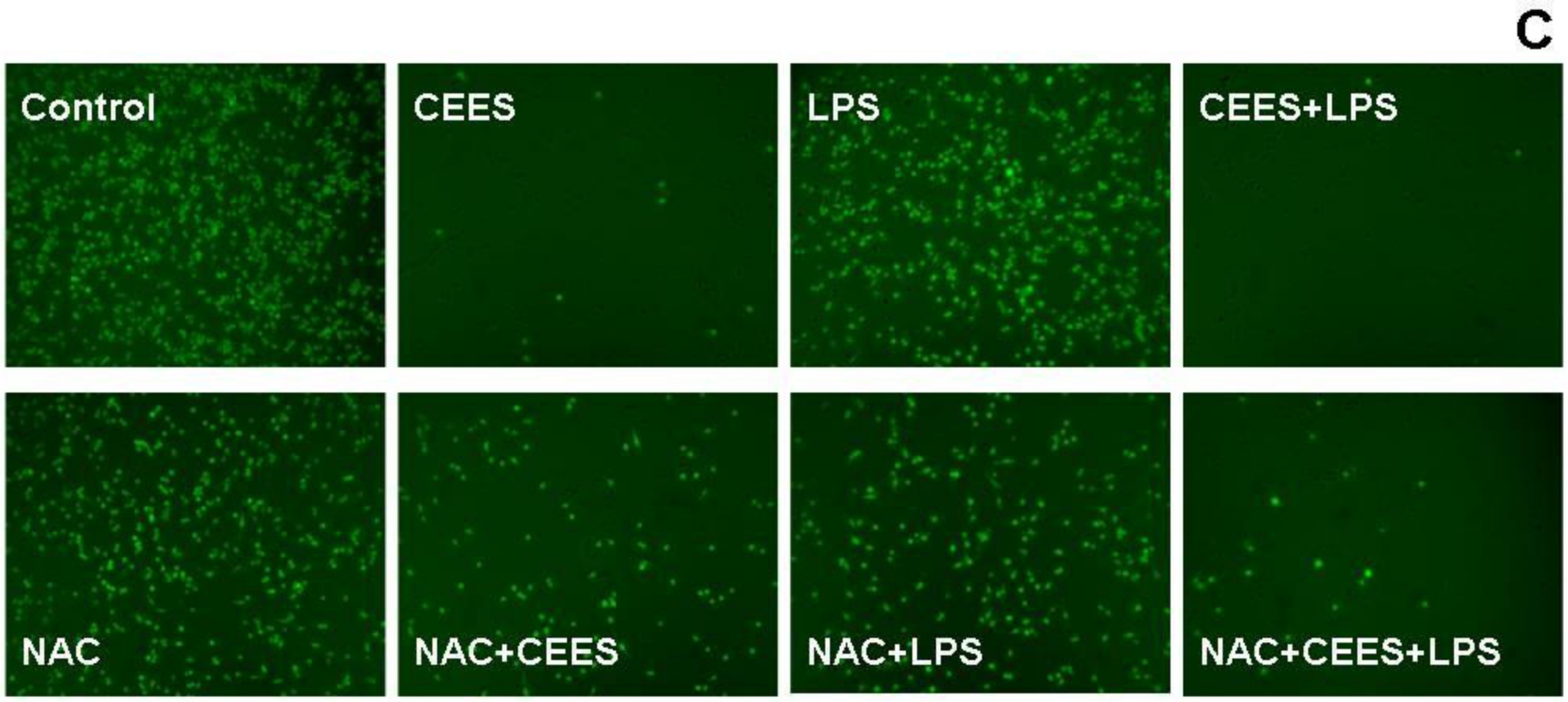
C
Control
CEES
LPS
CEES+LPS
NAC
NAC+CEES
NAC+LPS
NAC+CEES+LPS

Figure 4

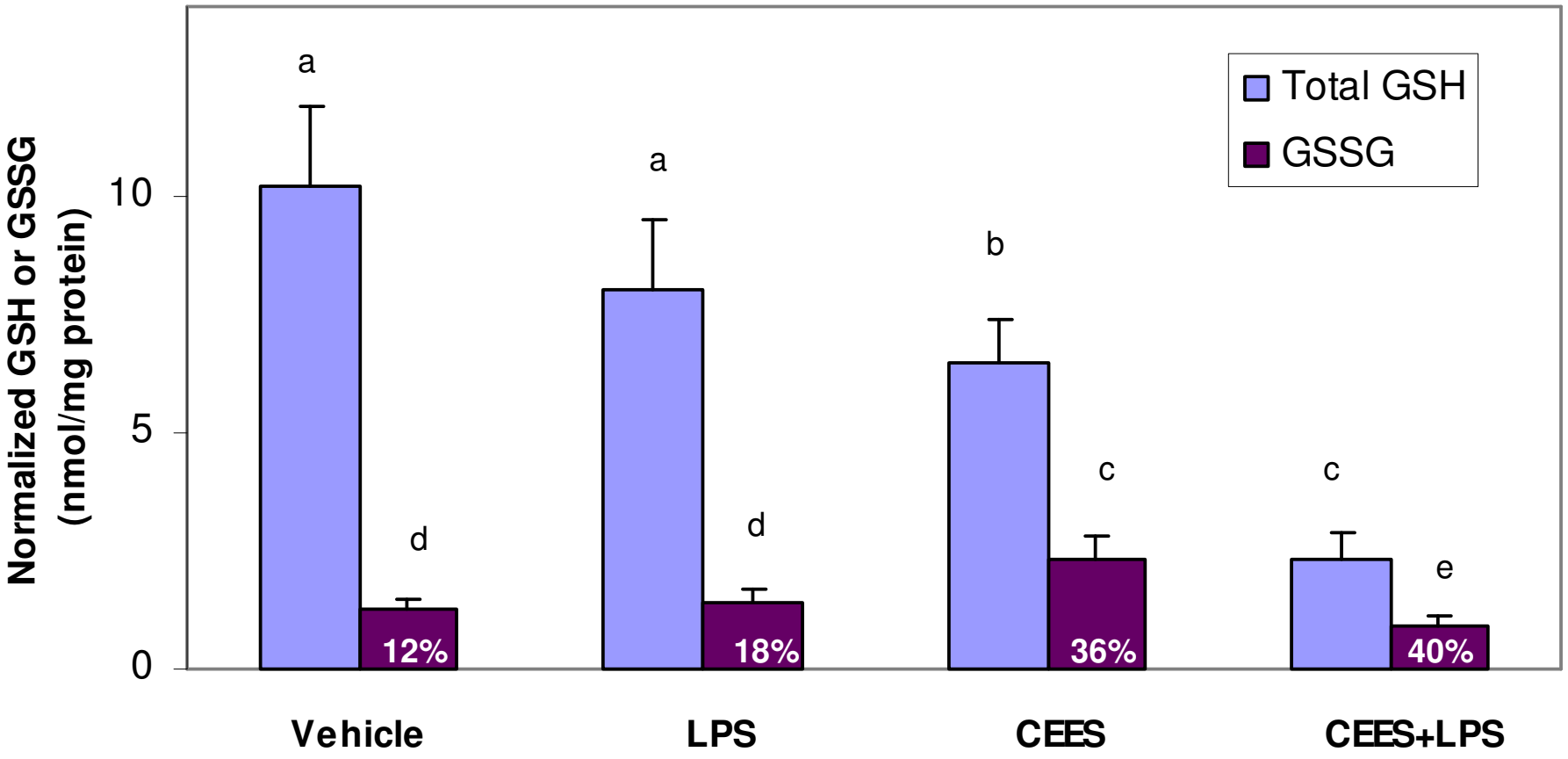
Normalized GSH or GSSG
(nmol/mg protein)
10
5
0
Total GSH
GSSG
a
d
12%
a
d
18%
b
c
36%
c
e
40%
Vehicle
LPS
CEES
CEES+LPS

Figure 5

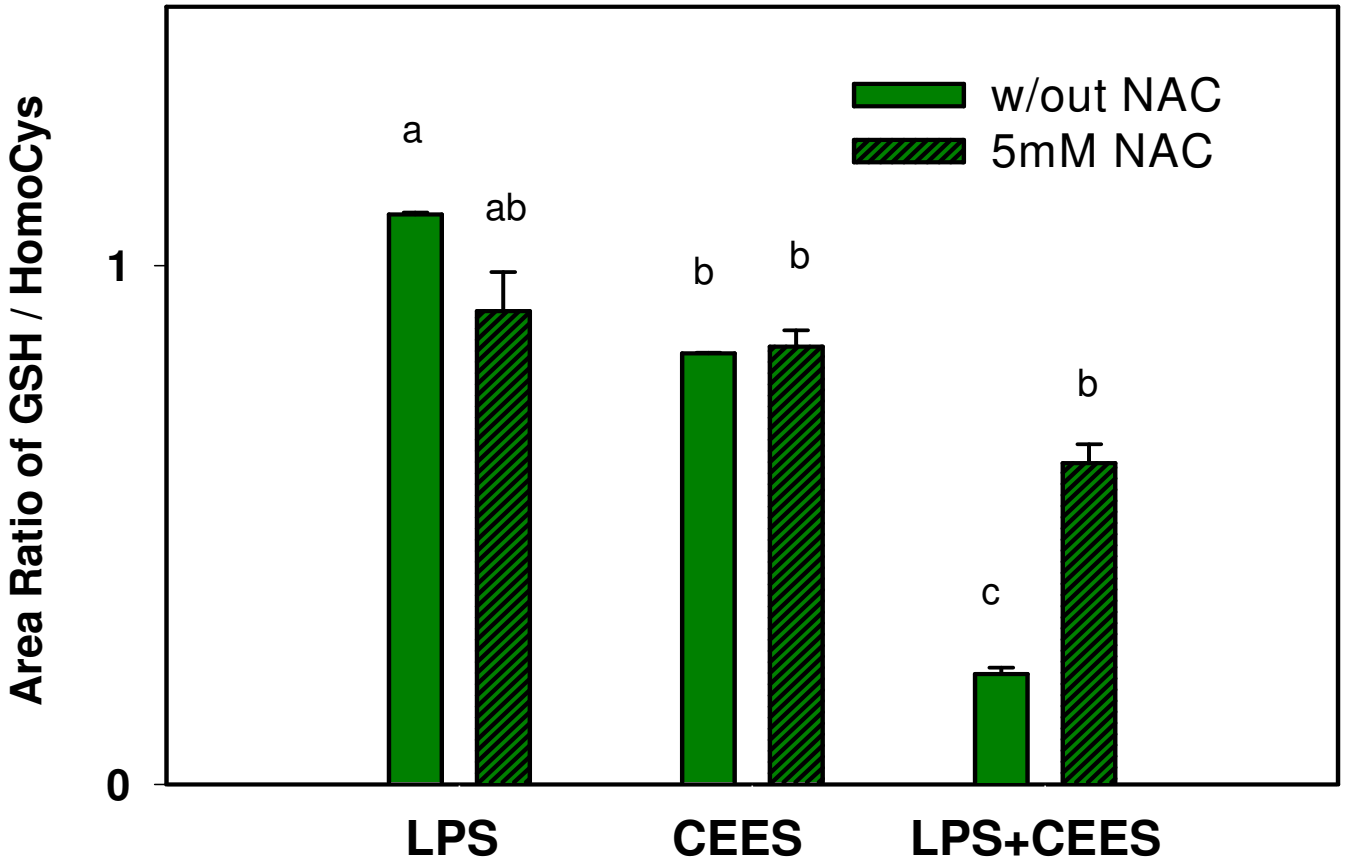
w/out NAC
5mM NAC
Area Ratio of GSH / HomoCys
1
0
a
ab
b
b
c
b
LPS
CEES
LPS+CEES

Figure 6

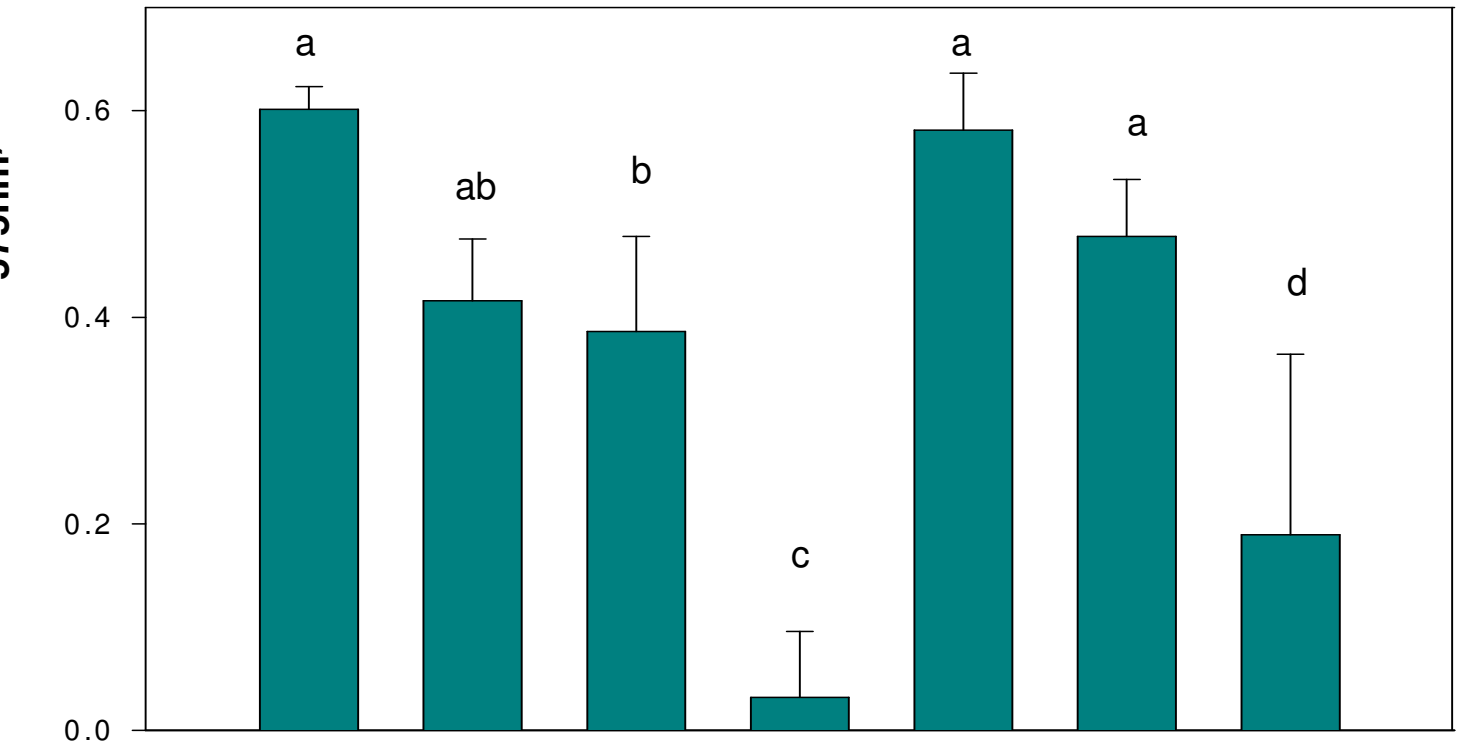

50ng/mL	-	+	-	+	-	+	+	LPS 50ng/
S 500 µM	-	-	+	+	-	-	+	CEES 500 µ
10 µg/mL	-	-	-	-	+	+	+	PMB 10 µg

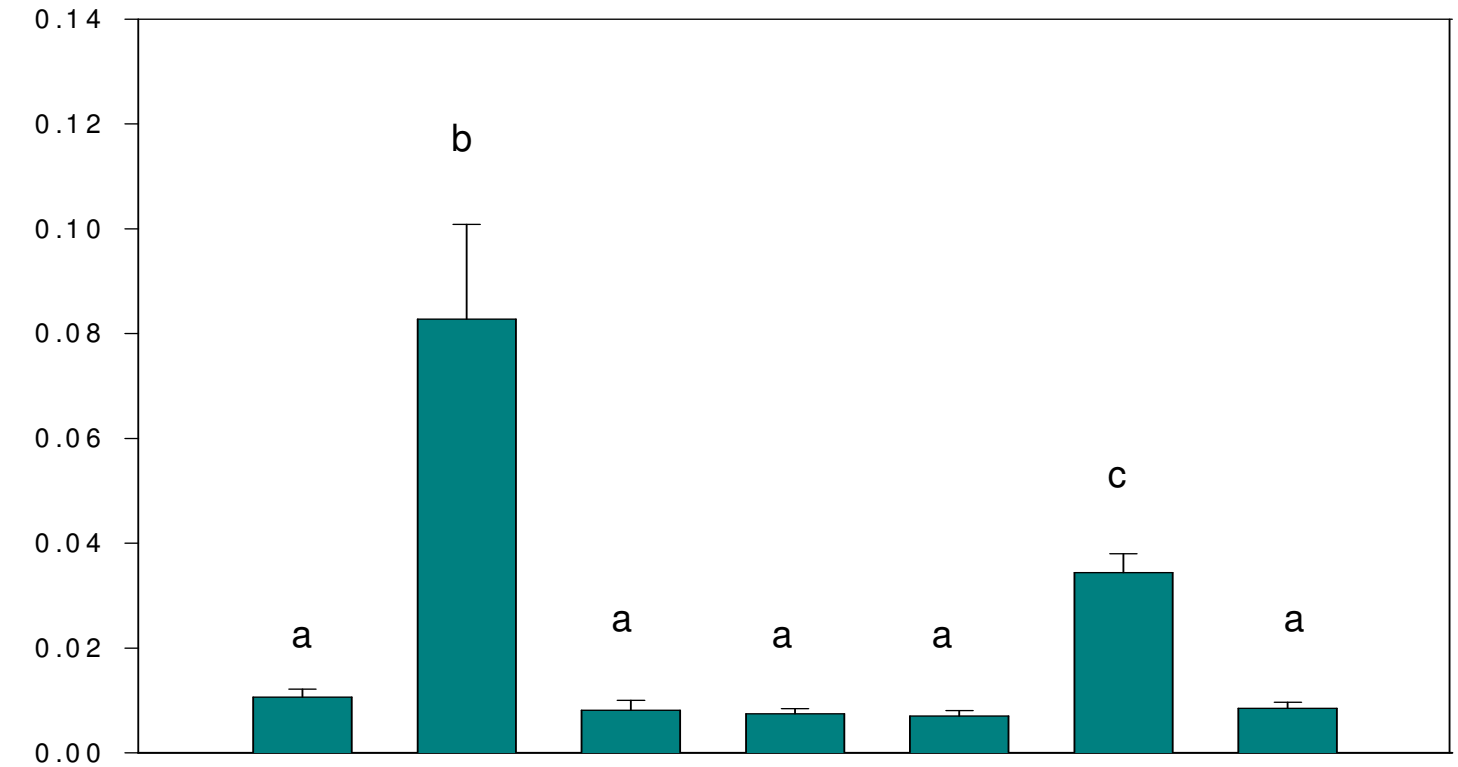

50ng/mL	-	+	-	+	-	+	+	LPS 50ng/
S 500 µM	-	-	+	+	-	-	+	CEES 500 µ
10 µg/mL	-	-	-	-	+	+	+	PMB 10 µg

Figure 7

Chapter 21

Preparation, Characterization, and Use of Antioxidant-Liposomes

Hongsong Yang, Victor Paromov, Milton Smith, and William L. Stone

W.L. Stone
Department of Pediatrics, James H Quillen College of Medicine, East Tennessee State University, Johnson City, TN 37614-0578, USA. E-mail: stone@etsu.edu

Abstract

Antioxidant liposomes provide a unique means of delivering both water and/or lipid soluble antioxidants to tissues thereby affecting disease states or signal transduction pathways modulated by oxidative stress. Considerable evidence suggests that liposome-encapsulated antioxidants can be superior to the corresponding free antioxidants in this regard. This chapter will provide practical details on the preparation, characterization, and use of antioxidant liposomes. Methods will be described for the small-scale preparation (1 ml) and large-scale (100 ml/hour) preparation of antioxidant liposomes as well as the techniques for characterizing their size distribution and their physical and chemical stability. The use of antioxidant liposomes in an in vitro situation will also be detailed.

Key words Antioxidants, Liposomes, Vitamin E, Oxidative stress, Cellular uptake, Glutathione, Phospholipid

21.1 Introduction

A liposome is a vesicle composed of a closed phospholipid bilayer (the lipid phase) encapsulating an aqueous phase: they are also the smallest artificial vesicles that can be produced from natural nontoxic phospholipids and cholesterol. Liposomes have often been used as a drug delivery system since they have a unique ability to simultaneously deliver lipid-soluble as well as water-soluble agents [1, 2]. Similarly, antioxidant liposomes provide a unique

From: *Methods in Molecular Biology*, *vol. 477: Advanced Protocols in Oxidative Stress I*,
Edited by: D. Armstrong, DOI: 10.1007/978-1-60327-517-0_21, © Humana Press, New York, NY

molecular tool for delivering both water- and lipid-soluble antioxidants to tissues or cells. The therapeutic use of antioxidant liposomes is particularly relevant for diseases in which oxidative stress plays a key role [3, 4]. Oxidative stress is a condition in which the production of damaging free radical species/reactive oxygen species exceeds the capacity of antioxidant protection mechanisms to prevent cellular damage. Free radicals are molecules with unpaired electrons, which are often highly reactive and damaging to biological systems, particularly the biological membranes of subcellular organelles.

Lipid-soluble antioxidants such as vitamin E or coenzyme Q10 (CoQ10) can be incorporated into the hydrophobic lipid phase of liposomal bilayers. Vitamin E is a term referring to at least eight different isoforms including four tocopherols (alpha-, beta- gamma-, and delta) and four corresponding tocotrienols (alpha-, beta- gamma-, and delta-). Alpha-tocopherol is the primary form of vitamin E found in human plasma since the other isoforms are rapidly metabolized by the liver before being secreted into plasma [5]. Moreover, the liver also contains an alpha-tocopherol transfer protein, which selectively promotes the secretion of alpha-tocopherol out of the liver into very low density lipoprotein [6]. Oral administration with forms of vitamin E other than alpha-tocopherol is not, therefore, effective at increasing their plasma levels.

Increasing evidence shows that the different vitamin E isoforms have distinct chemical and biological properties [7, 8, 9]. Moreover, many of the biological properties of vitamin E isoforms appear unrelated to their role as antioxidants [10]. Evidence suggest, for example that gamma-tocopherol [11, 12, 13] as well as tocotrienols have the potential to kill many types of cancer cells by activating apoptosis [14, 15, 16, 17]. Intravenous injection with liposomes containing non-alpha-tocopherol isoforms would bypass the selectivity imposed by the liver, allowing the unique properties of each vitamin E isoform to be therapeutically exploited.

Water-soluble antioxidants such as urate [18], ascorbate, N-acetyl-L-cysteine (NAC), or glutathione (GSH) can be encapsulated into the interior aqueous domain of antioxidant-liposomes. NAC is the acetylated from of L-cysteine and it is an excellent source of sulfhydryl (SH) groups. NAC is converted in the body into metabolites capable of stimulating GSH synthesis, promoting detoxification, and it also acts directly as a free radical scavenger. Fan et al. [19] have found that liposomal encapsulated NAC provides a longer lasting protection against acute respiratory distress syndrome than does free unencapsulated NAC. Water-soluble antioxidant enzymes such as superoxide dismutase or glutathione peroxidase can also be incorporated into the aqueous domain of antioxidant liposomes [4].

Although general guidelines for the preparation and size characterization of liposomes have been described [20], this chapter will focus on the specific preparation and characterization of antioxidant liposomes.

21.2 Materials

21.2.1 Equipment

1. Mini-Extruder set including extruder, stand/heating block, filter support, gas-tight syringe, and polycarbonate membranes, Avanti Polar Lipids Inc. (Alabaster, AL).
2. Model M-100L Microfluidizer (a bench top instrument) from Microfluidics (Newton, MA).
3. Nicomp 380 DLS from Particle Sizing Systems (Port Richey, FL).
4. Spectra Max Plus 384 microplate reader (Molecular Devices, Sunnyvale, CA).
5. Coulochem II Electrochemical Detector, ESA Model 580 Solvent Delivery, Model 5011 Analytical Cell, a Model 5020 Guard Cell (Chelmsford, MA).

21.2.2 Reagents and Buffers

1. Cholesterol, C8667 (Sigma-Aldrich.com, St. Louis, MD).
2. Phospholipon 85G (PL8G) and phospholipon 90H (PL90H)(Lipoid LLC, Newark, NJ).

21.2.2.1 Lipids for Liposome Formulation

3. L-α-phosphatidic acid, Avanti Product Number 109774 (Avanti Polar Lipids Inc., Alabaster, AL).

21.2.2.2 Organic Solvents for Liposome Formulation

1. Methylene chloride (dichloromethane), D151 (Fisher Scientific).
2. Ethanol, 042104 (Aaper Alcohol and Chemical Co., Shelbyville, KY).
3. Chloroform, C606 (Fisher Scientific).

21.2.2.3 Lipid-soluble Antioxidants

1. RRR-α-tocopherol (AT), R951027A1 and RRR-γ-tocopherol (DT), R951027A5 (Cognis Corporation (LaGrange, IL).
2. δ-Tocotrienol (DT3), Cayman Product 10008513 (Cayman Chemicals, Ann Arbor, Michigan).

21.2.2.4 Water-soluble Antioxidants

1. N-Acetyl-L-cysteine (NAC), A8199 (Sigma).
2. L-Glutathione reduced (GSH), G4251 (Sigma).

21.2.2.5 GSH/GSSG Assay

1. The assay buffer is Dulbecco's Phosphate-Buffered Saline (PBS) (Mediatech Inc., Herdon, VA) supplemented with 2 mM ethylenediaminetetraacetic acid (EDTA) Sigma-Aldrich, St. Louis, MO.
2. A 0.1 mM GSH solution (30.7 mg/l) is prepared in PBS and stored at 4°C (for up to 2 weeks). The solution is used to prepare GSH standards.
3. A 108 μl aliquot of 2-vinylpyridine (2-VP) (Sigma) is added to 1.00 ml of ethanol (1.00 M) and prepared immediately prior to the assay.
4. A 1.00 mM Ellman's reagent is prepared by dissolving 40 mg of 5,5′-dithio-bis(2-nitrobenzoic acid), (DTNB) (Invitrogen, Eugene, OR) in 100 ml of PBS immediately prior to the assay.
5. A 2 mM stock solution of reduced β-nicotinamide adenine dinucleotide 2′-phosphate tetrasodium salt (NADPH) (Sigma-Aldrich, St. Louis, MO) is prepared by dissolving 1.7 mg of NADPH in 1.00 ml of PBS immediately prior to the assay (stored at 4°C).
6. Glutathione Reductase (GR) (Roche Diagnostics, Indianapolis, IN).
7. Fisherbrand Flat-bottom 96-well clear plastic plate (Fisher Scientific, Hampton, NH).

21.2.2.6 Vitamin E Assays

1. A lysis buffer is prepared by mixing a 40.0 ml aliquot of 50 mM HEPES/NaOH buffer (pH = 7.50) with 1.0 ml of Triton X-100, 5.0 ml of 2 mM EDTA, and 54.0 ml of distilled water and stored at 4°C.
2. Stock solutions for the mobile phase are: (a) 1 M ammonium acetate/acetic acid (NH_4OAc/HOAc) Buffer (pH = 4.40) prepared by dissolving 77.10 g of NH_4OAc in 1.0 l of polished water and adjusting the pH to 4.40 with HOAc (J.T. Baker Chemical Co., Phillipsburg, NJ); (b) 3.0 mM of citric acid is prepared by dissolving 0.1441 g of citric acid in polished water to a final volume of 250 ml. All solutions in the mobile phase are prepared from "polished water" which is distilled water filtered through a Sep-Pak cartridge (Water, Atlanta, GA).
3. A 10 μg/ml BHT solution in hexane is prepared by dissolving 10.0 mg of 2,6-ditertiary-butyl-4-methyl phenol (BHT) from Aldrich (Milwaukee, WIS) in 1.0 l hexane.
4. Mobile Phase is prepared by mixing a 80.0 ml aliquot of 1 M NH_4OAc/HOAc buffer (pH = 4.40) with 4.0 ml of 3.0 mM citric acid, adding polished water to give a final volume of 400 ml followed by filtration through a 0.22 μm filter

Millipore (Millipore Corp., Bedford, MA). This solution is then mixed with 3,600 ml of HPLC grade methanol (MeOH).

5. rac-5, 7-dimethyl tocol (Matreya, Pleasant Gap, PA).

21.2.2.7 Cell Culture with Antioxidant Liposomes

1. RAW264.7 murine macrophage-like cells are obtained from the American Type Culture Collection, Rockville, MD.

21.3 Methods

Antioxidant liposomes can be formulated with a wide variety of phospholipids, stabilizers, lipid-soluble antioxidants, and water-soluble antioxidants. It is critical to have an overall experimental design in mind for the use of a given liposomal formulation since this will dictate compositional issues. For example, for an in vitro tissue culture experiment, the stock liposomes will often be diluted to provide physiological levels of antioxidants.

21.3.1 Concentration Issues

Liposomes have two phases, an interior aqueous phase and hydrophobic lipid bilayer phase. For the bilayer phase, the most useful units of concentration are mole fraction but for the interior aqueous phase it is mM or μM. The mole fraction of component *i*, x_i, in the lipid bilayer is given by $x_i = n_i/n$ where n_i is moles of component *i* in the bilayer and *n* is total number of moles of all components in the bilayer. When a liposomal formulation is diluted into a buffer/culture medium, the mole fraction of any component (like a lipid-soluble antioxidant) in the lipid bilayer will not change. It is also useful, however, to express the concentration of a lipid-soluble component in molar units so one can evaluate if a "physiological" level of a lipid component is being utilized. In the case of vitamin E, the molar concentration is given as moles of liposomal vitamin E added to the buffer divided by the volume of the buffer; a physiological concentration is about 30 μM for α-tocopherol. It should be kept in mind, however, that all the vitamin E is in the liposomal lipid phase, not "free" in solution.

A water-soluble antioxidant can also be incorporated into the interior aqueous phase of liposomes and its initial concentration in the liposomal aqueous phase (assuming no in vitro loss) would be the same as its concentration in the aqueous phase of the "formulation buffer". If the water-soluble antioxidant were an ionic, hydrophilic compound (such as ascorbate or GSH) it would not diffuse through the lipid bilayer of the liposome and its concentration in the interior liposomal aqueous phase would stay constant even after subsequent dilution of the liposomes or removal of the exterior formulation buffer. It is still, however, useful to calculate

the molar concentration of the liposomal water-soluble antioxidant in the buffer or medium into which it is diluted, i.e., the moles of water-soluble antioxidant per liter of buffer/medium: again keeping in mind, that this is not the "true" free concentration of antioxidant.

21.3.2 Preparation of Antioxidant Liposomes by Extrusion (Small Scale)

Antioxidant liposomes can be made with a variety of techniques and compositional variations. Some liposomal components such as DPPC and tocotrienols can be very expensive and it might be necessary to make small-scale preparations for use in tissue culture experiments. In this case, the "mini" extrusion technique is a very useful apparatus and is available from Avanti Polar Lipids (see http://www.avantilipids.com/extruder.html) where its operation is also described in some detail.

As is the case for all liposomal preparations, the desired lipid components are first added together to form a homogenous solution using an organic solvent (see Note 1). The solvent is evaporated in a glass container leaving a thin lipid film, which is then hydrated and detached by vigorous mixing with the formulation buffer (which could contain water-soluble antioxidants) to form large multilamellar vesicles (LMVs), which are then reduced in size by energy input. For the extrusion technique, this energy input is accomplished by mechanically extruding the LMVs through a polycarbonate filter with a fixed pore size. This will yield large unilamellar vesicles (LUVs) with a diameter similar to the pore size of the polycarbonate filter.

21.3.2.1 Preparation of δ-Tocotrienol-Liposomes with NAC (NAC-DT3-Liposomes) by Mini-extrusion

Below, we provide a detailed procedure for the preparation of liposomes containing δ-tocotrienol (DT3) as the lipid-soluble antioxidant and NAC as the water-soluble antioxidant. In this example, phosopholipon 85G (PL85G) is used as the phospholipid source (soybean lecithin) and this particular phospholipid forms "liquid" bilayers at room temperature. In this example, the mole fractions (in the lipid bilayer) of PL85G to cholesterol to delta-tocotrienol are 0.666, 0.266, and 0.066, respectively (see Note 2). Cholesterol and vitamin E both make liposomes less permeable to aqueous dyes and more resistant to protein-induced disruption [21]. In this example, there are a total of 50 μmol of lipid per ml of formulation buffer and the concentration of NAC and DT3 are 75 and 3.33 mM (in the formulation buffer), respectively.

1. Stock solutions of PL85G (30 mg/ml), cholesterol (20 mg/ml), and DT3 (24 mg/ml) are made in methylene chloride (see Note 3). The formulation buffer contains 61.2 mg of NAC in 5.00 ml of PBS with the pH adjusted to 7.4 (see Note 4). The NAC solution is passed through a sterile 0.2 μm filter into a sterile 10 ml test tube.
2. The stock solutions (4.5 ml of PL85G, 1.3 ml of cholesterol, and 275 μl of delta-T3) are added to a round bottom

test tube (55 ml, Pyrex, No. 9826, 25 mm OD × 150 mm) with a Teflon-lined screw cap. The dichloromethane solvent is evaporated using a stream of nitrogen in a fume hood.

3. After the solvent is completely removed, the lipid film is hydrated in 5 ml of sterile 75 mM NAC in PBS with vigorous vortexing for at least 2 min (see Note 5).
4. A 1 ml aliquot of the fully hydrated lipid sample is loaded into one of the gas-tight syringes and placed into one end of the mini-extruder. A second, empty, gas-tight syringe is placed into the other end of the mini-extruder and the fully assembled apparatus placed in the extruder stand. The syringe plunger containing the sample is transferred through the polycarbonate filter to the receptor syringe and this process is repeated at least five times (or 10 passes). Polycarbonate filters are available from 0.2 to 1.0 μm.
5. If liposomes are made with a 0.2 mm polycarbonate filter, they can be passed through a 0.4 μm filter for sterilization.

21.3.3 Preparation of Antioxidant Liposomes by High Pressure Homogenization (Large Scale)

For in vivo animal experiments, it is often necessary to have liposomal volumes much greater than the 1 ml produced by the mini-extruder. In addition, it may be required that the liposomes used for an in vivo animal experiment be identical to those used in a potential large-scale clinical experiment. In this case, the ability to scale-up a bench size production to a commercial scale production, without loss of liposomal characteristics, would be a very important quality control issue. High pressure homogenization (HPH), as performed by the Model M-100L Microfluidizer (a bench top instrument) with a throughput of up to 270 ml/minute can be scaled-up without loss of liposomal physiochemical properties. We routinely use this apparatus to produce 100 ml aliquots of antioxidant liposomes for use in animal models. Avestin Inc. (Ottawa, Canada) produces an apparatus that produces liposomes by a combination of homogenization and extrusion. HPH works by using air pressure to push a large piston which, in turn, pushes a smaller plunger thereby transferring the intensified pressure to the product stream (LMVs in our case) contained within an interaction chamber with microchannels. This process causes the LMVs to undergo shear, impact, and cavitation forces resulting in unilamellar vesicles.

Talsma et al. [22] have compared the HPH technique for preparing liposomes with the extrusion method and the ultrasonication method. In agreement with the data presented by Talsma et al. [22], we have found that about three to five cycles of homogenization, with chamber pressure of 17,000 psi, are sufficient to produce liposomes with a minimum mean particle size. In general, ultrasonication produces liposomes with a mean particle size similar to that achieved by HPH [22]. We have found,

however, that sonication is not suitable for the preparation of antioxidant liposomes since it promotes the oxidative loss of any added antioxidants.

The total amount of lipid per ml of formulation buffer is also a factor influencing liposomal characteristics. In general, we have found that concentrations of 50 μmol of lipids per ml of formulation buffer produce liposomes with a narrow size distribution but higher levels increase the solution viscosity and result in liposomes with an increased size distribution as well as an increased mean particle size.

In the example below, we describe the details to produce 50 ml of antioxidant liposomes containing both alpha-tocopherol and gamma-tocopherol as lipid-soluble antioxidants and GSH as a water-soluble antioxidant. Phospholipon 90 H (PL90H) is the primary phospholipid used but phosphatidic acid (PA) was also used to impart a negative charge to the liposomes to help maintain a fully dispersed particulate state. The mole ratios of PL90H: cholesterol: PA: AT: GT in this preparation are 10:4:0.1:1:1, respectively.

1. A stock solution of PL90H (see Note 6) is made in chloroform (20.0 g in 100.0 ml of $CHCl_3$). Stock solution of cholesterol (2.0 g/100.0 ml), phosphatidic acid (2.5 g/100 ml), α-tocopherol (0.50 g AT/10.0 ml), and γ-tocopherol (0.50 g GT/10.0 ml) are prepared in methylene chloride.
2. The stock solutions (12.3 ml each of PL90H, 0.86 ml of PA, 24 ml of cholesterol, 2.7 ml of AT, and 2.6 ml of GT) are added to a 500 ml Pyrex round bottom flask with a 24/40 ground glass joint. The solvent is removed by rotary evaporation producing a thin film of lipid on the inside of the round bottom flask. The solvent should be completely removed by application of a vacuum with mild heating (37°C).
3. After the solvent is completely removed, the lipid film is hydrated in 100 ml of sterile 75 mM GSH in PBS with vigorous agitation until all the lipid is removed from the inner glass surface of the round bottom flask (see Note 5). The temperature of the PBS solution should be above the gel-liquid transition temperature for PL90H, which is 51°C.
4. The HPH pump is primed with ethanol, then with distilled water followed by sterile PBS. The 100 ml of fully hydrated lipid sample is then placed in the product inlet reservoir and pumped through the Microfluidizer using a pressure of 17,000 psi until the reservoir is almost drained. The product is collected and passed through pump for an additional four times (resulting in a total of five passes).
5. It is sometimes desirable to remove the formulation buffer containing the external water-soluble antioxidant(s), leaving only the liposomal encapsulated water-soluble antioxidant(s).

This can be done in large scale by sedimenting the liposomes (three times) by centrifugation (15,000 rpm in an SS-34 rotor in a Sorvall RC-5B centrifuge for 15 min) followed by their resuspension in PBS buffer. Alternatively, the liposome sample can be placed inside dialysis tubing and dialyzed against multiple changes of PBS buffer.

21.3.4 Size Measurements by Dynamic Light Scattering

Particle size is an important factor modulating the uptake of liposomes [23, 24]. Chono et al. [23] have found, for example, that the uptake of liposomes by rat alveolar macrophages increases with particle size over a range from 100 to 1000 nm. It is important, therefore, to characterize antioxidant liposomes by measuring their particle size distribution. This is most readily accomplished by the use of dynamic light scattering (DLS), which has a very large size range from 0.005 to 2 microns (1 micron is 10^{-6} m or 1000 nm). For DLS, light from a laser is focused into a glass tube containing a diluted sample of the liposome suspension, which scatters some of the light in all directions. For a laser light beam, it is possible to observe time-dependent fluctuations in the scattered intensity due to the Brownian motion of the liposomes. Analysis of the time dependency of the intensity fluctuations yields the diffusion coefficient of the liposomes. Knowing the viscosity of the medium, the hydrodynamic diameter of the liposomes can be calculated from the Stokes Einstein equation. In the example provided below, a Nicomp 380 DLS from Particle Sizing Systems (Port Richey, FL) is utilized.

1. Dilute 10 µl the liposome sample (assuming a concentration of about 50 µmol of total lipids/ml) into 1.00 ml of PBS buffer, which should give a scattering intensity of 300 kHz.
2. The particle size distribution is analyzed using the software (CW388) accompanying the Nicomp instrument. The simplest particle distribution for liposomes is a smooth Gaussian unimodal distribution with a well-defined mean diameter and half width. If, however, this distribution does not the raw data very well (see Note 7), it is then necessary to attempt a fit assuming a discrete distribution of particle sizes, i.e., a distribution analysis. AQ1

21.3.5 Chemical Stability of Antioxidant Liposomes

The chemical stability of the antioxidants incorporated into antioxidant liposomes is an important quality control issue. Below, we describe the analytical procedures to measure GSH (a water soluble) or vitamin E (lipid soluble) isomers in antioxidant liposomes.

21.3.5.1 GSH Assay Using the Enzymatic Recycling Method

The assay detailed below provides specific details for measuring both reduced GSH and oxidized GSH (GSSG) in liposomes using the Tietze's enzymatic recycling method [25], but this method can easily be adopted to measuring cellular level as well.

This assay uses the Tietze's enzymatic recycling method [25] in which GSH reacts with DTNB (5,5′-dithio-bis-2-nitrobenzoic acid) yielding 5-thio-2-nitrobenzoic acid (TNB) as well as a mixed disulfide between GSH and TNB that is subsequently reduced by glutathione reductase, recycling GSH and producing more TNB. The rate of TNB production is directly proportional to the concentration of total GSH in the sample. Since this assay utilizes glutathione reductase, it measures the concentration of both GSH and GSSG (total GSH). In order to measure just GSSG, 2-vinylpyridine is first used to derivatize GSH alone [26] leaving just GSSG. The concentration of GSH in sample can be calculated as the difference between total GSH and GSSG. We have found it convenient to utilize a GSH assay kit from World Precision Instruments, (Sarasota, FL) but other sources are also available (see 703002 Glutathione Assay Kit from Cayman Chemical Company, Ann Arbor, MI).

1. Liposome samples containing GSH are diluted in PBS to give a final GSH concentration in the range of 5–30 μM. A 100 μl of each diluted sample is pipetted into two plastic microcentrifuge tubes, one for total GSH and the other for GSSG measurements.
2. GSH standards (6, 12, 18, 24, and 30 μM) are prepared from the 0.1 mM stock solution by dilutions in PBS and assayed in parallel with the samples. PBS is used as a blank reference (0 μM GSH).
3. A 2-μl aliquot of 1.00 M 2-VP solution in ethanol is added to each GSSG sample tube (see Note 8).
4. After vortexing for 30 seconds, the sample and standard tubes are incubated at room temperature for 60 minutes. A 25-μl aliquot of sample/standard is placed in each well of a clear plastic 96-well plate and all samples/standards assayed in triplicate.
5. The assay cocktail is prepared by mixing 1 ml of DTNB stock, 1 ml of NADPH stock, 0.2 ml of glutathione reductase stock, and 7.8 ml assay buffer. This cocktail should be used within 20 min after preparation.
6. A 100 μl of the assay cocktail is added to each sample/standard followed by careful shaking or 2 seconds and then inserted into the Spectra Max Plus 384 microplate reader. The absorbance at 405 nm is measured for 10 min at 2 min intervals at room temperature.
7. For each standard/sample, the average OD (of the triplicates) is plotted as function of time, and slopes for each curve (δOD) calculated (only in the linear part of the curves) by **δOD = OD final − OD initial**. The δOD values for the standards are plotted as a function of the GSH concentration

and the resulting graph should be linear, i.e., $\delta OD = a \cdot$ **GSH concentration** $+ b$. The a and b parameters of the formula for the linear trend line of the plot are determined using Microsoft Excel (graph function "Add Trend line"). The total GSH or GSSG concentrations can be calculated by:

$$\text{Total GSH or GSSG} = (\delta \text{ OD-}b)/a$$

The GSH concentrations diluted samples are calculated as the differences in total GSH and GSSG. Concentrations that are out of the 5–30 μM range are disregarded. Finally, GSH and GSSH concentrations in the liposomal samples are calculated using the appropriate dilution ratios.

Figure 21.1 shows ratio of GSSG (in GSH equivalents) to GSH assayed as a function of storage time for GSH-liposomes and GSH-α-tocopherol liposomes stored at room temperature (RT) or 4°C. These data show that GSH is oxidized fairly rapidly at room temperature compared to 4°C. Moreover, the presence of α-tocopherol does not retard GSH oxidation. These data suggest that GSH-liposomes would have to be used relatively soon after being formulated. A chelating agent such as ethylenediaminetetraacetate (EDTA) or urate [18] could be used as a preservative for both lipid- and water-soluble antioxidants.

21.3.5.2 Vitamin E Assay Using HPLC with Electrochemical Detection (HPLC-ECD)

The HPLC method described below utilizes a highly sensitive coulometric electrochemical detection technique suitable for measuring vitamin E isomers in 10^6 cells. Although we describe an assay for measuring vitamin E in adherent cultured cells, this technique

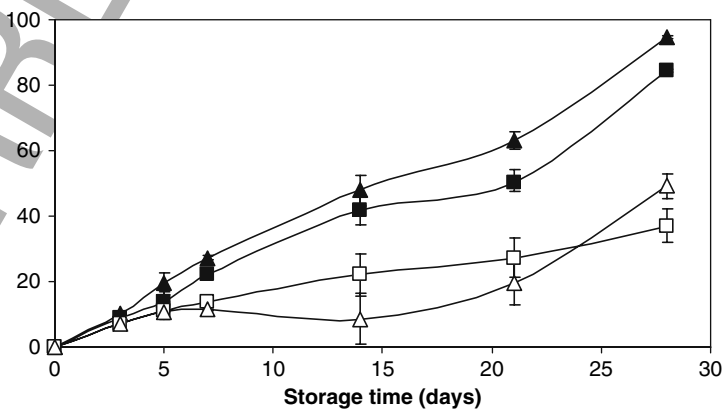

Fig. 21.1 GSH oxidation to GSSG in liposomes during storage. GSH-liposomes (square symbols) and GSH-α-tocopherol liposomes (triangular symbols) were stored at room temperature (solid symbols) or at 4°C (open symbols). Total GSH (GSH + GSSG) and GSSG concentrations within the liposome samples were measured after 3, 5, 7, 14, 21, and 28 days of storage using the Tietze method. Oxidation of GSH encapsulated in the liposomes was expressed as a percent of GSH converted to GSSG relatively to the total GSH content of each sample

can be readily adopted for measuring vitamin E levels in liposomes or tissue samples. The particular HPLC system we use consists of a Coulochem II Electrochemical Detector, an ESA Model 580 Solvent Delivery Module, a HR-80 column (C 18, 3 μm, 8 cm), a Model 5011Analytical Cell, a Model 5020 Guard Cell.

1. The culture medium is removed from 2×10^6 cells in a microplate by washing three times with cold PBS buffer. The cells are then overlaid with 400 μl of lysis buffer, scraped, and collected into a glass vial.
2. The lysed cell sample is mixed with 1.0 ml ethanol containing rac-5, 7-dimethyl tocol as an internal standard and 1.0 ml hexane containing 10 μg/ml BHT.
3. After vortexing for 4 min, the mixture is centrifuged at 1020 × g for 5 min, and a 400-μl aliquot of the supernatant fluid is removed, dried under nitrogen, and taken up in 100 μl of mobile phase and filtered using 0.45 μm syringe filter.
4. The flow rate is adjusted to 1.2 ml/min and the second analytical cell potential set to 400 mV and the potential of the guard cell electrode, used to eliminate interference by electro-active impurities in the mobile phase, set to 300 mV.

It is important to measure the response factor for each vitamin E isomer with respect to the internal standard (they are all different). This is accomplished by preparing standard solutions with known concentrations of vitamin E isomer (the extinction coefficients are listed in Note 9). The standard solutions are mixed with internal standard and the areas of peaks measured using the HPLC-ECD method. The response factors of a particular vitamin E isomer relative to the internal standard (DMT) are calculated by the following formula where $\text{area}_{(\text{DMT})}$ and [DMT] are the area and concentration of the internal standard; $\text{area}_{(\text{A})}$ and [A] are the area and concentration of the vitamin E isomer:

$$\text{Response Factor of A} = [\text{A}]/[\text{DMT}] \times \text{area}_{(\text{DMT})}/\text{area}_{(\text{A})}$$

With the response factor (F), we can easily obtain the concentration of A in the cellular extract from the known concentration of DMT and measured areas of DMT and A by:

$$\text{Concentration of A} = \text{F} \times [\text{DMT}] \times \text{Area}_{(\text{A})}/\text{Area}_{(\text{DMT})}$$

21.3.6 The Uptake of liposomes Containing Both α-Tocopherol and γ-Tocopherols by RAW 264.7 Murine Macrophages

The example provided below details the procedure for measuring the cellular uptake of vitamin E by RAW 264.7 murine macrophages incubated with liposomes containing both α-tocopherol and γ-tocopherol (AT,GT-liposomes). The liposomes used here were prepared by the HPH technique using the protocol described above except no NAC was present. Blank liposomes were also prepared in this experiment and they contain neither lipid- nor water-soluble antioxidants.

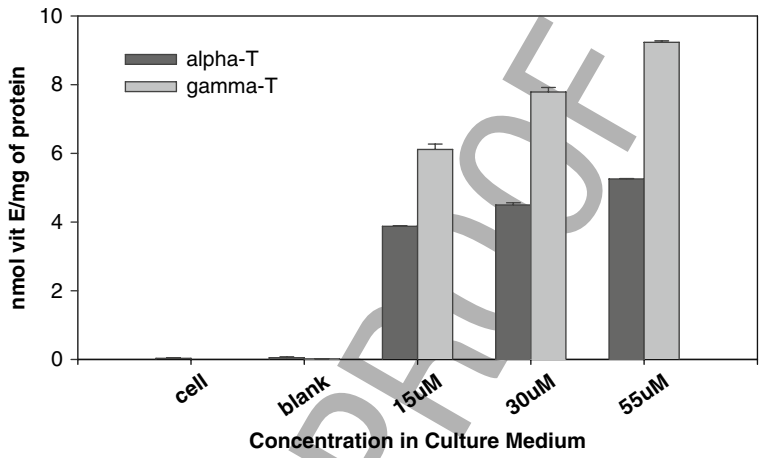

Fig. 21.2 RAW264.7 macrophage cellular uptake of tocopherols after incubation with α/γ-tocopherol antioxidant liposomes for 24 hours. The vitamin E content of RAW264.7 macrophages dramatically increases by incubation (for 24 hours) with liposomes containing both alpha- and gamma-tocopherol. The levels of liposomal vitamin E present in the medium varied from 0 to 55 μM. Physiological levels of vitamin E are in the 10–30 μM range

1. The stock liposomes contained 3.2 mM of α-tocopherol (AT) and 3.2 mM of γ-tocopherol (GT).
2. A 2.5 ml aliquot of 5×10^5 cells/ml is placed in each well of a 12-well plate and the cells incubated overnight to about 90% confluence.
3. The medium is removed from each well and fresh medium added with different concentrations of AT,GT-liposomes, black liposome or PBS into wells. After 24 hours of incubation, the medium from each well is removed, the cells lysed, and assayed for tocopherols as detailed in Sect. 21.3.5.2.
4. The total proteins in the lysed cell samples (Note 10) are measured using BCA assay and the final data presented as nmol of tocopherols/mg of protein.

Figure 21.2 shows the cellular uptake of tocopherols incubated with diluted samples of the AT,GT-liposomes for 24 hours. It is clear that the cells alone or cells incubated with the blank liposomes have very low endogenous tocopherol levels. In marked contrast, the cells incubated with the AT,GT-liposomes show a marked increase in the intracellular levels of both α-tocopherol and γ-tocopherol.

21.4 Notes

1. Vitamin E rapidly decays in halogenated solvents like chloroform or methylene chloride and therefore cannot be stored in these solvents for any length of time. Ethanol is a

suitable solvent for the long-term storage of tocopherols and tocotrienols and ethanol is miscible with methylene chloride or chloroform. Moreover, the molar extinction coefficients for most vitamin E isomers are given in ethanol.

2. Vitamin E can be added to liposomes at a level up to 33 mol% and, in general, has an effect similar to cholesterol [21].
3. The total lipid concentration is typically in the range of 10–30 mg of lipid per ml of organic solvent. Also note that methylene chloride is generally considered less toxic than chloroform.
4. It is important to adjust the pH of the NAC solution to 7.4 with NaOH or it will be acidic and potentially toxic.
5. When a water-soluble antioxidant is added to the PBS or culture medium, it is possible to increase the efficiency of entrapment into the liposomal aqueous phase by 3–5 freeze/thaw cycles.
6. Phospholipon 90H (PL90H) is not very soluble in methylene chloride and it is, therefore, necessary to use chloroform as the solvent.
7. The Nicomp software provides a "Chi Squared" parameter to help evaluate the type of particle distribution in a sample. A value less than 2 indicates a unimodal distribution and a value greater than 3 suggests a bimodal (or greater) distribution.
8. All work with 2-VP should be kept under the hood as the chemical is both toxic and volatile.
9. The molar extinctions coefficients for tocopherols (Ts) and tocotrienols (T3) are provided below.

Substance	M.W.	λ_{Max} (nm) in ethanol	ε (per cm per M) in ethanol
α-T	430.7	292	3270
β-T	416.7	296	3730
γ-T	416.7	298	3810
δ-T	402.7	298	3520
α-T3	424.7	292	3870
β-T3	410.7	295	3600
γ-T3	410.7	298	4230
δ-T3	396.7	292	3300
rac-5,7-dimethyl tocol	416.7	292	3460

10. It is important to make the BSA protein standard in the exact solution that the protein to be assayed is in, i.e., the lysis buffer.

Acknowledgments

This work was support by two United States Army Medical Research Command Grants: "The Influence of Antioxidant Liposomes on Macrophages Treated with Mustard Gas Analogues", USAMRMC Grant No. 98164001, and "Topical Application of Liposomal Antioxidants for Protection against CEES Induced Skin Damage", USAMRMC Grant No. W81XWH-05-2-0034.

References

1. Ciobanu, M., Heurtault, B., Schultz, P., Ruhlmann, C., Muller, C. D., and Frisch, B. (2007) Layersome: development and optimization of stable liposomes as drug delivery system. *Int J Pharm*. AQ2
2. Zaru, M., Mourtas, S., Klepetsanis, P., Fadda, A. M., and Antimisiaris, S. G. (2007) Liposomes for drug delivery to the lungs by nebulization. *Eur J Pharm Biopharm*. AQ3
3. Stone, W. L., Mukherjee, S., Smith, M., and Das, S. K. (2002) Therapeutic uses of antioxidant liposomes. *Methods Mol. Biol.* ***199***, 145–161.
4. Stone, W. L., and Smith, M. (2004) Therapeutic uses of antioxidant liposomes. *Mol. Biotechnol. 27*, 217–230.
5. Sontag, T. J., and Parker, R. S. (2007) Influence of major structural features of tocopherols and tocotrienols on their omega-oxidation by tocopherol-omega-hydroxylase. *J. Lipid Res. 48*, 1090–1098.
6. Mustacich, D. J., Bruno, R. S., and Traber, M. G. (2007) Vitamin E. *Vitam. Horm.* ***76***, 1–21.
7. Krishnan, K., Campbell, S., Abdel-Rahman, F., Whaley, S., and Stone, W. L. (2003) Cancer chemoprevention drug targets. *Curr. Drug Targets* ***4***, 45–54.
8. Stone, W. L., Krishnan, K., Campbell, S. E., Qui, M., Whaley, S. G., and Yang, H. (2004) Tocopherols and the treatment of colon cancer. *Ann. N Y Acad. Sci.* ***1031***, 223–233.
9. Stone, W. L., and Papas, A. M. (1997) Tocopherols and the etiology of colon cancer. *J. Natl. Cancer Inst.* ***89***, 1006–1014.
10. Azzi, A. (2007) Molecular mechanism of alpha-tocopherol action. *Free Radic. Biol. Med.* ***43***, 16–21.
11. Campbell, S. E., Stone, W. L., Lee, S., Whaley, S., Yang, H., Qui, M., Goforth, P., Sherman, D., McHaffie, D., and Krishnan, K. (2006) Comparative effects of RRR-alpha- and RRR-gamma-tocopherol on proliferation and apoptosis in human colon cancer cell lines. *BMC Cancer.* ***6***, 13.
12. Jiang, Q., Wong, J., and Ames, B. N. (2004) Gamma-tocopherol induces apoptosis in androgen-responsive LNCaP prostate cancer cells via caspase-dependent and independent mechanisms. *Ann. N Y Acad. Sci.* ***1031***, 399–400.
13. Jiang, Q., Wong, J., Fyrst, H., Saba, J. D., and Ames, B. N. (2004) Gamma-tocopherol or combinations of vitamin E forms induce cell death in human prostate cancer cells by interrupting sphingolipid synthesis. *Proc. Natl. Acad. Sci. U S A.* ***101***, 17825–17830.
14. Har, C. H., and Keong, C. K. (2005) Effects of tocotrienols on cell viability and apoptosis in normal murine liver cells (BNL CL.2) and liver cancer cells (BNL 1ME A.7R.1), in vitro. *Asia Pac. J. Clin. Nutr.* ***14***, 374–380.
15. McIntyre, B. S., Briski, K. P., Gapor, A., and Sylvester, P. W. (2000) Antiproliferative and apoptotic effects of tocopherols and tocotrienols on preneoplastic and neoplastic mouse mammary epithelial cells. *Proc. Soc. Exp. Biol. Med.* ***224***, 292–301.
16. Srivastava, J. K., and Gupta, S. (2006) Tocotrienol-rich fraction of palm oil induces

cell cycle arrest and apoptosis selectively in human prostate cancer cells. *Biochem. Biophys. Res. Commun.* ***346***, 447–453.

17. Sylvester, P. W. (2007) Vitamin E and apoptosis. *Vitam. Horm.* ***76***, 329–356.
18. Ma, Y. S., Stone, W. L., and LeClair, I. O. (1994) The effects of vitamin C and urate on the oxidation kinetics of human low-density lipoprotein. *Proc. Soc. Exp. Biol. Med.* ***206***, 53–59.
19. Fan, J., Shek, P. N., Suntres, Z. E., Li, Y. H., Oreopoulos, G. D., and Rotstein, O. D. (2000) Liposomal antioxidants provide prolonged protection against acute respiratory distress syndrome. *Surgery* ***128***, 332–338.
20. Woodle, M. C., and Papahadjopoulos, D. (1989) Liposome preparation and size characterization. *Methods Enzymol.* ***171***, 193–217.
21. Halks-Miller, M., Guo, L. S., and Hamilton, R. L., Jr. (1985) Tocopherol-phospholipid liposomes: maximum content and stability to serum proteins. *Lipids* ***20***, 195–200.
22. Talsma, H., Ozer, A. Y., van Bloois, L., and Crommelin, D. J. A. (1989) The size reduction of lipsomes with a high pressure homogenizer (microfluidicsTM). Characterization of a prepared dispersions and comparison with conventional methods. *Drug Dev. Ind. Pharm.* ***15***, 197–207.
23. Chono, S., Tanino, T., Seki, T., and Morimoto, K. (2007) Uptake characteristics of liposomes by rat alveolar macrophages: influence of particle size and surface mannose modification. *J. Pharm. Pharmacol.* ***59***, 75–80.
24. Chono, S., Tauchi, Y., and Morimoto, K. (2006) Influence of particle size on the distributions of liposomes to atherosclerotic lesions in mice. *Drug Dev. Ind. Pharm.* ***32***, 125–135.
25. Tietze, F. (1969) Enzymic method for quantitative determination of nanogram amounts of total and oxidized glutathione: applications to mammalian blood and other tissues. *Anal. Biochem.* ***27***, 502–522.
26. Griffith, O. W. (1980) Determination of glutathione and glutathione disulfide using glutathione reductase and 2-vinylpyridine. *Anal. Biochem.* ***106***, 207–212.

Chapter 21

Q. No.	Query
AQ1	Please check construction of the sentence: "If, however, this distribution **does not the raw data** very well (see Note 7), . . ."
AQ2	Please provide volume and page range for reference [1].
AQ2	Please provide volume and page range for reference [2].